LUND UNIVERSITY

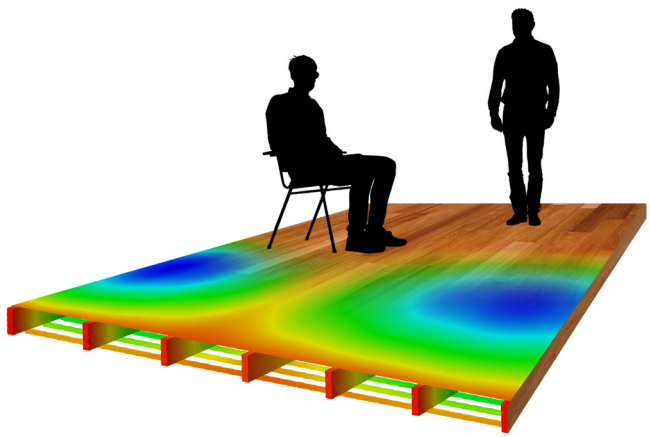

VIBRATIONS IN LIGHTWEIGHT BUILDINGS
Perception and Prediction

JUAN NEGREIRA

Engineering Acoustics

Licentiate Dissertation

DEPARTMENT OF CONSTRUCTION SCIENCES
DIVISION OF ENGINEERING ACOUSTICS

ISRN LUTVDG/TVBA--13/3130--SE (1-181) | ISSN 0281-8477
LICENTIATE DISSERTATION

VIBRATIONS IN LIGHTWEIGHT BUILDINGS

Perception and Prediction

JUAN NEGREIRA

Printed by Media-Tryck LU, Lund, Sweden, September 2013 *(Pl)*.

For information, address:
Div. of Engineering Acoustics, LTH, Lund University, Box 118, SE-221 00 Lund, Sweden.
Homepage: http://www.akustik.lth.se

Acknowledgments

The work on this Licenciate dissertation was carried out at the Department of Construction Science of Lund University (Division of Engineering Acoustics), with Dr. Delphine Bard as my main supervisor, and Professor Göran Sandberg as my co-supervisor, the period of time involved being from January 2011 to September 2013. The research reported on here was funded by the Silent Spaces project, a part of the EU program Interreg IV-A and by the Vinnova and Formas project AkuLite. The author highly appreciates the financial support.

First, I would like to thank my supervisor Dr. Delphine Bard for her continuous support and encouragement. I am also pleased to extend my greetings to all my colleagues at the Department of Construction Sciences for fruitful (and occasionally not that fruitful but very funny) discussions having taken place during *fika* breaks as well as in our office. Mr. Bo Zadig is also acknowledged for his invaluable help with the design of certain pictures included in the dissertation. A word of thanks to Arnaud Trollé, for nice talks, his very hard work and inestimable aid in matters related to statistics.

Living abroad is not always easy. *Ups and downs* kick in more frequently due to the closest ones being far away. These difficulties would never be possible to overcome without my family and my friends. Being always understanding and supportive, they, either from down south and also from Sweden – the friends who share daily experiences here with me–, backi me up in every decision I make and cheer me up in every problem I face. Deserving of special mention are my parents Juan and Mariluz, for their endless love, patience, support and understanding throughout all my life. They have always unconditionally stood behind the cause. Nothing would be as it is if they didn't encourage me to fight for what I am capable of, plus a little bit extra. I am also deeply grateful to my *brother* Alberto, for always being there when needed, every time reachable just a phone call away. *¡Moitas grazas!*

Juan Negreira
Lund, September 2013

Abstract

When the Swedish construction code (in 1994) allowed wooden multi-storey buildings to be built, this type of lightweight construction became popular due to its low cost and ease of construction, and also because wood is a plentiful resource in Sweden. Drawbacks in such buildings are disturbing vibrations and noise propagating in the construction, especially through junctions. In lightweight constructions using timber floors, vibrations can cause some nuisances for the inhabitants and complaints are often reported. Still, no vibration limits are given in any international standard due the complexity involved, simply certain guidelines and guide values being suggested instead. The vibrational response of wooden buildings has therefore become an issue to be tackled during their design phase.

The aims of the present Licenciate dissertation can in general terms be divided into two basic categories: the development of indicators of human exposure to floor vibrations, and the development of numerical prediction tools for the verification of vibratory and acoustic performance before a building is actually put up.

The appended publications **Paper A** and **Paper B**, aimed at supplementing the lack of existing studies addressing human response to floor vibrations. In order to obtain a better estimate of an acceptable level of vibrations in dwellings, measurements on real floors while people walked on the them, as well as when they sat down while another person was walking, were performed, measuring the accelerations, velocities and deflections they were exposed to. Indicators of human response to vibrations were extracted by determining relationships between people's answers to questionnaires about their perception and experience of the vibrations, and different parameters as determined by measurements. Several indicators were found to describe people's answers to questions both regarding vibration annoyance and vibration acceptability. Also, the applicability of several serviceability criteria found in the literature was checked. Ultimately, it was shown that multilevel regression, not widely used as yet in this field, can be a valuable tool for modelling repeated measures data that involves substantial inter-individual differences in rating, as the case of our study.

On the other hand, there still exist no reliable methods for predicting the vibratory and acoustic performance of a lightweight building. Nowadays, product development is carried out on an empirical basis, involving both observations and the experience of engineers. Time and costs can be reduced by addressing, during the design phase, issues of vibration, for instance by using numerical methods such as finite element simulations as prediction tools. These predictions tools allow one to simulate buildings before they are built so as to examine their vibratory and acoustic performance. Development of such accurate finite element prediction tools is also dealt with in this work. In line with

this, finite element models of a prefabricated timber volume element based building were created in the appended **Paper C**, the flanking transmission occurring being specifically analysed. Also, in the basis of conclusions drawn in that study, a method for extracting the properties of elastomers was developed in **Paper D**, so as to have reliable assessments of the material properties involved as input for the finite element models employed. This was done through performing analytical calculations, and carrying out finite element simulations and mechanical testing in a uni-axial testing machine.

More adequate knowledge of the vibrational performance of lightweight wooden buildings such as obtained here by use of measurements and of finite element simulations is seen here as paving the way for further development in this area.

Contents

Paper C
Investigation of the vibration transmission through a lightweight junction with elastic layer using the finite element method.
J. Negreira, A. Sjöström, D. Bard.
Proceedings of Internoise 2012, New York, USA.

Paper D
Characterisation of an elastomer for noise and vibration isolation in lightweight timber buildings.
J. Negreira, P-E. Austrell, O. Flodén, D. Bard
Submitted for publication. September 2013.

Part I

Introduction and overview of the work

1 Introduction

As a consequence of numerous urban fires that occurred during the 1800s, Swedish laws prohibiting the use of wooden frames in multi-storey constructions were passed in the year 1874, these being the first building regulations in the country's history [1]. This century-old ban was revoked in 1994, the year in which Swedish building regulations were revised with the aim of their harmonising with the building rules of the European Union. Since then, there has been a rapid growth in constructions of these types due to wood being a plentiful resource in Sweden and considerable research concerning such buildings having been carried out within recent years.

Lightweight constructions have many advantages [2], some of these being related to matters of sustainability such as wood's providing storage of carbon dioxide (CO_2), its use resulting in reduced amounts of waste at construction sites, relatively little energy being required for wooden buildings to be produced, and wood being a renewable raw material. Other advantages are of basically pragmatic character, such wood's being light in weight, its enabling a high degree of prefabrication to be attained, the ease of assembly of the building parts involved, the possibility of the thermal insulation attained being improved without the facade walls needing to be thickened, and the foundations being simpler, cheaper and lighter than the corresponding ones in traditional concrete constructions. Current architectural trends have also contributed to the use of wood. Accordingly, lightweight timber frame constructions have been steadily increasing their market share, to the detriment of heavy constructions, such as concrete buildings.

Nevertheless, there are many problems to be overcome in the use of timber as a construction material in multi-story buildings. Achieving a high level of acoustic quality, especially in the low frequency range (defined in the dissertation as up to 200 Hz), is a major challenge, various problems in connection with this being a major drawback in the use of lightweight timber structures. The differences in weight, stiffness, density and repartitioning as compared with more traditional materials have repercussions on how sound propagates throughout the structures, this triggering problems with sound insulation that can make acoustic comfort difficult to attain.

In most European countries, requirements for acoustic approval of a building have been developed on the basis of the performance of traditional heavy constructions, the principles applying there being extrapolated directly to lightweight timber buildings, even in spite of their different behaviours. Due to this, there unfortunately are not particularly many examples of acoustically successful multi-storey lightweight wooden framed constructions. Even if buildings comply with present-to-day regulations, complaints by inhabitants often arise due to the occurrence of low frequency noise which is outside the

scope of the standards. Accordingly, solutions for successfully achieving such acoustic comfort, regarding both sound and vibration, as well as improvement of the standards that presently exist are called for.

Although Sweden is undoubtedly a precursor in matters of lightweight timber constructions, there still remains a great deal to investigate before the vibrational behaviour of wooden structures can be regarded as readily predictable. Convincing the market that wood is a natural structural material adequate for use in multilevel buildings is still a challenge, further knowledge being needed, in particular regarding the acoustic and vibrational behaviour of such timber structures [3].

1.1 Aim and objective

The authorisation for the construction of wooden multi-storey buildings in Sweden brought with it an increase in the demand for open planning of both residential and office buildings that involved use of long-span floor structures. Wood is high in both strength and stiffness in relation to its weight. This makes it possible to build very long spans, especially with use of glue-laminated (glulam) timber. However, slender floor constructions involving long spans have low resonance frequencies that, in combination with a low degree of damping, are easily excited by such human activities as walking, running and jumping. Since people tend to be very sensitive to the vibrations thus produced, floors of this sort are often regarded as annoying. Accordingly, obtaining adequate indicators of human response to vibrations in lightweight structures dynamically excited by human activities can contribute very much to obtaining better estimates of what can be regarded as acceptable levels of vibrations in dwellings. Attempting to develop such indicators is one major objective of the dissertation.

Today there are still no methods that have been clearly shown to be reliable and have come into any sort of general use for predicting the vibratory and acoustic performance of lightweight buildings, specifically those of wood. At the same time, such predictive tools as finite element (FE) models can be conceived as being promising in this respect. In order to construct large wooden buildings of high performance in terms of limiting vibrations and structure-borne sound, adequate predictive tools are needed, so that structural adjustment of the sort needed can be made before such a building is erected. Time and costs can be markedly reduced here by addressing vibration issues during the design phase of the building, where prototypes and the performance of experiments on buildings already constructed can be both time-consuming and expensive. Gaining insight into and developing FE tools for predictive purposes here is thus a second major objective of the dissertation. The importance of developing predictive tools of this sort is specifically pointed out, for example, in [3, 4].

It is known that the evaluation methods in use today substantially underrate the effects of low frequency sound, there thus being a definite need of research to increase knowledge within this area and ultimately improve the evaluation methods employed. Gaining knowledge of the impact sound in the low frequency range on lightweight timber structures, though making use of both measurements and numerical simulations is thus sought in the dissertation.

1.2 Outline

The dissertation is divided into two parts:

Part I is an extended summary of the different topics dealt with in the papers that are appended, its aim being to provide a broad and theoretical overview of the topic. It is, in turn, structured as follows:

After presenting in this here **Chapter 1** the introduction and the aim and objectives of the dissertation, **Chapter 2** provides an overview of building with wood, describing various lightweight materials commonly used in timber buildings, and also touching upon such topics as building techniques, the current building regulations in Sweden and problems concerned with acoustics and vibrations in buildings of the sort described. **Chapter 3** considers floor vibrations in detail. It presents an extensive review of literature concerning existent serviceability criteria as well as of the theoretical background of the topic in question. **Chapter 4** describes the measurement devices and sensors employed, the excitation sources, as well as the various techniques and post-processing methods taken up in one of the four papers that are appended. **Chapter 5** introduces briefly the theoretical background of the statistical methods employed in one of the four appended papers, methods involved in relating subjective responses in a questionnaire concerned with how people experienced vibrations on the floors of the sort studied here to objective measurements performed on those floors at the same time people walked or sat on them. **Chapter 6** deals with the finite element (FE) method from a theoretical point of view, this being the basic tool used here in developing numerical prediction tools for predicting the acoustic performance of lightweight timber buildings. **Chapter 7** summarises all of the appended papers and the conclusions drawn there, and **Chapter 8** discusses the conclusions of the present work as a whole and suggests paths for further research in the areas dealt with.

Part II, in turn, compiles all the appended publications.

2 Building in wood

Acoustics encompasses both sound and vibration. At the present time, proper acoustics (i.e. fulfilment of the current standards) serves as a performance characteristic for building with wood, being a prerequisite for the acceptance of timber constructions by the building industry, by building owners and by consumers [3]. The dwindling share of single-family houses in the construction market in deference to wooden multi-storey constructions in Sweden since 1994 [2], has led to the regulations regarding both impact and airborne sound insulation becoming more stringent due to complaints of noise disturbances by the inhabitants of such buildings. Accordingly, new materials and new building techniques have been developed.

2.1 Engineered wood products

Wood is a natural structural material that generally has a high strength-to-weight ratio, that represents a renewable resource, and that is considered by many to be aesthetically appealing. Due to its anisotropy, strength and stiffness, its properties can vary considerably with different load orientations. Wood is generally both strong and stiff when loaded parallel to the grain, but is relatively weak when loaded perpendicular to it.

Engineered wood products (EWP) represent a broad class of materials intended for structural applications used very much in prefabricated timber constructions. In contrast to lumber or solid sawn timber, which is obtained by sawing logs or cants into individual solid elements, EWP are typically manufactured from wood which has been reduced to smaller pieces by sawing, peeling, chipping, slicing or defibration. EWP are comprised of such constituents, as sawn laminations, veneers, strands, flakes, and sawdust that are bonded together by use of adhesives and through application of heat and pressure to form panel-like, or timber-like elements of differing size or shape to create structural products of different kinds. One type of EWP, that of glulam, is manufactured in a different manner, its being made by simply gluing either sawn timber or laminates into larger units. Albeit EWP are more expensive for building purposes than sawn timber is, and the fact that adhesives have been added to the natural material of which they consist, EWP have distinct advantages [5]:

- The possibility of producing products of any size, regardless of the tree dimensions.
- Better and more efficient utilisation of the raw wood material.

- The strength-reducing effects present in solid wood are neutralised in part, the extent to which this occurs depending upon the type of EWP involved.
- The dimensional stability and tolerances they possess are significantly better, in general, than those of sawn timber.
- Their ready adaptation to market requirements (in terms of customised sizes, the specific properties sought, and the like).

EWP are found on the market for many different uses, the most prominent types of these being the following: structural wood panels (plywood, oriented strand board – OSB –, and cross-laminated timber – CLT –), structural composite lumber (laminated veneer lumber – LVL –, parallel strand lumber – PSL –, laminated strand lumber – LSL –, glued laminated timber – glulam –, and wood I-joists) and non structurally load-bearing components (particleboard). Figures 2.1(a)-2.1(f) show some of these EWP commonly used in the prefabricated constructions of the sort deal with in the dissertation.

(a) Plywood, [6].

(b) OSB, [7].

(c) CLT, [8].

(d) LVL, [9].

(e) Glulam, [9].

(f) Particle board, [10].

Figure 2.1: Different EWP.

Accounts of the properties of each of the aforementioned materials, as well as further information regarding them, can be found in the literature, for example [5, 11]. In [12], it is concluded, however, that if reliable results are to be obtained when carrying out FE simulations of lightweight wooden structures, for example, considerable research is called for, since so much is still unknown or uncertain regarding the properties of complex wooden structures built of such materials. There is thus a strong need of knowledge for enabling the correct modelling of such structures and their components to be carried out.

2.2 Building methods

Although lightweight timber frame buildings can be put up completely on site, the tendency leans towards them being erected by assembling prefabricated elements at the building site. The higher the degree of prefabrication is, the less weather-dependent the building process becomes, the time spent at the construction site being reduced and moisture problems thus also being avoided to a considerable degree. In addition, the level of quality control is higher indoors, in a factory, due to optimisation of the production techniques there. It also makes it possible to manufacture and assemble at different locations with a high degree of accuracy with regard to size. Moreover, prefabrication can improve production economy, in terms both of reducing the working time and the material wastage, all of this resulting in less expensive tenements [13, 14].

Only prefabricated structures are dealt with in the dissertation, due to the fact that buildings with massive wooden floors do not have that severe problems with regard to low frequency sound insulation (owing to their higher mass) and also that the market is moving towards prefabricated constructions being involved for the most part. At present time, three main prefabricated building methods can be distinguished in Europe [2]:

Platform-frame method

The floor elements here are fixed on top of the walls of the lower level and are most often continuous from one room to another on the same floor, their thus becoming a working platform for construction of the next building layer. This is the standard approach in lightweight frame construction in Europe.

Balloon-frame method

With use of this method, also known as the Chicago method, the walls are continuous over many storeys, the floors hanging between the walls, so to speak. Although this method provides advantages in terms of better air tightness of the building, its use is not widespread, due to the construction problems it results in, such as limitations in the height of the building, prefabrication problems and difficulties in the on site mounting of the construction in question. Some mixed balloon and platform-frame methods exist, however, in which the floors are fixed to notches in the walls.

Box-assembly

In this method, also called timber volume element (TVE) based buildings, prefabricated box-like elements are stacked together to assembly the complete building. Each box can be regarded as a closed three-dimensional structure built up by the floor, ceiling and walls. The degree of prefabrication performed at the factory is considerable so that the work on site required is held to a strict minimum. The costs and the difficulties in transportation can be the main drawbacks of this building approach.

A distinct advantage often present in this type of building system as regards vibrations and acoustic performance is that, for any two volumes placed above the other, the upper

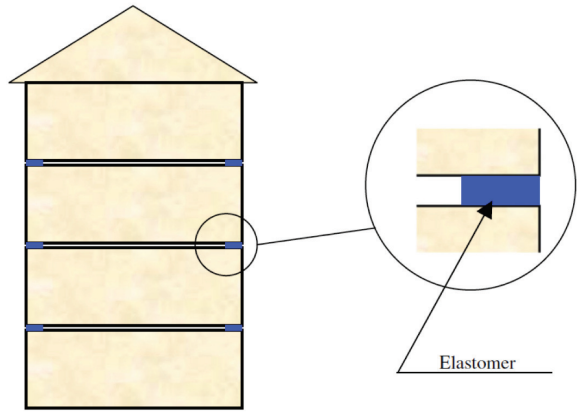

Figure 2.2: Box-assembly building method, [13]

volume contains the upper part of the floor to it, being the ceiling comprised in the lower volume. An elastomer is usually inserted in between the two volumes. It is precisely the fact of having an elastic strip between any two volumes one above the other, the floor of the one above and the ceiling of the one below being split from one another, that distinguish volume technique from more traditional lightweight building technique [13]. The only mechanical contact between two adjacent TVEs is by means of these elastomers that are placed on the flanks, its reducing the flanking transmission markedly if the correct elastomer is used; see Figure 2.2.

Considerable research on lightweight timber buildings has been carried out. According to [13], however, there is still a lack of systematic studies dealing specifically with volume based element buildings. It is still a question, therefore, to what extent the knowledge regarding traditional lightweight buildings attained thus far is directly applicable to volume system. Different FE prediction tools of buildings that were built following this method, will be taken up in the dissertation.

The type of method selected determines the types of junctions present in a building's structure, its having important consequences for the flanking transmission found between adjacent rooms.

2.3 Sound transmission

Various concepts employed in the dissertation are defined in this section. Disturbing sounds (noise) or vibrations in a building environment can stem from sounds or vibrations travelling from one part of it to another. On the basis of the noise source, one can distinguish between two types of transmission:

Airborne sound transmission

When sound waves travel through the air and reach a building element they cause it to vibrate. The vibrations produced travel throughout the element in question and radiate out to the other side of it through creating pressure differences that propagate and create noise. Typical airborne transmission sources are speech, HiFi systems (such as speakers), and appliances. The sound transmission path here is one in which the energy is carried for the most part by the air, and only to a minor extent via structural or solid-borne waves [15]; see Figure 2.3(a). The airborne sound is outside the major scope of the dissertation and will thus not be specifically dealt with.

Structure-borne sound transmission

The direct impact of an object in striking a separating surface of a building, such as a floor, causing both sides of the building element involved to vibrate, and generating sound waves that propagate through it and transmit the sound then to an adjacent room is called structure-borne sound. Typical impact sources are footsteps when people walk, jump or run, and dropped objects, the dropping of which can be heard in a room below; see Figure 2.3(b). Structure-borne sound is of central interest in the dissertation, particularly that in the low frequency range.

Both airborne and impact sources generate direct transmission and **flanking transmission** to adjacent rooms; see Figure 2.3. A typical example of flanking transmission is when the vibrations of a floor spread to the load-bearing walls and result in sound radiation from the walls, which sometimes is greater than that from the floor. Indeed, flanking transmission is often one of the main acoustic problems in lightweight constructions, especially as regards impact sounds. With use of suitable devices for suppressing flanking transmission, sound insulation can be improved by approximately 15 dB [3]. Theoretically, it can be reduced in line with three different principles [3]:

- Reduction of noise (air-borne or impact) transmitted into the plate-like structures in the source room, the reduction being achieved, for example, by increasing the surface weight of the upper part of the floors by means of an extra layer of heavy material, thus improving the noise-reduction performance of the floor in regards to low frequencies.
- Reducing the transmission of noise from the plate-like structures in the source room to those in the receiving room. Means of accomplishing this have been widely used in Sweden, especially in buildings made of volume elements (TVEs), the noise transmission be lessened by use of an elastic layer (cf. Figure 2.2).
- Reducing the radiation of noise from the plate-like structures in the receiving room by use of walls made of plasterboard placed on top of wooden studs rather than of massive wooden structures.

In practice, splitting the construction frameworks of adjoining apartments or rooms would be a safe solution in terms of reducing flaking transmission, yet this is often not a practicable approach due to factors of stabilisation affected by, for example, wind loads.

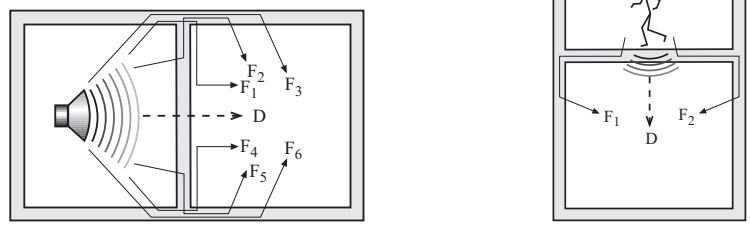

(a) Airborne sound transmission. (b) Impact sound.

Figure 2.3: Sound transmission types. "D" denotes direct transmission whereas "F_i" indicates different flanking paths.

2.3.1 Low frequency issues

Whereas heavy constructions do not present problems in regard to sound insulation at low frequencies, due to the large mass they possess, lightweight wooden constructions are prone to suffer low acoustic and vibratory quality at lower frequencies. As advanced, low frequency vibrations will referred as to those up to 200 Hz in the following, if not otherwise stated. Major topics to consider in regard to the acoustic quality of housing, as far as the lower frequencies concerned, are those described in Section 2.3 [3], specifically air-borne sound insulation, impact sound insulation and flanking transmission.

Statistical methods based on the assumption of the presence of a diffuse field are often employed in calculations. These methods are not appropriate to use for low frequencies, due to the lightweight elements there being exposed to non-diffuse conditions because of the internal damping being greater than that for heavy elements, this producing a high degree of uncertainty and variability in measurement results obtained. Persons walking, running or jumping, as well as appliances, traffic, airplanes, fans and other HVAC systems, etc. need to be dealt with properly if acoustic comfort (both in terms of buildings complying with regulations and providing comfort for the occupants) is to be achieved.

2.4 Requirements and subjective judgements

Due to the high degree of variability of vibratory and acoustic behaviour that characterises wood as a load-bearing material, large risks are always involved in assembling buildings of the types just described, the most important being that of the comfort of occupants. Greater knowledge in this regard concerning wood can reduce the risks of using it, enhance the positive qualities of choosing wood as a construction material and aid the industry in constructing these types of buildings. In line with this, the development and modification of excitation sources in ways conducive to sound reduction, and improvements in the prediction and evaluation methods employed, particular in connection with vibrations and low frequency sound are needed in order to better ensure the comfort of inhabitants.

2.4.1 Building regulations

The current requirements for acoustically approve a building are, in most countries, based on evaluations of the acoustic performance from the 100 Hz third octave band and upwards. At the same time, an increasing need has been felt to look carefully at the performance of buildings at levels below 100 Hz, especially as regards lightweight buildings [2]. These regulations rate dwellings on the basis of single number descriptors.

In Sweden, the national building regulations (BBR) establish for both air-borne and impact sound, a classification system stemming from two standards (SS-25267 [16] for dwellings and SS-25268 [17] for premises of other types), each of which involves four sound classes, denoted as A, B, C and D. Class C is the minimum requirement for the acceptance of a building, classes A and B being recommended for the achievement of a good sound climate, at the same time as class D, despite its limitations, may be regarded as acceptable in certain rebuilding projects. For classes A, B and C, the extended-frequency-adaptation terms that take account of low frequencies are included nowadays in the SS-25267 (2007) standard. Thus, the frequency range of analyses has been widened to include either of the following: 50-3150 Hz or 50-5000 Hz. For class D, however, the traditional frequency range of analyses, that of 100-3150 Hz, still applies [3]. Thus, the correction terms are $C_{50-3150}$ and $C_{I,50-2500}$, for air-borne and impact sound insulation, respectively. The limiting values are given, therefore, in terms of $R'_w + C_{50-3150}$ and $L'_{n,w} + C_{I,50-2500}$, in addition to R'_w and $L'_{n,w}$. The symbol ($'$) accompanying the descriptors means it was extracted through on site measurements being made. Its absence denotes the measurements in question having been performed in a laboratory environment.

The current international descriptors for evaluating airborne and impact sound insulation on the basis of measurements carried out are defined in the standards ISO 717-1:1996 [18] and ISO 717-2:1996 [19], respectively, which also include the low frequency bands of 50, 63 and 80 Hz in the rating procedures as spectrum-adaptation terms to be added to the single-number quantities when this is required in the country that is applying.

Table 2.1: Sound classes proposed in SS-2526 in terms of the minimal sound insulation from spaces outside the dwelling to spaces inside the dwelling. There are a few exceptions, however, depending of the type of the space outside the dwelling. For further information, see [16].

Sound Class	A [dB]	B [dB]	C [dB]	D [dB]
Air-borne sound insulation ($R'_w + C_{50-3150}$)	61	57	53	49
Impact sound insulation ($L'_{n,w} + C_{I,50-2500}$)	48	52	56	60

There is also a series of European prediction standards (EN-12354 [20]) for calculation of the total resulting airborne and impact sound insulation. These standards predict the acoustic performance of buildings from the standpoint of the performance of individual building elements. These standards make use of a simplified statistical energy analysis (SEA) model for predicting the apparent sound reduction index between two rooms, the contributions of the flanking paths being accounted for in this. There is interest worldwide in applying the EN-12354 model to lightweight building elements. Unfortunately, the

existing prediction models for sound transmission appear only to be only reliable for monolithic weakly-damped building elements made of concrete or brickwork [21]. Lightweight elements typically do not meet the requirements of an SEA subsystem (at low frequencies the prediction uncertainty of SEA-like models increases due to the lower modal density found there). Accordingly, applying the EN-12354 model to these elements may result in inaccurate predictions. Several investigations have led to corrections factors for applying these prediction standards to lightweight buildings having been developed as part of the work of the COST Action FP0702 [2], yet there is a long way to go before the calculation-prediction model can be expected to be accurate and reliable enough.

Regarding vibration requirements, the Eurocode standards [22] provide common structural design rules for the design of whole structures and of component products. The Eurocodes are a set of harmonised technical rules developed by the European Committee for Standardisation for the structural design of construction work carried out within the European Union. Specifically, the design of timber structures is dealt with in EC5-1-1 and in the serviceability limit state design guidelines regarding floor-vibration performance. Calculations in accordance with Eurocode 5, as well as further explanation of the procedures in question are to be found in the appended **Paper A**. There is still concern nowadays, however, regarding the guidelines proposed in [22], due to the complexity that vibration issues involve. Thus, it is stated in [23], for example, that the current EC5-1-1 design criteria do not adequately address issues concerning the dynamic response of timber flooring systems and associated vibrational problems. Reconsideration of the design criteria is thus called for.

Note that in the course of the present work, no standard measurements were performed and reported on in the publications that are appended. Instead of studying directly the sound pressure levels involved, the low frequency vibrations that caused the sound pressure were either measured by means of accelerometers (**Paper A**) or were evaluated from the FE models (**Paper C**). In line with this, it was shown in [12] that assessing vibrations by means of accelerometers provides information regarding the major flanking paths at different frequencies. Use of them is assumed to be a reliable way of studying low frequency sounds.

2.4.2 Subjective ratings

Results of the evaluation procedures currently employed often fail to correlate adequately measurements of impact sound insulation with acoustic quality as perceived by residents, and with complaints of impact noise produced, despite the building having been classified as fulfiling higher than the minimum (Swedish) demands according to the standardised assessment procedure employed [3].

The lowest frequency of analysis in the standards for acoustically approved buildings in Sweden is 50 Hz. Since a great part of the vibration energy of a floor is contained in the first few modes (up to approximately 20 Hz), these are believed to be the vibrations that cause most of the vibration annoyance, yet since such low frequencies are outside the scope of the standards, they are not accounted for in the single number descriptors contained in the standards. Reformulation of the standards and the evaluation methods employed is thus needed.

In line with this, the Swedish project AkuLite (which provided funding supporting work on the present dissertation) is about to publish final reports (cf. [24] amongst others) that highlight the importance of extending the frequency range of analysis down to 20 Hz, due to discrepancies found in statistical analysis carried out between subjective ratings provided by questionnaires and single number quantities obtained by following international standards. These reports show that the correlations between objective and subjective data increase markedly if low frequencies (as assessed by means of accelerometers or sound level meters) are included. The lower the lowest frequency included is, the higher the correlation is, in principle, between objective and subjective measurements.

2.5 Challenges

Nordic and international standardisation groups and the Swedish Standards Organisation have found problems in the following areas to be in need of further work [25]:

- The acoustic requirements for buildings are often based on various judgements of highly uncertain character and on doubtful background data.
- New products and combinations of these are often approved on the basis of principles of evaluation that are out of date and should be reconsidered.
- There is thus a need of field studies in greater depth so as to enable the principles of evaluation to be better adapted to modern housing design and modern building structures.

Although the number of investigations concerned with vibrations in lightweight buildings has increased in the recent years, paving the way for providing greater acoustic comfort for their inhabitants, there is still a long way to go before the performance of lightweight buildings can be adequately predicted and be approved amid occupants of these buildings.

As already indicated, results of the evaluation procedures currently employed often fail to correlate closely enough measured impact sound insulation with perceived acoustic quality, in particular due to increased low frequency noise not being adequately addressed by the single number quantities employed. Thus, finding sources having a spectrum close to that of the human footfall is of crucial importance for achieving the aim of the approval of buildings for residence being linked with the human comfort they provide. These sources should then be the basis for the standardised evaluation and measurement methods employed. The acoustic performance of the buildings should be measured uniformly, regardless of which laboratory the measurement or calculations were carried out at, the latter being an important demand recently pointed out from the sector of the building industry to the research community. A major problem to be dealt with here is the variability that can be noted in the assessment of theoretically identical buildings, leading to highly unpredictable results in many cases, and sometimes to unnecessarily expensive sound insulation that leads to higher rents. According to [3], there is also the need of more adequate knowledge of the causes of the extreme variability often found in

the sound insulation in buildings, so that measures can be taken to avoid it, improved it and reliably predict it. Various factors to be tackled are:

- Problems of measurement repeatability.
- The effects of different interior solutions involving large and small rooms, open plan spaces, and the like.
- Production variations: tolerances, workmanship, installations, materials, etc.
- The positioning of different rooms and units within a building: floors, the preload of rooms above, the effects of adjacent constructions, etc.
- Transportation of building units, especially of rooms and of flat modules, in order to avoid, for example, damages in the building units.

The importance of wooden buildings in Sweden is highlighted in a governmental publication from 2004 [1], where several challenges for strengthening wood as a competitive material in all types of buildings in Sweden, eventually Europe, were pointed out. Specifically, the following objectives for newly produced construction works were accentuated for the following 10-15 years:

- The share of annually produced apartment buildings with wooden frames be at least 30 %.
- Wood as a construction material should be considered as an alternative for public buildings from an economic and environmental point of view.
- At least 25 % of annually constructed bridges should be built using wood of some sort.

Gaining knowledge of variability of these different types can contribute to the further development of theoretical models for prediction and of prediction tools. These should all stem from knowledge gained through research within the field. If the development of truly reliable prediction tools and evaluation methods can be achieved, building in wood can provide enormous advantages, both pragmatically and aesthetically.

3 Floor vibrations

In broad strokes, floor vibrations can be divided into two types [26]: local deflection and resonant vibration. Local deflection, only experienced by the active person or another person relatively close to the former, appears in the direct vicinity of the occupant when an induced force is applied, its value increasing with decreasing stiffness. It is typical of lightweight constructions. Resonant vibration, in turn, generally occurs as a result of a lack of damping, force at hand generating a long-lasting vibration of the floor, its magnitude being larger the lower the damping is. All in all, vibration problems can be broken down to three main factors: the source, the path and the receiver [11]. The parameters that affect the dynamic behaviour of a floor are the following [26]:

- Stiffness, which determines the springiness of the floor. The higher it is the better, since the deflection due to a force that is applied is lower. Alhough increasing the stiffness of the floor might seem preferable, this would go counter to the main advantages of lightweight buildings, those of their being light and cheap. An increase in stiffness could only be achieved by either increasing the existing physical dimensions or by making the material of which is composed stronger, which would mean an increase in mass density.

- Damping, an increase in it being beneficial. Although any given material has its own internal damping, it is not straightforward and easy to assess the damping of a structure, due to the joints, couplings, screws etc. present in it. Damping will be dealt with further in Section 3.2.5.

- Mass: low mass being economically desirable, allowing supporting walls to be slimmer. Regarding floor vibrations, however, it can be stated as a rule of thumb that the greater the mass, the better it is, since the response of the floor to an impact force is lower in amplitude. Further analyses would be nevertheless needed when adding mass, as the fundamental frequency of the floor would change, its being then likely to be excited by other different types of loads present.

- Fundamental frequency, which is a function of the mass, the stiffness and the damping. Human response to floor vibrations is often assumed to be a result of the first natural frequency (referred here to as fundamental frequency), as it will be taken up in Section 3.1.

3.1 Literature review

The acceptance of vibrations in buildings is a really complicated issue due to the numerous factors affecting the perception of those vibrations; see Figure 3.1. Many design criteria stemming from research on human response to vibrations have been proposed, still complains from inhabitants arising in lightweight timber buildings. A summary of research in the area of human response to floor vibrations, as well as a compilation of the serviceability criteria found applicable to timber constructions nowadays will be presented here first. This literature review is also included in the appended **Paper A**.

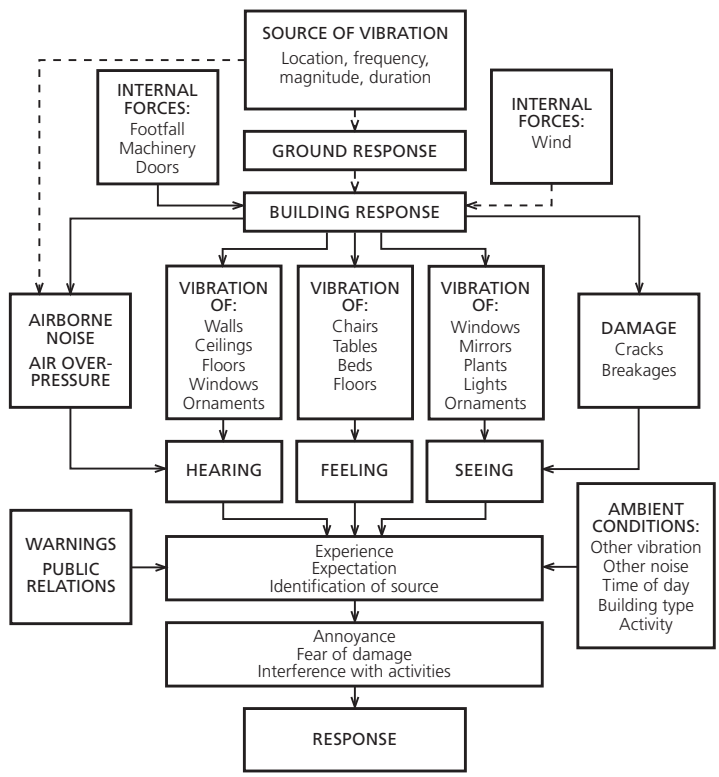

Figure 3.1: Factors affecting the acceptability of building vibrations, [11].

3.1.1 Factors affecting human response to floor vibrations

Extensive research in the area of human perception of whole-body vibration, and human response to such vibration has been carried out. According to [27], human response to whole-body vibration can be divided into five categories: (i) degraded comfort, (ii) interference with activities, (iii) impaired health, (iv) occurrence of motion sickness and (v) perception of low-magnitude vibration. In the case of vibration in buildings, human response to it can be said to consist of annoyance and of a reduction in comfort.

Due to the complexity, sensitivity and variability of the human body, there are no clearly stated limits for acceptable vibration levels that are used in buildings nowadays but simply certain guidelines that have been developed [27]. The response of a human to vibration not only depends upon a large number of variables but is also highly subjective. For instance, people differ in how they react in response to what are nominally the same vibration levels (reflecting inter-subject differences in this respect), and a given person may respond differently to a particular level or type of vibration under differing circumstances (intra-subject differences) [28].

More specifically, one can say that human response to whole-body vibration depends both on psychological and on physiological variables. Thus, characteristics of the vibration, i.e. its amplitude, frequency, duration and direction, may very well influence the perception of it as much as age, gender, posture, fitness, type of activity being performed, attitude, expectations, context or motivation do [28].

Moreover, if humans are subjected to vibrations for too long a time, there is the risk of health problems being involved. According to [29], long-term high-intensity whole-body vibrations can result in an increased health risk for the lumbar spine and the connected nervous system of the segments affected. The digestive system, the genital/urinary system, and the female reproductive organs are also assumed to be affected, although the probability of this can be regarded as being lower. Such effects have only been investigated in the case of seated persons, no corresponding research having been carried out on standing or recumbent persons thus far. It has also been found that it normally takes several years for the health changes involved to occur.

3.1.2 Criteria for human perception of vibrations

Pioneering work in the field of human perception of structural vibrations is that of Reiher and Meister [30], in which human sensitivity to vibrations was investigated. Ten test persons were exposed to vertical and to horizontal steady-state vibrations while standing or lying on a platform, the frequencies ranging from 5 to 100 Hz and the amplitudes from 0.01 mm to 10 mm. Subjects' reactions were classified and were labelled in categories extending from "barely perceptible" to "intolerable". The perception threshold was reached at a constant value of the product of displacement amplitude and frequency, and thus at a constant vibration velocity. A vibration perception scale was proposed on the basis of these findings. The scale was eventually modified in [31] to make it applicable as well to vibrations due to walking impact, its being observed that for transient vibrations the main factor affecting human beings was that of damping, variations in amplitude and in frequency having little effect. It was suggested that if the amplitude scale is increased by a factor of ten the original Reiher-Meister scale can be seen as applicable to floor systems having less than 5 % critical damping. The resulting modified Reiher-Meister scale is shown in Figure 3.2. In [32], transient vibrations from a single-frequency component were investigated. A number of 40 persons standing in a room with a floor 4.9×8.5 m^2 in size were exposed to vertical vibrations created by a shaker of varying frequency, peak amplitude and damping. The vibrations involved (including both damped and undamped ones) were then rated on a 1-5 scale extending from "imperceptible" to "severe". Statistical analyses were carried out for identifying possible relationships between the response rate

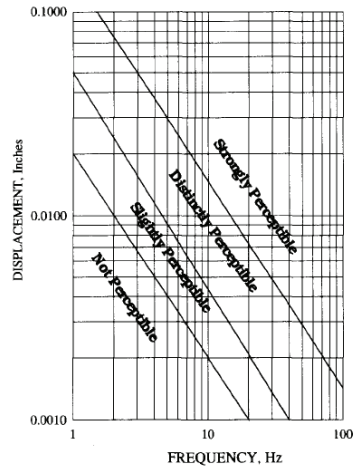

Figure 3.2: Modified Reiher-Meister scale [31].

and various parameters. For damped vibrations, the following equation was proposed as predicting the response rate R_{WP}:

$$R_{WP} = 5.08 \left(\frac{f u_{max}}{\zeta^{0.217}} \right)^{0.265}, \tag{3.1}$$

where f is the frequency, u_{max} the peak displacement in inches and ζ the damping ratio. The following equation was proposed for predicting the response to undamped vibrations:

$$R_{WP} = 6.82 \left(f u_{max} \right)^{0.24}, \tag{3.2}$$

values for R_{WP} ranging from 1 to 5, labelled respectively as following: 1 "imperceptible", 2 "barely perceptible", 3 "distinctly perceptible", 4 "strongly perceptible" and 5 "severe vibration". The investigations performed also showed the product of the frequency and the displacement to be constant and the transient vibrations of a given frequency and peak displacement to become progressively less perceptible as the damping was increased.

A vibration criterion for the degree of acceleration and damping appropriate for quiet human occupancies such as residential buildings and offices was developed in [33]. As the damping increases, the steady-state response produced by walking becomes a series of transient responses, resulting in a less significant response. A human perception scale for the degree of damping required was presented as a function of the product of initial displacement and the frequency in [34], the same parameters as in [32] being used.

In [35], springiness and vibrations in timber floors and steel floors were investigated in a laboratory environment with use of subjective rating tests, 15 persons taking part. A rating of different timber test floors in comparison with a reference floor was also carried out. The tests on laboratory timber floors showed both a reduction in the length of the span and the existence of a ceiling to have a positive effect in terms of subjective judgements of the level of vibration, but the use of glue to fix the deck to the joists to

have little effect in this respect. It was also pointed out that the spacing between adjacent natural frequencies should be one of at least 5 Hz in order to prevent annoyance.

Field tests were carried out and vibration ratings were collected in [36]. Human perception here was found to not be correlated with either peak acceleration, filtered peak acceleration, RMS acceleration, the fundamental frequency or the product of the fundamental frequency and peak acceleration. In [37], it was reported that in terms of the subjective assessments made, none of the structural modifications investigated there except for those of a reduction in joist depth and the introduction of rubber inserts, resulted in any improvement in dynamic serviceability.

There are several different standards concerning human perception of structural vibrations that are or have been employed, the three most prominent ones being the following.

ISO 2631-1:1997

The International Standard ISO 2631-1:1997 [29], (*Vibration and shock – Evaluation of human exposure to whole-body vibration – Part 1: General requirements*) provides guidelines on how to perform vibration measurements, what to report, and how to evaluate the results obtained, these guidelines being used to standardise reporting and to simplify comparisons. Although this standard is provided with three annexes containing suggestions, as well as current information on the possible effects of vibrations on health, comfort and perception, and motion sickness, it does not present any vibration exposure limits for whole-body vibrations.

ISO 2631-2:1989

This older version of the standard just referred to [38] has been cancelled and been replaced with the newer edition [39]. In the earlier version, tentative vibration serviceability limits were given in the form of base curves for the vibration magnitudes that cause approximately the same degree of annoyance. The base curves were to be used together with multiplication factors, taking into consideration the time of day and the type of occupied space involved (office, residential, etc.). In the latest edition of the standard, these base curves have been withdrawn, the reason given being the following: "Guidance values above which adverse comments due to building vibration could occur are not included anymore since their possible range is too widespread to be reproduced in an International Standard" [39].

ISO 2631-2:2003

The second part of the ISO standard 2631 [39] (*Mechanical vibration and shock – Evaluation of human exposure to whole-body vibration – Part 2: Vibration in buildings – 1 Hz to 80 Hz –*) is applicable to the evaluation of vibrations in buildings with respect to matters of comfort and the annoyance of occupants. No limit values are stated, due to the considerable differences in the research findings concerning this that have been reported. Instead, methods of measurement and evaluation concerned with whole-body vibrations in buildings have been suggested in order to encourage a uniform approach to the collection of data. A frequency weighting, W_m, (coincident with the W_k as defined

in [29]) is recommended for use, irrespective of the measurement posture of an occupant (its being sufficient to simply consider vibrations in the direction having the highest frequency-weighted magnitude).

In [26], it was concluded that the frequency weighting of the ISO standard 2631-2 [39] and the overall weighted amplitude value obtained succeed well in describing the degree of annoyance felt regarding a single sinusoidal vibration, but that they are less accurate in regard to a vibratory signal involving only a limited number of discrete frequencies. To overcome these difficulties, a prediction model was developed in which both the overall weighted amplitude and the fundamental frequency are taken account of. This model, proposed in [26], is as follows:

Sinusoidal case:
$Annoyance = -1.26 + 0.39 \cdot weighted\ total\ amplitude$

Multiple Frequency case:
$Annoyance = -3.17 + 0.43 \cdot weighted\ total\ amplitude + 0.24 \cdot fundamental\ frequency$

Amplitude given in [mm/s^2] RMS, frequency in [Hz]
The frequency weighting: done according to ISO2631-2:2003

Interpretation:
if $Annoyance \leq 4$, the floor is acceptable
if $Annoyance > 4$, the floor is unacceptable

3.1.3 Design criteria to minimise annoying vibrations

Various design criteria for minimising annoying vibrations in floor systems exist in the literature, hereunder gathered and classified in accordance with the parameters they use.

Criteria-limiting point-load deflections

The earliest attempts to provide some degree of control over vibration problems in timber floors involved limiting the static deflection of joists under uniformly distributed load conditions so as to ensure the floor stiffness being sufficient [40]. For instance, the traditional $L/360$ deflection limit (L being the span of the floor) was in broad use for a considerable period of time. A numerical investigation performed in [41] led to an improved stiffness-based criterion for floor vibration serviceability being developed, one that limited the midspan deflection of the floor system to 1 mm for a point load of 1 kN, independent of the span. In [42], another stiffness-based criterion, one incorporated into the National Building Code of Canada and requiring that the static deflection produced by a 1 kN load at midspan be limited to $8.0/L^{1.3}$, and also that it not be greater than 2 mm for spans ranging from 3 to 6 m in length, was employed.

If the same traditional design criteria for deflection, making use of static response parameters, are employed, vibration serviceability is not guaranteed [43]. As a consequence, research aimed at gaining an understanding of the factors that affect human response to floor vibrations has increased ever since and has paved the way for the development of design approaches for studying the dynamic parameters involved.

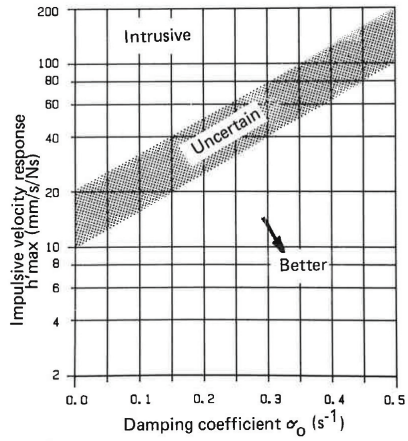

Figure 3.3: A preliminary proposal for classifying the response of a floor construction in terms of impact load [44].

Criteria for limiting-point load deflection, for velocity due to unit impulse, and for RMS velocity

Criteria taking account of several different modes of vibration as well as of modal damping, of limiting-point load deflection, of the velocity due to a unit impulse and of the RMS velocity, can be found in [35] and [44]. The development of these criteria was based on measurements of floors and subjective evaluation of their vibration performance, mainly in single-family houses. Three types of limits are to be noted: (i) the floor system needs to have a flexibility of no more than 1.5 mm/kN in the case of a concentrated load located at midspan; (ii) for floors with a fundamental frequency greater than one of 8 Hz, the values of the velocity due to a unit impulse (h'_{max}) and of a damping coefficient ($\sigma_0 = f_1\zeta$ [Hz]) need to fall within a given region of the graph $h'_{max} = f(\sigma_0)$ in order to ensure that the performance achieved will be acceptable (cf. Figure 3.3); and (iii) the root-mean-square velocity for steady-state vibration needs to be less than tabulated values as given for acceptable floor systems. Actually, the use of such tabulated values has never been proposed, the recommendation being that one instead compare the root-mean-square velocity with corresponding values for similar floor constructions that show acceptable vibration performance. Yet values of this sort have never been available either. Rather, the first two criteria, namely (i) and (ii), have provided the basis for the vibration serviceability criteria in Eurocode 5 [22].

Criteria limiting the fundamental frequency and the frequency-weighted RMS acceleration

The design criterion developed in [45] requires that the fundamental frequency of a floor be greater than 8 Hz, and that the frequency-weighted root-mean-square acceleration obtained during the first second of vibration be less than 0.45 m/s^2 when loaded by a specific impulse. The first part of the criterion is determined by the stiffness and the mass

of the floor system, whereas the second part is a function of the damping that takes place. Theoretically, therefore, it is necessary that the designer estimate the damping of the floor structure at the time that designing is carried out. Since doing this is virtually impossible, however, due to the damping of the timber floors varying considerably depending upon the construction type selected, and the techniques and workmanship employed, methods requiring that damping calculations be performed may not be practical for design engineers to utilise.

Criteria limiting the fundamental frequency

The investigation performed in [43] suggests that if the stiffness of a floor is sufficient to maintain the fundamental frequency of the floor system at a level above that of 15 Hz in the case of unoccupied floors, and above 14 Hz in the case of occupied floors, the furniture or whatever and the persons involved being included, acceptable levels of vibration will be obtained.

The work presented in [26] is in opposition to the latter reference, as it shows that human perception of vibration is strongly affected by the composition of the vibration signal in terms of the number of frequency components involved and their mutual amplitude relationships. Thus, in line with [26], it can be argued that the multiple natural frequencies inherent in a floor need to be taken account of in determining the design rules to be followed. This is in agreement with the criteria for design rules proposed in [35] and [46] (in which it is suggested that up to the 8^{th} harmonic should be taken account of), its contradicting many presently used floor design criteria that often rely on the fundamental frequency alone.

Criteria limiting the fundamental frequency and point-load deflection

In [47], rules for the design of floors with "high-" and with "low-" requirements and those with "no-" requirements, resulting in the fundamental frequency being maintained at above a level of 8 and of 6 Hz for "high-" and for "low-" requirement floors, respectively, were proposed. A stiffness criterion is also specified there (such that the deflection due to a static load of 2 kN is to be less than the limit value w_{limit}, the size of which depends upon the requirements that apply to the floor in question).

Suggested criteria and limiting values for the classifying of floors into five different classes (A-E) are proposed in [48]. It was found there that the point load deflection and the fundamental frequency are two of the best indicators of vibration performance in the case of lightweight floors.

A criteria-limiting combination of parameters

The approaches just mentioned are semi-empirical in nature, their providing satisfactory solutions for the particular categories of floors for which the methods were developed. None of them appear to work entirely satisfactorily when applied to other types of floors, however [40]. In [49], a new design method consisting of a vibration-controlled criterion and a calculation method for determining the criterion parameters were developed. The

design criterion states that if the ratio (fundamental frequency)/(1 kN deflection)$^{0.44}$ of an unoccupied floor is larger than 18.7, the floor is most likely satisfactory for the occupants.

In [50], the ratio of the peak acceleration achieved by walking, to the force of gravity, is used as a design guideline, its value depending upon the use to which the building is to be put. Its value given as

$$\frac{a_p}{g} = \frac{P_0 e^{-0.35 f_n}}{\beta W} \leq \frac{a_0}{g}, \tag{3.3}$$

where P_0 is a constant applied force (0.29 kN for floors and 0.41 kN for footbridges), f_n the fundamental frequency of the floor structure, β the damping ratio, W the floor's effective weight, a_0/g the tabulated acceleration limit and a_p/g the estimated peak acceleration (in units of g).

Eurocode 5

The methods presented in [35] and [44] served as the basis for the vibrational serviceability criteria developed in Eurocode 5 [22]. The Eurocodes are a set of harmonised technical rules developed by the European Committee for Standardisation for the structural design of construction work carried out within the European Union.

Specifically, the design of timber structures is dealt with in EC5-1-1 and in the serviceability limit state design guidelines regarding floor-vibration performance. The design criteria are applicable to residential wood-based plate-type floors with a fundamental frequency greater than 8 Hz, in which the human sensitivity is related to the effects of the vibration amplitude and velocity caused by the dynamic footfall forces involved [51]. If the fundamental frequency of the floor is lower than this, a special investigation of the floor in question is needed.

The effects are divided into low- and high-frequency ones. The low frequency contributions that come from step actions are dealt with by a static criterion that limits the deflection caused by a static point load applied at the point on the floor that results in a maximum vertical deflection. The high-frequency effect is a consequence of the heel impact actions that occur, its being taken account of by use of a dynamic criterion that limits the maximum initial value of the vertical floor vibration velocity caused by an ideal unit-impulse load. Three points must thus be checked on:

- The fundamental frequency of the floor, f_1, should be at least 8 Hz in order for the floor to be regarded as a high-frequency one (otherwise a special investigation of it is needed), the requirement thus being that

$$f_1 \geq 8 \text{ Hz}. \tag{3.4}$$

- The maximum instantaneous vertical deflection, w, due to a single force should be less than a deflection of a varying size a (see Figure 3.4 regarding a):

$$\frac{w}{F} \leq a \text{ [mm/kN]}. \tag{3.5}$$

- The maximum initial value of the vertical floor vibration velocity, v, produced by an impulse of 1 [N·s], applied at the point on the floor giving the maximum response

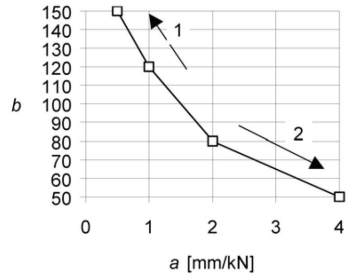

Figure 3.4: Recommended range of the relationship between a and b: 1 better performance, 2 poorer performance. Each country is able state values for a and b in their National Annex [22].

– where components above 40 Hz can be disregarded – should verify the inequality (see the dimension b in Figure 3.4):

$$v \leq b^{(f_1\zeta-1)} \text{ [m/Ns}^2\text{]}. \tag{3.6}$$

where F is a vertical concentrated static force applied to any point on the floor, taking account of the load distribution, and ζ is the modal damping ratio (a value of 1 % is recommended in [22] unless some other value has been found to be more appropriate).

Design tools

Various numerical methods, the FE method, for example, are sometimes used as design tools nowadays for checking on the serviceability of floors of different types, in line with the development of commercial solutions in the form of different softwares. Often highly versatile, they can enable floors to be very much improved and various criteria described above to be verified during the design phase. Examples of the use of such tools are to be found in [52, 53, 23].

3.2 Structural dynamics: Governing theory

Vibrations normally appear in systems subjected to time-varying forces, such as produced by people walking, jumping or running, which is often the case in dwellings. When analysing and dealing with such dynamic events, the magnitude of the force may not be as important as its frequency. Thus, it is of utmost importance to describe and analyse a vibratory signal both in the time domain (a magnitude being plotted versus the time), or in the frequency domain (a magnitude being plotted versus the frequency); see Figure 3.5. Fourier analysis methods, such as the Fast Fourier Transform (FFT), can readily make the shift from one domain to the other.

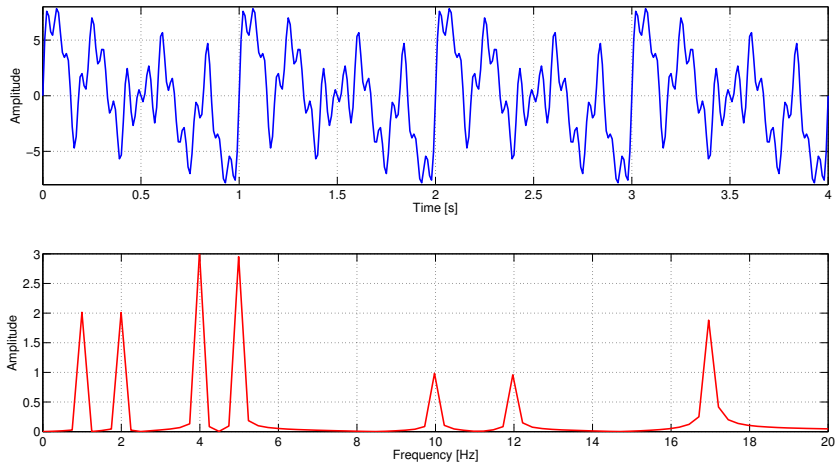

Figure 3.5: Time domain signal (above) and correspondent frequency content (below).

In studying a structure, a modelling simplification can be made by discretising it, when possible. The degrees of freedom (DOF) involved can be defined as the number of independent displacements required to define the exact position of the system at any given time. Hence, it is straightforward to make the distinction between discrete systems, in which a finite number of DOFs is needed to describe completely, and continuous systems, for which an infinite number of DOFs are needed for defining their position at any given time. Discrete systems lead to a system of ordinary differential equations, whereas continuous systems yield a system of differential equations with partial derivatives, often solved by use of the FE method techniques, as it will be taken up further in Chapter 6. The theory presented hereafter is summarised from the account of it found in [54, 55, 12].

3.2.1 Single-degree-of-freedom systems

The easiest way to describe a dynamic system, such as a floor subjected to human walking, for example, is by use of a single-degree-of-freedom (SDOF) system. The classical SDOF system is a mass-spring-damper system, which can be seen as representing a simplified floor structure. Considering the spring and the damper to both be massless, the mass to be a lumped mass and all the motions to be in the vertical direction, as shown in Figure 3.6, the force equilibrium equation given by Newton's second law of motion represents the differential equation that describes the motion of the system:

$$m\ddot{u}(t) + c\dot{u}(t) + ku(t) = f(t), \tag{3.7}$$

$f_s(t) = ku(t)$ being the elastic force, $f_d(t) = c\dot{u}(t)$ the damping force (related to the velocity of the structure), c the viscous damping coefficient given in [N·s/m], $f(t)$ the time-dependent external force applied, $f_I(t) = m\ddot{u}(t)$ the inertial force of the mass, and

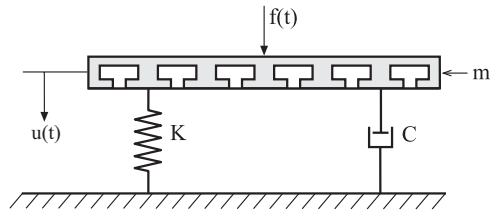

Figure 3.6: Mass-spring-damper SDOF system.

u the only DOF necessary to describe the system. The displacements of the system, $u(t)$, can be easily obtained by solving Equation (3.7), supplementing it with the initial conditions that are involved.

Undamped SDOF system

Although real structures always having damping effects, the solution to the undamped system has an important value theoretically. The solution to the undamped ($c = 0$) equation

$$m\ddot{u}(t) + ku(t) = f(t), \tag{3.8}$$

consists in a particular solution in which the system is subjected to harmonic loading, $u_p(t)$, and in a homogeneous solution in which no load is involved, $u_h(t)$, i.e.

$$u(t) = u_p(t) + u_h(t). \tag{3.9}$$

- The particular solution is arrived at through solving the equation

$$m\ddot{u}_p(t) + ku_p(t) = f_0 \cos(\omega t). \tag{3.10}$$

  The response of a system subjected to a harmonic force is also harmonic, and because of linearity and superposition, the responses is the sum of the responses of the harmonic components of the original forces

$$u_p(t) = U_{p,ud} \cos(\omega t) = \frac{u_s}{1 - \left(\frac{\omega}{\omega_n}\right)^2} \cos(\omega t) = \frac{u_s}{1 - \beta^2} \cos(\omega t), \tag{3.11}$$

  $U_{p,ud}$ being the amplitude of the particular solution of the undamped SDOF system, obtained by inserting Equation (3.11) into Equation (3.10), $\beta = \omega/\omega_n$, $u_s = f_0/k$ being the static displacement and $\omega_n = \sqrt{k/m}$ the undamped natural frequency involved.

- The homogeneous part of the solution stems from solving

$$m\ddot{u}_h(t) + ku_h(t) = 0, \tag{3.12}$$

  the solution having the form

$$u_h(t) = A_1 \cos(\omega_n t) + B_1 \sin(\omega_n t). \tag{3.13}$$

Hence, by use of Equations (3.11) and (3.13), Equation (3.9) can be rewritten as

$$u(t) = \frac{u_s}{1-\beta^2}\cos(\omega t) + A_1\cos(\omega_n t) + B_1\sin(\omega_n t). \tag{3.14}$$

The constants A_1 and B_1 are determined by the initial conditions, i.e. the initial displacement and velocity of the SDOF system. Note that if the excitation frequency ω coincides with one of the natural frequencies of the system, infinite displacements are obtained, i.e. resonance occurs; see Figure 3.9.

Damped SDOF system

The solution to the damped SDOF, stemming from Equation (3.7), is

$$m\ddot{u}(t) + c\dot{u}(t) + ku(t) = f_o\cos(\omega t), \tag{3.15}$$

being also composed of both a particular and a homogeneous solution; see Equation (3.9).

- The particular solution is given as

$$u_p(t) = U_{p,d}\cos(\omega t - \alpha), \tag{3.16}$$

$U_{p,d}$ being the amplitude of the particular solution of the damped SDOF system and $H(\omega)$ the amplitude response, both given as

$$U_{p,d}(\omega) = u_s\frac{1}{\sqrt{\left(1-\beta^2\right)^2 + \left(2\zeta\beta\right)^2}} = u_s H(\omega), \tag{3.17}$$

the phase response α being

$$\alpha(\omega) = \tan^{-1}\left(\frac{2\zeta\beta}{1-\beta^2}\right), \tag{3.18}$$

and ζ, the viscous damping ratio, being defined as

$$\zeta = \frac{c}{c_{cr}} = \frac{c}{2m\omega_n}. \tag{3.19}$$

The critical damping c_{cr} is defined as the lowest level of viscous damping, one in which the mass exhibits no oscillation when displaced from the equilibrium; ζ is dimensionless and is usually expressed as a percentage. A system is classified as underdamped if $\zeta < 1$, as critically damped if $\zeta = 1$, and as overdamped if $\zeta > 1$.

One can then define the frequency response function (FRF) as the complex non-dimensional relationship of a system's input to its output, i.e.

$$\text{FRF} = G(\omega) = H(\omega)e^{-i\alpha(\omega)}. \tag{3.20}$$

Some common FRFs that depend upon the input and the output considered are referenced to as follows: compliance (displacement/force), mobility (velocity/force), accelerance (acceleration/force), and mechanical impedance (applied force/velocity) [11].

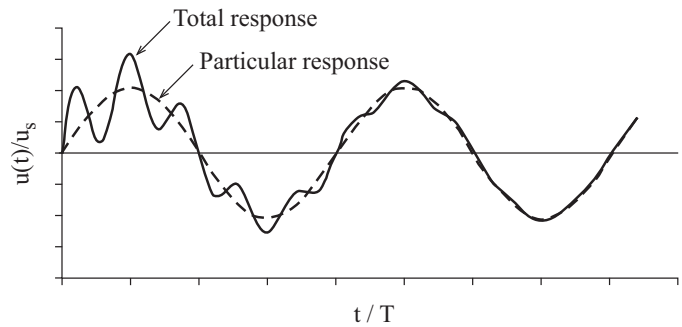

Figure 3.7: Example on the total response of a damped system subjected to a harmonic force, [54].

- The homogeneous part of the solution can be written as

$$u_h(t) = e^{-\zeta\omega_n t}\left(A_2\cos(\omega_D t) + B_2\sin(\omega_D t)\right), \tag{3.21}$$

  the damped natural frequency being given as

$$\omega_D = \omega_n\sqrt{1-\zeta^2}. \tag{3.22}$$

The total response thus becomes

$$u(t) = \frac{u_s}{\sqrt{\left(1-\beta^2\right)^2 + \left(2\zeta\beta\right)^2}}\cos(\omega t - \alpha) + e^{-\zeta\omega_n t}\left[A_2\cos(\omega_D t) + B_2\sin(\omega_D t)\right]. \tag{3.23}$$

The constants A_2 and B_2 are again determined by the initial conditions, i.e. the initial displacement and velocity of the damped SDOF. Note that the particular solution is controlled by the ratio β. Thus, if the loading frequency ω approaches the natural frequency of the system, ω_n, the solution is dominated by the damping in accordance with $U_{p,d} \approx u_s/(2\zeta)$ (cf. Section 3.2.3). The homogeneous solution, in turn, vanishes with increasing time, the system response being defined by just the particular solution after some time has passed, i.e. $u(t) \approx u_p(t)$; see Figure 3.7.

3.2.2 Multi-degree-of-freedom systems

More than one DOF is normally needed in fact to describe a structure completely. It is possible, however, to create an approximate model of it, referred to as multi-degree-of-freedom system (MDOF) with a finite number of DOFs by considering a finite number of massless elements and a finite number of node displacements, the mass being lumped on these nodes. Newton's second law of motion equation here yields the differential equation for an n-degree-of-freedom discrete system subjected to small displacements in generalised coordinates

$$\mathbf{M}\ddot{\mathbf{u}}(t) + \mathbf{C}\dot{\mathbf{u}}(t) + \mathbf{K}\mathbf{u}(t) = \mathbf{f}(t), \tag{3.24}$$

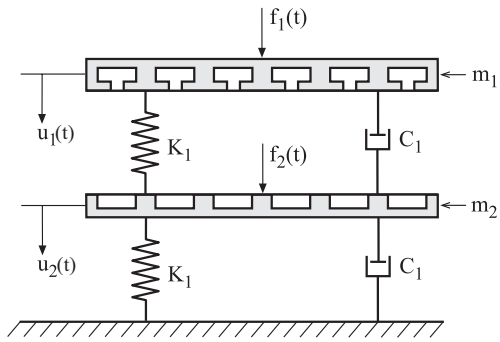

Figure 3.8: A two-DOF system: a mass-spring-damper MDOF system.

where n is the number of DOFs, $\mathbf{M}(n \times n)$ is the mass matrix (symmetric and positive-definite), $\mathbf{C}(n \times n)$ is the damping matrix, $\mathbf{K}(n \times n)$ is the stiffness matrix (symmetric and whether positive or semi-positive-definite), $\mathbf{f}(t)$ is the external load vector containing the dynamic external forces and having the dimensions $(n \times 1)$, $\mathbf{u}(t)$ being the displacement vector with the dimensions $(n \times 1)$. The load and the corresponding displacements can be expressed as a complex harmonic function

$$\begin{aligned} \mathbf{f} &= \hat{\mathbf{f}} e^{i\omega t}, \\ \mathbf{u} &= \hat{\mathbf{u}} e^{i\omega t}, \end{aligned} \tag{3.25}$$

$\hat{\mathbf{f}}$ and $\hat{\mathbf{u}}$ denoting the complex load and the displacement amplitude, respectively. Inserting Equation (3.25) into Equation (3.24) yields the equation of motion in the frequency domain

$$\mathbf{D}(\omega)\hat{\mathbf{u}} = \hat{\mathbf{f}}, \tag{3.26}$$

$\mathbf{D}(\omega)$ being the frequency-dependent dynamic stiffness matrix given as

$$\mathbf{D}(\omega) = -\omega^2\mathbf{M} + i\omega\mathbf{C} + \mathbf{K}. \tag{3.27}$$

3.2.3 Natural frequencies and modes

Modal analysis can be used to determine natural frequencies (those of free vibration) and the vibrational mode shapes (the spatial pattern of free vibration) of a structure. Taking Equation (3.24) and particularising it for the free vibrational case ($\mathbf{f} = \mathbf{0}$) in an undamped system ($\mathbf{C} = \mathbf{0}$), results in

$$\mathbf{M}\ddot{\mathbf{u}} + \mathbf{K}\mathbf{u} = \mathbf{0}, \tag{3.28}$$

with the initial conditions of $\mathbf{u}(0) = \mathbf{u}_0$ and $\dot{\mathbf{u}}(0) = \dot{\mathbf{u}}_0$. The free vibration of an undamped system in one of its vibration modes can be described as

$$\mathbf{u}(t) = q_n(t)\phi_n, \tag{3.29}$$

with the deflected shape ϕ_n being constant over time. The time variation of the displacements is described by the harmonic function

$$q_n(t) = A_n \cos(\omega_n t) + B_n \sin(\omega_n t), \tag{3.30}$$

A_n and B_n being constants of integration determined on the basis of the initial conditions. Combining Equations (3.29) and (3.30) yields

$$\mathbf{u}(t) = \phi_n \left(A_n \cos(\omega_n t) + B_n \sin(\omega_n t) \right), \tag{3.31}$$

ω_n and ϕ_n being unknowns. Substituting Equation (3.31) in (3.28)

$$\left[-\omega_n^2 \mathbf{M} \phi_n + \mathbf{K} \phi_n \right] q_n(t) = \mathbf{0}. \tag{3.32}$$

Equation (3.32) can be satisfied in two ways, either by the trivial solution $q_n(t) = 0$, meaning there to be no motion of the system, or through the natural frequencies ω_n and the modes of vibration ϕ_n satisfying the matrix eigenvalue problem

$$\left[\mathbf{K} - \omega_n^2 \mathbf{M} \right] \phi_n = 0, \tag{3.33}$$

the quantities to determine being ω_n and $\phi_n(t)$ (the matrices $\mathbf{K}$ and $\mathbf{M}$ being known). This system of equations is homogeneous, its coefficient matrix being singular. Hence, it has a solution different from the trivial zero (no-motion), one of

$$\left| \mathbf{K} - \omega_n^2 \mathbf{M} \right| = 0, \tag{3.34}$$

A polynomial of n order in ω_n^2 is obtained in expanding the determinant (called the characteristic equation or frequency equation), with n being the number of DOFs necessary to describe the system, its having n positive and real roots since both $\mathbf{M}$ and $\mathbf{K}$ are symmetric and positive-definite. The positive-definite property of $\mathbf{K}$ is assured for all structures supported in a way preventing rigid-body motion, and for $\mathbf{M}$ making sure that all masses are non-zero in each of the DOFs.

In solving the frequency equation, the n roots ω_n^2 determine the n natural frequencies ω_n ($n = 1, 2...n$) of vibration. When a natural frequency ω_n is known, Equation (3.33) can be solved to obtain the corresponding vector ϕ_n to within a multiplicative constant, referred to as the natural mode of vibration or the natural shape of vibration. Note that the eigenvalue problem does not fix the absolute amplitude vectors but simply the shape of the vector given by the relative displacements ϕ_j ($j = 1, 2, ...n$). As many eigenvectors (ϕ_n) as eigenvalues (ω_n^2) exist.

In summary, when a structure is disturbed from its static equilibrium position and is allowed to oscillate without any external dynamic excitation, it vibrates with certain frequencies ω_n, i.e. the natural frequencies. Associated with each natural frequency is a modal shape of the structure, which can be defined as the deformed shape of the structure at the specific frequency involved. A structure has an unlimited number of natural frequencies, these being a property of the structure, their in principle depending upon the mass and the stiffness as well as on their distribution. If the FE method is used to model the structure, it will have as many natural frequencies and corresponding mode shapes as there are DOFs. The natural frequencies of a damped system differ somewhat from the natural frequencies of the same system without damping. For lightly damped structures (which is normally the case for lightweight timber structures), however, the natural frequencies of the damped vibrations are approximately the same as the natural frequencies of the structure without damping [54]; see Equation (3.22).

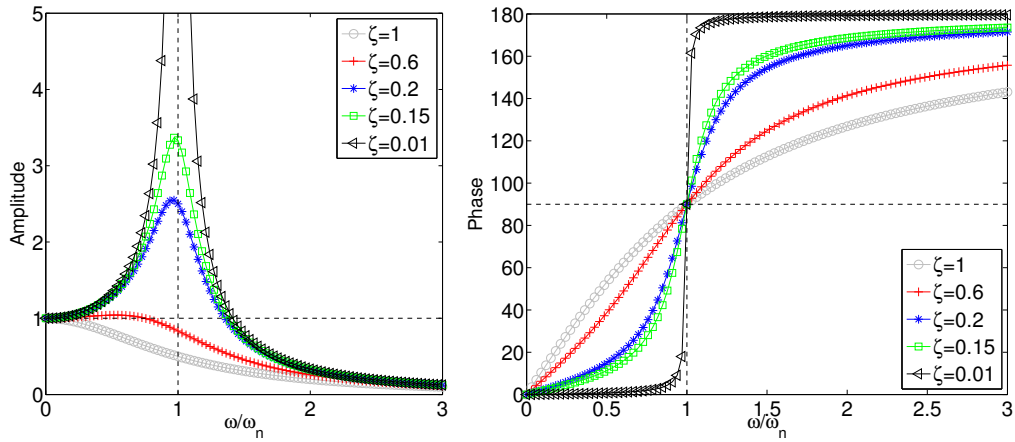

Figure 3.9: Amplitude response (left) and phase (right) of a resonant structure.

Resonance

If a structure is subjected to a dynamic force having a frequency close to one of its natural frequencies, the response can be strongly enhanced, increasing its amplitude. Both the amplitude and the acceleration become very high then. This phenomenon is that of resonance. Without the presence of any damping, this amplitude gradually increases towards infinity. Some damping is, however, always present in structures (joints, micro-cracks) preventing both this crescent and uncontrolled oscillations from occurring [54].

It is in fact the presence of resonances that annoys inhabitants, since the modes of vibration (especially the first few modes) contain almost all of the vibration energy of the floor, making it vibrate excessively. In Figure 3.9, the effects of various damping ratios on the resonant response in terms both of the amplitude response and the phase response are depicted. The amplitude response $H(\omega)$ shown on the vertical axis of the plot at the left is the ratio of the dynamic deformation to the static deformation, whereas the horizontal axis shows the ratio of the current excitation frequency to the natural frequency. As one can see, damping needs to be incorporated into the structure in order for resonant vibrations to be minimised.

3.2.4 Wave propagation

Bending waves are likely to be excited in bodies or structures where one or two dimensions are becoming small compared to the wavelength at an actual frequency, i.e. it is the dominant type of wave in construction elements (beams, plates). If the plates of the floor structure are sufficiently thin, the shear wave propagation can be ignored and the acoustic wave propagation that leads to sound radiation are only the bending waves since they create larger lateral displacements compared with in-plane waves (quasi-longitudinal and transversal shear waves). A propagating bending wave causes both rotation and lateral displacement of the beam or plate elements when impinging upon the boundaries

from a variety of angles. For more information about wave propagation see e.g. [56, 57].

In many areas of civil engineering, wood is not considered to be a linear elastic material. In earthquakes analyses, for example, strains can be of such magnitude that non-linearities cannot be neglected. In the case under study of human-made vibrations or serviceability loads, however, strains are usually at a level such that an assumption of linear elasticity applies. Damping, since it generally plays an important role in terms of dynamic responses that occur, is thus usually applied to the linear elastic material under such conditions.

3.2.5 Damping

In order to have a floor which is light in weight, provides open-space and yet is not that prone to vibration, damping needs to be incorporated into its makeup. Damping is, in general terms, the reduction of a vibration response due to the dissipation of energy. There is a lack of knowledge concerning the actual physical phenomena and mechanisms that cause damping, due to the fact that these properties of materials are not well established. Although certain analytical calculations to predict damping can be carried out, so as to be able to include it in the overall calculations, the damping generally needs to be determined on the basis of measurement data from similar existent structures or by carrying out new measurements on similar structures. This is due to the fact that damping properties cannot be calculated directly in a reliable and accurate way.

There are different methods for estimating damping via measurements either in the time domain or the frequency domain [11], namely logarithmic decrement, envelope fitting, phase plot diagrams, resonant amplification, half-power bandwidth, resonant energy loss per cycle, identification of damping parameters from the FRF, phase angle methods, laboratory visco-elastic methods, acoustic methods, and others. Once the damping parameters are extracted via measurements (or predicted via calculations), they can be described and be introduced into the models via either mathematical models (viscous and hysteric models), physical mechanisms (material, structural and fluid damping), or rheological models (Maxwell, Kelvin-Voigt, etc) [11].

A broader explanation of damping can be found in [11]. Different experimental methods for evaluating damping have been developed and also several analytical models for predicting damping have been derived. Albeit damping mechanisms are non-linear, linear damping models often suffice for small oscillations and slight damping, which are the types of cases under study in the present dissertation. Thereafter, a brief explanation account of the mathematical way of modelling damping used in **Papers C** and **Paper D** is provided.

Rayleigh damping

In **Paper C**, damping is modelled for the wooden parts as Rayleigh damping, which can be used for both transient and steady-state analyses. It is a procedure for determining the classical damping matrix by use of damping ratios. It assumes that both mass and stiffness are evenly distributed. In damping of this kind, it is considered that the damping matrix is a linear combination of the mass matrix and the stiffness matrix, in accordance

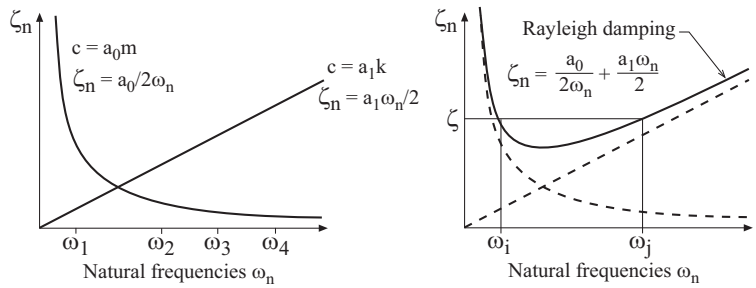

Figure 3.10: (Left) Mass damping and stiffness damping, (right) Rayleigh damping, [54].

with Equation (3.35); see Figure 3.10.

$$\mathbf{C} = a_o\mathbf{M} + a_1\mathbf{K}, \tag{3.35}$$

the damping ratio for the n^{th}-mode being given by

$$\zeta_n = \frac{a_0}{2}\frac{1}{\omega_n} + \frac{a_1}{2}\omega_n. \tag{3.36}$$

This damping ratio is shown to not be constant for all modes of vibration. The constants a_0 and a_1 are based on the damping of two natural frequencies of the structure.

$$a_0 = \zeta\frac{2\omega_i\omega_j}{\omega_i + \omega_j} \qquad\qquad a_1 = \zeta\frac{2}{\omega_i + \omega_j}, \tag{3.37}$$

ζ being constant for both modes of vibration, i and j, which normally conforms with experience.

In applying this procedure to a practical problem, i and j with specified damping ratios should be chosen so as to ensure that reasonable values for the damping ratios are obtained for all modes that contribute significantly to the response [54].

Although the assumption that the damping is proportional to the mass and to the stiffness matrices has no rigorous physical basis, it has been shown to provide good approximations. Also, in practice, the damping distribution is rarely known in sufficient detail to warrant use of any other, more complicated model [58]. In general, it is more important to damp the lower frequencies due to their being more difficult to damp, and also because the annoyance in lightweight buildings is mostly caused by low frequencies. As stated in the formula, a_0 is more important for lower modes, whereas a_1 is important mainly for the higher frequencies (the lower frequencies being damped by the mass, whereas the higher frequencies are damped by the stiffness).

A loss factor that takes account of propagating waves in steady-state analyses can be used to introduce rate-independent linear damping into the system. Accordingly, in **Paper C**, in the first instance and due to the lack of data on the material at that point, the structural damping of the blocks of elastomer was added in the form of a loss factor, defined [54] as

$$\eta = \frac{1}{2\pi}\frac{E_D}{E_{S_0}} = \frac{1}{2\pi}\frac{\pi c\omega u_o^2}{k\frac{u_0^2}{2}} = \frac{c\omega}{k}, \tag{3.38}$$

where in a steady-state the energy dissipated in the form of viscous damping in a given cycle of harmonic vibration is denoted as $E_D = \pi c \omega u_o^2$ and the strain energy as $E_{S_o} = k u_0^2/2$, c being the damping constant and u_o the amplitude of motion. The relationship between structural damping and Rayleigh damping in steady-state analyses can be expressed as

$$\eta = 2\zeta \frac{\omega}{\omega_n}, \tag{3.39}$$

and when the exciting frequency is equal to the eigenfrequency it can be expressed as

$$\eta = 2\zeta. \tag{3.40}$$

This approach of adding structural damping and employing a linear elastic material model was found in **Paper C** to not be accurate enough in the case of the elastomers. Accordingly, **Paper D** deals with extraction of the linear viscoelastic properties of the resilient strips used at the junctions of lightweight volume based wooden buildings.

Damping materials used in junctions of wooden buildings

Traditionally, in single-family timber houses, the different elements converging at junctions were connected by use of screws or nails, sometimes in combination with glue. The authorisation of the construction of multi-storey wooden buildings in Sweden led to the development of new construction techniques in line with requirements becoming more demanding. There are many methods used to decrease flanking transmission. These include the addition of extra wall plates with distances on the sending room or on the walls of the receiving room [59], hanging the ceiling on resilient channels [59], use of decoupled radiation-isolated walls [59], or of roller bearings [60], the addition of extra mass and damping to the floor through insertion of an extra board layer [61], use of elastic glue between boards [61], and utilisation of a floating floor [61].

Elastomers: A more recent method is that of placing construction elements (e.g. floor, walls, or the whole room) on top of a resilient layer – in the form of blocks, strips or a layer covering the entire surface. Although this technique is used in many types of lightweight constructions, use of it in volume based wooden buildings (cf. Section 2.2) has become more widespread. Elastomers have a behaviour that can be described as being both elastic and viscous, depending upon the frequency [12]. In using resilient strips in between parts of lightweight buildings, it is very important to design and select the appropriate stiffness for the material so that the degree of isolation desired can be achieved, since a load higher than the recommended one can compress the elastomer to such an extent that its isolating properties are greatly reduced. A more thorough review of the literature concerning work with insulators of this kind is presented in **Paper D**.

3.2.6 Linear viscoelastic materials

In **Paper C** it is argued that efforts should be made to provide blocks of elastomer with more reliable properties. **Paper D** deals then with the accurate assessment of the properties of an elastomer for their use as input to FE software. More specifically,

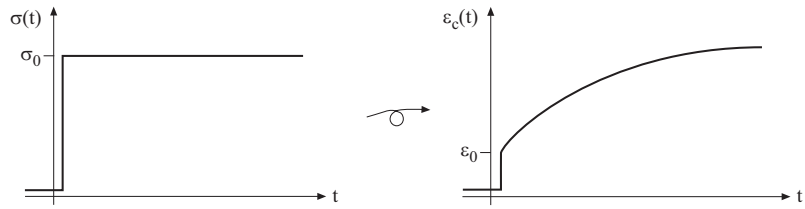

Figure 3.11: Creep behaviour.

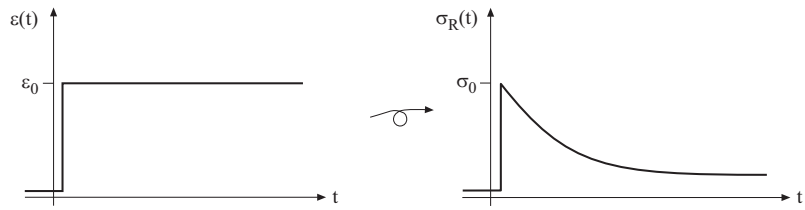

Figure 3.12: Relaxation behaviour.

the linear viscoelastic frequency-dependent properties of elastomers were assessed. The theoretical background of this can be briefly describes as follows.

Viscous materials resist shear flow and strain linear with time when a stress is applied. Elastic materials strain when stretched, their returning to their original state once the stress ceases. Viscoelastic materials possess both viscous and elastic properties, to varying degrees while undergoing deformations. The elastic properties are the result of bond stretching along crystallographic planes in an ordered solid, whereas the viscous behaviour comes from atoms or molecules diffusing within the material. The material properties vary over time or, in the frequency domain, vary with the frequency. Specifically, if the material is subjected to deformations or stresses sufficiently small so that its rheological properties do not depend upon the value of the deformation stress, the material behaves in a linear viscoelastic way, this being the simplest response of a viscoelastic material. Also, their effective stiffness depends upon the rate of application of the load.

Linear viscoelastic models include phenomena of creep and of relaxation. Creep is an increasing strain in response to step-stress loading (cf. Figure 3.11), whereas relaxation is a decrease in stress in response to a step-strain loading (cf. Figure 3.12). The notation henceforth is that used in [62]. For a linear viscoelastic material the creep compliance can be defined as $J_C(t) = \epsilon(t)/\sigma_0$, which is a characteristic function independent of the stress step σ_0, its being unique for a given linear viscoelastic material. In the same way, the relaxation modulus, independent of the strain step ϵ_0 and also specific for a linear viscoelastic material involved, is defined as $E_R(t) = \sigma(t)/\epsilon_0$. It can be shown that the instantaneous elasticity, i.e. the relationship between creep compliance and relaxation modulus at $t = 0$ equals $E_R(0) = 1/J_C(0)$.

The behaviour of a linear viscoelastic material can be defined on the basis of these single-step response functions. Linearity and Boltzmann's superposition principle lead to the constitutive equation defined as a convolution integral (also called the hereditary

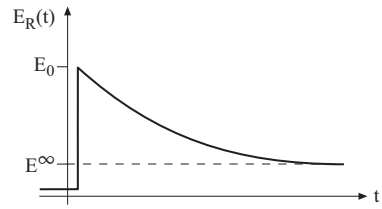

Figure 3.13: The relaxation modulus of a viscoelastic solid, E_0 being the instantaneous modulus and $E\infty$ the long-term modulus.

integral). The hereditary integral indicates that the internal stresses of a viscoelastic material are not dependent on the instantaneous deformation alone, but are also depend upon the past history of deformation. The stress response corresponding to any given strain history (and vice versa) can be obtained from this integral. The constitutive model is defined by the relaxation modulus, or for the inverse relation, the creep compliance as shown in Equations (3.41) and (3.42).

$$\sigma(t) = \int_{-\infty}^{t} E_R(t-\tau)\frac{d\epsilon}{d\tau}d\tau, \tag{3.41}$$

$$\epsilon(t) = \int_{-\infty}^{t} J_C(t-\tau)\frac{d\sigma}{d\tau}d\tau, \tag{3.42}$$

where t is the time, $\sigma(t)$ the stress, $\epsilon(t)$ the strain, and $E_R(t)$ and $J_C(t)$ denoting the relaxation and creep functions. Note too that elastomers are solid materials, so that it is required that the creep response be limited, and that the relaxation limit differs from zero, as shown in Figure 3.13. An example of a relaxation process can be obtained by assuming the following simple exponential law, in which t_r is the relaxation time, according to

$$E_R(t) = E\infty + (E_0 - E\infty)e^{-t/t_r}. \tag{3.43}$$

The response of linear viscoelastic materials to stationary sinusoidal strain history is of interest in the application under study, since steady-state dynamic analyses when simulating building structures are often carried out. When elastic materials are exposed to this kind of excitations, the stress and the strain involved are in phase, so that the response of the one caused by the other is immediate. In purely viscous materials, strain lags stress by a 90 degree phase lag. Viscoelastic materials exhibit a behaviour that is somewhere in between the two types of behaviours just described, their presenting some lag in relation to strain. Thus, the stress corresponding to a harmonic strain can be expressed in terms of a complex modulus. The constitutive relation (3.41) will be used for determining an expression for the complex modulus. Let a sinusoidal strain in complex notation be

$$\epsilon^* = \epsilon_0 e^{i\omega t} = \epsilon_0(\cos(\omega t) + i\sin(\omega t)). \tag{3.44}$$

Through carrying out certain mathematical manipulations of a sort shown in [62], for example, it can be shown that the hereditary integral in Equation (3.41) can be replaced by

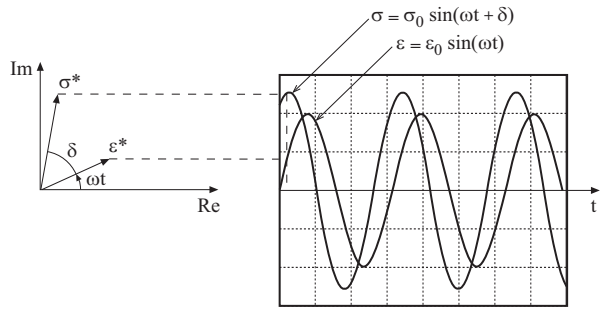

Figure 3.14: The real and the imaginary part of the complex strain and stress that the harmonic motion involves.

the relationship between the complex strain and the stress given by a simple multiplication by a complex function, the so-called the complex modulus,

$$\sigma^* = E^*(\omega)\epsilon^*, \tag{3.45}$$

the complex modulus being

$$E^*(\omega) = E_\infty(1 + i\omega e^*(\omega)), \tag{3.46}$$

where e^* is the Fourier transform of the dimensionless relaxation function

$$e^*(\omega) = \mathscr{F}(e(\tau)) = \int_0^\infty e^{-i\omega\tau} e(\tau) d\tau. \tag{3.47}$$

The response to a steady-state sinusoidal strain is thus, as suggested, an out-of-phase steady-state sinusoidal stress of the same frequency (cf. Figure 3.14), as given by

$$\sigma^* = \sigma_0 e^{i(\omega t+\delta)}. \tag{3.48}$$

Looking at Equation (3.45), one can see that the complex modulus can be also written as

$$\sigma^* = |E^*| e^{i \arg(E^*)} \epsilon_0 e^{i\omega t} = |E^*| \epsilon_0 e^{i(\omega t + \arg(E^*))}. \tag{3.49}$$

Comparing Equations (3.45) and (3.49), suggests an interpretation of the complex modulus in terms of measurable quantities as

$$|E^*| = \frac{\sigma_0}{\epsilon_0} \qquad \text{and} \qquad \arg(E^*) = \delta, \tag{3.50}$$

meaning that the absolute value $|E^*(\omega)|$ is the amplitude ratio of stress to strain (called the dynamic modulus) and the phase angle $\arg(E^*(\omega))$ represents the phase shift between stress and strain. The complex modulus can thus be expressed in polar form as

$$|E^*| = \frac{\sigma^*}{\epsilon^*} = \frac{\sigma_0 e^{i(\omega t+\delta)}}{\epsilon_0 e^{i\omega t}} = \frac{\sigma_0}{\epsilon_0} e^{i\delta}, \tag{3.51}$$

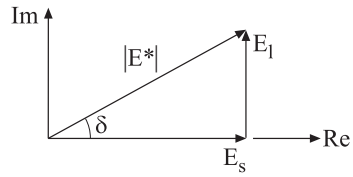

Figure 3.15: Complex representation of E^*.

and in rectangular form as

$$E^* = \frac{\sigma_0}{\epsilon_0}\cos\delta + i\frac{\sigma_0}{\epsilon_0}\sin\delta = E_s + iE_l, \tag{3.52}$$

where the real part E_s is called the storage modulus (it represents an in-phase response, i.e. the elastic response) whereas the imaginary part E_l is termed the loss modulus (it represents the out-of phase response, i.e. the energy dissipation); see Figure 3.15. An alternative version of this rectangular form is:

$$E^* = E_s(1 + \tan\delta), \tag{3.53}$$

$\tan\delta$ being termed the loss factor. The relationship between the polar and the rectangular form of the complex modulus can be simplified for low values of δ. The approximations involved are

$$\sin\delta \approx \tan\delta \approx \delta \qquad \text{and} \qquad \cos\delta \approx 1 \tag{3.54}$$

In addition, dynamic measurements of linear viscoelastic materials under harmonic loading show curves of dynamic modulus and damping looking like those in Figure 3.16, where E_0 is the instantaneous Young's modulus for very fast loading and E^∞ the long term modulus for very slow or no loading rate.

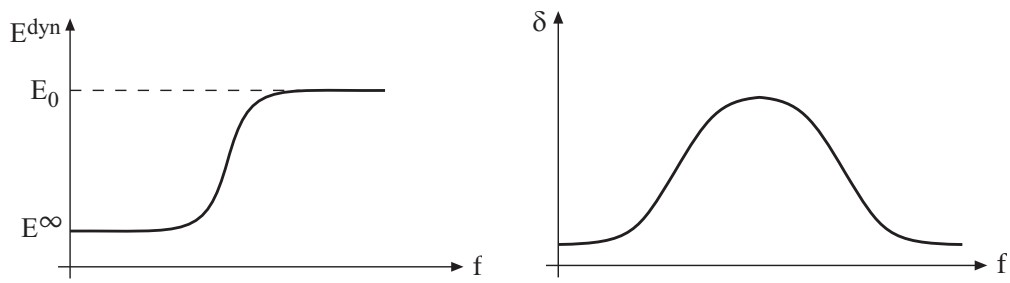

(a) Dynamic modulus.

(b) Damping.

Figure 3.16: Dynamic measurements of linear viscoelastic materials.

4 Measurements

In the appended **Paper A**, measurements were performed on lightweight wooden prefabricated floors in efforts to find indicators of human response to vibrations through comparing objective data concerning the floors with results of questionnaires answered by persons experiencing the vibrations on the floors involved while they were walking or seated on them. In this chapter, a brief overview of the most prominent excitation methods, as well as sensors and transducers, used nowadays in floor vibratory measurements, is presented. The extraction methods employed are also described.

4.1 Excitation methods

Human footfalls such as occur though adults walking and children running and jumping, for example, are the main sources of impact noise in dwellings, due to the disturbing vibrations created, especially in lightweight timber buildings, the most severe problems being at low frequencies, since the sound of footsteps produces a high degree of noise disturbance [3, 63]. The low resonance frequencies of floors of these kinds, in combination with low damping, makes them prone to easily being excited by such human activities. Thus, finding a source with a spectrum close to that of the human footfall is of crucial importance for attaining the approval of buildings in terms of how they react being consistent with human comfort.

Several excitation methods which exist today that can be used in evaluating floor vibrations, some of them standardised and others non-standardised, are described in the following.

4.1.1 Standardised sources

ISO tapping machine

The ISO tapping machine (cf. Figure 4.2(a)) consists of five steel hammers, each of them hitting the floor with two taps per second, which gives it ten taps per second altogether. This means one hit every 0.1 second with a short delay in between. Albeit various investigations have pointed out that the ISO tapping machine does not properly mimic human-step excitations, it is still used nowadays for measurement excitation in certain standardised procedures [19]. The device was developed after the construction of wooden multi-storey houses in Sweden was prohibited. Several adjustments to the

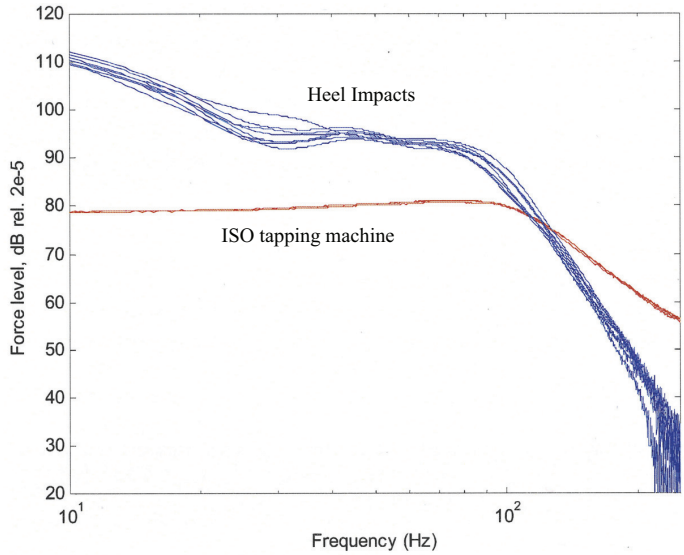

Figure 4.1: Force spectra of repeated heel impacts and repeated impacts produced by an ISO tapping machine, [4].

standards in terms of the evaluation procedures employed were undertaken in 1999 (see Section 2.4.1), yet these were found to not be sufficient in evaluating the vibratory and acoustic performance of wooden structures [4]. This is due to the fact that the amplitude of the input force amplitude of the tapping machine, in the low frequency range, is lower than that produced by the heel impact; see Figure 4.1. It is indeed in the low frequency range where lightweight timber constructions show higher impact sound levels than traditional concrete constructions do. This highlights the need for a source and for methods being employed that produce vibrations having a realistic frequency content, one that wooden houses generally are exposed to.

Rubber tire

The Japanese standard [64] describes a method in which a 3 kg rubber tire (cf. Figure 4.2(b)) is dropped from a height of 300 to 900 mm, producing a peak force of 1250 to 2400 N. This method was adopted to simulate children jumping and to study the impact sound insulation in thin concrete floor constructions. For further information regarding this, see for example [65].

The lack of standardised requirements is closely coupled with the sparseness of systematised measuring methods and sources. Certain non-standardised methods for assessing vibrations in floors and aimed at obtaining knowledge of the various types of buildings have come about in the recent years, the most prominent of these being those listed in Section 4.1.2.

4.1.2 Non-standardised sources

Shaker

Producing a continuous excitation is sometimes preferred in order to study the result spectrum with a high degree of resolution. Accordingly, an alternative to the tapping machine is to make use of an electrodynamic shaker, the applied load of which can be measured by means of force transducers. An electro-mecanical shaker, that can generate a broad range of different types of signals (sine, stepped sine, pure random, pseudo-periodic random, burst random and chirp), depending upon the needs that arise, gives a better (higher) signal to noise ratio than a tapping machine does.

In broad terms, a shaker (cf. Figure 4.2(c)) consists of a loudspeaker which is fed with a signal and is connected to the floor by a connecting rod (called a stinger), which in turn sets the floor into motion when it starts playing the signal and setting the membrane into motion. The stinger possesses a high degree of axial stiffness and a low bending stiffness, so that it can be considered to represent a point load on the floor, without there being any rotatory loading (the attachment needs to be carefully made so that no reaction forces from the main body of the shaker will be transmitted). A shaker is commonly used for modal analysis measurements.

Japanese ball

This hollow heavy-soft spherical impact source (cf. Figure 4.2(d)) is made of natural rubber and polybutadiene and is described in terms of the Japanese standard [66]. It weights 2.55 kg and is 183 mm in diameter [4]. Its properties when it is dropped from a height of 1 meter height are similar to those of the relevant human impacts, allowing it to be used for floor vibration measurements for frequencies below approximately 70 Hz [4].

Impact hammer

This consists basically of a hammer with a force transducer placed on its tip; see Figure 4.2(e). The tip can be changed depending upon the material being tested (using tips of differing stiffness). Hammer testing is commonly used for modal analysis measurements, since it is quick, easy and relatively cheap. The convenience of this technique is attractive, its requiring very little hardware (the impact hammer itself and a single accelerometer suffice) and the measurements it provides are not time-consuming at all. When the tip of the modal hammer hits a structure, a wide range of frequencies is excited very quickly. Hammer testing is decried mainly because of its lack of repeatability [11].

In the dissertation, non-standardised excitations sources were employed. In line with this, in the appended **Paper A** both a shaker and real human walking were used for excitation purposes during the measurements carried out.

(a) Tapping machine, [67].

(b) Rubber tire, [67].

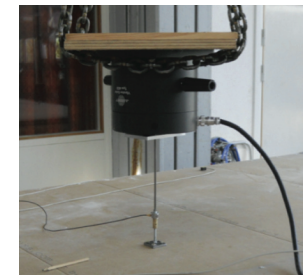

(c) Shaker.

(d) Japanese ball.

(e) Impact hammer, [68].

Figure 4.2: Excitation sources.

4.2 Sensors and transducers

In [69], a sensor is defined as a device that when exposed to a physical phenomenon (a given temperature, displacement, force, or whatever) produces a proportional output signal (electrical, mechanical, magnetic, etc.), or also as a device that responds to a change in such a physical phenomenon. A transducer, in turn, is defined as a device that converts one form of energy into another. In another words, a sensor is the complete assembly required to detect and communicate the occurrence of a particular event, whereas a transducer is the element within that assembly that has the function simply of detecting that event.

Sensors can be classified in terms of the functioning of the power supply [69], as being passive (or self powered), i.e. the power is provided by a sensed physical phenomenon (e.g. a theromometer) or as being active, when external power is necessary for operation. As regards the output signal, they can be either analog (if the signal is continuous) or digital (if the output signal is digitalised).

Transducers can, in turn, be either non-contact (detection occurring by means of eddy-currents or on the basis of optical proximity), or contact (mechanical contact is needed for detection to occur, such as for instance with piezoelectric, or piezoresistive sensors).

4.2.1 Accelerometers

An accelerometer is a device that measures accelerative forces by producing an output voltage proportional to the actual acceleration. The main parameters of accelerometers (and, in general terms, of any sensor) are the following [69, 70]:

- Sensitivity: the ratio of accelerometer's electrical output to its mechanical input, as expressed in terms of voltage per physical unit (e.g. [mV/ms^{-2}]). In analog sensors it is given as the slope of the output and input signals.
- Frequency response: the dependence of the charge or voltage sensitivity upon frequency. It defines the useful frequency range having linear sensitivity. The lower as well as the upper frequency limits are controlled by the following:
  - Upper frequency limit: this depending primarily upon the mounting resonance.
  - Lower frequency limit: this being restricted mainly by the pre-amplifier employed. Since accelerometers exposed to variations in temperature generate a low frequency response, pre-amplifiers can be set so as to have some cut-off frequency in the lower region to avoid it.
- Phase response: this corresponds to the time delay between the mechanical input and the resulting electrical output. In general, this delay is not the same for all frequencies.
- Transient response: response to shocks and transient vibrations.
  - Zero shift: phase nonlinearities in the preamplifier, or in the accelerometers.
  - Ringing: the transient containing high frequency components that excite the resonance of the accelerometer. It can be reduced by setting a mounting resonance of no less than 10/T, T being the length of the transient in seconds.
- Resolution: the smallest input increment that can be reliably detected.
- Weight: as a rule of thumb, the weight of the accelerometer should be no more than a tenth of the effective weight of the vibration test specimen.
- Dynamic range: the range over which the electrical output of the accelerometer is directly proportional to the acceleration at its base.
  - Lower limit: the practical limit (noise level) of the measuring system.
  - Upper limit: in general, the smaller the accelerometer, the higher vibration level is. This characteristic is of interest especially in the case of shock measurements.
- Environmental characteristics: the sensitivity of an accelerometer is also affected by the environment, especially the temperature, humidity, acoustic field, magnetic field and radiation. If measurements under severe conditions are of interest, special accelerometers should be employed.

- Repeatability (reproducibility): the ability to provide identical outputs for inputs that are the same. It can be affected by such factors as electrical noise and hysteresis. Averaging or low-pass filtering can be used to increase the repeatability.
- Linearity and accuracy: the ability to indicate the direct (linear) relationship between the input and the output with a minimal degree of fluctuation. It is expressed as a percentage of the full-scale values.
- Impedance: the ratio of the voltage to the current flow of the sensor. In general, high input impedance is required in order to reduce effectively the current flowing from the source. The output impedance needs to be low since it has to behave as a source of current.
- Eccentricity: geometrical non-linearity.
- Saturation: this defines the maximum output capability, i.e. reaching saturation by increasing the input signal, the output remains at the same level.
- Deadband: a region of input close to zero at which the output remains zero. Once the input travels outside the deadband, the output varies with input.

Fixation

In general, the types of fixations for accelerometers are the following [71, 72]:

- Threaded stud: the best fixation that can be achieved is by attaching the accelerometer to the structure with use of a threaded stud. It is recommended that one uses a thin layer of grease to increase the contact stiffness. Fixation of this type is often not possible due to its damages the structure it is attached to, however.
- Beeswax: a thin layer of beeswax can be used to stick the accelerometer to the structure. Temperature limitations (up to 40°) as well as limitations in acceleration (at about 100 m/s^2 in the case of clean surfaces) often restrict its use. Use of beeswax for fixation was employed in **Paper A**.
- Cement: if it is not possible to drill a hole, cement (e.g. epoxy or cyanoacrylate) can be used instead. This fixation method was also used in **Paper A**.
- An isolated stud and a mica washer: can be used if there is the requirement that the accelerometer be isolated from the object electrically (to prevent ground loops).
- Permanent magnet: for flat magnetic surfaces. A permanent magnet also isolates the accelerometer electrically. The resonant frequency is then reduced, but is still reasonably high, even for accelerations of up to 1000 or 2000 m/s^2.
- Hand held: suitable for *quick-look survey work*, although not generally recommended [73]. Due to the low stiffness involved, this introduces error but is suitable up to a level of 1 kHz.
- Others [73]: vacuum mounting, double-sided adhesive disk, quick mount.

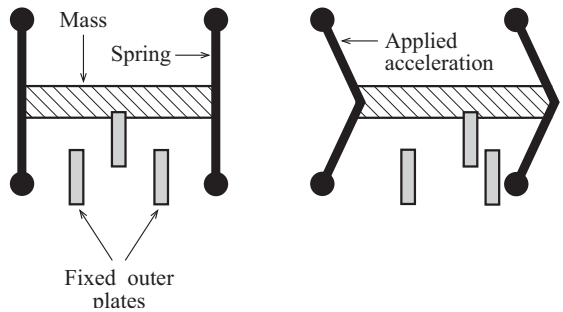

Figure 4.3: MEMS accelerometer. The movable plate attached to the movable mass makes the capacitance between the two fixed plates vary. The output voltage measured between these two plates is proportional to the sensed acceleration.

Types of accelerometers

There are different types of accelerometers (MEMS, piezoelectric, mechanical, Hall effect, etc.), only the first two of these, which are described below, being used in the course of the dissertation work.

MEMS accelerometers: The development of MEMS accelerometers (micro-electro-mechanical systems) was provoked by the need of having a device that was smaller, increasing its applicability. MEMS provide more compact and robust sensing than piezoelectric accelerometers do.

The way that MEMS accelerometers measure the acceleration is by their sensing changes in capacitance when the geometry of a capacitor changes (in terms either of the area of the electrodes, the distance between them or the permitivity of the material separating them [74]). A typical MEMS accelerometer is composed of a movable proof mass provided with a plate (representing a capacitor) that is fastened to a reference frame by a mechanical suspension system, as shown in Figure 4.3. The deflection of the mass, which is attached to the surface to be measured, and that is caused by the vibrations that are occurring, provokes a difference in capacitance between the outer plates and thus in the output voltage, its being proportional to the sensed acceleration.

All MEMS accelerometers used in the dissertation were built at our department, by buying the chip and carrying out the casing and cabling ourselves. The accelerometers were of types ADXL203 and ADXL 202E, by *Analog Devices*. We also carried out the **calibration** of them, using the back-to-back calibration method, which is described in the standard [75], in which the uncertainties involved when calibrating sensors using this method are also discussed.

In general terms, back-to-back calibration can be described as a comparative method, in which an unknown accelerometer is mounted as close as possible to a reference accelerometer, for which its sensitivity over the frequency range in known. Both accelerometers are then driven by a carefully controlled shaker, a frequency sweep being carrying out. Measuring the output voltage of both accelerometers and knowing the sensitivity of

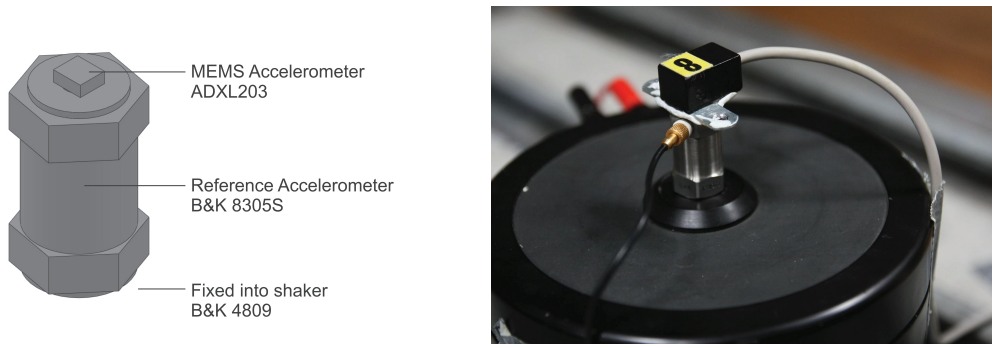

(a) Scheme, [76].

(b) Laboratory setup, [76].

Figure 4.4: Back-to-back calibration.

the reference one, enables the sensitivity of the other one to be calibrated as follows:

$$S(f)_{\text{unknown}} = S(f)_{\text{ref}} \frac{V(f)_{\text{unknown}}}{V(f)_{\text{ref}}} \tag{4.1}$$

$S(f)$ being the frequency-dependent sensitivity and $V(f)$ the output voltage for each frequency of the accelerometer in question (unknown or reference). The calibration accuracy achieved can well be better than 2 % [75]. Images of the procedure and the setup employed are shown in Figures 4.4(a) and 4.4(b). A report concerning all of the calibration procedures and many other aspects of the procedures employed is being prepared in [76].

Piezoelectric: A piezoelectric accelerometer uses the piezoelectric effect of quartz or ceramic crystals to provide an electrical output which is proportional to the sensed acceleration. The piezoelectric effect produces a charge which is emitted by the crystal when it is subjected to a compressive force. A force applied to a quartz crystal lattice structure alters the alignment of the positive and the negative ions, which results in an accumulation of these charged ions on the opposing surfaces. These charged ions accumulate on an electrode that is ultimately conditioned by transistor microelectronics and designed to measure the acceleration. The piezoelectric crystal is normally bonded to a mass such that when the accelerometer is subjected to a force, the mass in question compresses the crystal, which produces an electric signal proportional to the acceleration; see Figure 4.5.

Piezoelectric accelerometers can be used over a wide range of frequencies, their showing an excellent linearity over a very wide dynamic range, the measurements they provide being attainable with excellent accuracy over a wide range of environmental conditions. They require no power supply, are extremely durable since they contain no movable parts, are extremely compact and have a high sensitivity-to-mass ratio [70]. Their price is one of their main disadvantages, as they are much more expensive than MEMS accelerometers.

During their use, their **calibration** was checked on the calibration chart, this being their theoretical calibration as it is since the sensitivity value in question is based on factory calibration. As stated in [71], the accuracy of factory calibration is better than ± 2 % and includes the effects of the connection cable supplied with the accelerometer.

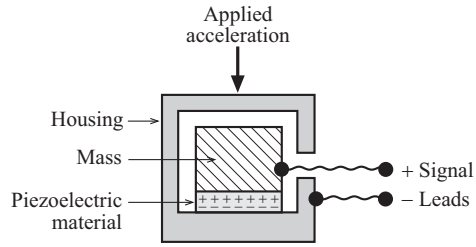

Figure 4.5: A piezoelectric accelerometer.

4.2.2 Deflectometers

In **Paper A**, the deflections of floors were measured while people were walking on them. The distance gauges employed were made by *Duncan Electronics*, the type being 9600 Series (cf. Figure 4.6). They have a sensitivity of 5 volts per 12.5 mm and are of the resistive type. The gauges consist of a copper coil along which a slider that moves together with the measured surface. The measuring tip is spring loaded, when it is fully extended the voltage level being 5 V and when it is fully depressed 0 V. Due to the construction of the sensor, care needs to be taken in the placement of the gauge so that the neutral position of the measured object corresponds to a depression of 6.25 mm of the measuring tip, i.e. half the measuring capacity of the gauge. The casing and cabling of the deflectometers was carried out at our department.

4.2.3 Force transducers

In **Paper A**, the force produced by the shaker when performing the experimental modal analysis (cf. Section 4.3.1) was also measured. The force transducer is a *Brüel&Kjær* 8200 (cf. Figure 4.7), a piezoelectric charge transducer. The range of usable force is 1000 N in the tensile and 5000 N in the compressive mode. The working principle of the transducer is the same as in piezoelectric accelerometers, its involving the piezoelectric effect of quartz, a quartz crystal producing an electrical charge when stressed. The charge is proportional to the stressing force and thus provides a direct measure of the force applied. Since the transducer has a very low internal capacitance, it needs to be used together with charge amplifiers, these permitting the use of long cables without its disturbing the sensitivity of the measurement system.

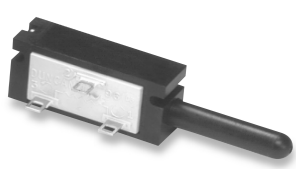

Figure 4.6: Deflectometer by Duncan Electronics (Series 9600), [77].

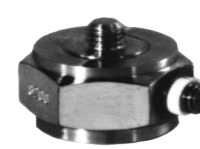

Figure 4.7: Force transducer B&K 8200, [78].

4.3 Extraction

4.3.1 Experimental modal analysis

Experimental modal analysis (EMA) involves measuring and analysing the dynamic response of a structure when excited by a load (either continuous one created by a shaker or an impact one induced by a modal hammer). The response to the load involved is recorded by sensors, which generally are accelerometers, these being placed strategically at one or more spots for registering the vibration modes when post-processing the signals with data acquisition hardware and software that are adequate for the purpose in question. The FRF obtained gives the structure's magnitude and phase response over the frequency range of interest. Modal parameter extraction algorithms are used to identify the modal parameters from the FRF data, through fitting the measurement data to appropriate mathematical expressions. This is done by minimising the squared error (or squared difference) between the analytical function and the measured data. Since EMA is a linear theory, the FRF obtained is also linear. Hence, the validity of the FRF is assessed by the coherence function, γ^2, which is similar to the square of the correlation coefficient used in statistics; the value of it comes closer and closer to 1.0, the better the coherence is between the input and output signal there at each fundamental frequency involved. Values lower than 0.75 are normally considered poor, due to this being a sign of noise in the measured input or output signal, such values thus being disregarded [11]. The full frequency response matrix, $\mathbf{H}$, be written [11] as

$$\begin{bmatrix} X_1 \\ X_2 \\ \vdots \\ X_n \end{bmatrix} = \begin{bmatrix} H_{11} & H_{12} & ... & H_{1n} \\ H_{21} & H_{22} & ... & H_{2n} \\ \vdots & \vdots & \vdots & \vdots \\ H_{n1} & H_{n2} & ... & H_{nn} \end{bmatrix} \begin{bmatrix} F_1 \\ F_2 \\ \vdots \\ F_n \end{bmatrix} \tag{4.2}$$

the H_{ij} terms being defined as

$$H_{ij}(\omega) = \frac{X_i(\omega)}{F_j(\omega)} = \frac{\text{Response } \text{“}i\text{”}}{\text{Excitation } \text{“}j\text{”}} \tag{4.3}$$

where $X_i(\omega)$ is the Fourier transform of the response $x_i(t)$, and $F_j(\omega)$ is the Fourier transform of the excitation $f_j(t)$.

EMA was used specifically in **Paper A** so as to extract the dynamic properties of the floor structures under study, those of the eigenfrequencies, damping ratios, mode shapes and modal densities involved. An electro-mechanical shaker was hung from an overhead crane so as to isolate its main body from the structure and thus simply transmit, through the stinger, the signal fed into it, whereas piezoelectric accelerometers were attached all over the floor surface (the SIMO protocol being used, in terms of which the single input was that of the shaker and the multiple output was that of the accelerometers). A pseudo-random excitation signal was fed into the shaker. Such a signal is achieved by a set spectral frequency lines over a frequency band of interest being inverse transformed to the time domain so as to create an excitation signal. Due to the sinusoidal nature of such a signal,

the effects of leakage are non-existent, providing the system is excited for sufficiently long a time for a steady-state response to be achieved. This works very well with structures that are fairly linear in character. For signal excitations of other types, see e.g. [79].

Once the FRFs were acquired by the data acquisition system, modal parameters were identified by curve fitting, through matching a mathematical expression to a set of empirical data points (a poly-reference method of this sort was used in **Paper A**). For information regarding the poly-reference method and other types of fitting, as well as for further information regarding EMA, see for example [80].

5 Analysis of subjective responses

In order to obtain greater insight into human response to vibrations, specifically floor vibrations here, the data stemming from the questionnaires were confronted with objective measurements performed on the floors under study. Several statistical studies were performed. Specifically, in **Paper B**, the data analysis carried out aimed eventually at finding a satisfactory indicator for two subjective attributes – vibration annoyance and vibration acceptability –, in the form of an objective parameter that could best explain the subjective data. To this end, use was made of multilevel regression.

The large amount of non-subject-dependent objective parameters available made it impossible to determine by means of multilevel regression analysis the relationships between each and every one of these objective parameters, on the one hand, and the subjective data, on the other. Thus, a preliminary analysis based on use of Principal component analysis (PCA) was carried out first, in order to select beforehand a small number of objective parameters that could be thought to best explain the subjective data.

A brief review of the statistical methods used in **Paper B** is presented below, its not being a major objective of the dissertation to delve deeply into them.

5.1 Principal component analysis

Principal component analysis (PCA) is a technique involving multivariate statistics, mainly descriptive, used for reducing the dimension of a set of multidimensional data. The technique is useful for finding the separate sources of variability in a set of data and ordering them in terms of importance.

The mathematical procedures involved use an orthogonal transformation to convert a set of n observations of p variables that are possibly correlated with one another, into a set of values of linearly uncorrelated variables q (where $q \leq p$) termed principal components. The idea is that, if a variable is a function of one or more other variables, it contains redundant information and therefore the size of the model should be reduced. This transformation is defined in such a way that the first principal component has the largest possible variance (its thus accounting for as much of the variability in the data as possible), and that each succeeding component, in turn, has the highest variance possible under the constraint that it be orthogonal to (i.e. uncorrelated with) the preceding components. After a reduction of this sort, the q new components (the number of new components to consider is up to the analyst) are obtained as linear combinations of the original variables. For further information concerning standard PCA, see e.g. [81, 82].

Two types of PCA were employed in **Paper B**: the PCA of binary data (De Leeuw's model being used specifically [83]) in order to deal with the vibration acceptability data, and the PCA of metric data (the MDPREF model being used here [84, 85]) to deal with the vibration annoyance data. Both types of PCA are explained in the following.

5.1.1 PCA of metric data – MDPREF

In this study, the annoyance scores uttered by the subjects on the five different floors involved were analysed by use of the MDPREF model. The analysis was carried out by use of the program *MDPREF*. The model makes it possible to inspect inter-individual differences graphically. Furthermore, it is possible to go on then to identification of those vibratory features of the floors that can account for the vibration annoyance scores uttered by the subjects.

Theoretical framework: MDPREF is a multidimensional scaling model that belongs to the family of scalar product models [85]. It is commonly applied to metric data set up in a rectangular two-mode matrix. This matrix, termed $\mathbf{S}$, contains scores; in that which follows, it will be supposed that $\mathbf{S}$ contains vibration annoyance scores uttered by a given number of subjects (N subjects arranged in rows) to a set of stimuli (n stimuli arranged in columns).

The aim of the model is to represent the stimuli and the subjects in a joint space. More precisely, MDPREF provides a configuration of n points representing the stimuli, and of N unit vectors passing through the origin representing the subjects. These entities are placed in the space in such a way that the orthogonal projections of the different points onto each vector are in maximal agreement with the annoyance scores uttered in response to the stimuli by the various subjects (see Figure 5.1). The vibration annoyance scores increase in continuous fashion along the subject vector. The further a stimulus is projected onto the vector for a given subject, the more it is judged to be annoying to the subject.

The MDPREF algorithm is based on the singular value decomposition (SVD) of matrix $\mathbf{S}$ according to the Eckart-Young procedure [86]. In that sense, MDPREF strongly resembles PCA. Indeed, the algorithm determines by diagonalisation the eigenvalues of the major (i.e. the product $\mathbf{S}\mathbf{S}^t$) and the minor (i.e. the product $\mathbf{S}^t\mathbf{S}$) covariance matrices and their associated eigenvectors. The magnitude of the eigenvalues common to both covariance matrices makes it possible to estimate the number of principal factors, r, to be retained. In the r-dimensional space, the components of the subject vectors are determined by computing the product of the matrix of the r first eigenvectors of $\mathbf{S}\mathbf{S}^t$ and of the diagonal matrix of the r first eigenvalues; the coordinates of the stimulus points being given by the components of the r first eigenvectors of $\mathbf{S}^t\mathbf{S}$ [87].

Data pre-processing: The respective row mean is substracted from each of the entries. This removes any effects due to the differences in the values used by the individual subjects.

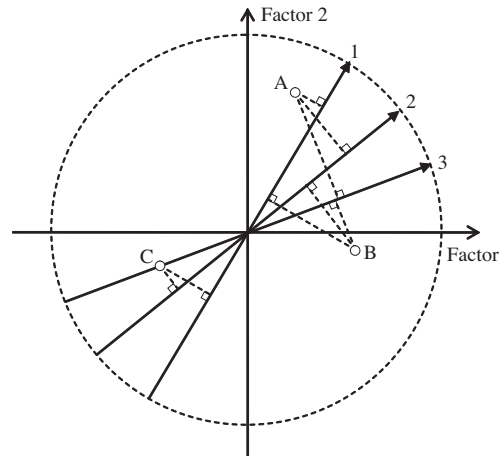

Figure 5.1: llustration of a representation space provided by MDPREF. Let a 2-dimensional space in which three stimuli A, B and C and three subjects 1, 2 and 3 are represented. In the example shown here, the respective projections of points A, B and C onto the vectors 1, 2 and 3 reproduce the annoyance scores given by the three subjects to the three stimuli.

Dimensionality selection: The number of principal components to be retained can be determined by means of the *scree test* method [88], used in PCA. The test applies to a plot of the eigenvalues of the covariance matrices $\mathbf{SS}^t$ and $\mathbf{S}^t\mathbf{S}$ in terms of the number of the principal components associated with them, an illustration of this being presented in Figure 5.2. According to this method, the appropriate dimensionality can be estimated by the number of the principal factors the associated eigenvalue of which is located at the end of the line that can join up a maximal number of low eigenvalues "at one go". In Figure 5.2, since a line going through eigenvalues 3 to 10 can be drawn, the number of components to be retained can be considered likely to be equal to 3.

Interpretation – General issues: From the MDPREF space produced, the inter-individual differences in rating involved can be assessed by inspecting the relative locations of the respective subject vectors. Indeed, the cosine of the angle between two subject vectors provides a measure of the extent of agreement there is between the scores uttered by two subjects. When both vectors are perfectly represented in the space, the cosine of the angle is equivalent to the correlation coefficient between the two series of scores, whereas when it is not the case that both vectors are not perfectly represented in the space, the cosine of the angle is always lower than the correlation coefficient between the two series of scores [89].

The links between the subject vectors and the axes of the space are then examined. The direction in which a subject vector points gives an idea of how the subject combines the vibratory features of the floors to utter what, after the data analysis required, represent her/his vibration annoyance scores, this assuming that the factors have a psychological meaning and that they refer to vibratory features of the floors. The cosine of the angle

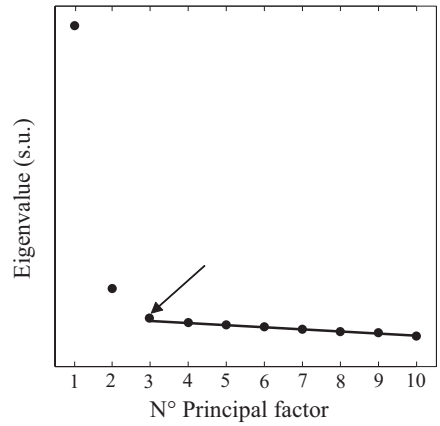

Figure 5.2: Example of a plot of the eigenvalues obtained in relation to the number of associated principal components involved. The number of the principal factors to be retained can be considered likely to be equal to 3, since a line going through eigenvalues 3 to 10 can be drawn "at one go".

between the subject vector and the axis also provides a measure of the importance the subject attaches to the component in question [89]. If the subject vectors are closely related to an axis (i.e. are close to this axis), and are located on the same side of this axis, then the axis denotes a component of consensus among the subjects. In contrast, if some of the subject vectors have a positive component along an axis whereas others have a negative component, this axis denotes a component of inter-individual differences [90].

To investigate the assumption that the components have a psychological meaning, the links between the components, on the one hand, represented by the axes, and the vibratory indices, on the other, computed on the basis of the vibratory measurements obtained for the various floors, as represented in the vector space as vectors by use of PREFMAP procedure [89], are examined. An index vector points in a direction such that the projections of the stimulus points onto the vector are in maximal agreement with the index values, the non-normalised vector length being equivalent to the correlation coefficient between the projections and the index values, this indicating the quality of the representation of the index within the vector space [90].

Thus, an index vector very close to the axis in question suggests that the components refer very clearly to the vibratory features described by the index, these vibratory features appearing rather clearly to be used by the subjects to utter their degree of annoyance as expressed in the annoyance scores. For further information regarding the analysis of the results, see also **Paper B**.

5.1.2 PCA of binary data – the De Leeuw model

In the present study, the vibration acceptability responses were analysed by use of De Leeuw's model, in practice the analysis being carried out by use of the *R* code that De Leeuws developed [83]. Regarding the output of the MPREF model, it is possible, in inspecting the

inter-individual differences in question graphically, to identify the vibratory features of the floors that can account for the vibration acceptability responses uttered by the subjects. The theoretical framework of this model will now be presented briefly, the general issues regarding the interpretation of the solution being basically the same as for MDPREF.

Suppose $\mathbf{P} = p_{ij}$ is an $n \times m$ binary data matrix, a matrix of observed acceptability judgements in this case, the elements of which are equal to one or to zero (i.e. the vibrations being acceptable or non-acceptable respectively). The rows in $\mathbf{P}$ refer to the different subjects, whereas the columns refer to the floors. $\mathbf{P}$ is to be fitted to a predicted matrix $\mathbf{\Pi}(X, Y)$ (the acceptability matrix as given by the PCA). The predicted matrix is a function of X, an $n \times r$ matrix of row scores, and of Y, an $m \times r$ matrix of column scores. The parameter r is the dimensionality of the solution. The computational problem is that of minimising the distance between $\mathbf{P}$ and $\mathbf{\Pi}(X, Y)$ over X and Y, the distance being measured by the loss function

$$\mathscr{D}(X, Y) = -\sum_{i=1}^{n}\sum_{j=1}^{n}\left[p_{ij}\log\pi(x_i' y_j) + (1 - p_{ij})\log(1 - \pi(x_i' y_j))\right]. \tag{5.1}$$

Two different ways of specifying the function π, which maps the parameters in X and Y, to the zero-one scale of the outcomes are given in [83]. In the *logit* case, $\pi(x)$ is

$$\boldsymbol{\psi(x)} = \int_{-\infty}^{x}\psi(x)\mathrm{d}t = \frac{1}{1 + e^{-x}}, \tag{5.2}$$

where the standard logistic density function is given by

$$\psi(x) = \frac{e^{-x}}{(1 + e^{-x})^2}. \tag{5.3}$$

By defining a matrix $\mathbf{\Lambda} = \lambda_{ij}$ in terms of *logits*, i.e. $\lambda_f = \psi^{-1}(\pi(x', y_f))$, the basic relationship to be fitted can be written as $\mathbf{\Lambda} = XY'$. This shows the problem being dealt with is a fixed-rank-approximation problem on the *logit* scale, a problem usually solved by PCA or, equivalently, by SVD in the linear case in which $\mathbf{\Lambda}$ is observed directly. Similarly, this model provides a multidimensional space consisting of a configuration of floor points and of subject vectors that pass through the origin. A vector endpoint represents the point of maximum acceptability for the subject in question. For further information regarding logistic PCA, see [83] and also **Paper B**.

5.2 Multilevel regression analysis

Multilevel regression has advantages over classical regression for the modelling of repeated measures data. Notably, a multilevel regression formulation complies strictly with the hierarchical structure of the repeated measures data involved, like that in **Papers A** and **Paper B**, which consists of observations nested within individuals in question as the data is collected. It thus takes account of the fact that the observations are not independent. For an introduction to multilevel regression models, the reader can be

referred to the textbooks [91, 92]. Although not a new idea, this conception of things has become much more popular as the growth of computing power and the availability of appropriate softwares have increased.

More generally, a multilevel model is considered to be a regression model (either a linear or a generalised regression model) in which the parameters, i.e. the regression coefficients, are modelled at a second level. In modelling repeated measures data, the feature that distinguishes multilevel models from classical regression models is in the modelling of the variation between individuals [91]. Multilevel models can be used on data with many levels, although 2-level models are the most common. The dependent variable need to be examined at the lowest level of analysis [93]. In what concerns repeated measures data, the lowest level of analysis is the occasion level.

Conceptually, such models are often viewed as representing hierarchical system of regression equations. Assume there to be data on J individuals, and there to be a different number of occasions N_j for each individual involved. On the occasion (the lowest) level, there is a set of dependent variables Y_{ij} and a set of explanatory variables X_{ij}, whereas on the individual level one has the explanatory variable Z_j. Thus, a separate regression equation can be applied to each individual in accordance with

$$Y_{ij} = \beta_{0j} + \beta_{1j}(X_{1ij}) + e_{ij}. \tag{5.4}$$

The β_j values are modelled by explanatory variables at the individual level:

$$\begin{aligned} \beta_{0j} &= \gamma_{00} + \gamma_{01} Z_j + u_{0j}, \\ \beta_{1j} &= \gamma_{10} + \gamma_{11} Z_j + u_{1j}. \end{aligned} \tag{5.5}$$

Sustitution of Equations (5.5) in (5.4) gives

$$Y_{ij} = \gamma_{00} + \gamma_{10} X_{ij} + \gamma_{11} Z_j X_{ij} + u_{1j} X_{ij} + u_{0j} + e_{ij}. \tag{5.6}$$

There is generally more than one explanatory variable at the lowest level, and also more than one at the highest level. Let P be the number of explanatory variables X at the lowest level ($p = 1...P$) and Q be the number of explanatory variables Z at the highest level ($q = 1, ..., Q$). Equation (5.6) then becomes

$$Y_{ij} = \gamma_{00} + \sum_{p=1}^{P} \gamma_{p0} X_{pij} + \sum_{q=1}^{Q} \gamma_{0q} Z_{qj} + \sum_{p=1}^{P} \sum_{q=1}^{Q} \gamma_{pq} Z_{qj} X_{pij} + \sum_{p=1}^{P} u_{pj} X_{pij} + u_{0j} + e_{ij}. \tag{5.7}$$

Prior to the analysis to be carried out, the researcher must first decide, which predictors, if any, are to be included in it. Secondly, she or he must decide whether the parameter values (i.e. the elements that are to be estimated) are to be fixed or random. Fixed parameters are composed of a constant that applies to all the individuals, whereas a random parameter has a different value for each of the individuals [94]. The types of models to be selected between are the random-intercepts model, the random-slope model and the random-intercepts-random-slope model [94]. In **Paper B**, a random intercept and random-intercept-random-slope model were tested. The first of these is a model in which the intercepts are allowed to vary across individuals. This model assumes that the slopes involved are fixed (the same across each of the individuals included). The second model is a model in which both the intercepts and the slope are allowed to vary across individuals. For further information regarding these models, see **Paper B**.

6 Finite element method

6.1 Introduction

Partial differential equations (PDE) arise in the mathematical modelling of many engineering problems. The analytical solutions of PDEs are often either impossible or impracticable to obtain by use of classical analytical methods. The FE method is a numerical approach by which boundary value differential equations, both linear and non-linear, can be solved in an approximate manner.

In broad strokes, one can say that the differential equation, or equations describing the physical problems considered, are assumed to hold over a particular region of the structure under study (1D, 2D or 3D regions). This region is divided into smaller parts (finite elements), and what is usually a polynomial approximation of the solution for each such element (as regards acceleration, velocity, temperature, etc.) is then sought. The assembly of all the elements involved is called an FE mesh. The correct choice of elements for a particular simulation is essential if accurate results at a reasonable computational cost are to be obtained. Having determined the behavior of each individual element, these are then assembled by use of some specific rules to obtain a solution for the entire region, which eventually enables one to obtain an approximate solution for the body as a whole [95]. This procedure will be explained in theoretical terms in the sections that follow. The notation of the theoretical background presented will follow the one provided in [95]. For a broader discussion of the FE method, see for example [96].

6.2 Finite element formulation of elasticity

The differential equations defining the problem under study, together with the boundary conditions applying to the region of validity, or what is termed as strong formulation of the problem, is first transformed into a finite set of algebraic equations that hold across this region of interest, this being called the weak formulation of the problem in question. The algebraic approximations of all the small regions involved (the finite elements) are assembled by use of certain mathematical manipulations, so as to obtain the FE formulation of the problem, as explained in the following.

Strong formulation

For 3D problems, the differential equations of motion of a body as given by Newton's second law, small deformations being assumed, are

$$\tilde{\boldsymbol{\nabla}}^{\boldsymbol{T}}\boldsymbol{\sigma} + \mathbf{b} = \rho\frac{\partial^2\mathbf{u}}{\partial t^2}, \tag{6.1}$$

where $\boldsymbol{\sigma}$ is the vector representing the stresses, $\mathbf{b}$ the body force vector, ρ the material density, $\mathbf{u}$ the displacement vector, t the time, and $\tilde{\boldsymbol{\nabla}}^{\boldsymbol{T}}$ a differential operator matrix, as given as

$$\tilde{\boldsymbol{\nabla}}^{\boldsymbol{T}} = \begin{bmatrix} \frac{\partial}{\partial x} & 0 & 0 & \frac{\partial}{\partial y} & \frac{\partial}{\partial z} & 0 \\ 0 & \frac{\partial}{\partial y} & 0 & \frac{\partial}{\partial x} & 0 & \frac{\partial}{\partial z} \\ 0 & 0 & \frac{\partial}{\partial z} & 0 & \frac{\partial}{\partial x} & \frac{\partial}{\partial y} \end{bmatrix}; \quad \boldsymbol{\sigma} = \begin{bmatrix} \sigma_{xx} \\ \sigma_{yy} \\ \sigma_{zz} \\ \sigma_{xy} \\ \sigma_{xz} \\ \sigma_{yz} \end{bmatrix}; \quad \mathbf{b} = \begin{bmatrix} b_x \\ b_y \\ b_z \end{bmatrix}; \quad \mathbf{u} = \begin{bmatrix} u_x \\ u_y \\ u_z \end{bmatrix}. \tag{6.2}$$

Carrying out the matrix multiplications yields the three differential equations of motion

$$\begin{aligned} \frac{\partial\sigma_{xx}}{\partial x} + \frac{\partial\sigma_{xy}}{\partial y} + \frac{\partial\sigma_{xz}}{\partial z} + b_x &= \rho\frac{\partial^2 u_x}{\partial t^2} \\ \frac{\partial\sigma_{yx}}{\partial x} + \frac{\partial\sigma_{yy}}{\partial y} + \frac{\partial\sigma_{yz}}{\partial z} + b_y &= \rho\frac{\partial^2 u_y}{\partial t^2} \\ \frac{\partial\sigma_{zx}}{\partial x} + \frac{\partial\sigma_{zy}}{\partial y} + \frac{\partial\sigma_{zz}}{\partial z} + b_z &= \rho\frac{\partial^2 u_z}{\partial t^2}. \end{aligned} \tag{6.3}$$

At the surface boundary of the body ($\mathbf{n}$ being a normal vector pointing outwards the body), the traction vector $\mathbf{t}$ must fulfill the natural boundary conditions along a surface Γ_h, as well as the essential boundary conditions (the prescribed displacements $\mathbf{g}$) along the boundary, denoted as Γ_g, where

$$\mathbf{t} = \boldsymbol{\sigma}\mathbf{n} = \begin{bmatrix} \sigma_{xx}n_x + \sigma_{xy}n_y + \sigma_{xz}n_z \\ \sigma_{yx}n_x + \sigma_{yy}n_y + \sigma_{yz}n_z \\ \sigma_{zx}n_x + \sigma_{zy}n_y + \sigma_{zz}n_z \end{bmatrix} \quad \text{on } \Gamma_h, \tag{6.4}$$

$$\mathbf{u} = \mathbf{g} = \begin{bmatrix} g_x \\ g_y \\ g_z \end{bmatrix} \quad \text{on } \Gamma_g. \tag{6.5}$$

The differential equations (6.3) together with the boundary conditions given in Equations (6.4) and (6.5), and the region of interest in which the equations hold, represent the so-called strong formulation of the problem in question.

Weak formulation

In order to derive the weak formulation of the FE problem in question, a time independent weight vector $\mathbf{v}$ is introduced. The weak form is a variational statement of the problem in which one integrates against the test function $\mathbf{v}$. This has the effect of relaxing the problem, where instead of finding an exact solution everywhere, a solution that on the average satisfies the strong formulation over the domain in question is sought. A solution of the strong form also satisfies the weak form, the two being identical [95]. The weight function has the following form:

$$\mathbf{v} = \begin{bmatrix} v_x & v_y & v_z \end{bmatrix}^T . \tag{6.6}$$

Multiplying the Equations (6.3) in the order stated by v_x, v_y and v_z respectively, and integrating the expressions over the volume V, yields

$$\underbrace{\int_V \mathbf{v}^T \rho \ddot{\mathbf{u}} \mathrm{d}V}_{\text{(I)}} = \underbrace{\int_V \mathbf{v}^T \tilde{\boldsymbol{\nabla}}^{\boldsymbol{T}} \boldsymbol{\sigma} \mathrm{d}V}_{\text{(II)}} + \underbrace{\int_V \mathbf{v}^T \mathbf{b} \mathrm{d}V}_{\text{(III)}} . \tag{6.7}$$

Integrating by parts through applying the Green-Gauss theorem to term (II), the traction vector emerges, giving

$$\int_V \mathbf{v}^T \tilde{\boldsymbol{\nabla}}^{\boldsymbol{T}} \boldsymbol{\sigma} \mathrm{d}V = \underbrace{\int_S \mathbf{v}^T \mathbf{t} \mathrm{d}S}_{\text{(IV)}} - \underbrace{\int_V \left(\tilde{\boldsymbol{\nabla}} \mathbf{v} \right)^T \boldsymbol{\sigma} \mathrm{d}V}_{\text{(V)}} . \tag{6.8}$$

Inserting terms (IV) and (V) in Equation (6.7) gives the weak formulation

$$\underbrace{\int_V \mathbf{v}^T \rho \ddot{\mathbf{u}} \mathrm{d}V}_{\text{(I)}} = \underbrace{\int_S \mathbf{v}^T \mathbf{t} \mathrm{d}S}_{\text{(IV)}} - \underbrace{\int_V \left(\tilde{\boldsymbol{\nabla}} \mathbf{v} \right)^T \boldsymbol{\sigma} \mathrm{d}V}_{\text{(V)}} + \underbrace{\int_V \mathbf{v}^T \mathbf{b} \mathrm{d}V}_{\text{(III)}} . \tag{6.9}$$

The advantages of the weak formulation as compared with the strong formulation are [95]:

- The FE equations are based on the weak formulation.
- The strong formulation presents a second derivative, whereas the weak formulation has only the first derivative, due to the integration that is performed. It is thus much better to deal with approximating functions which are differentiable once (whereas if the strong formulation had been considered instead, the approximating functions would have to be differentiable twice).
- Whereas the strong formulation varies when discontinuities in the problem are present, the weak form retains its form, its thus being invariant.

Establishing the FE equations

The weak form, as given in Equation (6.9), involves the displacements $\mathbf{u}$ and the arbitrary weight function $\mathbf{v}$, certain approximations being needed in order to achieve the FE formulation.

Choice of approximating functions: The region is now to be divided into finite elements, a piecewise-approximation across these elements being carried out first, and then, on the basis of these results, its being established for the entire region. The approximations over each of the elements can be selected from a variety of different types (exponential functions, trigonometrical, etc.), the use of polynomial functions being especially advantageous and convenient to use due to their simplicity.

Obviously, the smaller the elements considered over the region are, the more accurate the final solution will be, at the same time the computational cost increasing as the number of elements increases. In the limiting case in which the elements are infinitely small, the approximate solution is infinitely close to the exact solution (this is the so-called convergence requirement). The convergence requirement is fulfiled if and only if the two following conditions are met:

- The approximations of the vector $\mathbf{u}$ must be able to represent an arbitrary constant rigid-body motion and an arbitrary constant strain state (completeness requirements).
- The approximations of the displacement vector $\mathbf{u}$ must vary in a continuous manner over the boundaries of the elements (compatibility or conforming requirement).

Although in some cases the compatibility requirement may be relaxed and convergence still be achieved (in the case of non-conforming elements), the fulfilment of completeness is a necessary condition for convergence to be satisfied.

Irrespective of the particular type of element selected, the approximation of the unknown function, i.e. the displacement field within each element in this case, is carried out as an interpolation between the displacement of the nodal points of the element (the superscript e denoting element-wise quantities), expressed as

$$\mathbf{u} = \mathbf{N}^{\mathrm{e}}\mathbf{a}^{\mathrm{e}}, \tag{6.10}$$

where $\mathbf{a}^{\mathrm{e}}$ contains the nodal displacements of all the nodal points n_e, and $\mathbf{N}^{\mathrm{e}}$, the element shape functions, given by

$$\mathbf{u} = \begin{bmatrix} u_x \\ u_y \\ u_z \end{bmatrix}; \mathbf{N}^{\mathrm{e}} = \begin{bmatrix} N_1^{\mathrm{e}} & 0 & 0 & N_2^{\mathrm{e}} & 0 & 0 & ... & N_{n_e}^{\mathrm{e}} & 0 & 0 \\ 0 & N_1^{\mathrm{e}} & 0 & 0 & N_2^{\mathrm{e}} & 0 & ... & 0 & N_{n_e}^{\mathrm{e}} & 0 \\ 0 & 0 & N_1^{\mathrm{e}} & 0 & 0 & N_2^{\mathrm{e}} & ... & 0 & 0 & N_{n_e}^{\mathrm{e}} \end{bmatrix}; \mathbf{a}^{\mathrm{e}} = \begin{bmatrix} u_{x1} \\ u_{y1} \\ u_{z1} \\ \vdots \\ u_{xn_e} \\ u_{yn_e} \\ u_{zn_e} \end{bmatrix}. \tag{6.11}$$

Note that the polynomial forms of the shape functions N_i^{e} vary for each type of element (tetrahedral, quadrilateral, etc.) and node (i.e. their depending upon the coordinates), here simply the general notation being given. The particularisation to a specific type of element is explained, for example, in [95, 96]. The vector $\mathbf{a}^{\mathrm{e}}$ has the dimension $3n_e \times 1$. The matrix $\mathbf{N}^{\mathrm{e}}$ has as many rows as there are displacement components for each node (three components in the case presented here, in the x-, y- and z-directions) and as many columns as there are DOFs in each of the nodes ($3 \times 3n_e$).

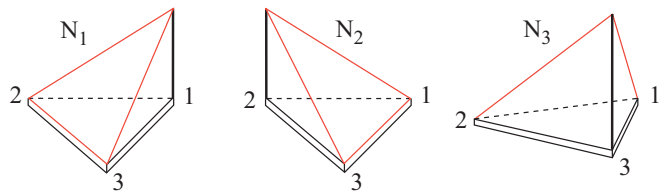

Figure 6.1: Linear shape functions for a triangular 2D element [97].

All N_i^{e}, regardless of the order of approximation (i.e. linear, quadratic, etc.) must possess the following property:

$$N_i^{\mathrm{e}} = \begin{cases} 1 & \text{at nodal point } i \\ 0 & \text{at all other nodal points} \end{cases} \tag{6.12}$$

In addition, one should recall that an element shape function related to a specific nodal point is zero along its element boundaries, which do not contain the nodal point in question. Also, the element shape functions must also comply with the following property:

$$\sum_{i=1}^{n_e} N_i^{\mathrm{e}} = 1. \tag{6.13}$$

Moreover, one should note that the interpolation scheme matches that of the adjacent elements since they share common nodes, the function varying (linearly for linear elements, quadratically for quadratic elements, and so on) between those nodes. To illustrate the latter relationships, the linear shape functions for a triangular 2D element are shown in Figure 6.1.

Once the displacements have been interpolated, the strains within each of the elements can also be obtained according to

$$\boldsymbol{\varepsilon} = \mathbf{B}^{\mathrm{e}}\mathbf{a}^{\mathrm{e}} \qquad \text{where} \qquad \mathbf{B}^{\mathrm{e}} = \tilde{\boldsymbol{\nabla}}\mathbf{N}^{\mathrm{e}}, \tag{6.14}$$

the dimension of $\mathbf{B}^{\mathrm{e}}$ being $6 \times 3n_e$ and

$$\boldsymbol{\varepsilon}^T = \left[\begin{array}{cccccc} \varepsilon_{xx} & \varepsilon_{yy} & \varepsilon_{zz} & \gamma_{xy} & \gamma_{xz} & \gamma_{yz} \end{array} \right]. \tag{6.15}$$

Choice of a weight function: Different methods of weighted residuals (MWR) exist for solving differential equations approximately, specifically the collocation method, the sub-domain method, the method of moments, and the least squares method; see [95, 96]. Consider the 1D differential equation

$$Lu(x) + g(x) = 0 \qquad\qquad a \leq x \leq b, \tag{6.16}$$

in which $u(x)$ is the unknown function and the function $g(x)$ is known, L denoting a linear differential operator. The two boundary conditions are assumed to be (if L is a second-order operator), $u(a) = u_a$ and $u(b) = u_b$. Methods for solving Equation (6.16) for

arbitrary forms of L and g are sought. This requires a reformulation of Equation (6.16) through its multiplication by an arbitrary function $v(x)$, the form of which is given in Equation (6.6), the resulting expression then being integrated as follows over the region of interest,

$$\int_a^b v(Lu+g)\mathrm{d}x = 0. \tag{6.17}$$

Since a numerical solution is sought, an approximation of the unknown variable, u, needs to be selected, this approximation being a linear combination of basis functions (trial functions ψ_i) chosen from a linearly independent set,

$$u^{app} \cong u = \psi_1 a_1 + \psi_2 a_2 + ... + \psi_n a_n = \sum_{i=1}^{n} a_i \psi_i = \begin{bmatrix} a_1 \\ a_2 \\ \vdots \\ a_n \end{bmatrix} \begin{bmatrix} \psi_1 & \psi_2 & \dots & \psi_n \end{bmatrix} = \boldsymbol{\psi}\mathbf{a}. \tag{6.18}$$

Thus, Equations (6.16) and (6.17) take the form

$$\int_a^b v(Lu^{app}+g)\mathrm{d}x = 0 \tag{6.19}$$

$$Lu^{app} + g = e \tag{6.20}$$

where e is the residual, the approximation not generally satisfying Equation (6.16) exactly. The residual (or error) depends upon the unknown parameters given by $\mathbf{a} = a_1, ... a_n$. The objective then is to choose a weight function v allowing these parameters to be determined, which implies, in turn, that the approximate solution Equation (6.18) provides is known. In other words, the notion of using the MWR is to force the weighted residual to a value zero, on the average, over the domain, i.e.

$$\int_V v_i e\mathrm{d}x = 0 \quad \text{with} \quad i = 1, 2, ...n, \tag{6.21}$$

where the number of weight functions v_i is exactly equal to the number of unknown constants a_i in u^{app}. The result is a set of n algebraic equations for the unknown constants a_i. The weight functions can be expressed by

$$v = V_1 c_1 + V_2 c_2 + ... + V_n c_n = \begin{bmatrix} V_1 \\ V_2 \\ \vdots \\ V_n \end{bmatrix} \begin{bmatrix} c_1 & c_2 & \dots & c_n \end{bmatrix} = \mathbf{V}\mathbf{c} = \mathbf{c}^T\mathbf{V}^T, \tag{6.22}$$

where $\mathbf{c}$ is an arbitrary vector and $\mathbf{V}$ are known functions of x. In inserting Equation (6.22) into (6.21), and since the expression must hold for any $\mathbf{c}^T$-matrices, n integral equations are obtained,

$$\begin{aligned} \mathbf{c}^T \int_a^b \mathbf{V}^T e\mathrm{d}x &= \mathbf{0}, \\ \int_a^b \mathbf{V}^T e\mathrm{d}x &= \mathbf{0}, \end{aligned} \tag{6.23}$$

where the residual e depends on the n unknowns $a_1 ... \ a_n$. The latter is a system of equations of the form $\mathbf{Ka} = \mathbf{f}$ (shown by insertion Equation (6.18) in (6.21)), through which is possible to determine those n unknowns, for which

$$\mathbf{K} = \begin{bmatrix} \int_a^b V_1 L(\psi_1)\mathrm{d}x & \int_a^b V_1 L(\psi_2)\mathrm{d}x & ... & \int_a^b V_1 L(\psi_n)\mathrm{d}x \\ \int_a^b V_2 L(\psi_1)\mathrm{d}x & \int_a^b V_2 L(\psi_2)\mathrm{d}x & ... & \int_a^b V_1 L(\psi_n)\mathrm{d}x \\ \vdots & \vdots & \vdots & \vdots \\ \int_a^b V_n L(\psi_1)\mathrm{d}x & \int_a^b V_n L(\psi_2)\mathrm{d}x & ... & \int_a^b V_n L(\psi_n)\mathrm{d}x \end{bmatrix}; \mathbf{f} = - \begin{bmatrix} \int_a^b V_1 g\mathrm{d}x \\ \int_a^b V_2 g\mathrm{d}x \\ \vdots \\ \int_a^b V_n g\mathrm{d}x \end{bmatrix}. \quad (6.24)$$

It will be observed that the derivative of the approximating function is employed here. This yields

$$\tilde{\boldsymbol{\nabla}}\mathbf{v} = \mathbf{Bc} \quad (6.25)$$

This procedure applies to all MWR, its being the $\mathbf{V}$ that is selected which distinguishes the different methods. It is not required that the weight functions be approximated by use of the same interpolants that are used for the trial solutions, although, for most problems it is advantageous to use the same approximation for the weight functions as for the trial solutions, this being what is commonly done. The method that possesses the latter distinguishing feature is called the Galerkin method. Use of the Galerkin method (see [95, 96] for more information), allows one to state that

$$V_i = \psi_i. \quad (6.26)$$

When using the Galerkin method in combination with the weak form, a symmetric coefficient matrix arises. This matter, as well as the applicability of this method to differential equations, generally suggest its fundamental importance in setting up the FE formulation.

FE equations: The FE approximations given in Equations (6.10) and (6.25) are then inserted into the terms (I), (III), (IV) and (V) as indicated in Equation (6.9).

$$\begin{aligned}
(I) \qquad & \int_V \mathbf{v}^T \rho \ddot{\mathbf{u}} \mathrm{d}V = \mathbf{c}^T \underbrace{\int_V \mathbf{N}^{\mathrm{eT}} \rho \mathbf{N}^{\mathrm{e}} \mathrm{d}V}_{\text{mass matrix } \mathbf{M}^{\mathrm{e}}} \ddot{\mathbf{a}}^{\mathrm{e}} \\
(III) \qquad & \int_V \mathbf{v}^T \mathbf{b} \mathrm{d}V = \mathbf{c}^T \underbrace{\int_V \mathbf{N}^{\mathrm{eT}} \mathbf{b} \mathrm{d}V}_{\text{body forces } \mathbf{f}_b^{\mathrm{e}}} \\
(IV) \qquad & \int_S \mathbf{v}^T \mathbf{t} \mathrm{d}S = \mathbf{c}^T \int_S \mathbf{N}^{\mathrm{eT}} \mathbf{t} \mathrm{d}S = \mathbf{c}^T \underbrace{\int_{\Gamma_h} \mathbf{N}^{\mathrm{eT}} \mathbf{h} \mathrm{d}S}_{\text{applied force } \mathbf{f}_s^{\mathrm{e}}} + \mathbf{c}^T \underbrace{\int_{\Gamma_g} \mathbf{N}^{\mathrm{eT}} \mathbf{t} \mathrm{d}S}_{\text{reaction force } \mathbf{f}_r^{\mathrm{e}}} \\
(V) \qquad & \int_V \left(\tilde{\boldsymbol{\nabla}} \mathbf{v} \right)^T \boldsymbol{\sigma} \mathrm{d}V = \mathbf{c}^T \int_V \left(\tilde{\boldsymbol{\nabla}} \mathbf{N}^{\mathrm{e}} \right)^T \boldsymbol{\sigma} \mathrm{d}V = \mathbf{c}^T \int_V \mathbf{B}^{\mathrm{eT}} \boldsymbol{\sigma} \mathrm{d}V.
\end{aligned} \quad (6.27)$$

Finally, summing all of the terms and cancelling $\mathbf{c}$ due to its arbitrary nature,

$$\begin{aligned} \mathbf{c}^T\mathbf{M}^{\mathrm{e}}\ddot{\mathbf{a}}^{\mathrm{e}} + \mathbf{c}^T \int_V \mathbf{B}^{\mathrm{eT}}\boldsymbol{\sigma}\mathrm{d}V = \mathbf{c}^T\left(\mathbf{f}_s^{\mathrm{e}} + \mathbf{f}_r^{\mathrm{e}} + \mathbf{f}_b^{\mathrm{e}}\right) \Rightarrow \\ \mathbf{M}^{\mathrm{e}}\ddot{\mathbf{a}}^{\mathrm{e}} + \int_V \mathbf{B}^{\mathrm{eT}}\boldsymbol{\sigma}\mathrm{d}V = \mathbf{f}^{\mathrm{e}}, \end{aligned} \tag{6.28}$$

which is the FE formulation valid for any constitutive relationship. Particularising for the linear elastic solid dynamic case and under conditions of zero initial strains, where $\boldsymbol{\sigma} = \mathbf{D}\boldsymbol{\varepsilon} = \tilde{\boldsymbol{\nabla}}\mathbf{N}^{\mathrm{e}}\mathbf{a}^{\mathrm{e}} = \mathbf{B}^{\mathrm{e}}\mathbf{a}^{\mathrm{e}}$, yields

$$\begin{aligned} \mathbf{M}^{\mathrm{e}}\ddot{\mathbf{a}}^{\mathrm{e}} + \underbrace{\int_V \mathbf{B}^{\mathrm{eT}}\mathbf{D}\mathbf{B}^{\mathrm{e}}\mathrm{d}V}_{\text{stiffness matrix } \mathbf{K}}\mathbf{a}^{\mathrm{e}} = \mathbf{f}^{\mathrm{e}} \Rightarrow \\ \mathbf{M}^{\mathrm{e}}\ddot{\mathbf{a}}^{\mathrm{e}} + \mathbf{K}^{\mathrm{e}}\mathbf{a}^{\mathrm{e}} = \mathbf{f}^{\mathrm{e}}, \end{aligned} \tag{6.29}$$

which is the element-wise FE formulation of a dynamic undamped problem, in which

$$\begin{aligned} \mathbf{M}^{\mathrm{e}} = \int_V \mathbf{N}^{\mathrm{eT}}\rho\mathbf{N}^{\mathrm{e}}\mathrm{d}V; \qquad \mathbf{K}^{\mathrm{e}} = \int_V \mathbf{B}^{\mathrm{eT}}\mathbf{D}\mathbf{B}^{\mathrm{e}}\mathrm{d}V \\ \mathbf{f}_b^{\mathrm{e}} = \int_V \mathbf{N}^{\mathrm{eT}}\mathbf{b}\mathrm{d}V; \qquad \mathbf{f}_s^{\mathrm{e}} = \int_{\Gamma_h} \mathbf{N}^{\mathrm{eT}}\mathbf{h}\mathrm{d}S; \qquad \mathbf{f}_r^{\mathrm{e}} = \int_{\Gamma_g} \mathbf{N}^{\mathrm{eT}}\mathbf{t}\mathrm{d}S \end{aligned} \tag{6.30}$$

If damping is present in the system, the term $\mathbf{C}^{\mathrm{e}}\dot{\mathbf{a}}^{\mathrm{e}}$ is added to the the left-hand side of Equation (6.29) to account for the damping forces present in the structure, the damping matrix $\mathbf{C}^{\mathrm{e}}$ being easily created by assuming Rayleigh damping, for example, as explained in Section 3.2.5. The equation of the dynamic damped problem in its complete form look like the one given in Equation (3.24).

Equation of motion of the whole system: The equilibrium equation obtained for each finite element can be applied to all of the finite elements in the structure. Once all the matrices have been created for each of the elements, the assembly process must be carried out according to

$$\bigcup_e \mathbf{M}^{\mathrm{e}}\ddot{\mathbf{a}}^{\mathrm{e}} + \bigcup_e \mathbf{K}^{\mathrm{e}}\mathbf{a}^{\mathrm{e}} = \bigcup_e \mathbf{f}^{\mathrm{e}}, \tag{6.31}$$

where $\bigcup_e$ is used here in order to indicate the assembly (union) of the magnitudes in question in accordance with the DOF of the structure. This yields the equation of motion for the system as a whole.

One can readily see that the size of the global stiffness, mass matrices and damping (if present) matrices $\mathbf{K}$, $\mathbf{M}$ and $\mathbf{C}$, respectively, is $n_{DOF_{total}} \times n_{DOF_{total}}$, whereas the size of the correspondent element matrices $\mathbf{K}^{\mathrm{e}}$, $\mathbf{M}^{\mathrm{e}}$ and $\mathbf{C}^{\mathrm{e}}$ is $n_{DOF_{el}} \times n_{DOF_{el}}$. The global and element force vectors, in turn, have the dimensions $n_{DOF_{total}} \times 1$ and $n_{DOF_{el}} \times 1$, respectively.

Finally, the boundary conditions must be applied in the correspondent positions of the matrix, i.e. in the DOF in question in order to reduce the order of the resultant system and allow its calculation. For further information regarding the assembly process, see for example, [95, 96].

6.2.1 Finite elements

Depending on the dimension, the basic finite elements can be divided into three different categories:

- Line elements: truss, beam and restriction elements.
- Area elements: plane stress, plain strain, axisymmetric, membrane, plate and shell.
- Volume elements: tetrahedral and hexahedral solid elements.

The criteria for selection of the proper element for each specific problem depends on many factors, such as the type of load applied (traction or compression, moment...), types of variables to be evaluated (displacements, rotations...), the geometry of the problem in question, etc. These need to be analysed by the analyst prior to performing the calculations.

Isoparametric elements

Normally, the sides of quadrilateral elements must be parallel to the coordinate axes in order for them to behave in a compatible manner. This restriction is very difficult to fulfil, however, when modelling bodies with arbitrary geometries. This can be done, nevertheless, with use of isoparametric elements, since the functions used for interpolating the geometry are coincident with those used for interpolating the displacements. Therefore, this was the type of elements used in the appended papers.

Consider a cubic domain bounded in a $\xi\eta\zeta$-coordinate system (parent domain) and also bounded by $\xi = \pm 1$, $\eta = \pm 1$ and $\zeta = \pm 1$. The transformation through which the parent domain is transformed into another, more complicated region is called *mapping*. The mapping that occurs transforms the parental domain into a global cartesian xyz-coordinate system as follows:

$$x = x(\xi, \eta, \zeta); \qquad y = y(\xi, \eta, \zeta); \qquad z = z(\xi, \eta, \zeta). \tag{6.32}$$

This relationship is univocal, i.e. for every point given by its $\xi\eta\zeta$-coordinates in the parent domain there exists a unique point given by its xyz-coordinates in the global domain. Differentiating Equation (6.32) and using the chain rule, leads to an expression that allows the following transformation between two domains to occur,

$$\begin{bmatrix} dx \\ dy \\ dz \end{bmatrix} = \begin{bmatrix} \frac{\partial x}{\partial \xi} & \frac{\partial x}{\partial \eta} & \frac{\partial x}{\partial \zeta} \\ \frac{\partial y}{\partial \xi} & \frac{\partial y}{\partial \eta} & \frac{\partial y}{\partial \zeta} \\ \frac{\partial z}{\partial \xi} & \frac{\partial z}{\partial \eta} & \frac{\partial z}{\partial \zeta} \end{bmatrix} \begin{bmatrix} d\xi \\ d\eta \\ d\zeta \end{bmatrix} = \mathbf{J}^{-1} \begin{bmatrix} d\xi \\ d\eta \\ d\zeta \end{bmatrix}, \tag{6.33}$$

where the matrix $\mathbf{J}$, which is related to the mapping, is the so-called Jacobian matrix. Equation (6.33) requires $\det\mathbf{J} \neq 0$. It should be emphasised that, even when the mapping is unique, this does not necessarily imply that it is possible to invert Equation (6.32) and obtain explicit solutions in the form of $\xi = \xi(x, y, z)$, $\eta = \eta(x, y, z)$ and $\zeta = \zeta(x, y, z)$ [95].

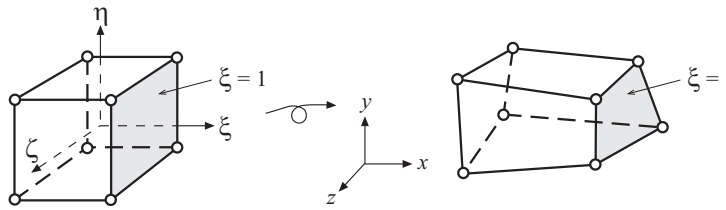

Figure 6.2: An eight-node three-dimensional isoparametric element [95].

If an element behaves in a conforming, i.e. compatible, manner in the parent domain, its isoparametric version also behaves in a conforming way, no mismatch between adjacent elements existing. The completeness criterion is satisfied with use of Equation (6.13). If the compatibility and completeness requirements are fulfiled individually, then the element in question fulfils the convergence criterion as well. Mapping an element requires that the vertex-nodes on the parent domain also be located in the boundary after the transformation has taken place [95].

6.3 Finite element prediction tools

In the present dissertation, intensive use was made of the FE method, specifically as provided by the FE package *Abaqus*, a software for finite element analysis created by Dassault Systems [58], in efforts to seek and develop prediction tools for lightweight timber buildings.

The costly process of using test buildings is common, even though the measurement results obtained are not directly applicable to buildings of slight different construction [3]. Prediction models, despite their being highly useful for the designing of new buildings, through their serving to prevent the need of severe and costly changes in the aftermath of construction, are still very much lacking today, this being an extreme drawback in the designing of multi-storey wooden buildings. Gaining an adequate understanding of the dynamic behaviour of multi-storey lightweight buildings, also at low frequencies, requires the use FE models here that represent the geometry of the buildings in great detail, since small structural modifications can have a strong effect on the vibration transmission paths there. One of the major objectives of the appended publications presented in the dissertation is to develop methods of applying the FE predictions tools considered in the low frequency range.

The vibration transmission between two adjacent storeys in a TVE-based building was investigated in **Paper C** [98], in which results obtained through use of an FE model of two adjacent TVEs for checking on a variety of construction configurations within the volume elements were analysed (cf. Figure 6.3(a)). Knowledge of the behaviour of the structure was gained by investigating the parameters affecting the response that was found to occur, this enabling a more refined model to be developed on the basis of these

findings. The relative differences between the modelled results were of greater importance than the absolute correlation between the output from the simulations and the existent measurements. One major conclusion was that the FE model needed to be developed further in order to eventually more adequately mimic the experimental data.

In line with this, the initial development of the FE model here involved efforts to obtain a more accurate material model of an elastomer placed between different storeys in a TVE-based building; see Figure 2.2. A method for determining linear viscoelastic properties of the material, one based on the laboratory testing, material modelling and FE simulations of a test block used in the actual constructions involved was developed in **Paper D** [99].

To unerringly predict the real behaviour of the types of construction under study and match the FE results there with the actual measurements, still further construction features need to be looked into, such as the following:

- A further development which is currently underway involves the inclusion of air and insulation in the wall and floor-ceiling cavities as in reality, since only structural vibration transmission has been considered in [98].

- The assembling of more TVEs, both in the vertical and the horizontal direction, encompassing the entire building in this way, studying the global modes of vibration involved and examining the flanking transmission in one specific room. Account in particular would be taken above all of the low frequency range, which is of greatest concern in lightweight buildings. A major problem is that in assembling the many different volume elements into a global model, the number of DOFs quickly increases to the point of exceeding the limits of the computer capacity available, at least for calculation times that are reasonable. Reduction methods, component mode synthesis (CMS) [100], for example, will thus eventually need to be adopted for performing calculations for applying the FE model to the building as a whole.

- Simplification of the elastomer blocks employed, through use of a simplified approach of considering the elastomers as constituting a discrete spring-and-dashpot system. This is seen as being a very suitable and efficient approach to carry out time-consuming FE simulations, one that enables substructuring reduction techniques to be employed in, when eventually assembling the different parts involved into an entire building.

- Mimicking the conditions under which the measurements are performed on site, a step which is regarded as being of crucial importance, like the scaling of the input force in the FE model to the source spectra of the excitation employed (a Japanese ball, an ISO tapping machine, an impact hammer, etc.), as well as consideration of the right boundary conditions being needed in connection with this.

- Some other improvements as the inclusion of tie plates and metal studs between different TVEs, the consideration of different types of connections between buildings parts, and the like.

Some ongoing developments on the FE model dealt with in **Paper C** described above, are published in an AkuLite-project report, [101].

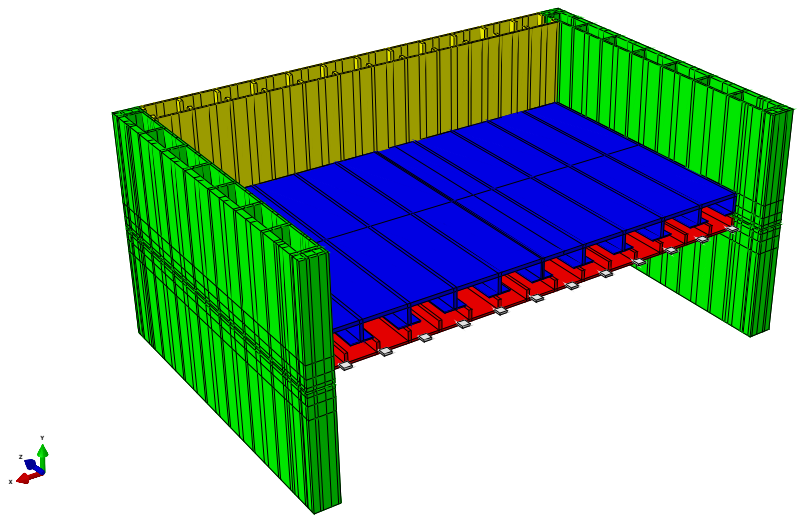

(a) Entire FE model. For clarity, two apartment separating walls were removed.

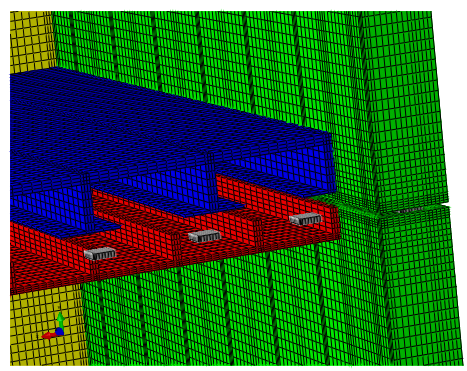

(b) Detail of the junction.

Figure 6.3: One of the FE models used in **Paper C**, its representing two halves of two TVEs, one stacked on top of the other. The blocks of elastomer are shown in grey colour, the floor in blue, the ceiling in red, the inner walls (apartment separating walls) in yellow and the outer (facade) walls in green.

7 Appended papers

Paper A
Psycho-vibratory evaluation of timber floors – Part I: Existent criteria, measurement protocol and analysis of objective data.
J. Negreira, K. Jarnerö, A. Trollé, L-G. Sjökvist, D. Bard.
Submitted for publication. June 2013.

Paper B
Psycho-vibratory evaluation of timber floors – Part II: Towards the determination of a design indicator of vibration acceptability and vibration annoyance.
A. Trollé, L-G. Sjökvist, K. Jarnerö, J. Negreira, D. Bard.
Submitted for publication. June 2013.

Paper C
Investigation of the vibration transmission through a lightweight junction with elastic layer using the finite element method.
J. Negreira, A. Sjöström, D. Bard.
Proceedings of Internoise 2012, New York, USA.

Paper D
Characterisation of an elastomer for noise and vibration isolation in lightweight timber buildings.
J. Negreira, P-E. Austrell, O. Flodén, D. Bard.
Submitted for publication. September 2013.

7.1 Summary of the appended papers

7.1.1 Paper A

In lightweight housing constructions containing timber floors, vibrations can be a nuisance for inhabitants. The vibrational response of wooden floor systems is thus an issue in need of being dealt with more adequately in the designing of such buildings. Studies addressing human response to vibrations are needed in order to be able to better estimate what level of vibrations in dwellings can be seen as acceptable. In the present study, measurements on five different floors were performed in a laboratory environment. Acceleration

measurements were carried out while a person either was walking on a particular floor or was seated in a chair placed there as the test leader was walking on the floor. These participants filled out a questionnaire regarding their perception and experiencing of the vibrations in question. Independent of the subjective tests, acceleration measurements were also carried out, using a shaker as a source of excitation, with the aim of determining the dynamic characteristics of the floors. Also, static load tests were performed using displacement gauges in order to measure the floor deflections. The ultimate aim of the study was to develop an indicator of human response to vibrations, based on relationships between the questionnaire responses obtained and the parameter values determined on the basis of the measurements carried out. This indicator was to be one that could eventually be used as a design guideline for manufacturers regarding the vibration serviceability of different timber floors. This part of the overall study, i.e. *Part I*, i.e. **Paper A**, presents a literature review of the topics dealt with, a description of the measurements performed, an analysis of the objective data obtained, as well as a classification of the floors in accordance with several different serviceability criteria. *Part II*, i.e. **Paper B**, in turn, deals with the statistical analysis of the objective and the subjective data with the aim of developing an indicator of vibration acceptability and vibration annoyance. The criteria used for classification of the floors ([22], [43] and [49]) were found to describe well the performance of the floors in terms of vibration acceptability, especially in the case of measured data, certain discrepancies being found when calculated data were employed.

7.1.2 Paper B

This paper is the second part of a report on work dealing with the psycho-vibratory evaluation of timber floors. The companion paper, *Part I* (here in the dissertation denoted as **Paper A**), reviewed the existent criteria for the vibration serviceability of timber floors and described measurements performed in a laboratory environment at two locations in Sweden (SP in Växjö and LU in Lund). The data stemming from those measurements served as input for the present study, aimed at obtaining further knowledge concerning human response to vibrations in wooden floors. The study involved primarily the conjoint analysis of merged subjective data and objective parameters, with the goal of determining a design indicator both of vibration acceptability and of vibration annoyance, use being made of multilevel regression. Although the sample of floors tested was small (5 altogether), certain clear trends could be noted. In particular, the first eigenfrequency (calculated in accordance with Eurocode 5) and Hu and Chui's criterion (calculated from measured quantities) proved to be the best indicators of vibration annoyance, and the Maximum Transient Vibration Value (computed on the basis of the accelerations experienced by the test subjects) to be the best indicator of vibration acceptability.

7.1.3 Paper C

When the Swedish construction code in 1994 allowed wooden multi-storey buildings, this type of lightweight structures became popular due to low cost and ease of construction. A drawback in those buildings is disturbing vibrations and noise propagating in the con-

struction, especially through the junctions, for example between floor and wall. These structures should not just meet the demands of structural integrity but also the dynamic requirements. Therefore, gaining knowledge about their dynamic behaviour is of crucial importance. To reduce noise and vibration through the junctions, rubber foam materials may be introduced between the walls and the floors and ceilings. Hence, finite element simulations are useful as a prediction tool during the design phase. In this study, the properties of a junction when introducing a rubber foam material – Sylodyn® – in between were investigated by means of the finite element method using the commercial software *Abaqus*. The flanking transmission was specifically analysed. The main conclusion was that in order to mimic the measurements with numerical FE simulations, the model had to be further refined and developed, as non-realistic results, such as nearly total vibration reduction within a junction, were sometimes obtained.

7.1.4 Paper D

Lightweight timber constructions have gained popularity in Sweden since 1994, when the national building regulations revoked a ban on constructing wooden multi-storey buildings. Since then, regulations regarding impact and airborne sound insulation have become increasingly stringent due in particular to complaints by inhabitants and the development accordingly of new building techniques. In line with this, elastomers have frequently been used at junctions between walls, floors and ceilings so as to reduce low frequency noise travelling through the structure. The development of prediction tools by using numerical methods such as the finite element (FE) method, for example, is needed in tackling flanking transmission problems during the design phase of buildings, this saving time and costs for builders. In order to create accurate models, the exact material properties involved are required as input. The properties of elastomers are often provided by manufacturers in the form of a data sheet. These properties are often closely linked to such structural effects as shape factors and boundary conditions of the samples and tests. Material properties are normally of interest for modelling arbitrary sizes and shapes of the elastomers selected, depending on the type of construction involved. Thus, accurate and handy methods for the characterisation of elastomers are needed in order to obtain precise material properties to serve as inputs for simulations. The present research concerns the characterisation of an elastomer, the properties of the elastomer material being investigated by comparing results obtained by analytical calculations, FE simulations, and mechanical testing in a uni-axial testing machine. Frequency-dependent material properties were obtained, separating geometry and material dependence. A method, one based on results of the present study, for extracting the material properties of an elastomer from the manufacturer's data sheet and solely based on the knowledge of the static modulus of elasticity, is presented. These properties are to ultimately serve as input to commercial FE softwares for setting up models acting as prediction tools of lightweight wooden buildings.

8 Conclusions

8.1 Concluding remarks

Although research within the field of lightweight wooden buildings has increased in recent years, much is left yet to do in investigating the vibratory and acoustic behaviour of such constructions, before the performance in all of them can be regarded as predictable and as satisfactory for those living in them. There are two major goals connected with achieve this that were aimed at in the dissertation:

- Gaining more adequate insight into human response and perception of floor vibrations.
- Developing more adequate numerical prediction tools for use in connection with lightweight wooden buildings.

Human response to floor vibrations was studied through carrying out of psycho-vibratory tests of five different timber floors in which 60 participants took part, their describing how they experienced both the vibrations they produced in walking on the floors and while seated in a chair experiencing the vibrations another person produced in strolling by. How they experienced those vibrations was assessed via questionnaires and was related to different objective parameters that were measured (accelerations, deflections, and the like). It was shown that the non-standarised criteria found in the literature ([22], [43] and [49]) described the floors rather well in terms of vibration acceptability as shown by the measured data that were obtained, certain discrepancies being found when calculated data were employed. In the course of the study, multilevel regression was employed for investigating relationships between the subjects' answers to the questionnaire and both measured and calculated objective parameters of the floors in question in efforts to determine the best indicators of vibration acceptability and vibration annoyance, its being found to be a valuable tool for modelling repeated measures data that involve substantial inter-individual differences in rating. Two of the objective parameters tested were found to be the best indicators of vibration annoyance, the one being Hu and Chui's criterion, $r_{HC,m}$ (calculated from measured quantities), the other being the first eigenfrequency calculated in accordance with Eurocode 5, $f_{1,c,EC5}$. The Maximum Transient Vibration Value, MTVV, determined on the basis of the accelerations experienced by the subjects, proved to be the best indicator of vibration acceptability.

It was also shown that the effects of changes in buildings could be assessed during their design phase by use of prediction tools based on such numerical methods as the

FE method, thus avoiding the high costs of constructing prototypes and performing measurements that otherwise be required. Accurately assessing the dynamic behaviour of a building here in an adequate way requires use of FE models representing the geometry of the building in great detail, since small modifications in the structure can strongly affect the vibration transmission paths. Accurate properties of the materials involved are also needed, as small differences in these could have a marked effect on the final results. Timber volume element (TVE) based buildings were analysed here in particular, due to the recent growth of interest in Sweden in their being built, and also because of the systematisation of the method of building. A first step in the present project was to carry out several parametric studies aimed at obtaining a better understanding of the FE models involved. On the base of these, it was concluded that further refinement of the model or methodology was needed if on site measurement results obtained in similar buildings were to be ultimately mimicked. An initial advance made there was to obtain reliable-appearing material properties of the elastomers used at the junctions of buildings of this type, since the first material model employed appeared to not lead to realistic conclusions regarding the functioning of the resilient material. A method for extracting the material properties of the elastomer from a data sheet provided by the manufacturer, such properties there often being linked with structural effects such as shape factors and the boundary conditions of the samples and tests, was developed, one in which only the static modulus of elasticity is needed in order to obtain the frequency-dependent linear viscoelastic material properties of the elastomer.

All in all, the research reported on here aimed at being able to predict more accurately and better understand the low frequency sound. The results obtained provided insight into two basic pillars of research in investigating vibrations in lightweight buildings, the one being that of research on human perception of floor vibrations and the other being research concerned with the development of numerical prediction tools. Many problems remain, however, still nowadays, as highlighted in several reports (still to be published) within the framework of the Swedish project AkuLite (cf. [24] amongst others). It was noted there that despite the lightweight wooden buildings complying with the standardised criteria currently employed, subjective vibratory studies of modern timber framework buildings still frequently show inhabitants of these buildings to often be annoyed by vibrations. Thus, further work in the field is called for. The conclusions just drawn paved the way to further research reported on in Section 8.2.

8.2 Proposals for further work

The findings obtained concerning the psycho-vibratory tests that were carried out were obtained in what can be considered a pilot study, in the sense of its involving only a small sample of wooden floors (five different ones), although there was a sufficiently large number of subjects to provide clear statistical support for the conclusions drawn concerning these floors. This can serve as a starting point to a follow up study involving a larger sample of wooden floors, making it possible to extract power laws concerning vibration acceptability and annoyance. This could be of critical importance, since reconsideration of the existent criteria and the development of new ones seem called for.

Particular efforts should be directed at the development of better prediction tools. In [3] the necessity of developing such tools for purposes of prognosis is specifically emphasised. One should be aware, however, that wooden frame constructions can be quite complex, showing strong variations both within each floor and wall element, as well as in the couplings, material and facade elements, making the development of a general prediction tool difficult. At the same time, the steady increase in the industrial production of volume buildings makes the development of a thoroughly appropriate engineering prediction model seem more feasible than before, due in part to the standardisation of the building technique. This is the main type of buildings the dissertation has dealt with and regarding which research should continue.

The future improvements of the models (apart from the first presented in **Paper D**) which can lead to the development of a model able to predict the behaviour of the buildings in question in a highly realistic way (some already advanced in Section 6.3) are:

- Models involving the inclusion of air and insulation in the wall and in floor-ceiling cavities, since only structural vibration transmission has been considered in practical terms thus far. Fluid-structure interaction can affect the vibrational behaviour here through the propagation of vibrations through acoustic media.

- Models involving the assembly of more TVEs than two, both in the vertical and in the horizontal direction, so as to simulate the behaviour of the entire building and be able to take account of global modes of vibration.

- Relating the results such models provide to specific measurements that are undertaken in order to validate the predictive tools that are employed will be important. Both the model in question and the measurements would need to have the same boundary conditions, the same input load (done by scaling the input force in the FE model to the source spectra of the excitation source employed in the measurements), and the like.

Bibliography

[1] Näringsdepartementet: Mer trä i byggandet: underlag för en nationell strategi att främja användning av trä i byggandet (in Swedish), (*More wood in construction: basis for a national strategy to promote use of wood in construction*), Ds 2004: 1, Ministry of Industry, Employment and Communications, Government of Sweden, Stockholm, 2004.

[2] COST Action FP0702: Net-Acoustics for Timber based lightweight buildings and elements. eBook, 2012.

[3] J. Forssén, W. Kropp, J. Brunskog, S. Ljunggren, D. Bard, G. Sandberg, F. Ljunggren, A. Ågren, O. Hallström, H. Dybro, K. Larsson, K. Tillberg, L-G. Sjökvist, B. Östman, K. Hagberg, Å. Bolmsvik, A. Olsson, C-G. Ekstrand, M. Johansson: Acoustics in wooden buildings. State of the art 2008. Vinnova project 2007-01653, Report 2008:16, SP Trätek (Technical Research Institute of Sweden), Stockholm, 2008.

[4] A. Homb: Low frequency sound and vibrations from impacts on timber floor constructions. PhD thesis, NTNU (Norwegian university of science and technology), Trondheim, Norway, 2005.

[5] S. Thelandersson, H.J. Larsen: Timber engineering. Wiley, Chichester, UK, 2003.

[6] J. Gibson McIlvain: Lumber supplier. Web, seen on May 15$^{\text{th}}$ 2013.

[7] Egger International. Web, seen on May 15$^{\text{th}}$ 2013.

[8] AzkoNobel wood coatings. Web, seen on May 15$^{\text{th}}$ 2013.

[9] Buildipedia. Web,seen on May 15$^{\text{th}}$ 2013.

[10] Alibaba: Global Trade Products. Web, seen on May 15$^{\text{th}}$ 2013.

[11] N. Labonnote: Damping in timber structures. PhD thesis. Norwegian University of Science and Technology, Trondheim, Norway, June 2012.

[12] Å. Bolmsvik: Structural-acoustic vibrations in wooden assemblies – Experimental modal analysis and finite element modelling. PhD thesis. Linnaeus University, Sweden, 2012.

[13] F. Ljunggren, A. Ågren: Potential solutions to improved sound performance of volume based lightweight multi-storey timber buildings. Applied Acoustics **72** (2011) 231–240.

[14] A. Ågren: Acoustic highlights in Nordic light weight building tradition – focus on ongoing development in Swedish. Proceedings of BNAM, Bergen, Norway, 2010.

[15] C. L. Morfey: Dictionary of acoustics. Academic Press, Trowbridge, UK, 2001.

[16] SS 25267: Acoustics – Sound classification of spaces in buildings – Dwellings. Swedish Standards Institute, Stockholm, Sweden, 2007.

[17] SS 25268: Acoustics – Sound classification of spaces in buildings – Institutional premises, rooms for education, preschools, leisure.time centres, rooms for office work and hotels. Swedish Standards Institute, Stockholm, Sweden, 2007.

[18] ISO 701-1: Acoustics – Rating of sound insulation in buildings and of building elements – Part 1: Airborne sound insulation. International Organization for Standardisation, Geneva, Switzerland, 1996.

[19] ISO 701-2: Acoustics – Rating of sound insulation in buildings and of building elements – Part 2: Impact sound insulation. International Organization for Standardisation, Geneva, Switzerland, 1996.

[20] EN 12354-1 to 6: Building acoustics – Estimation of acoustic performance in buildings from the performance of elements. European Committee for Standardisation, Brussels, Belgium, 2000.

[21] S. Schoenwald: Flanking sound transmission through lightweight framed double leaf walls – Prediction using statistical energy analysis. PhD thesis, Technische Universiteit Eindhoven, The Netherlands, 2008.

[22] EN 1995-1-1: Eurocode 5 – Design of timber structures – Common rules and rules for buildings. European Committee for Standardisation, Brussels, 2004.

[23] J. Weckendorf: Dynamic Response of Structural Timber Flooring Systems. PhD thesis, Edinburgh Napier University, UK, 2009.

[24] K. Jarnerö, D. Bard, C. Simmons: Vibration performance of apartments buildings with wooden framework – Residents' survey and field measurements. AkuLite Rapport 6, SP Rapport 2013:17, ISBN: 978-91-87461-02-6, 2013.

[25] K. Hagberg: Evaluation of sound insulation in the field. Licenciate dissertation, Department of Construction Sciences, Division of Engineering Acoustics, Lund University, Sweden, 2005.

[26] F. Ljunggren: Floor Vibration – Dynamic Properties and Subjective Perception. PhD thesis, Department of Human Work Sciences, Division of Sound and Vibration, Luleå University of Technology, Sweden, 2006.

[27] M. J. Griffin: Handbook of human vibration. Academic Press Limited, London, UK, 1996.

[28] A. Pavic, P. Reynolds: Vibration Serviceability of Long-Span Concrete Building Floors. Part 1: Review of Background Information. The Shock and Vibration Digest **34(3)** (2002) 191–211.

[29] ISO 2631-1: Vibration and shock – Evaluation of human exposure to whole-body vibration – Part 1: General requirements. International Organization for Standardisation, Geneva, Switzerland, 1997.

[30] H. Reiher, F. J. Meister: The effect of vibration on people. Published in German in 1931, English Translation in Report No. F-TS-616-R.E.Headquarters, Air Material Command, Wright Field, Ohio, USA, 1949.

[31] K. H. Lenzen: Vibration of steel joist-concrete slab floors. AISC Engineering Journal **3** (1966) 133–136.

[32] J. F. Wiss, R. A. Parmelee: Human perception of transient vibrations. Journal of the Structural Division ASCE **100(4)** (1974) 773–787.

[33] D. E. Allen, J. H. Rainer: Vibration criteria for long-span floors. Canadian Journal of Civil Engineering **3** (1976) 165–173.

[34] T. M. Murray: Acceptability criterion for occupant-induced floor vibrations. Engineering Journal AISC **2nd Qtr.** (1981) 62–70.

[35] S. Ohlsson: Floor Vibrations and Human Discomfort. PhD thesis, Chalmers University, Göteborg, Sweden, 1982.

[36] S. R. Alvis: An Experimental and Analytical Investigation of Floor Vibrations. M.Sc. Thesis, Virginia Polytechnic Institute and State University, USA, 2001.

[37] E. S. Bernard: Dynamic serviceability in lightweight engineered timber floors. ASCE Journal of Structural Engineering **134(2)** (2008) 258–268.

[38] ISO 2631-2: Evaluation of human exposure to whole-body vibration – Part 2: Continuous and shock-induced vibration in buildings (1 Hz to 80 Hz). International Organization for Standardisation, Geneva, Switzerland, 1989.

[39] ISO 2631-2: Vibration and shock – Evaluation of human exposure to whole-body vibration – Part 2: Vibration in buildings (1 Hz to 80 Hz). International Organization for Standardisation, Geneva, Switzerland, 2003.

[40] L. J. Hu, Y. H. Chui: Vibration serviceability of timber floors in residential construction. Progress in Structural Engineering and Materials **3** (2001) 228–237.

[41] R. O. Foschi, A. Gupta: Reliability of floors under impact vibration. Canadian Journal of Civil Engineering **14** (1987) 683–689.

[42] D. M. Onysko: Performance and acceptability of wood floors – Forintek studies. National Research Council of Canada, Publication 28822, Forintek Canada Corp., Ottawa, 1988.

[43] J. D. Dolan, T. M. Murray, J. R. Johnsson, D. Runte, B. C. Shue: Preventing annoying wood floor vibrations. Journal of Structural Engineering **125(1)** (1999) 19–24.

[44] S. Ohlsson: Springiness and human-induced floor vibrations – A design guide. Swedish Council for Building Research, Stockholm, 1988.

[45] I. Smith, Y.H. Chui: Design of light-weight wooden floors to avoid human discomfort. Canadian Journal of Civil Engineering **15** (1988) 254–262.

[46] B. R. Ellis: On the response of long-span floors to walking loads generated by individuals and crowds. The Structural Engineer **78(10)** (2000) 17–25.

[47] P. Hamm, A. Richter, S. Winter: Floor vibrations – New results. Proceedings of the 11th World Conference on Timber Engineering, Riva del Garda, Italy, 2010.

[48] T. Toratti, A. Talja: Classification of human induced floor vibrations. Building Acoustics **13(3)** (2006) 211–221.

[49] L. J. Hu, Y. H. Chui: Development of a design method to control vibrations induced by normal walking action in wood-based floors. Proceedings of the 8th World Conference on Timber Engineering, Lahti, Finland, 2004.

[50] D. E. Allen, T. M. Murray: Design criteria for vibrations due to walking. Engineering Journal AISC **30(4)** (1993) 117–129.

[51] J. Porteus, A. Kermani: Structural timber design to Eurocode 5, Wiley, 2008.

[52] A. A. Al-Foqaha'a, W. F. Cofer, K. J. Fridley: Vibration Design Criterion for Wood Floors Exposed to Normal Human Activities. Journal of Structural Engineering **125** (1999) 1401–1406.

[53] I. Glisovic, B. Stevanovic: Vibrational Behaviour of Timber Floors. Proceedings of the 11th World Conference on Timber Engineering, Riva del Garda, Italy, 2010.

[54] A. K. Chopra: Dynamics of structures. Prentice Hall, New Jersey, USA, 2007.

[55] R. R. Craig Jr, A. J. Kurdila: Fundamentals of Structural Dynamics, Hoboken, John Wiley & Sons, New Jersey, USA, 2006.

[56] C. Hopkins: Sound Insulation. Elsevier, Oxford, UK, 2007.

[57] O. A. B. Hassan: Building Acoustics and Vibration: Theory and Practice. World Scientific, Singapore, 2009.

[58] Dassault Systèmes: Abaqus theory manual, Version 6.11, 2012.

[59] A. Ågren, F. Ljunggren, Å. Bolmsvik: Flanking transmission in light weight timber houses with elastic flanking isolators. Proceedings of Internoise, New York, USA, 2012.

[60] S. Ljunggren: Measurement of the performance of noise controlling devices in buildings of massive wood. Working Report 2001:42001. Department of Civil and Architectural Engineering, Division of Building Technology, KTH, Stockholm, Sweden, 2001.

[61] F. Ljunggren, A. Ågren: Potential solutions to improved sound performance of volume based lightweight multistory timber buildings. Applied Acoustics **72** (2011) 231–240.

[62] P-E. Austrell: Modeling of elasticity and damping for filled elastomers. PhD thesis, Division of Structural Mechanics, Lund University, Sweden, 1997.

[63] L. C. Forthergill, T. Carman: A comparison of methods for rating the insulation of floors against impact sound. Building Research and Practice. The Journal of CIB **18**(4) (1990), 245–249.

[64] JIS A 1418-1: Measurement of floor impact sound insulation of buildings – Part 1: Method using standard light impact source. Japanese Standards Association, Tokio, Japan, 2000.

[65] W. Shi, C. Johansson, U. Sundbäck: An investigation of the characteristics of impact sound sources for impact sound insulation measurement. Applied Acoustics **51**(1) (1997), 85–108.

[66] JIS A 1418-2: Measurement of floor impact sound insulation of buildings – Part 2: Method using standard heavy impact sources, Japanese Standards Association, Tokio, Japan, 2000.

[67] SP Technical Research Institute of Sweden. Web, seen on July 25$^{\text{th}}$ 2013.

[68] Brüel&Kjær. Web, seen on July 25$^{\text{th}}$ 2013.

[69] R. H. Bishop: The mechatronics handbook, CRC Press, Boca Raton, USA, 2002.

[70] Brüel&Kjær: Piezoelectric Accelerometers and Vibration Preamplifiers. Theory and Application Handbook, Brüel&Kjær, Nærum, Denmark, 1978.

[71] Brüel&Kjær: Measuring Vibration. Primer, Nærum, Denmark, 1982.

[72] ISO 5348: Mechanical vibration and shock – Mechanical mounting of accelerometers. International Organization for Standardisation, Geneva, Switzerland, 1998.

[73] IEEE 1293: IEEE Standard Specification Format Guide and Test Procedure for Linear, Single-Axis, Non-gyroscopic Accelerometers, Institute of Electrical and Electronics Engineers, New York, USA, 1999.

[74] M. Andrejasi: MEMS accelerometers – A seminar, University of Ljubljana, Faculty for mathematics and physics, Department of Physics, Ljubljana, Slovenia, 2008,

[75] ISO 16063: Methods for the calibration of vibration and shock transducers – Part 21: Vibration calibration by comparison to a reference transducer, International Organization for Standardisation, Geneva, Switzerland, 2003.

[76] R. Darula, A. Sjöström, J. Negreira: Calibration of MEMS accelerometers. In preparation to be published as an internal report. Department of Construction Sciences, Lund University, Sweden.

[77] Duncan Electronics Division: Miniature spring return linear motion position sensor, Data Sheet, BEI Technologies.

[78] Brüel&Kjær: Force Transducers – Types 8200 and 8201, Product Data, Nærum, Denmark.

[79] B. J. Schwarz, M. H. Richardson: Experimental Modal Analysis. In CSI Reliability Week, Orlando, USA, 1999.

[80] W. Heylen, S. Lammens, P. Sas: Modal analysis – Theory and testing, Heverlee, Katholieke Universiteit Leuven, Belgium, 2007.

[81] A. Grané: Análisis de componentes principales (in Spanish). Lecture notes, Department of Statistics, University Carlos III Madrid, Spain, 2012.

[82] P. González Martín, A. Díaz de Pascual, E. Torres Lezama, E. Garnica Olmos: Una aplicación del análisis de componentes principales en el área educativa (in Spanish). Faculty of economic and social sciences and institute of economic and social research, Mérida, Venezuela, Revista Economía **9** (1994) 55–72.

[83] J. De Leeuw: Principal component analysis of binary data: Applications to roll-call analysis. Technical Report n°364, UCLA Department of Statistics, Los Angeles, CA, USA, 2003.

[84] J. J. Chang, J. D. Carroll: How to use MDPREF: A computer program for multidimensional analysis of preference data. Technical Report, Bell Telephone Laboratories, Murray Hill, NJ, USA, 1969.

[85] J. D. Carroll: Individual differences and multidimensional scaling. In R. N. Shepard, A. K. Romney, et S. B. Nerlove (editors): Multidimensional Scaling: Theory and Applications in the Behavioral Sciences, **1** (1972) 105–155. Seminar Press, New York and London.

[86] C. Eckart, G. Young: The approximation of one matrix by another of lower rank. Psychometrika **1** (1936), 211–218.

[87] The New MDSX Project: The MDS(X) Series of Multidimensional Scaling Programs. User's manual, Technical Report 51, Inter-University / Research Council Series, Inter-University/Research Council Series, 1981.

[88] R. B. Cattell: The Scree Test for the Number of Factors, Multivariate Behavioral Research **1** (1966) 245–276.

[89] A. P. M. Coxon: The user's guide to multidimensional scaling, Heinemann Educational Books, London, England, 1982.

[90] M. R. Schroeder, D. Gottlob, K. F. Siebrasse: Comparative study of european concert halls: Correlation of subjective preference with geometric and acoustic parameters, Journal of the Acoustical Society of America **56**(4) (1974), 1195–1201.

[91] A. Gelman, J. Hill: Data analysis using regression and multilevel/hierarchical models. Cambridge University Press, New York, NY, USA, 2007.

[92] J. J. Hox: Multilevel analysis – Techniques and applications, Hogrefe and Huber, New York, USA, 2010.

[93] H. Goldstein: Multilevel Statistical Models. Wiley, London, England, 2011.

[94] B. G. Tabachnick, L. S. Fidell: Using multivariate statistics. Pearson A & B, Boston, USA; 2007.

[95] N. Ottosen, H. Petersson: Introduction to the finite element method. Prentice Hall, England, 1992.

[96] K. J. Bathe: Finite Element Procedures. Prentice Hall, New York, USA, 1996.

[97] J. T. Celigüeta Lizarza: Método de los elementos finitos para análisis estructural (in Spanish), Unicopia C.B., San Sebastián, Spain, 2000.

[98] J. Negreira Montero, A. Sjöström, D. Bard, Investigation of the vibration transmission through a lightweight junction with elastic layer using the finite element method, Proceedings of Internoise 2012, New York, USA, 2012.

[99] J. Negreira, P-E. Austrell, O. Flodén, D. Bard: Characterisation of an elastomer for noise and vibration isolation in lightweight timber buildings. Submitted for publication, September 2013.

[100] R. R. Craig: Structural Dynamics; An Introduction to Computer Methods, John Wiley & sons Inc., New York, United States, 1981.

[101] J. Negreira, D. Bard: Finite element modelling of a Timber Volume Element based building with elastic layer insolators, AkuLite final report, SP Rapport 2013:27, Sweden, 2013.

Part II

Appended publications

Paper A

Psycho-vibratory evaluation of timber floors – Part I: Existent criteria, measurement protocol and analysis of objective data.

J. Negreira[1], K. Jarnerö[2], A. Trollé[3], L-G. Sjökvist[2], D. Bard[1].

[1]Lund University,
Department of Construction Sciences, Division of Engineering Acoustics,
P.O. Box 118, 221 00 Lund, Sweden.

[2]SP Technical Research Institute of Sweden, SP Wood Technology,
Vidéum Science Park, SE-35196, Växjö, Sweden.

[3]Université de Lyon, Labex CeLyA,
École Nationale des Travaux Publics de l'État, Laboratoire Génie Civil et Bâtiment,
Rue M. Audin, 69518 Vaulx-en-Velin Cedex, France.

Submitted for publication, June 2013.

Contributions: In this paper, Juan Negreira carried out all measurements performed at Lund University and post processed them. Likewise, he made the merging of the data coming from both laboratories (Lund University and SP Technical Research Institute of Sweden), as well as all the writing of the article. All other authors proofread the paper, and contributed with ideas about the experimental procedure. Specifically, those working at SP also performed the same measurements as those done in Lund at a different time. The raw data obtained at SP was sent to Lund University and served as input to carry out the merging.

Psycho-vibratory evaluation of timber floors – Part I: Existent criteria, measurement protocols and analysis of objective data

J. Negreira[1], K. Jarnerö[2], A. Trollé[3], L-G. Sjökvist[2], D. Bard[1].

[3]Lund University, Department of Construction Sciences, Division of Engineering Acoustics, P.O. Box 118, 221 00 Lund, Sweden.

[2]SP Technical Research Institute of Sweden, SP Wood Technology, Vidéum Science Park, SE-35196, Växjö, Sweden.

[3]Université de Lyon, Labex CeLyA, École Nationale des Travaux Publics de l'État, Laboratoire Génie Civil et Bâtiment, Rue M. Audin, 69518 Vaulx-en-Velin Cedex, France.

Abstract

In lightweight housing constructions containing timber floors, vibrations can be a nuisance for inhabitants. The vibrational response of wooden floor systems is thus an issue in need of being dealt with more adequately in the designing of such buildings. Studies addressing human response to vibrations are needed in order to be able to better estimate what level of vibrations in dwellings can be seen as acceptable. In the present study, measurements on five different floors were performed in a laboratory environment. Acceleration measurements were carried out while a person either was walking on a particular floor or was seated in a chair placed there as the test leader was walking on the floor. These participants filled out a questionnaire regarding their perception and experiencing of the vibrations in question. Independent of the subjective tests, acceleration measurements were also carried out, using a shaker as a source of excitation, with the aim of determining the dynamic characteristics of the floors. Also, static load tests were performed using displacement gauges in order to measure the floor deflections. The ultimate aim of the study was to develop an indicator of human response to vibrations, based on relationships between the questionnaire responses obtained and the parameter values determined on the basis of the measurements carried out. This indicator was to be one that could eventually be used as a design guideline for manufacturers regarding the vibration serviceability of different timber floors. This part of the overall study, i.e. *Part I*, presents a literature review of the topics dealt with, a description of the measurements performed, an analysis of the objective data obtained, as well as a classification of the floors in accordance with several different

serviceability criteria. *Part II*, in turn, deals with the statistical analysis of the objective and the subjective data with the aim of developing an indicator of vibration acceptability and vibration annoyance.

Keywords: Psycho-vibratory evaluation, Vibrations, Timber floors, Lightweight, Measurements, Serviceability criteria, Vibration annoyance, Vibration acceptability, Eurocode 5.

1 Introduction

Timber floors have traditionally been designed with respect to their static load-carrying capacity and static stiffness when uniformly distributed loads are involved [1]. This criterion has proved to not be sufficient in regard to vibration serviceability, however, for timber constructions in particular, complaints by inhabitants there being frequent, even when present-day building code regulations are met [2].

In 1994, Swedish building regulations authorised the construction of wooden multi-storey buildings. This led to an increasing demand for open planning in both residential and office buildings, involving use of long-span floor structures. Wood is high both in strength and in stiffness in relation to its weight, making it possible to build very long spans, especially with use of glue-laminated (glulam) timber. However, slender floor constructions involving long spans have low resonance frequencies that, in combination with low damping, are easily excited by such human activities as walking, running and jumping. Since humans are very sensitive to the vibrations thus produced, floors of this sort are often regarded as annoying. Accordingly, obtaining adequate indicators of human response to vibrations in slender or lightweight structures dynamically excited by human activities is of considerable importance.

In the present work, in efforts to assess how floor vibrations are perceived under various conditions, psycho-vibratory tests of five different prefabricated floor structures were carried out in a laboratory environment at two different locations in Sweden (Lund University – referred to here as LU – and the SP Technical Research Institute of Sweden – referred to as SP). A total of 60 persons participated in the tests conducted (31 persons at LU and 29 at SP). The floors in question were presented to the subjects in random order. The tests were divided into two parts: a "seated subtest" in which the subject was seated in a chair placed on the floor and experienced the vibrations created by a person who was walking on the floor, and a "walking subtest" in which the subject was asked to walk on the floor, being able in so doing to experience vibrations this produced. A questionnaire concerning different subjective attributes was presented to the subjects after each subtest. During the psycho-vibratory tests, objective measurements were also carried out on the floors in order to assess accelerations experienced by the subjects that could eventually be compared with their answers given in the questionnaires. The accelerations were measured at several points on the surface of the floors during the "walking subtest", and on the chair when the "seated subtest" was carried out. In addition, in order to assess certain measurable physical properties of the floors, i.e. properties not dependent on the subjects, static and dynamic tests were carried out separately.

Analyzing the data from the questionnaires and comparing it with the accelerations experienced by the subjects, as well as with the objective non-subject-dependent measures obtained, enabled design indicators of different subjective attributes (vibration acceptability and vibration annoyance) to be determined.

The results of the present investigation are reported in two articles, that designated as *Part I* reviewing the criteria currently applied to the vibration serviceability of timber floors, describing the measurement protocols employed, analysing the objective data obtained and presenting a classification of the floors in terms of several serviceability criteria in present use. *Part II*, in turn, analyses both the objective and the subjective data with the aim of obtaining indicators of vibration acceptability and vibration annoyance.

2 Literature Review

A summary of research in the area of human response to floor vibrations, as well as a compilation of the serviceability criteria found applicable to timber constructions nowadays will be presented here first.

2.1 Factors affecting human response to floor vibrations

Extensive research in the area of human perception of whole-body vibration, and human response to such vibration has been carried out. According to [3], human response to whole-body vibration can be divided into five categories: (i) degraded comfort, (ii) interference with activities, (iii) impaired health, (iv) occurrence of motion sickness and (v) perception of low-magnitude vibration. In the case of vibration in buildings, human response to it can be said to consist of annoyance and of a reduction in comfort.

Due to the complexity, sensitivity and variability of the human body, there are no clearly stated limits for acceptable vibration levels that are used in buildings nowadays but simply certain guidelines that have been developed [3]. The response of a human to vibration not only depends upon a large number of variables but is also highly subjective. For instance, people differ in how they react in response to what are nominally the same vibration levels (reflecting inter-subject differences in this respect), and a given person may respond differently to a particular level or type of vibration under differing circumstances (intra-subject differences) [4].

More specifically, one can say that human response to whole-body vibration depends both on psychological and on physiological variables. Thus, characteristics of the vibration, i.e. its amplitude, frequency, duration and direction, may very well influence the perception of it as much as age, gender, posture, fitness, type of activity being performed, attitude, expectations, context or motivation do [4].

Moreover, if humans are subjected to vibrations for too long a time, there is the risk of health problems being involved. According to [5], long-term high-intensity whole-body vibrations can result in an increased health risk for the lumbar spine and the connected nervous system of the segments affected. The digestive system, the genital/urinary system, and the female reproductive organs are also assumed to be affected, although the probability of this can be regarded as being lower. Such effects have only been investi-

gated in the case of seated persons, no corresponding research having been carried out on standing or recumbent persons thus far. It has also been found that it normally takes several years for the health changes involved to occur.

2.2 Criteria for human perception of structural vibrations

Pioneering work in the field of human perception of vibration is that of Reiher and Meister [6], in which human sensitivity to vibrations was investigated. Ten test persons were exposed to vertical and to horizontal steady-state vibrations while standing or lying on a platform, the frequencies ranging from 5 to 100 Hz and the amplitudes from 0.01 mm to 10 mm. Subjects' reactions were classified and were labelled in categories extending from "barely perceptible" to "intolerable". The perception threshold was reached at a constant value of the product of amplitude (displacement) and frequency, and thus at a constant vibration velocity. A vibration perception scale was proposed on the basis of these findings. The scale was eventually modified in [7] to make it applicable as well to vibrations due to walking impact, its being observed that for transient vibrations the main factor affecting human beings was that of damping, variations in amplitude and in frequency having little effect. It was suggested that if the amplitude scale is increased by a factor of ten the original Reiher-Meister scale can be seen as applicable to floor systems having less than 5 percent critical damping. The resulting modified Reiher-Meister scale is shown in Figure 1.

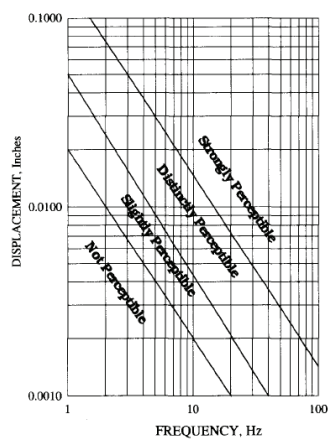

Figure 1: Modified Reiher-Meister Scale [7].

In [8], transient vibrations from a single-frequency component were investigated. A number of 40 persons standing in a room with a floor 4.9×8.5 m^2 in size were exposed to vertical vibrations created by a shaker of varying frequency, peak amplitude and damping. The vibrations involved (including both damped and undamped ones) were then rated on a 1-5 scale extending from "imperceptible" to "severe". Statistical analyses were carried out for identifying possible relationships between the response rate and various parameters. For damped vibrations, the following equation was proposed as predicting

the response rate R_{WP}:

$$R_{WP} = 5.08 \left(\frac{f u_{max}}{\zeta^{0.217}} \right)^{0.265} \tag{1}$$

where f is the frequency, u_{max} the peak displacement in inches and ζ the damping ratio. The following equation was proposed for predicting the response to undamped vibrations:

$$R_{WP} = 6.82 \left(f u_{max} \right)^{0.24} \tag{2}$$

values for R_{WP} ranging from 1 to 5, labelled respectively as following: 1 "imperceptible", 2 "barely perceptible", 3 "distinctly perceptible", 4 "strongly perceptible" and 5 "severe vibration".

The investigations performed also showed the product of the frequency and the displacement to be constant and the transient vibrations of a given frequency and peak displacement to become progressively less perceptible as the damping was increased.

A vibration criterion for the degree of acceleration and damping appropriate for quiet human occupancies such as residential buildings and offices was developed in [9]. As the damping increases, the steady-state response produced by walking becomes a series of transient responses, resulting in a less significant response. A human perception scale for the degree of damping required was presented as a function of the product of initial displacement and the frequency in [10], the same parameters as in [8] being used.

In [1], springiness and vibrations in timber floors and steel floors were investigated in a laboratory environment with use of subjective rating tests, 15 persons taking part. A rating of different timber test floors in comparison with a reference floor was also carried out. The tests on laboratory timber floors showed both a reduction in the length of the span and the existence of a ceiling to have a positive effect in terms of subjective judgements of the degree of vibration, but the use of glue to fix the deck to the joists to have little effect in this respect. It was also pointed out that the spacing between adjacent natural frequencies should be one of at least 5 Hz in order to prevent annoyance.

Field tests were carried out and vibration ratings were collected in [11]. Human perception here was found to not be correlated with either peak acceleration, filtered peak acceleration, RMS acceleration, the fundamental frequency or the product of the fundamental frequency and peak acceleration. In [12], it was reported that in terms of the subjective assessments made, none of the structural modifications investigated there except for those of a reduction in joist depth and the introduction of rubber inserts, resulted in any improvement in dynamic serviceability.

There are several different standards concerning human perception of structural vibrations that are or have been employed, the three most prominent ones being the following.

2.2.1 ISO 2631-1:1997

The International Standard ISO 2631-1:1997 [5], (*Vibration and shock – Evaluation of human exposure to whole-body vibration – Part 1: General requirements*) provides guidelines on how to perform vibration measurements, what to report, and how to evaluate the results obtained, these guidelines being used to standardise reporting and to simplify comparisons. Although this standard is provided with three annexes containing suggestions,

as well as current information on the possible effects of vibrations on health, comfort and perception, and motion sickness, it does not present any vibration exposure limits for whole-body vibrations.

2.2.2 ISO 2631-2:1989

This older version of the standard just referred to [13] has been cancelled and been replaced with the newer edition [14]. In the earlier version, tentative vibration serviceability limits were given in the form of base curves for the vibration magnitudes that cause approximately the same degree of annoyance. The base curves were to be used together with multiplication factors, taking into consideration the time of day and the type of occupied space involved (office, residential, etc.). In the latest edition of the standard, these base curves have been withdrawn, the reason given being the following: "Guidance values above which adverse comments due to building vibration could occur are not included anymore since their possible range is too widespread to be reproduced in an International Standard" [14].

2.2.3 ISO 2631-2:2003

The second part of the ISO standard 2631 [14] (*Mechanical vibration and shock – Evaluation of human exposure to whole-body vibration – Part 2: Vibration in buildings – 1 Hz to 80 Hz –*) is applicable to the evaluation of vibrations in buildings with respect to matters of comfort and annoyance of occupants. No limit values are stated, due to the considerable differences in the research findings concerning this that have been reported. Instead, methods of measurement and evaluation concerned with whole-body vibrations in buildings have been suggested in order to encourage a uniform approach to the collection of data. A frequency weighting W_m (coincident with the W_k as defined in [5]) is recommended for use, irrespective of the measurement posture of an occupant (its being sufficient to simply consider vibrations in the direction having the highest frequency-weighted magnitude).

In [15], it was concluded that the frequency weighting of the ISO standard 2631-2 [14] and the overall weighted amplitude value obtained succeed well in describing the degree of annoyance felt regarding a single sinusoidal vibration, but that they are less accurate in regard to a vibratory signal involving only a limited number of discrete frequencies. To overcome these difficulties, a prediction model was developed in which both the overall weighted amplitude and the fundamental frequency are taken account of. This model, proposed in [15], is as follows:

Sinusoidal case:
$Annoyance = -1.26 + 0.39 \cdot weighted\ total\ amplitude$

Multiple Frequency case:
$Annoyance = -3.17 + 0.43 \cdot weighted\ total\ amplitude + 0.24 \cdot fundamental\ frequency$

Amplitude given in [mm/s^2] RMS, frequency in [Hz]
The frequency weighting: done according to ISO2631-2:2003

Interpretation:
if $Annoyance \leq 4$, the floor is acceptable
if $Annoyance > 4$, the floor is unacceptable

2.3 Design criteria to minimise annoying vibrations in floor systems

2.3.1 Criteria-limiting point-load deflections

The earliest attempts to provide some degree of control over vibration problems in timber floors involved limiting the static deflection of joists under uniformly distributed load conditions so as to ensure the floor stiffness being sufficient [16]. For instance, the traditional $L/360$ deflection limit (L being the span of the floor) was in broad use for a considerable period of time. A numerical investigation performed in [17] led to an improved stiffness-based criterion for floor vibration serviceability being developed, one that limited the midspan deflection of the floor system to 1 mm for a point load of 1 kN, independent of the span. In [18], another stiffness-based criterion, one incorporated into the National Building Code of Canada and requiring that the static deflection produced by a 1 kN load at midspan be limited to $8.0/\mathrm{L}^{1.3}$, and also that it not be greater than 2 mm for spans ranging from 3 to 6 m in length, was employed.

If the same traditional design criteria for deflection, making use of static response parameters, are employed, vibration serviceability is not guaranteed [19]. As a consequence, research aimed at gaining an understanding of the factors that affect human response to floor vibrations has increased ever since and has paved the way for the development of design approaches for studying the dynamic parameters involved.

2.3.2 Criteria for limiting-point load deflection, for velocity due to unit impulse, and for RMS velocity

Criteria taking account of several different modes of vibration as well as of modal damping, of limiting-point load deflection, of the velocity due to a unit impulse and of the RMS velocity, can be found in [1] and [20]. The development of these criteria was based on measurements of floors and subjective evaluation of their vibration performance, mainly in single-family houses. Three types of limits are to be noted: (i) the floor system needs to have a flexibility of no more than 1.5 mm/kN in the case of a concentrated load located at midspan; (ii) for floors with a fundamental frequency greater than one of 8 Hz, the values of the velocity due to a unit impulse (h'_{max}) and of a damping coefficient ($\sigma_0 = f_1\zeta$ [Hz]) need to fall within a given region of the graph $h'_{max} = f(\sigma_0)$ in order to ensure that the performance achieved will be acceptable (Figure 2); and (iii) the root-mean-square

velocity for steady-state vibration needs to be less than tabulated values as given for acceptable floor systems. Actually, the use of such tabulated values has never been proposed, the recommendation being that one instead compare the root-mean-square velocity with corresponding values for similar floor constructions that show acceptable vibration performance. Yet values of this sort have never been available either. Rather, the first two criteria, namely (i) and (ii), have provided the basis for the vibration serviceability criteria in Eurocode 5 [21].

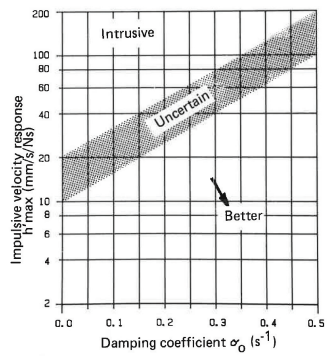

Figure 2: A preliminary proposal for classifying the response of a floor construction in terms of impact load [20].

2.3.3 Criteria limiting the fundamental frequency and the frequency-weighted RMS acceleration

The design criterion developed in [23] requires that the fundamental frequency of a floor be greater than 8 Hz, and that the frequency-weighted root-mean-square acceleration obtained during the first second of vibration be less than 0.45 m/s^2 when loaded by a specific impulse. The first part of the criterion is determined by the stiffness and the mass of the floor system, whereas the second part is a function of the damping that takes place. Theoretically, therefore, it is necessary that the designer estimate the damping of the floor structure at the time that designing is carried out. Since doing this is virtually impossible, however, due to the damping of the timber floors varying considerably depending upon the construction type selected, and the techniques and workmanship employed, methods requiring that damping calculations be performed may not be practical for design engineers to utilise.

2.3.4 Criteria limiting the fundamental frequency

The investigation performed in [19] suggests that if the stiffness of a floor is sufficient to maintain the fundamental frequency of the floor system at a level above that of 15 Hz in the case of unoccupied floors, and above 14 Hz in the case of occupied floors, the furniture or whatever and the persons involved being included, acceptable levels of vibration will be obtained.

The work presented in [15] is in opposition to the latter reference, as it shows that human perception of vibration is strongly affected by the composition of the vibration signal in terms of the number of frequency components involved and their mutual amplitude relationships. Thus, in line with [15], it can be argued that the multiple natural frequencies inherent in a floor need to be taken account of in determining the design rules to be followed. This is in agreement with the criteria for design rules proposed in [1] and [24] (in which it is suggested that up to the 8^{th} harmonic should be taken account of), its contradicting many presently used floor design criteria that often rely on the fundamental frequency alone.

2.3.5 Criteria limiting the fundamental frequency and point-load deflection

In [25], rules for the design of floors with "high-" and with "low-" requirements and those with "no-" requirements, resulting in the fundamental frequency being maintained at above a level of 8 and of 6 Hz for "high-" and for "low-" requirement floors, respectively, were proposed. A stiffness criterion is also specified there (such that the deflection due to a static load of 2 kN is to be less than the limit value w_{limit}, the size of which depends upon the requirements that apply to the floor in question).

Suggested criteria and limiting values for the classifying of floors into five different classes (A-E) are proposed in [26]. It was found there that the point load deflection and the fundamental frequency are two of the best indicators of vibration performance in the case of lightweight floors.

2.3.6 A criteria-limiting combination of parameters

The approaches just mentioned are semi-empirical in nature, their providing satisfactory solutions for the particular categories of floors for which the methods were developed. None of them appear to work entirely satisfactorily when applied to other types of floors, however [16]. In [27], a new design method consisting of a vibration-controlled criterion and a calculation method for determining the criterion parameters were developed. The design criterion states that if the ratio (fundamental frequency)/(1 kN deflection)$^{0.44}$ of an unoccupied floor is larger than 18.7, the floor is most likely satisfactory for the occupants.

In [28], the ratio of the peak acceleration achieved by walking, to the force of gravity, is used as a design guideline, its value depending upon the use to which the building is to be put. Its value given as

$$\frac{a_p}{g} = \frac{P_0 e^{-0.35 f_n}}{\beta W} \leq \frac{a_0}{g} \tag{3}$$

where P_0 is a constant applied force (0.29 kN for floors and 0.41 kN for footbridges), f_n the fundamental frequency of the floor structure, β the damping ratio, W the floor's effective weight, a_0/g the tabulated acceleration limit and a_p/g the estimated peak acceleration (in units of g).

2.3.7 Eurocode 5

The methods presented in [1] and [20] served as the basis for the vibrational serviceability criteria developed in Eurocode 5 [21]. The Eurocodes are a set of harmonised technical

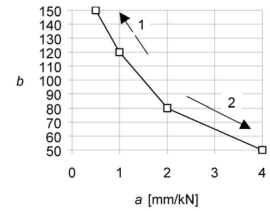

Figure 3: Recommended range of the relationship between a and b: 1 better performance, 2 poorer performance.

rules developed by the European Committee for Standardisation for the structural design of construction work carried out within the European Union.

Specifically, the design of timber structures is dealt with in EC5-1-1 and in the serviceability limit state design guidelines regarding floor-vibration performance. The design criteria are applicable to residential wood-based plate-type floors with a fundamental frequency greater than 8 Hz, in which the human sensitivity is related to the effects of the vibration amplitude and velocity caused by the dynamic footfall forces involved [22]. If the fundamental frequency of the floor is lower than this, a special investigation of the floor in question is needed.

The effects are divided into low- and high-frequency ones. The low-frequency contributions that come from step actions are dealt with by a static criterion that limits the deflection caused by a static point load applied at the point on the floor that results in a maximum vertical deflection. The high-frequency effect is a consequence of the heel impact actions that occur, its being taken account of by use of a dynamic criterion that limits the maximum initial value of the vertical floor vibration velocity caused by an ideal unit-impulse load. Three points must thus be checked on:

- The fundamental frequency of the floor, f_1, should be at least 8 Hz in order for the floor to be regarded as a high-frequency one (otherwise a special investigation of it is needed), the requirement thus being that

$$f_1 \geq 8 \text{ Hz} \tag{4}$$

- The maximum instantaneous vertical deflection, w, due to a single force should be less than a deflection of a varying size a (see Figure 3 regarding a):

$$\frac{w}{F} \leq a \text{ [mm/kN]} \tag{5}$$

- The maximum initial value of the vertical floor vibration velocity, v, produced by an impulse of 1 [N·s], applied at the point on the floor giving the maximum response – where components above 40 Hz can be disregarded – should verify the inequality (see the dimension b in Figure 3):

$$v \leq b^{(f_1 \zeta - 1)} \text{ [m/Ns}^2\text{]} \tag{6}$$

where F is a vertical concentrated static force applied to any point on the floor, taking account of the load distribution, and ζ is the modal damping ratio (a value of 1 % is recommended in [21] unless some other value has been found to be more appropriate).

For more detailed information regarding Eurocode 5 calculations, see Section 5.3.1.

2.3.8 Design tools

Various numerical methods, the finite element method, for example, are sometimes used as design tools nowadays for checking on the serviceability of floors of different types, in line with the development of commercial solutions in the form of different softwares. Often highly versatile, they can enable floors to be very much improved and various criteria described above to be verified during the design phase. Examples of the use of such tools are to be found in [29], [30] and [31].

3 The floors tested

In the present investigation, five separate floors (shown in Figures 4 - 8) differing one from another but each of a type used frequently in residential buildings, the suppliers of each playing an active role in the Swedish construction market, were tested in a laboratory environment. Due to differences between them in the structural conceptions they embodied (box-floor-type, surface-floor-type), they can differ in design, in their dimensions and in various construction features. Although the floors differed in their vibration properties, the range in vibration performance they represented was not large at all, each of them being known from earlier to display fairly good vibration performance in a normal building environment. This could make it difficult for the persons participating in the testing conducted to distinguish clearly between the floors in terms of their vibration performance. Table 1 shows the manufacturers of the floors together with the labelling used in the investigation, the design features of the floors being listed in Table 2.

Table 1: Suppliers of the floors and the labels given them.

Supplier	Label
Moelven Töreboda	A
Martinssons Byggsystem	B
Lindbäcks Bygg	C
Masonite Beams	D
Masonite Lättelement	E

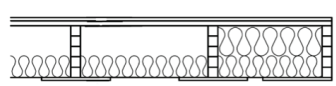

Figure 6: Lindbäcks Bygg.

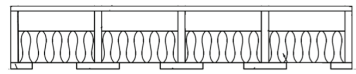

Figure 4: Moelven Töreboda.

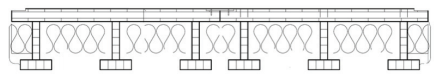

Figure 5: Martinssons Byggsystem.

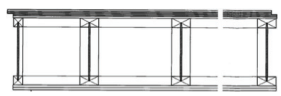

Figure 7: Masonite Beams.

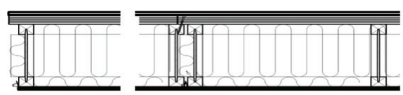

Figure 8: Masonite Lättelement.

During the tests, each floor was simply supported on two sides by glulam beams having dimensions 90×180 mm^2. The glulam beams, in turn, were supported by studs at a centre-to-centre distance from one another of 600 mm. These studs were stabilised by use of plywood slabs, and they were bolted to the concrete floor of the laboratory, as shown in Figure 9. In attaching the floor elements to the supporting beams, the floor suppliers' instructions were followed. A floor resting on its supports is shown in Figure 10.

Figure 9: Floor supports used.

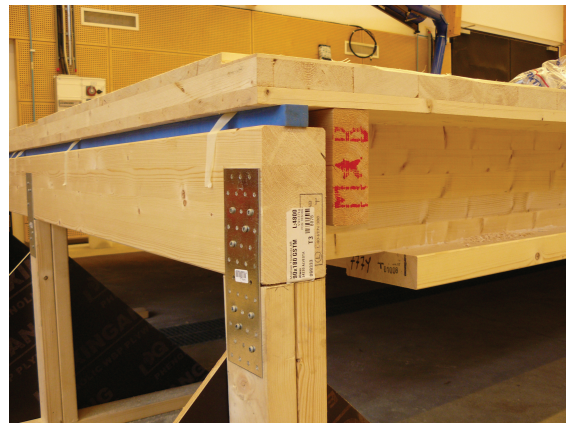

Figure 10: Floor supports joined to a glulam beam by means of a tie plate, the floor resting on top. In this case, the floor is required to rest on top of an elastomer, blue in colour in the picture, according to the manufacturer's instructions.

Table 2: Floor design, all sizes in [mm].

Feature/Label	A	B	C	D	E
Length [m]	6800	8500	3700	7966	8100
Width [m]	4800 (2x2400)	4800 (4x1200)	2400	4804 (2x2402)	4848 (2x2424)
Flooring	-	-	13 mm gypsum boards	-	13 mm gypsum boards
Sheating	33 mm Kerto Q511	73 mm CLT	22 mm chipboards	43 mm plyboard	43 mm plyboard
Beams	Web: Kerto S80 51x360 s587 Flange: Kerto S16 45x300	Web: Glulam C40 42x220 s400 Flange: Glulam C40 42x180	Web: Glulam 42x225 s600 Flange: Plywood 12x300	Web: Masonite beam HB 350 C24 s480 Flange: 45x98	Masonite beam H300 C24 s585 Flange: 45x45
Remarks	-	-	-	Beam in one of the long sides H350 C24 Flange width: 45	Tension flange 0.7 mm perforated steel sheet
Strutting	2 rows of beams Kerto S75 52x360 L_1=2392 L_2=4362	-	-	2 rows of Masonite beams H350 K24 L_1=3079 L_2=6079	2 rows of Masonite beams H300 K24 L_1=3079 L_2=6079
Junction (between floor elements)	WT-T screw 6.5x130 s300 every second from left and right element respectively	Plywood strip 12x160 P30 screwed with WFR 4x50 s125	-	Glued with SikaBond-540 Chipped nails 34x45 s300	Overlapping plyboard screwed with 5x90 s300
No. Elements	2	4	1	2	2
Ceiling	-	-	-	2x13 mm gypsum board	13 mm gypsum board

4 Measurement procedures

4.1 Non-subject-dependent measurements

Prior to the subjective psycho-vibratory testing that was carried out, objective measurements of each of the five floors were performed in order to determine the values for various

static and dynamic parameters for each of them, those of subfloor and floortop deflections, eigenfrequencies, eigenmodes and modal damping ratios. These parameters were used to classify the floors in terms of various criteria taken up in the literature review, use being made here both of methods proposed in Eurocode 5 [21], and of methods employed by Hu and Chui [27] and by Dolan *et al* [19], as taken up in Section 5.3. The parameters assessed on the basis of the objective measurements that were taken were also used in the statistical analysis to determine which parameters were correlated most closely with vibration acceptability and with vibration annoyance (see the companion paper).

4.1.1 Eigenmodes, eigenfrequencies and damping ratios

Dynamic tests were carried out in order to measure the eigenfrequencies and damping ratios of the floors and determine the mode shapes involved. Excitation was performed by use of a shaker driven by a pseudo-random signal, the strength of it being measured by a force transducer attached to the floor by a wood screw and to the shaker by a threaded rod. The vertical floor accelerations were measured by accelerometers located at ten separate points placed within one quadrant of the floor area. The test setup is shown in Figure 11.

For frequencies of up to 40 Hz, the eigenfrequencies, damping ratios ζ [%], mode shapes and modal density, n_{40}, were extracted from the measured frequency response functions (FRFs) using the Matlab toolbox *VibraTools Suite* [32]. In order to extract the aforementioned parameters, a poly-reference time domain method [33] was used for determining the poles and the modal participation factors, a least-squares frequency-domain method then being employed to fit estimates made to the measured data. Also, the impulse velocity response was calculated from the driving point mobility.

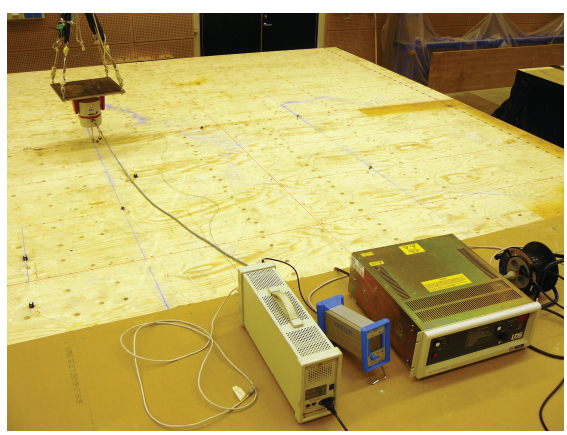

Figure 11: Shaker, accelerometers and other equipment used for the measurements.

4.1.2 Subfloor deflection

In order to classify the floors in terms described by Hu and Chui [27] and in Eurocode 5 [21], the midspan deflection produced by a static point load of 1 kN was measured. The

deflection measurement procedure was based on that proposed in [34].

The displacement gauge was fastened to a reference system consisting of a magnetic stand that was attached to a metal weight hung from an overhead crane. The loading was performed by a person weighing approximately 80 kg who stood with his feet straddling the measurement point, facing in the direction of the floor-load-bearing beams. The deflection was averaged from five measurements performed in the same way for each of the floors in order to ensure good repeatability. The deflection produced by a 1 kN point load, $d_{1,m}$, was then obtained by extrapolation.

4.1.3 Floortop deflection

The floortop deflection, i.e. the deflection on the sheating of the floor, was measured. For each of the wooden floors (A to E), two displacement gauges were placed on the upper surface of the floor in question, the first one located at the midpoint of the floor and the second one placed 0.6 m from it (see Figure 12). The gauges were fixed to a reference system consisting of a metallic portal frame (moved from one floor to another) that remained motionless during recordings. This setup was the same for each of the floors.

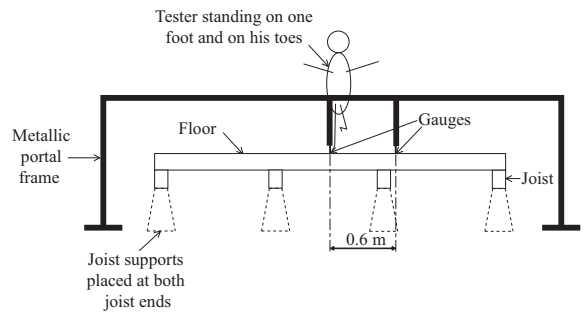

Figure 12: Side view of the floortop deflection measurement setup.

The measurement procedure was based on that proposed in [26]. The midpoint was loaded by the tester's weight of approximately 80 kg. The displacement time histories were recorded by both gauges while the tester was standing on his toes of one foot in the middle of the floor (see Figure 12). Three trials were carried out for each floor, in order to ensure a good repeatability. The maximum displacement recorded by the one gauge was subtracted from that recorded by the other, the resulting difference being extrapolated in the manner proposed in [26] so as to obtain the floortop deflection, $d_{2,m}$, produced by a 1 kN point load.

4.2 Subject-dependent measurements

The subject-dependent measurements made during the subjective tests that were carried out were obtained both at *LU* and at *SP*. A total of 60 persons differing in age and gender (31 at *LU* and 29 at *SP*) participated in the tests. All of them performed the following

tasks on each floor, the tasks at both locations being the same, the five different floors being presented to each subject in random order:

- Seated subtest: the subject was first seated in a chair placed at the observation point in question (located 0.6 m from the midline of the floor, see Figure 13), he or she gazing in the direction of the walking line. The experimenter walked along the walking line at a step velocity of about 2 Hz, back and forth between the two limits indicated by the red lines in Figure 13, his passing the observation point three times. Three accelerometers were used during the test, the first one placed on the floor between the feet of the subject, the second one placed under the chair seat, and the third one placed on the backrest of the chair (marked by crosses in Figure 13). Although the acceleration would normally be measured on the upper surface of the seat [5], in this case it was placed beneath the seat so as to not create discomfort for the test person. A situation similar to this was investigated in [15], its being shown there that the transmissibility, i.e. the gain between the one way of measuring and the other – under the seat versus on top of it – both types of measurements being performed by a seated person, was approximately 1.0, showing that this alternative also works properly.

- Walking subtest: after the seated subtest was completed, the chair was removed and the subject was asked to walk in a rather free manner along the walking line, between the two limits marked by the red lines in Figure 13. No other specific instruction was given to the subject concerning his or her way of walking. Five accelerometers were placed along the walking line to measure the floor vibrations (their locations being marked by crosses in Figure 13).

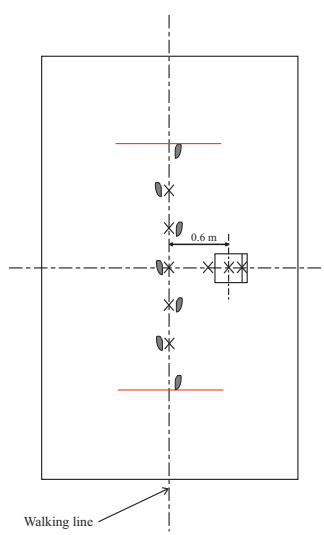

Figure 13: Measurement setup.

Figure 14 shows a subject performing the seated and the walking test, respectively.

Figure 14: Measurement pictures showing the seated (left) and the walking (right) subtest.

After each completion of the one subtest or the other for a given floor, subjects were asked, as to describe, through filling in a questionnaire, their experiences of the floor in question in terms of various subjective attributes, there being one such questionnaire to be filled out following the seated subtest and another following the walking subtest. The questionnaires of this sort used at *LU* were not identical with these used at *SP*, the questionnaires for use in the two organisations having been developed separately, yet questions concerning certain matters of central interest – primarily matters of whether one is annoyed by vibrations and whether or not one considers the level of vibration present to be acceptable – were either exactly the same or rather similar in both cases, which led to a merging of the questionnaire results of this character in reporting the results here. The reasoning behind this merging of results and the methods involved are taken up in the companion paper, *Part II*.

For the seated subtest at *LU*, subjects were asked about noise annoyance, vibration annoyance, vibration acceptability and springiness. For the walking subtest, subjects were asked about vibration annoyance, vibration acceptability and springiness. The definition of springiness given to the subjects was "resistance of a material to a shock". In response to questions concerning noise annoyance and vibration annoyance evaluation, subjects were asked to express a judgment on a 11-point numerical scale ranging from "0" ("not at all annoyed") to "10" ("extremely annoyed"). In response to questions concerning springiness, subjects were asked to express a judgment on a 11-point numerical scale ranging from "0" ("very bad") to "10" ("very good"). Finally, regarding vibration acceptability, subjects were requested to express a dichotomic judgment: "acceptable" or "not acceptable".

For the seated subtest at *SP*, subjects were asked about noise annoyance, vibration annoyance and vibration acceptability. They were also asked to describe in their own words their perceptions while the test leader was walking. For the walking subtest there, the subjects were asked about springiness, annoyance and acceptability. They were also asked to describe in their own words their experiencing of the floor response while walking on the floor. The definition of springiness given to the subjects here was "the resilience or flexibility of the floor under a step". Finally, subjects there were asked to judge how

they experienced the floor vibrations, as well as the quality of the floors, and whether they would accept having such vibrations in a living room in a new residential building. Subjects' answers to all these questions were to be given on a six-point categorical scale, for instance "definitely not acceptable", "not acceptable", "barely acceptable", "acceptable", "fully acceptable", "acceptable with any reservations whatever". Subjects were also asked to rank the floors on a scale from the one they would prefer most to have at home to the one they would prefer least.

For each subtest and floor, the time histories of acceleration obtained in each of the accelerometers were recorded simultaneously during testing. The objective parameters extracted for each subject during the subjective testing carried out are presented below.

4.2.1 Overall frequency-weighted RMS accelerations

For each accelerometer, the frequency-weighted RMS (Root-Mean-Square) acceleration, a_w, was computed in accordance with Equation (7) (see standard [5], section 6.4.2),

$$a_w = \left[\sum_i \left(W_{m,i} a_i \right)^2 \right]^{\frac{1}{2}} \tag{7}$$

where $W_{m,i}$ are the weighting factors for the different third-octave bands i of the acceleration spectrum, as given in Annex A of the standard [14], and a_i are RMS values computed for the different third-octave bands i of the acceleration spectrum.

An overall frequency-weighted RMS acceleration was determined finally on the basis of the root-sum-of-squares of the frequency-weighted RMS accelerations as computed for the different accelerometers (see standard [5], section 8.2.3).

4.2.2 Overall frequency-weighted RMS velocities

In addition, for each accelerometer, velocity time histories were determined by integration on the basis of the acceleration time histories. The frequency-weighted RMS velocity, v_w, was computed then as

$$v_w = \left[\sum_i \left(K_{b,i} v_i \right)^2 \right]^{\frac{1}{2}} \tag{8}$$

where $K_{b,i}$ are the weighting factors for the different third-octave bands i of the velocity spectrum, as given in the standard [35], and v_i are the RMS values computed for the different third-octave bands i of the velocity spectrum.

In the end, an overall frequency-weighted RMS velocity was determined from the root-sum-of-squares of the frequency-weighted RMS velocities computed for the different accelerometers (see standard [5], section 8.2.3).

Note that the frequency-weighted RMS values are highly dependent upon the time window for analysis. Accordingly, this time window needs be chosen carefully and be stated in connection with the results. In the present case, frequency-weighted RMS values were computed using a time window corresponding to only one of the three "walking lines" (a "walking line" is defined as one completed stroll along the floor in the one direction

or the other). Thus, the periods of time in which the subject just stood on the floor, not creating any noticeable vibrations, or moved by simply turning around, were not taken into account in the computations. Had such periods of time been taken into account, the frequency-weighted RMS values could well have been markedly reduced.

4.2.3 Maximum Transient Vibration Value ($MTVV$)

For each accelerometer, the maximum transient vibration value was computed by use of Equation (9) (see the standard [5], section 6.3.1).

$$MTVV = max\left[a_w(t_0)\right] \tag{9}$$

where $a_w(t_0)$ is defined as follows:

$$a_w(t_0) = \sqrt{\frac{1}{\tau}\int_{t_0-\tau}^{t_0}\left[a_w(t)\right]^2 dt} \tag{10}$$

where $a_w(t)$ is the instantaneous frequency-weighted acceleration, τ is the integration time for the running average (1 second in the present case), t is the time and t_0 is the observation time. A Matlab code was created here in order to be able to calculate $MTVV$. With use of that code, the entire duration of the recording swept over, a one-second window being employed. Each of the computed $a_w(t_0)$ values was saved. The output produced, i.e. $MTVV$, is the "worst" (i.e. the maximum) of these values. In the end, an overall $MTVV$ was determined on the basis of the root-sum-of-squares of the $MTVV$s computed for the different accelerometers (see the standard [5], section 8.2.3).

5 Results

5.1 Non-subject-dependent objective parameters

5.1.1 Eigenmodes, eigenfrequencies and damping ratios

The eigenfrequencies, eigenmodes and modal damping ratios up of to 40 Hz were extracted (as described in Section 4.1.1), fairly close agreement of the LU and the SP results and good reproducibility of the measurements being obtained. It was thus concluded that the floors were mounted in a similar way at both locations, allowing the data to be used interchangeably, measurements at both locations thus theoretically providing basically the same results. The results obtained at SP are presented in Tables 3 and 4.

Not surprisingly, floor C, with the shortest span, has the highest fundamental frequency, whereas floors B, D and E, with the longest spans, have the lowest fundamendal frequencies. Also, floor C has the lowest value for n_{40}, whereas floors B and D have the highest values for n_{40}. In examining the modal damping ratios for the three first eigenmodes, one can note that floor C has the strongest damping properties, whereas floor B has the weakest damping properties.

Table 3: Measured eigenfrequencies below 40 Hz, i.e. n_{40}.

Floor Label	Mode number [Hz]											n_{40}
	1	2	3	4	5	6	7	8	9	10	11	
A	16.3	17.7	18.3	30	36	-	-	-	-	-	-	5
B	9.9	10.5	11.1	17.3	24.2	27.8	29.5	33.7	36.6	38.9	39.6	11
C	24.3	26.1	36	-	-	-	-	-	-	-	-	3
D	8.8	9.9	14	22.7	24	28.3	31.7	37	-	-	-	8
E	8.2	12	20.2	25.9	28.4	34.1	-	-	-	-	-	6

Table 4: Measured modal damping ratios below 40 Hz, i.e. ζ_i [%].

Floor Label	Modal damping ratio, ζ_i [%]										
	1	2	3	4	5	6	7	8	9	10	11
A	1.6	1.5	1.5	8	5	-	-	-	-	-	-
B	0.7	1.1	0.9	1.2	1.1	1.4	1.6	1	1.2	2.1	1.3
C	2.3	2.6	5	-	-	-	-	-	-	-	-
D	1.8	2.1	2.2	2	2	1.5	1.6	2	-	-	-
E	1.1	1.8	3.5	2.6	3.2	4	-	-	-	-	-

5.1.2 Floor deflections

The subfloor deflection, $d_{1,m}$, and the floortop deflection, $d_{2,m}$, were measured as described in Sections 4.1.2 and 4.1.3, respectively. The results are shown in Table 5.

The deflection $d_{1,m}$ appears to covary with $d_{2,m}$. For instance, floor A (the rigidity of which is among the highest, see Table 7) has the lowest subfloor and floortop deflection, whereas floor B has both the highest subfloor and floortop deflection.

Table 5: Measured subfloor deflection produced by a 1 kN load $d_{1,m}$ and floortop deflection $d_{2,m}$.

Floor	A	B	C	D	E
$d_{1,m}$ [mm/kN]	0.260	0.660	0.560	0.530	0.440
$d_{2,m}$ [mm/kN]	0.101	0.529	0.335	0.320	0.230

5.2 Subject-dependent objective parameters

The 2.5%, 50% and 97.5% percentiles for a_w, v_w and $MTVV$ for the seated test, for all floors and subjects, are given in Table 6. The parameter a_w appears to strongly covary with v_w and $MTVV$. Floors A and C have the lowest median values of a_w , v_w and $MTVV$, whereas floors B, D and E have the highest median values of a_w , v_w and $MTVV$. The dispersion of the a_w, v_w and $MTVV$ values for each of the floors is large. This high degree of dispersion may have come about through the large differences in weight between those participating in the test (extending from 50.7 to 140 kg). Indeed, subjects differing appreciably in weight have been found to differ in the levels of acceleration and velocity of vibration they experience [3]. This dispersion may also be due to differences between subjects in their manner of walking.

Table 6: Percentiles of weighted parameters for each of the floors for the subjects as a whole, in the seated subtest.

Floor	Percentile	a_w [m/s^2]	v_w [m/s]	$MTVV$ [m/s^2]
A	0.025	0.001	0.00004	0.004
	0.50	0.012	0.00030	0.034
	0.975	0.026	0.00070	0.054
B	0.025	0.003	0.00010	0.011
	0.50	0.054	0.00140	0.150
	0.975	0.144	0.00341	0.291
C	0.025	0.001	0.00005	0.003
	0.50	0.021	0.00060	0.058
	0.975	0.041	0.00110	0.091
D	0.025	0.003	0.00009	0.012
	0.50	0.055	0.00140	0.151
	0.975	0.116	0.00320	0.242
E	0.025	0.003	0.00010	0.009
	0.50	0.063	0.00160	0.163
	0.975	0.116	0.00331	0.292

5.3 Classification of the floors

5.3.1 Floor classification according to Eurocode 5 [21]

The degree to which the design guidelines given in Eurocode 5 [21] (see Section 2.3.7) were met was also investigated, for the calculated data, in line with instructions given in [22]. The calculations were carried out under the assumption that the floor was unloaded, i.e. that only the weight of the floor and other permanent actions need to be taken into account. For the individual materials of the floor structures, the mean values for the modulus of elasticity involved were employed, these being provided by the material suppliers. In calculating the flexural rigidity in the span direction, $(EI)_l$, composite action between the floor sheathing and the floor joists was assumed to occur on each of the floors. In calculating the corresponding flexural rigidity in the cross-joist direction $(EI)_b$, however, only the contribution from the floor sheathing was taken into account. The fact of not considering the positive effect of strutting between joists when calculating $(EI)_b$ means that the rigidity of the floors A, D and E is underestimated somewhat, since two rows of strutting are present in each of them. On the basis of the results of laboratory tests, the rotational rigidity $(EI)_T$ was assumed to be equal to $(EI)_l/500$ in the finite element (FE) analysis and hand calculations. Table 7 gives the physical properties of the floors.

For a rectangular floor having overall dimensions of $L \times B$, simply supported along all four edges and having timber beams with span of L, the fundamental frequency f_1 can be calculated in an approximate manner as

$$f_1 = \frac{\pi}{2L^2}\sqrt{\frac{(EI)_l}{m}} \tag{11}$$

where m is the mass per unit area given in [kg/m^2], L is the floor span given in [m], and

$(EI)_l$ is the equivalent plate bending stiffness of the floor about an axis perpendicular to the beam direction given in [N·m^2/m].

For floors having a fundamental frequency of more than 8 Hz, as calculated by use of Equation (11) (this is the case for all of the floors under study here), the requirements to be satisfied are the following:

- Low-frequency effects: the requirement given in Equation (5) needs to be met. The deflection value produced by a point load of 1 kN, w, given in [mm], as calculated using Equation (12), must not exceed the limit, a, given for each country in the National Annex. In the Swedish National Annex, the deflection limit a is equal to 1.5 mm, no consideration being taken of the floor span.

$$w = \frac{1000 k_{dist} l_{eq}^3 k_{amp}}{48 (EI)_{joist}} \tag{12}$$

  In calculating the deflection produced by a point load, w, account is taken of only a single joist. The effect of load sharing between joists is taken account of by use of the following reduction factor k_{dist}:

$$k_{dist} = max \left\{ k_{strut} \left[0.38 - 0.08 \ln \left[\frac{14 (EI)_b}{s^4} \right] \right] ; 0.30 \right\} \tag{13}$$

  where $(EI)_{joist}$ is the stiffness of a single joist in [N·mm^2], $(EI)_b$ is the flexural rigidity in the cross-joist direction as given in [N·mm^2/m], s is the spacing between joists in as given in [mm] and the factor k_{strut} takes the effect of strutting into account. If a single row or several rows of strutting exist, the value of k_{strut} is set to 0.97 (floors A, D and E), in the case of no strutting the value being equal to 1 (floors B and C). The parameter l_{eq} is the equivalent span of the floor joists in [mm], which equals here the span of the floor joists, since each of them is simply supported. In addition, k_{amp} is an amplification factor that takes into account the effects of shear deformations, its being equal to 1.05 for simply supported timber joists (floors A, B and C) and to 1.15 for simply supported glued thin webbed joists (floors D and E).

- High-frequency effects: when an impulse force of 1 [N·s] is applied to the centre of the floor in a manner simulating heel impact, the unit impulse velocity response v needs to comply with Equation (6), the value of v being given by Equation (14), and the value of b being set to 100 in the Swedish National Annex. For the relationship between a and b, see Figure 3. The value of v can, as an approximation, be taken as

$$v = \frac{4(0.4 + 0.6 n_{40})}{(mBL + 200)} \tag{14}$$

  where v is the unit impulse velocity response given in [m/(N·s^2)], n_{40} is the number of first-order modes having eigenfrequencies of up to 40 Hz, B is the floor width in [m], m is the mass per unit area in [kg/m^2] and L is the floor span in [m]. The value of n_{40} can be calculated as

$$n_{40} = \left[\left(\left(\frac{40}{f_1} \right)^2 - 1 \right) \left(\frac{B}{L} \right)^4 \frac{(EI)_l}{(EI)_b} \right]^{0.25} \tag{15}$$

where $(EI)_b$ is the equivalent plate bending stiffness of the floor about an axis parallel to the beams, given in [N·m^2/m]. Note that $(EI)_b < (EI)_l$.

For purposes of verification, eigenfrequencies of up to 40 Hz were also calculated for each of the floors, as displayed in Table 8, using the Matlab FE toolbox *Calfem* [36]. The mode shapes for floor D are shown, as an example, in Figure 15.

Table 7: Stiffness parameters (EI) (longitudinal – l –, transversal – b –, rotational – T – and single joist), floor geometry – the width of the exterior supports not being taken into account – (L length and B width) and mass m of the floors.

Floor	$(EI)_l$ [N·m^2/m]	$(EI)_b$ [N·m^2/m]	$(EI)_T$ [N·m^2/m]	$(EI)_{joist}$ [N·mm^2]	L [m]	B [m]	m [kg/m^2]
A	2.65E+07	5.99E+03	5.30E+04	1.56E+13	6.7	4.8	60
B	1.94E+07	2.06E+05	3.88E+04	0.77E+13	8.4	4.8	67
C	1.81E+06	2.40E+03	3.62E+03	0.11E+13	3.7	2.4	43
D	1.05E+07	2.91E+04	2.09E+04	0.50E+13	8.0	4.8	48
E	1.06E+07	2.62E+04	2.11E+04	0.62E+13	8.0	4.8	53

Table 8: Calculated eigenfrequencies of the different floors, obtained using the Matlab toolbox *Calfem* [36].

Floor Label	Mode number [Hz]											n_{40}
	1	2	3	4	5	6	7	8	9	10	11	
A	23.3	23.4	23.9	24.9	26.8	29.9	34.4	-	-	-	-	7
B	11.9	12.1	15.2	26.8	-	-	-	-	-	-	-	4
C	23.5	23.7	24.6	27.8	35.2	-	-	-	-	-	-	5
D	11.5	11.6	12.6	16.3	24.1	36.0	-	-	-	-	-	6
E	10.9	11.1	11.9	15.2	22.2	32.8	-	-	-	-	-	6

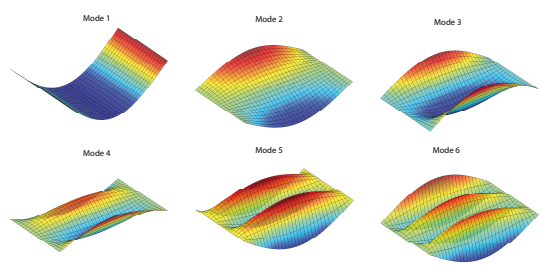

Figure 15: Eigenmodes for Floor E calculated with Calfem.

A summary of the calculations and requirements, as stated in [21] for the five floors under study, is presented in Table 9. All of the requirements are fulfilled for each of the floors.

It should be pointed out that there is still concern regarding both the accuracy of the proposed damping ratio ζ and the procedures for calculating n_{40}. This also raises

serious doubts regarding the accuracy of the simplified procedures used for calculating the impulse velocity response v. Specifically, it is stated in [31] that the current EC5-1-1 design criteria do not adequately address issues concerning the dynamic response of timber flooring systems and their associated vibrational problems. Reconsideration of the design criteria is thus called for.

Table 9: Calculations in terms of Eurocode 5 [21].

		Low frequency effects					High frequency effects					Requirements		
Floor	f_1 [Hz]	k_{strut}	k_{amp}	k_{dist}	w [mm]	a [mm]	n_{40}	v [mm/N·s^2]	v_{limit} [mm/N·s^2]	b	ζ [%]	$f_1 > 8$ Hz	$w/F \leq a$	$v \leq b^{(f_1\zeta-1)}$
A	23.5	0.97	1.05	0.396	0.167	1.5	7	8.54	29.18	100	1	✓	✓	✓
B	12.0	1	1.05	0.300	0.501	1.5	3	3.18	17.36	100	1	✓	✓	✓
C	23.5	1	1.05	0.300	0.498	1.5	4	19.19	29.57	100	1	✓	✓	✓
D	11.5	0.97	1.15	0.488	0.730	1.5	5	6.39	16.97	100	1	✓	✓	✓
E	11.0	0.97	1.15	0.300	0.593	1.5	5	6.12	16.58	100	1	✓	✓	✓

5.3.2 Floor classification according to Hu and Chui [27]

The criterion for floor vibration acceptability proposed in [27] states, regarding unoccupied floors, that if the ratio of the fundamental frequency, f_1, to the deflection due to a 1 kN point load, d_1, expressed as $r_{HC} = [f_1/{d_1}^{0.44}]$, is larger than 18.7, the floor in question is most likely satisfactory for occupants. In such a case, the criterion has been evaluated both with use of the measured first eigenfrequency and deflection as well as with use of the first eigenfrequency and deflection, as assessed on the basis of calculations.

The formulae used in the design method employed are based on the ribbed-plate theory. The floor stiffness parameters should then be calculated, taking account of the semi-rigid connections between the joist and the sheathing, the torsional rigidity of the joists and the sheathing stiffness in both the span and the across-joist directions. In addition, performance-enhancement-related construction details such as between-joist bridging, strong-back and strapping, are accounted for in the formulae presented in [27]. The deflection $d_{1,c,HC}$ in [m] due to a static point load P of 1 kN at the centre of the floor was calculated as

$$d_{1,c,HuChui} = \frac{4P}{LB\pi^4} \cdot \sum_{m=1,3,5\ldots} \sum_{n=1,3,5\ldots} \frac{1}{\left(\frac{m}{a}\right)^4 D_x + 4\left(\frac{mn}{ab}\right)^2 D_{xy} + \left(\frac{n}{b}\right)^4 D_y} \tag{16}$$

where P is in [N], L is the floor span in [m], B is the floor width in [m], D_x is the system flexural rigidity along the span direction in [N·m^2/m], D_y is the system flexural rigidity in the cross-joist direction in [N·m^2/m] and D_{xy} is the sum of the shear rigidity of the multi-layered floor deck and the torsion rigidity of the floor joist. To ensure convergence of the calculations, it is recommended to use three terms for $m = 1, 3, 5$ and eighteen terms for $n = 1, 3, 5 \ldots 35$.

The fundamental frequency $f_{1,c,HC}$ in [Hz] of a floor system was calculated as follows:

$$f_{1,c,HC} = \frac{\pi}{2\sqrt{\rho}} \sqrt{\left(\frac{1}{L}\right)^4 D_x + 4\left(\frac{1}{LB}\right)^2 D_{xy} + \left(\frac{1}{B}\right)^4 D_y} \tag{17}$$

where ρ is the mass per unit area in [kg/m^2]. Table 10 presents the results regarding the classification of the floors. In that table, the acceptability rate is the percentage of

Table 10: Classification of the floors according to Hu and Chui [27]. The subindex m denotes measured values whereas c indicates calculated values. In the last row, the percentages of subjects who considered the floor vibrations acceptable during the seated subtest are presented. It is often considered 50% of acceptability as the threshold for a floor being "acceptable".

Floor label	A	B	C	D	E
$f_{1,m}$ [Hz]	16.3	9.9	24.3	8.8	8.2
$d_{1,m}$ [mm]	0.26	0.66	0.56	0.53	0.44
$f_{1,c,HC}$ [Hz]	23.3	12.6	23.7	11.6	11.1
$d_{1,c,HC}$ [mm]	0.29	0.28	0.89	0.61	0.62
$r_{HC,m}$	29.5	11.9	31.4	11.6	11.8
$r_{HC,c}$	40.1	22.3	24.7	14.5	13.7
$r_{HC,m} > 18.7$	✓	×	✓	×	×
$r_{HC,c} > 18.7$	✓	✓	✓	×	×
Acceptability [%]	56.7	30.0	58.3	35.0	25.0

the participants who would accept the floor for their own houses. A value of 50% for acceptability can be considered as the threshold for a floor being acceptable.

Albeit the criterion computed from the calculated data fails to correctly describe the vibration acceptability for floor B, the criterion does accurately portray the vibration acceptability for the measured data. The mismatch for floor B may be due to the fact that it has a high cross-joist rigidity, due to the thick cross-laminated timber (CLT) plate there and the fact that the model proposed in [27] assumes lower cross-joist rigidity.

5.3.3 Floor classification according to Dolan *et al.* [19]

The design criterion presented in [19] states that if the stiffness of the floors is sufficient to mantain the fundamental frequency of the floor system at a level above 15 Hz for unoccupied floors, and above 14 Hz for occupied floors (i.e. including furniture and/or persons), an acceptable level of vibration will be obtained. The fundamental frequency, f_1, of the joists and the girders alone can be estimated using

$$f_1 = \frac{\pi}{2}\sqrt{\frac{gEI}{WL^3}} \tag{18}$$

where g is the acceleration due to gravity – equal to 9.81 [m/s^2] –, E the modulus of elasticity in [Pa], I the moment of inertia of the joist alone in [m^4] (without consideration of the composite action with the subflooring), W the weight of the floor system supported by the joist, given in [N], and L is the floor span in [m]. The weight, W, is taken as being simply the weight of the joist plus the weights of the subflooring and the finished flooring that are supported by a joist. The ceiling, floor covering, furniture, and other occupancy weights are not to be included in W. The same restrictions apply when calculating the fundamental frequency of the girder.

If the floor system includes joists and girders, the fundamental frequency can be esti-

mated using the Dunkerly equation:

$$f_1 = \sqrt{\frac{f_{joist} f_{girder}^2}{f_{joist} + f_{girder}^2}} \tag{19}$$

where f_{joist} is the fundamental frequency of the joist alone, given in [Hz], and f_{girder} is the fundamental frequency of the more flexible girder supporting the joists, also given in [Hz].

This criterion is simple to use and restricts only the stiffness of a floor system relative to its weight. Damping is not included since it cannot be effectively estimated or controlled by the designer, and if the level of damping is high, this improves the vibration performance of the system. The criterion involved also ignores any composite action between the joists and the sheathing which if present would improve performance and be effective at the low displacement amplitudes associated with vibrations. Both of these concerns have been investigated experimentally and been discussed in [19]. The results for each of the five floors can be seen in Table 11.

Table 11: Classification according to Dolan *et al* [19]. The subindex m denotes measured values, c indicates calculated values and D stands for Dolan.

Floor Label	A	B	C	D	E
$f_{1,m}$ [Hz]	16.3	9.9	24.3	8.8	8.2
$f_{1,c,D}$ [Hz]	15.9	6.1	21.9	2.9	2.2
$f_{1,m} > 15$ Hz	✓	×	✓	×	×
$f_{1,c,D} > 15$ Hz	✓	×	✓	×	×
Acceptability [%]	56.7	30.0	58.3	35.0	25.0

The criterion based on both the measured and the calculated fundamental frequencies appear able to predict the acceptability from the subjects standpoint. Despite this, it is our belief that the failure of the formulae involved to take account of composite actions between parts when the bending stiffness is calculated can lead to results being too conservative in predictions made on the basis of these calculations.

6 Discussion

For all of the floors, the degree to which the requirements proposed by Eurocode 5 [21] were met was checked. In fact, all of the floors met the requirements stated in EC5-1-1. This is not very surprising, however, since Eurocode 5 regulates the structural design of construction work carried out in the European Union and all of the floors under study were ones of a type used in real buildings there. Also, the requirements stated in EC5-1-1 were drawn up on the basis of measurements and subjective ratings made in lightweight timber houses, which happens to be our working scenario.

In addition, in considering the value of 50 % acceptability (i.e. half of the participants being ready to accept the floor within their own house) as the threshold for a floor being "acceptable", it was found that the Hu and Chui [27] criterion works well for the measured

data here, since it matches the acceptability results for all of the floors under study here. A match with the calculated data, however, fails for floor B, since the degree of acceptability for subjects cannot be predicted there. This is probably due to the assumption in the analytical formulae proposed that the connections between joists and sheathing be semi-rigid, whereas floor B has rigid connections and a high level of across-joist rigidity due to the thick CLT layer on the surface of it.

The applicability of Dolan *et al*'s criterion [19] was examined. It was observed that these guidelines could be applied and that they worked properly with use of the measured data for each of the five floors included in the study. Nonetheless, although the criteria worked properly as well for the calculated data, the fact that the composite action that occurs is not accounted for in the formulae proposed for use there means that the calculations underestimate the fundamental frequency, which could lead to the results obtained being unrealistically conservative.

7 Conclusions

Psycho-vibratory tests were performed on 5 different timber floors in a laboratory environment. A total of 60 persons participated in the tests. Acceleration measurements were carried out while the persons, tested individually, either were walking on the floor in question or were seated in a chair placed on it at the same time as the test leader was walking on the floor. After each subtest, questionnaires were handed out to the participants concerning different attributes of the floors. Non-subject-dependent measurements were also carried out in order to investigate the dynamic and static properties of each of the floors. Different measurement protocols were employed, these being put together by combining various existing methods reported in the literature. All of the data of this sort gathered were post-processed and were used for classification of the floors in accordance with different criteria.

The criteria employed, described in [21], [27] and [19], were found to describe fairly well the performance of the floors in terms of vibration acceptability (see Tables 9-11), especially in the case of measured data, certain discrepancies being found when calculated data were employed. The inconsistencies obtained may be due to the fact that the analytical formulae proposed for the different criteria described in [27] assume that semi-rigid connections are present and to [19] not taking account of composite action. Accordingly, results based on use of calculated data need to be interpreted with care.

Nevertheless, despite the timber floors basically complying with the criteria currently employed, subjective vibratory studies of modern timber framework buildings still frequently yield results showing the inhabitants involved to often be annoyed by vibrations [37]. This may be due in part to the design criteria employed being based originally on measurements and subjective ratings carried out in single-family houses. Thus, reconsideration of the questions of interest here and the development of new design criteria are needed.

Ultimately, design guidelines and indicators of vibration annoyance and vibration acceptability will be drawn up by analyzing statistically the objective and subjective data from the questionnaires, as will be taken up in the companion paper, designated as *Part II*.

Acknowledgements

This research reported on here was funded by the Silent Spaces project, a part of the EU program Interreg IV and by the Vinnova and Formas project AkuLite.

References

[1] S. Ohlsson: Floor Vibrations and Human Discomfort. PhD thesis, Chalmers University, Göteborg, Sweden, 1982.

[2] J. Forssén, W. Kropp, J. Brunskog, S. Ljunggren, D. Bard, G. Sandberg, F. Ljunggren, A. Ågren, O. Hallström, H. Dybro, K. Larsson, K. Tillberg, L-G. Sjökvist, B. Östman, K. Hagberg, Å. Bolmsvik, A. Olsson, C-G. Ekstrand, M. Johansson: Acoustics in wooden buildings. State of the art 2008. Vinnova project 2007-01653, Report 2008:16, SP Trätek (Technical Research Institute of Sweden), Stockholm, 2008.

[3] M. J. Griffin: Handbook of human vibration. Academic Press Limited, London, UK, 1996.

[4] A. Pavic, P. Reynolds: Vibration Serviceability of Long-Span Concrete Building Floors. Part 1: Review of Background Information. The Shock and Vibration Digest **34(3)** (2002) 191–211.

[5] ISO 2631-1: Vibration and shock – Evaluation of human exposure to whole-body vibration – Part 1: General requirements. International Organization for Standardization, Geneva, Switzerland, 1997.

[6] H. Reiher, F. J. Meister: The effect of vibration on people. Published in German in 1931, English Translation in Report No. F-TS-616-R.E.Headquarters, Air Material Command, Wright Field, Ohio, USA, 1949.

[7] K. H. Lenzen: Vibration of steel joist-concrete slab floors. AISC Engineering Journal **3** (1966) 133–136.

[8] J. F. Wiss, R. A. Parmelee: Human perception of transient vibrations. Journal of the Structural Division ASCE **100(4)** (1974) 773–787.

[9] D. E. Allen, J. H. Rainer: Vibration criteria for long-span floors. Canadian Journal of Civil Engineering **3** (1976) 165–173.

[10] T. M. Murray: Acceptability criterion for occupant-induced floor vibrations. Engineering Journal AISC **2nd Qtr.** (1981) 62–70.

[11] S. R. Alvis: An Experimental and Analytical Investigation of Floor Vibrations. M.Sc. Thesis, Virginia Polytechnic Institute and State University, USA, 2001.

[12] E. S. Bernard: Dynamic serviceability in lightweight engineered timber floors. ASCE Journal of Structural Engineering **134(2)** (2008) 258–268.

[13] ISO 2631-2: Evaluation of human exposure to whole-body vibration – Part 2: Continuous and shock-induced vibration in buildings (1 Hz to 80 Hz). International Organization for Standardization, Geneva, Switzerland, 1989.

[14] ISO 2631-2: Vibration and shock – Evaluation of human exposure to whole-body vibration – Part 2: Vibration in buildings (1 Hz to 80 Hz). International Organization for Standardization, Geneva, Switzerland, 2003.

[15] F. Ljunggren: Floor Vibration – Dynamic Properties and Subjective Perception. PhD thesis, Department of Human Work Sciences, Division of Sound and Vibration, Luleå University of Technology, Sweden, 2006.

[16] L. J. Hu, Y. H. Chui: Vibration serviceability of timber floors in residential construction. Progress in Structural Engineering and Materials **3** (2001) 228–237.

[17] R. O. Foschi, A. Gupta: Reliability of floors under impact vibration. Canadian Journal of Civil Engineering **14** (1987) 683–689.

[18] D. M. Onysko: Performance and acceptability of wood floors – Forintek studies. National Research Council of Canada, Publication 28822, Forintek Canada Corp., Ottawa, 1988.

[19] J. D. Dolan, T. M. Murray, J. R. Johnsson, D. Runte, B. C. Shue: Preventing annoying wood floor vibrations. Journal of Structural Engineering **125(1)** (1999) 19–24.

[20] S. Ohlsson: Springiness and human-induced floor vibrations – A design guide. Swedish Council for Building Research, Stockholm, 1988.

[21] EN 1995-1-1: Eurocode 5 – Design of timber structures – Common rules and rules for buildings. European Committee for Standardization, Brussels, 2004.

[22] J. Porteus, A. Kermani: Structural timber design to Eurocode 5, Wiley, 2008.

[23] I. Smith, Y.H. Chui: Design of light-weight wooden floors to avoid human discomfort. Canadian Journal of Civil Engineering **15** (1988) 254–262.

[24] B. R. Ellis: On the response of long-span floors to walking loads generated by individuals and crowds. The Structural Engineer **78(10)** (2000) 17–25.

[25] P. Hamm, A. Richter, S. Winter: Floor vibrations – New results. Proceedings of the 11th World Conference on Timber Engineering, Riva del Garda, Italy, 2010.

[26] T. Toratti, A. Talja: Classification of human induced floor vibrations. Building Acoustics **13(3)** (2006) 211–221.

[27] L. J. Hu, Y. H. Chui: Development of a design method to control vibrations induced by normal walking action in wood-based floors. Proceedings of the 8th World Conference on Timber Engineering, Lahti, Finland, 2004.

[28] D. E. Allen, T. M. Murray: Design criteria for vibrations due to walking. Engineering Journal AISC **30(4)** (1993) 117–129.

[29] A. A. Al-Foqaha'a, W. F. Cofer, K. J. Fridley: Vibration Design Criterion for Wood Floors Exposed to Normal Human Activities. Journal of Structural Engineering **125** (1999) 1401–1406.

[30] I. Glisovic, B. Stevanovic: Vibrational Behaviour of Timber Floors. Proceedings of the 11th World Conference on Timber Engineering, Riva del Garda, Italy, 2010.

[31] J. Weckendorf: Dynamic Response of Structural Timber Flooring Systems. PhD thesis, Edinburgh Napier University, UK, 2009.

[32] Axiom EduTech AB: VibraTools Suite [computer program], Ljusterö, Sweden 2007.

[33] W. Heylen, S. Lammens, P. Sas: Modal analysis – Theory and testing. Department of Mechanical Engineering, Katholieke Universiteit Leuven, Leuven, Belgium, 1995.

[34] L. J. Hu: Protocols for field testing of wood-based floor systems. Appendix V in Report of Serviceability design criteria for commercial and multi-family floors. Report No. 3 for Canadian Forest Service, FPInnovations, Quebec, 1998.

[35] DIN 45669-1: Measurement of vibration immission – Part 1: Vibration meters – Requirements and tests. Deutsches Institut für Normung, Berlin, 2010.

[36] P-E. Austrell, O. Dahlblom, J. Lindemann, A. Olsson, K-G. Olsson, K. Persson, H. Petersson, M. Ristinmaa, G. Sandberg, P-A. Wernberg: CALFEM – A finite element toolbox. Version 3.4., Division of Structural Mechanics, Lund University, Sweden, 2004.

[37] K. Jarnerö, D. Bard, C. Simmons: Vibration performance of apartments buildings with wooden framework Residents' survey and field measurements. AkuLite Rapport 6, SP Rapport 2013:17, ISBN: 978-91-87461-02-6, 2013.

[38] P. Holmlund: Absorbed power and mechanical impedance of the seated human exposed to whole-body vibration in horizontal and vertical directions. Department of Technical Hygiene, National Institute for Working Life, Umeå & Department of Applied Physics and Electronics, Umeå University, 1998.

[39] A. C. Johansson, Svikt och vibrationer hos lätta träbjälklag (Vibration performance of lightweight floor structures). M.Sc. Thesis, Division of Structural Engineering and Division of Engineering Acoustics, Lund University, Sweden, 1999.

[40] ISO 2631-1: Evaluation of human exposure to whole-body vibration – Part 1: General requirements. International Organization for Standardization, Geneva, Switzerland, 1985.

[41] S. Ohlsson: Serviceability limit states – Vibration of wooden floors. In: STEP 1, Centrum Hout, The Netherland, A18/1-A18/8, 1995.

[42] A. Pavic, P. Reynolds: Vibration Serviceability of Long-Span Concrete Building Floors. Part 2: Review of Mathematical Modelling Approaches. Shock and Vibration Digest **34(4)** (2002) 279–297.

[43] M. J. Griffin, K. C. Parsons: Whole-body vibration perception thresholds. Journal of Sound and Vibration **121(2)** (1988) 237–258.

[44] D. E. Allen, J. H. Rainer, G. Pernica: Vibration criteria for assembly occupancies. Canadian Journal of Civil Engineering **12** (1985) 617–623.

[45] A. Ebrahimpour, R. L. Sack: A review of vibration serviceability criteria for floor structures. Computers and Structures **83** (2005) 2488–2494.

[46] V. Radic, J. M. W. Brownjohn, A. Pavic: Human walking and running forces: Novel experimental characterization and application in civil engineering dynamics, Proceedings of 26$^{\text{th}}$ International Modal Analysis Conference (IMAC XXVI), Orlando, USA, 2008.

[47] P. Johansson: Vibration of Hollow Core Concrete Elements Induced by Walking, M.Sc. Thesis, Division of Structural Engineering and Division of Engineering Acoustics, Lund University, Sweden, 2009.

[48] C. Hopkins: Sound Insulation. Elsevier, Oxford, UK, 2007.

[49] A. K. Chopra: Dynamics of structures. Prentice Hall, New Jersey, USA, 2007.

[50] K. J. Bathe: Finite Element Procedures. Prentice Hall, New York, USA, 1996.

Paper B

Psycho-vibratory evaluation of timber floors – Part II: Towards the determination of design indicators of vibration acceptability and vibration annoyance.

A. Trollé[1], L-G. Sjökvist[2], K. Jarnerö[2], J. Negreira[3], D. Bard[3].

[1]Université de Lyon, Labex CeLyA,
École Nationale des Travaux Publics de l'État, Laboratoire Génie Civil et Bâtiment,
Rue M. Audin, 69518 Vaulx-en-Velin Cedex, France.

[2]SP Technical Research Institute of Sweden, SP Wood Technology,
Vidéum Science Park, SE-35196, Växjö, Sweden.

[3]Lund University,
Department of Construction Sciences, Division of Engineering Acoustics,
P.O. Box 118, 221 00 Lund, Sweden.

Submitted for publication, June 2013.

Contributions: The author of the dissertation performed 20% of the work, by helping Arnaud Trollé and the other authors discussing the results stemming from the statistical analysis during the merging of the data as well as proofreading the paper.

Psycho-vibratory evaluation of timber floors – Part II: Towards the determination of design indicators of vibration acceptability and vibration annoyance

A. Trollé[1], L-G. Sjökvist[2], K. Jarnerö[2], J. Negreira[3], D. Bard[3].

[1]Université de Lyon, Labex CeLyA, École Nationale des Travaux Publics de l'État, Laboratoire Génie Civil et Bâtiment, Rue M. Audin, 69518 Vaulx-en-Velin Cedex, France.

[2]SP Technical Research Institute of Sweden, SP Wood Technology, Vidéum Science Park, SE-35196, Växjö, Sweden.

[3]Lund University, Department of Construction Sciences, Division of Engineering Acoustics, P.O. Box 118, 221 00 Lund, Sweden.

Abstract

This paper is the second part of a report on work dealing with the psycho-vibratory evaluation of timber floors. The companion paper, *Part I*, reviewed the existent criteria for the vibration serviceability of timber floors and described measurements performed in a laboratory environment at two locations in Sweden (SP in Växjö and LU in Lund). The data stemming from those measurements served as input for the present study, aimed at obtaining further knowledge concerning human response to vibrations in wooden floors. The study involved primarily the conjoint analysis of merged subjective data and objective parameters, with the goal of determining a design indicator both of vibration acceptability and of vibration annoyance, use being made of multilevel regression. Although the sample of floors tested was small (5 altogether), certain clear trends could be noted. In particular, the first eigenfrequency (calculated in accordance with Eurocode 5) and Hu and Chui's criterion (calculated from measured quantities) proved to be the best indicators of vibration annoyance, and the Maximum Transient Vibration Value (computed on the basis of the accelerations experienced by the test subjects) to be the best indicator of vibration acceptability.

Keywords: Psycho-vibratory evaluation, vibration serviceability, timber floors, design indicators, vibration annoyance, vibration acceptability, Principal Component Analysis, multilevel regression.

1 Introduction

The present study aims at obtaining more thorough knowledge of the relationship between perceived vibrational discomfort and certain objective engineering parameters. The various considerations that led to this work are presented in greater detail in the companion paper, *Part I*, of this work. A total of 60 persons tested five separate timber floors, two different locations being involved (29 of the subjects being tested at SP in Växjö and 31 of them at LU in Lund), these persons providing judgments regarding the vibration performance of the floors by way of questionnaires. The experiments at both locations are described in detail in the companion paper. Objective static and dynamic parameters pertaining to the floors, such as their eigenfrequencies, eigenmodes, damping ratios, and subfloor and floortop deflections (see the companion paper), were also measured or calculated. In the present investigation, relationships between subjects' questionnaire responses of relevance and the objective parameters involved were examined. This paper describes efforts made to determine indicators of vibration acceptability and vibration annoyance by combining the outcomes (i.e. subjects' questionnaire responses and objective parameters) stemming from both locations. To this end, use was made of multilevel regression. Multilevel regression, not yet in wide use, appears to be a suitable statistical method for modelling repeated measures data in which inter-individual differences in rating are substantial. The paper can thus also be seen as an illustration of the usefulness of multilevel regression as a tool for modelling repeated measures data.

2 Methods

This section presents the methods used for merging the subjective data stemming from two separate though closely related studies, that at SP and that at LU (see section 2.1), and for analyzing the merged data obtained (see section 2.2).

2.1 Merging the subjective data

Of the rather many questions posed to subjects either at the SP location or at the LU location (see the companion paper), only two of them were considered to be equivalent in the sense that the subjects' answers to them at the two locations could be combined. These two questions concerned vibration annoyance and vibration acceptability, respectively.

At SP, the vibration annoyance question was: "How do you experience the vibrations when I walk on the floor?". The response scale was a six-point verbal one, having the following alternatives: "not at all disturbing", "barely disturbing", "a little disturbing", "disturbing", "very disturbing", "extremely disturbing". The vibration acceptability question was: "Considering a newly-built residential building: do you experience the vibrations that occur as?". The response scale was again a six-point verbal one, having the following alternatives: "definitely not acceptable", "not acceptable", "barely acceptable", "acceptable", "fully acceptable", "definitely acceptable". The questions and the answers were both in Swedish, and are translated here to English. At LU, the vibration annoyance question was "Imagine that you live in a newly-built multi-storey building equipped with this floor, you are seated on a chair and another person is walking by: what number

from 0 to 10 best shows how much you are bothered, disturbed or annoyed by the floor vibrations?". The response scale was an eleven-point numerical one, the numbers ranging from 0 to 10. Two labels, "not at all" and "extremely", were attached to the respective ends of the scale, at 0 and 10. The vibration acceptability question was "Imagine that you live in a newly built multi-storey building equipped with this floor, you are seated on a chair and another person is walking by: do you find the floor vibrations acceptable?". The two response alternatives were "Yes, acceptable" and "No, not acceptable". The questions and answers were available both in English and in Swedish.

One can note that both the vibration annoyance and the vibration acceptability questions were posed at each of the two laboratories in a situation in which the test person was seated in a chair placed on the floor in question while the test leader was walking by. Since the two studies differed in the response scale used regarding both vibration annoyance and vibration acceptability, the issue arose of how to merge the subjective data coming from the two locations, at SP and LU.

For the vibration annoyance question, the responses from both data sources could be translated into scores ranging from 0 to 100. This translation procedure is based on the assumption that the different response categories available divide up the range extending from 0 to 100 into equally spaced intervals (Miedema and Vos, 2004). The general rule followed here for assigning a particular score on the 0 to 100 scale is that described by Passchier-Vermeer and Zeichart (1998):

$$score\,(0\,\text{to}\,100) = 100(i - \frac{1}{2})/m \tag{1}$$

where m is the number of categories ($m = 6$ in the SP study, and $m = 11$ in the LU study) and $i = 1,....,\ m$ is the rank number of a given category, starting with the lowest response category. After this translation, the scores ranging from 0 to 100 from both studies could be merged.

Regarding the vibration acceptability question, in the SP study the responses were translated into dichotomic responses in accordance with the following rules: the responses "definitely not acceptable" and "not acceptable" were transformed into the response "no, not acceptable", and the responses "barely acceptable", "acceptable", "fully acceptable" and "definitely acceptable" were transformed into the response "yes, acceptable". After this transformation, the dichotomic responses from both studies could be merged.

2.2 Data analysis

The data analysis aimed at assessing relationships between the subjective data and the objective parameters involved, as well as at finding a satisfactory indicator for each of the two subjective attributes (vibration annoyance and vibration acceptability), that is, an objective parameter that best explains the subjective data. To this end, use was made of multilevel regression (see section 2.2.2).

The large amount of non-subject-dependent objective parameters available made it impossible to determine by means of multilevel regression analysis the relationships between each and every one of these objective parameters, on the one hand, and the subjective data, on the other. Thus, a preliminary analysis based on Principal Component Analysis

(PCA) was carried out first, in order to select beforehand a small number of objective parameters that could best explain the subjective data (see section 2.2.1).

2.2.1 Preliminary selection of relevant non-subject-dependent objective parameters

Vibration annoyance data The merged vibration annoyance scores ranging from 0 to 100 were analyzed using linear PCA, or more specifically the MDPREF model (Chang and Carroll, 1969). This model provides a multidimensional space in which the floors are represented by points and the subjects by unit vectors passing through the origin. These entities are located in such a way that the projections of the points on the vectors are in maximal agreement with the subjects' scores. A vector endpoint represents the point of maximum vibration annoyance of the subject in question. In order to identify the vibratory features of the floors able to affect vibration annoyance, the non-subject-dependent objective parameters were fitted into the space as non-normalized vectors, using a PREFMAP procedure (Chang and Carroll, 1972). An objective parameter vector then points in a direction such that the projections of the points on the vector are in maximum agreement with the values of the objective parameter. The length of the vector, which is equivalent to the linear correlation coefficient between the projections and the values of the objective parameter, indicates the quality of representation of the objective parameter in the space (Schroeder *et al.*, 1974).

The non-subject-dependent objective parameters that were fitted are presented in Table 1. Their values for each of the floors are shown in the companion paper.

Vibration acceptability data The merged binary responses were analyzed using logistic PCA, a tool especially well suited for analyzing binary data. More specifically, the model proposed by De Leeuw (2003) was employed. Similarly, this model provides a multidimensional space consisting of a configuration of floor points and of subject vectors passing through the origin. For convenience sake, the subject vectors were normalized *a posteriori*. A vector endpoint represents the point of maximum acceptability for the subject in question. In order to identify the vibratory features of the floors that could affect vibration acceptability, the objective parameters were also fitted into the space as non-normalized vectors by use of a PREFMAP procedure.

Again, all objective parameters shown in Table 1 were fitted.

2.2.2 Determination of an indicator of vibration annoyance and vibration acceptability

In efforts to find an adequate indicator of vibration annoyance and one of vibration acceptability, a regression analysis involving the vibration annoyance and the acceptability responses, on the one hand, and the relevant appearing objective parameters, on the other, was carried out. More specifically, for analyzing the repeated measures data that were collected, use was made of multilevel regression models, within a Bayesian framework. Although this regression method has been used for meta-analysis of *in situ* noise annoyance studies earlier (Miedema and Vos, 2004), it appears to not yet have been used

Symbol	Objective parameter
$d_{1,m}$	Measured subfloor deflection
$d_{1,c,EC5}$	Calculated subfloor deflection, according to Eurocode 5
$d_{1,c,HC}$	Calculated subfloor deflection, according to Hu and Chui
$d_{2,m}$	Measured floortop deflection
$n_{40,m}$	Measured number of modes below 40 Hz
$n_{40,c,EC5}$	Calculated number of modes below 40 Hz, according to Eurocode 5
$n_{40,c,FEM}$	Calculated number of modes below 40 Hz, obtained by use of Calfem simulations
$f_{1,c,EC5}$	Calculated first eigenfrequency, according to Eurocode 5
$f_{1,c,FEM}$	Calculated first eigenfrequency, obtained by use of Calfem simulations
$f_{1,c,HC}$	Calculated first eigenfrequency, according to Hu and Chui
$f_{1,c,D}$	Calculated first eigenfrequency, according to Dolan *et al.*
$f_{1,m,v}$	Measured first eigenfrequency in the SP study
v_m	Measured impulse velocity response
$v_{c,EC5}$	Calculated impulse velocity response, according to Eurocode 5
η_1	Measured damping ratio for the first eigenmode
η_2	Measured damping ratio for the second eigenmode
m	Mass
$(EI)_l$	Longitudinal stiffness of the load-bearing beams
$(EI)_b$	Transverse stiffness of the load-bearing beams
$r_{HC,c}$	Hu and Chui's criterion, as calculated from the calculated quantities $f_{1,c,HC}$ and $d_{1,c,HC}$
$r_{HC,m}$	Hu and Chui's criterion, as calculated from the measured quantities $f_{1,m,v}$ and $d_{1,m}$

Table 1: List of non-subject-dependent objective parameters.

for modelling subjective data collected under laboratory conditions. Multilevel regression has advantages over classical regression for the modelling of repeated measures data. Notably, multilevel regression formulation complies strictly with the hierarchical structure of repeated measures data that consists of observations nested within individuals. It thus takes account of the fact that the observations are not independent. For an introduction to multilevel regression models, the reader is referred to the textbooks of Gelman and Hill (Gelman and Hill, 2007) and Hox (Hox, 2010).

In carrying out the regression analysis here, a two-level random-intercept-only model (one which includes no explanatory variable at the occasion level) was first fitted to the subjective responses (either vibration annoyance or vibration acceptability responses). This model provides a baseline for comparisons with models that include occasion-level predictors, its for this reason being referred to henceforth here as a "null" model.

Following this, for each of the subjective attributes, objective parameters were inserted successively into two-level models as occasion-level predictors. For each objective parameter, two models, the one with a fixed regression slope and the other with a random regression slope, were tested. For each objective parameter, these two models were compared with the corresponding null model in order to check, for each of the objective parameters considered, to what extent it could account for the subjective responses obtained.

Finally, for each subjective attribute, the models of interest, each including an objective parameter thought to be able to account to some extent for the subjective responses obtained, were compared with one another. These comparisons aimed at determining which indicator is best, this being the one provided by the model making it possible to best explain the subjective responses obtained.

Note that the objective parameters tested are divided into two groups: (i) those determined on the basis of the measurements carried out separate from the subjective testing and which do not vary across individuals, these being referred to as non-subject-dependent objective parameters, and (ii) those determined on the basis of the measurements carried out during the subjective testing and that vary across individuals, these being referred to as subject-dependent objective parameters (see the companion paper).

Model specification A two-level random-intercept-only model (one that included no explanatory variable at the occasion level) was first fitted to the data in question. For the vibration annoyance data, this null model ($M0$) can be written as follows:

$$\begin{aligned} &Y_{fi} = (\beta_{00} + u_{0i}) + e_{fi} \\ &u_{0i} \sim N(0, \sigma^2_{u_0}) \text{ , for } i = 1, ..., I \\ &e_{fi} \sim N(0, \sigma^2_{e}) \text{ , for } i = 1, ..., I \text{ and } f = 1, ..., F \end{aligned} \tag{2}$$

where Y_{fi} is the vibration annoyance score obtained for floor f and individual i, F is the number of floors, I is the number of individuals, β_{00} is the fixed intercept, the terms u_{0i} are (random) residual error terms (for the intercept) at the individual level, and e_{fi} are (random) residual error terms at the occasion level. The residual errors u_{0i} are assumed to have a mean of zero, and a variance $\sigma^2_{u_0}$ that is to be estimated. The residual errors e_{fi} are assumed to have a mean of zero, and a variance σ^2_e which is to be estimated.

For the vibration acceptability data (binary data), this null model ($M0$) can be written as follows:

$$\begin{aligned} logit(p_{fi}) &= \beta_{00} + u_{0i} \\ u_{0i} &\sim N(0, \sigma^2_{u_0}) \text{ , for } i = 1, ..., I \end{aligned} \tag{3}$$

where p_{fi} is the probability that the binary response Y_{fi} obtained for floor f and individual i is equal to 1 (here 1 = "acceptable") and $logit(p_{fi}) = \log(p_{fi}/(1 - p_{fi}))$.

Two-level models with a fixed regression slope were then tested. For the vibration annoyance data, these models can be written as follows:

$$\begin{aligned} Y_{fi} &= (\beta_{00} + u_{0i}) + \beta_{10} X_{fi} + e_{fi} \\ u_{0i} &\sim N(0, \sigma^2_{u_0}) \text{ , for } i = 1, ..., I \\ e_{fi} &\sim N(0, \sigma^2_e) \text{ , for } i = 1, ..., I \text{ and } f = 1, ..., F \end{aligned} \tag{4}$$

where β_{10} is the fixed slope, X_{fi} is the value of the occasion-level predictor (i.e. the objective parameter which is being tested) for measurement occasion (i.e. floor) f and individual i.

For the vibration acceptability data, these models can be written as follows:

$$\begin{aligned} logit(p_{fi}) &= (\beta_{00} + u_{0i}) + \beta_{10} X_{fi} \\ u_{0i} &\sim N(0, \sigma^2_{u_0}) \text{ , for } i = 1, ..., I \end{aligned} \tag{5}$$

Finally, two-level models with a random regression slope were tested. For the vibration annoyance data, these models can be written as follows:

$$\begin{aligned} Y_{fi} &= (\beta_{00} + u_{0i}) + (\beta_{10} + u_{1i}) X_{fi} + e_{fi} \\ \begin{bmatrix} u_{0i} \\ u_{1i} \end{bmatrix} &\sim N\left(\mathbf{0}, \begin{bmatrix} \sigma^2_{u_0} & \sigma_{u_{01}} \\ \sigma_{u_{01}} & \sigma^2_{u_1} \end{bmatrix} \right), \text{for } i = 1, ..., I \\ e_{fi} &\sim N(0, \sigma^2_e) \text{ , for } i = 1, ..., I \text{ and } f = 1, ..., F \end{aligned} \tag{6}$$

where the terms u_{1i} are (random) residual error terms (for the slope) at the individual level. The residual errors u_{1i} are assumed to have a mean of zero, and a variance $\sigma^2_{u_1}$, which is to be estimated. The term $\sigma_{u_{01}}$ is the covariance between the residual error terms u_{0i} and u_{1i}.

For the vibration acceptability data, these models can be written as follows:

$$\begin{aligned} logit(p_{fi}) &= (\beta_{00} + u_{0i}) + (\beta_{10} + u_{1i}) X_{fi} \\ \begin{bmatrix} u_{0i} \\ u_{1i} \end{bmatrix} &\sim N\left(\mathbf{0}, \begin{bmatrix} \sigma^2_{u_0} & \sigma_{u_{01}} \\ \sigma_{u_{01}} & \sigma^2_{u_1} \end{bmatrix} \right), \text{for } i = 1, ..., I \end{aligned} \tag{7}$$

Computation Gamma distributions were used as non-informative prior distributions for the variance and the covariance parameters. The posterior distributions of the model parameters were computed using Markov Chain Monte Carlo simulations involving up to 40000 iterations. These computations were performed using the Software MLwiN© (Browne, 2009). For each model parameter, a median value (i.e. a point estimate) and a 95% credibility interval were determined from its posterior distribution.

Model comparison The models were compared in terms of the following criteria:

- DIC – Deviance Information Criterion. This criterion provides a measure of out-of-sample predictive error (Gelman and Hill, 2007). This fit measure takes the degree of complexity of the model into account. The DIC values are not bounded; the lower the value of DIC is, the better the predictive power of the model is assumed to be. In comparing two models, differences in DIC of more than 10 may definitely rule out the model having the higher DIC value, differences of between 5 and 10 being regarded as substantial (The BUGS Project, 2012). For differences in DIC of less than 5, it can be misleading to simply report the model having the lower DIC value (The BUGS Project, 2012).

- R_1^2 – The proportion of variance explained at the lowest level (the measurement occasion level). It is computed for the vibration annoyance data. This criterion, which provides a measure of the goodness-of-fit of the model to the data, is defined as follows (Gelman and Hill, 2007):

$$R_1^2 = 1 - \frac{E(V(e_{fi}))}{V(Y_{fi})} \tag{8}$$

  where V represents the finite-sample variance operator, the expectation $E()$ averages over the uncertainty in the fitted model (using the posterior simulations). The quantity R_1^2 varies between 0 and 1; the closer R_1^2 is to 1, the better the goodness-of-fit of the model to the data is.

- $\hat{\Delta}$ – The proportion of risk explained at the lowest level. It is computed for the vibration acceptability data. This criterion provides a measure of the goodness-of-fit of the logistic model to the data. It is defined as follows (Gelman and Hill, 2007; DeMaris, 2002):

$$\hat{\Delta} = 1 - \frac{E\left(\frac{\sum_{i=1}^{I}\sum_{f=1}^{F}\hat{p}_{fi}(1-\hat{p}_{fi})}{I\times F}\right)}{p(1-p)} \tag{9}$$

  where $\hat{p}_{fi}$ are the estimated probabilities that $Y_{fi} = 1$ (i.e. "acceptable"), the expectation $E()$ averages over the uncertainty in the fitted model (using the posterior simulations), p is the sample marginal probability that $Y_{fi} = 1$ (that is, p is given by the proportion of 1's occurring in the $I \times F$ binary responses). The quantity $\hat{\Delta}$ varies between 0 and 1; the closer $\hat{\Delta}$ is to 1, the better the goodness-of-fit of the logistic model to the data is.

Thus, for vibration annoyance, the model comparisons are based on two criteria: DIC and R_1^2. For vibration acceptability, the model comparisons are likewise based on two criteria, here DIC and $\hat{\Delta}$. A given model model will only be considered to clearly outperform another model if it performs better in terms of both criteria.

3 Results

The results of the present study that are reported in this section are ones obtained from the analysis of the merged data by use of the methods presented in section 2.2.

3.1 Preliminary selection of relevant objective parameters

3.1.1 Vibration annoyance data

The vibration annoyance data could be represented in a 2-D MDPREF space. The two first dimensions were found to account for 73% of the total variance. The optimal dimensionality was selected by use of the Scree test method (Cattell, 1966). It was applied to the plot of the eigenvalues against the number of dimensions. The space is shown in Figure 1. For greater readability, only the endpoints of the subject vectors are reported there. The labels that begin with "V" designate the subjects from the SP study, and those beginning with "L" the subjects from the LU study.

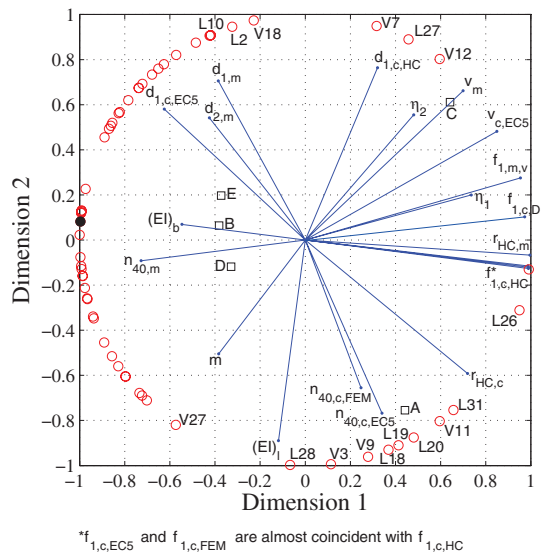

Figure 1: Vibration annoyance data – 2-D MDPREF space. □: floors; ○: endpoints of the subject vectors; •: endpoint of the average subject vector; —: objective parameter vectors.

Most of the endpoints of the subject vectors lie within the left-hand part of the space. This shows there to be a relatively close consensus among the subjects in terms of their responses. The average subject vector (marked in Figure 1 by a black circle), which appears in the left-hand part of the space, nearly coincides with the first dimension, indicating that consensus is basically found regarding this dimension of the space (its accounting for 50% of the total variance). Nevertheless, some endpoints are to be found elsewhere, notably in the upper and lower right-hand parts of the space. One can also note that the subject vectors in both studies are well mixed, there thus appearing to be no study effect on the vibration annoyance responses.

The $f_{1,c,EC5}$, $f_{1,c,FEM}$ and $f_{1,c,HC}$ vectors, which appear in the right-hand part of the space, are very close in position to the average subject vector. Their length (close to the unit) shows there to be a very high quality of representation ($r = 0.997$, $p = 0.001$, $r = 0.997$, $p = 0.001$, and $r = 0.994$, $p = 0.003$, respectively). Also, the $f_{1,m,v}$ and $f_{1,c,D}$

vectors, which appear in the right-hand part of the space, are likewise close in position to the average subject vector, although to a lesser extent. Their length reveals a very high quality of representation ($r = 0.993$, $p = 0.004$ and $r = 0.981$, $p = 0.015$, respectively). All in all, the first eigenfrequency is able, on the average, to explain the subjects' responses rather well. The higher the first eigenfrequency is, the lower on the average the level of vibration annoyance is. In addition, the $r_{HC,m}$ vector, which appears in the right-hand part of the space, is close in position to the average subject vector. Its length indicates it to have a very high quality of representation ($r = 0.998$, $p = 0.001$). These various observations show that Hu and Chui's criterion (calculated from measured quantities) can explain the subjects' responses on the average rather well. The higher this criterion is, the lower on the average the level of vibration annoyance is. The η_1 vector, finally, which appears in the right-hand part of the space, is close to the average subject vector, yet its somewhat shorter length indicates it to have a lower quality of representation ($r = 0.763$, $p = 0.323$), this objective parameter thus being correlated to a lesser degree with the average response.

	Vibration annoyance and vibration acceptability
Non subject-dependent indices	Calculated first eigenfrequency, obtained in accordance with Eurocode 5 ($f_{1,c,EC5}$)
	Hu and Chui's criterion ($r_{HC,m}$)
	Damping ratio for the first eigenmode (η_1)
Subject-dependent indices*	Frequency-weighted RMS acceleration (a_w)
	Frequency-weighted RMS velocity (v_w)
	Maximum Transient Vibration Value (MTVV)

*See *Part I* for further details of the procedure for calculating these indices.

Table 2: Objective parameters tested.

3.1.2 Vibration acceptability data

The vibration acceptability data were represented in a 2-D space. The space is shown in Figure 2; for greater readability, only the endpoints of the subject vectors are reported there. Again, the labels beginning with "V" designate the subjects from the SP study, and those beginning with "L" the subjects from the LU study.

Most of the endpoints of the subject vectors lie within the upper right-hand, lower right-hand and left-hand parts of the space. This dispersion shows the subjects' vibration acceptability responses to be less consensual than their vibration annoyance responses are. The average subject vector (marked by a black circle in Figure 2) appears in the lower right-hand part of the space. One can note too that the subject vectors in both studies are quite well mixed, no study effect on the vibration acceptability responses being evident, therefore.

The η_1 vector, which appears in the lower right-hand part of the space, is very close in position to the average subject vector. Its length shows it to possess a moderate quality of representation ($r = 0.890$, $p = 0.146$). These observations show that the damping ratio for the first eigenmode appears to be able to explain the subjects' responses on the average here rather well. The higher the value of η_1 is, the greater on the average vibration acceptability is assumed to be. The $f_{1,m,v}$, $f_{1,c,EC5}$, $f_{1,c,FEM}$, $f_{1,c,HC}$ and $f_{1,c,D}$ vectors, which appear in the lower left-hand part of the space, are less close in position

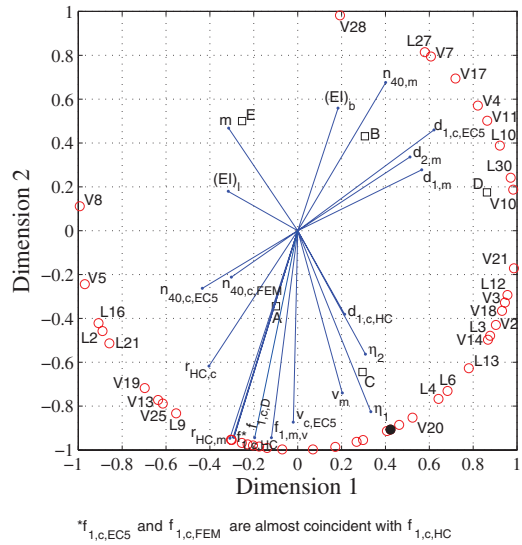

Figure 2: Vibration acceptability data – 2-D logistic PCA space. ○: endpoints of the subject vectors; ●: endpoint of the average subject vector; —: objective parameter vectors.

to the average subject vector. Their length indicates them to have a high quality of representation ($r = 0.952$, $p = 0.053$, $r = 0.986$, $p = 0.01$, $r = 0.986$, $p = 0.01$, $r = 0.982$, $p = 0.014$, and $r = 0.965$, $p = 0.034$, respectively). These observations show that the first eigenfrequency can on the average explain the subjects' responses rather well. The higher the first eigenfrequency is, the greater on the average the vibration acceptability is assumed to be. In addition, the $r_{HC,m}$ vector, which appears in the lower left-hand part of the space, is as close in position to the average subject vector. Its length shows it to have a very high quality of representation ($r = 0.998$, $p = 0.001$). This indicates Hu and Chui's criterion (calculated from measured quantities) to be able to explain the subjects' responses on the average rather well. The higher this criterion is, the greater on the average the vibration acceptability is assumed to be.

3.1.3 Discussion

The PCA results show there to be several non-subject-dependent objective parameters that can explain the subjective data rather well.

Regarding vibration annoyance, the linear PCA results show $f_{1,c,EC5}$, $f_{1,c,FEM}$, $f_{1,c,HC}$ and $r_{HC,m}$ to be the most relevant parameters for explaining, on the average, the subjects' responses. Regarding the first eigenfrequency, it appears as though any one of the three indices $f_{1,c,EC5}$, $f_{1,c,FEM}$ and $f_{1,c,HC}$ could be selected, since each of them seems equally relevant, although $f_{1,c,EC5}$ was finally selected due its widespread use and the ease of the calculations it involves. Although η_1 appeared to be correlated with the average response to a lesser extent, this design parameter seemed to possibly also be relevant in accounting for the subjects' responses, its thus being selected as well, and $r_{HC,m}$ finally being selected

too.

Regarding vibration acceptability, the logistic PCA results showed $f_{1,m,v}$, $f_{1,c,EC5}$, $f_{1,c,FEM}$, $f_{1,c,HC}$, $f_{1,c,D}$, η_1 and $r_{HC,m}$ to be the parameters most relevant on the average in accounting for the subjects' responses. As far as the first eigenfrequency is concerned, any one of the five indices that were tested could have been selected, since these appeared to be about equally relevant, yet $f_{1,c,EC5}$ was selected finally, in order to be consistent with the choice made regarding vibration annoyance, $r_{HC,m}$, and η_1 being selected as well.

3.2 Determination of indicators of vibration annoyance and vibration acceptability

All the objective parameters tested are presented in Table 2.

3.2.1 Vibration annoyance data

The null model $M0$ is shown in Table 3.

	Coefficient (95% CI)
Fixed part	
β_{00}	61.33 (56.73; 65.94)
Random part	
σ_e^2	387.2 (324.6; 466.2)
$\sigma_{u_0}^2$	234.3 (141.4; 383.8)
DIC	2641.2
$\boldsymbol{R}_1^2$	0.475

Table 3: Vibration annoyance – Null model $M0$. 95% CI: 95% Bayesian credibility interval; β_{00}: intercept; σ_e^2: variance of the residual errors at the occasion level; $\sigma_{u_0}^2$: variance of the residual errors u_0 (for the intercept) at the individual level; DIC: Deviance Information Criterion; R_1^2: proportion of variance explained at the occasion level.

Figures 3 and 4 show the differences in DIC and in R_1^2, respectively, between the null model $M0$ (taken as a reference model) and the models involving occasion-level predictors.

Models involving non-subject-dependent indices Including $f_{1,c,EC5}$ in a model as an occasion-level predictor with a fixed slope enables the model's goodness-of-fit and out-of-sample predictive power to be improved ($\Delta R_1^2 = 2.5\%$ and ΔDIC $\ll$-10 as compared with the null model $M0$). Employing a fixed-slope model involving $f_{1,c,EC5}$ is thus found to outperform the null model. Making the slope random then enables the model's goodness-of-fit and out-of-sample predictive power to be improved ($\Delta R_1^2 = 6.3\%$ and ΔDIC<-10 as compared with the fixed-slope model). In regard to both criteria, therefore, the random-slope model involving $f_{1,c,EC5}$ is the one to select. It should also be emphasized that 98% of the random slopes (the median values of these) are negative. Thus, for nearly all of the subjects, vibration annoyance is negatively correlated with $f_{1,c,EC5}$, so that the lower $f_{1,c,EC5}$ is, the greater the vibration annoyance is. Thus, there is rather close consensus

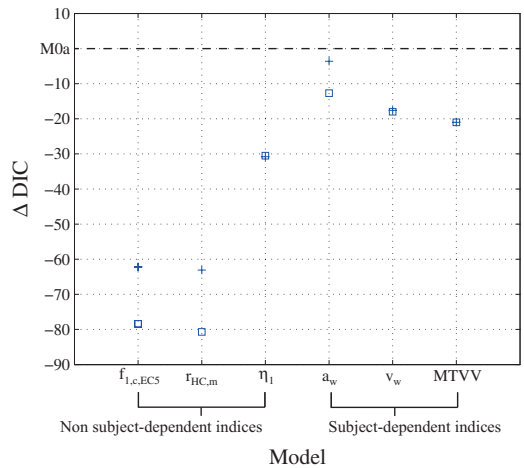

Figure 3: Vibration annoyance - Differences in DIC (ΔDIC) between null model $M0$, and the models involving occasion-level predictors. +: fixed-slope model; □: random-slope model.

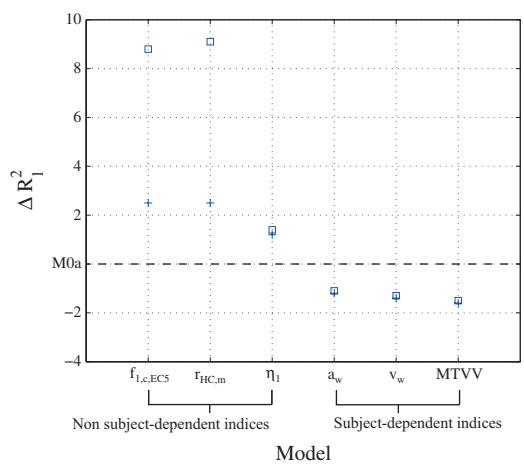

Figure 4: Vibration annoyance - Differences in R_1^2 (ΔR_1^2) between null model $M0$, and the models involving occasion-level predictors. +: fixed-slope model; □: random-slope model.

among the subjects in terms of the effect of $f_{1,c,EC5}$ on vibration annoyance. Accordingly, the model just described appears to definitely be the one to select. In making use of this model, $f_{1,c,EC5}$ can serve as a suitable indicator of vibration annoyance.

Including $r_{HC,m}$ in the model as an occasion-level predictor with a fixed slope enables the model's goodness-of-fit and out-of-sample predictive power to be improved ($\Delta R_1^2 =$ 2.5% and ΔDIC $\ll$-10 as compared with the null model $M0$). A fixed-slope model in which $r_{HC,m}$ is included thus outperforms the null model. In addition, making the slope random enables a further improvement in the goodness-of-fit and the out-of-sample predictive power to be achieved ($\Delta R_1^2 = 6.6\%$ and ΔDIC<-10 in comparison with the fixed-slope model). Thus, in terms of both criteria, a random-slope model involving $r_{HC,m}$ appears to be the one to select. It should also be emphasized that 98% of the random slopes (the median values of these) are negative. For nearly all the subjects, vibration annoyance is negatively correlated with $r_{HC,m}$, such that the lower $r_{HC,m}$ is, the greater the vibration annoyance is. Thus, there is rather close consensus among the subjects in terms of the effect of $r_{HC,m}$ on vibration annoyance. It is felt that the model just described should definitely be selected. In making use of this model, $r_{HC,m}$ can represent a suitable indicator of vibration annoyance.

Inserting η_1 into the model as an occasion-level predictor with a fixed slope tends to improve the model's goodness-of-fit ($\Delta R_1^2 = 2.5\%$ in comparison with the null model M0) and makes it possible to improve its out-of-sample predictive power (ΔDIC$\ll$-10 as compared with the null model $M0$). Making the slope random does not serve to further improve the goodness-of-fit or the out-of-sample predictive power of the model, however ($\Delta R_1^2 = 0.2\%$ and ΔDIC>0 in comparison with the fixed-slope model). Thus, a random-slope model containing η_1 does not outperform a fixed-slope model containing η_1. All in all, in making use of the fixed-slope model, η_1 appears to be an adequate indicator of vibration annoyance.

Finally, one can note that a random-slope model involving $r_{HC,m}$ appears to perform as well as a random-slope model involving $f_{1,c,EC5}$ does ($\Delta R_1^2 = 0.3\%$ and ΔDIC>-5). It appears, therefore, that $r_{HC,m}$ and $f_{1,c,EC5}$ are about equally good indicators of vibration annoyance. One can also note that the random-slope models involving $f_{1,c,EC5}$ or $r_{HC,m}$ clearly outperform the fixed-slope model involving η_1, in terms both of goodness-of-fit and of out-of-sample predictive power (at least $\Delta R_1^2 = 7.6\%$ and ΔDIC $\ll$-10). Thus, $f_{1,c,EC5}$ and $r_{HC,m}$ appear to be better than η_1 as indicators of vibration annoyance.

Models involving subject-dependent indices Including a_w in a model as an occasion-level predictor with a fixed slope does not serve to improve the model's goodness-of-fit or its out-of-sample predictive power ($\Delta R_1^2 = -1.2\%$ and ΔDIC>-5 as compared with the null model $M0$). A fixed-slope model involving a_w thus does not outperform the null model. Including a_w in the model as an occasion-level predictor with a random slope enables the model's out-of-sample predictive power to be improved (ΔDIC<-10 in comparison with the null model $M0$), but it does not serve to improve its goodness-of-fit ($\Delta R_1^2 = -1.1\%$ in comparison with the null model $M0$). Thus, a random-slope model does not clearly outperform the null model. Therefore, the models involving a_w do not clearly outperform the null model, a_w thus not being an indicator of vibration annoyance.

Including v_w in a model as an occasion-level predictor with a fixed slope enables the

model's out-of-sample predictive power to be improved (ΔDIC<-10 as compared with the null model $M0$), but it does not serve to improve its goodness-of-fit ($\Delta R_1^2 = -1.4\%$ in comparison with the null model $M0$). Thus, the fixed-slope model involving v_w appears to not clearly outperform the null model. Also, although including v_w in the model as an occasion-level predictor with a random slope enables the model's out-of-sample predictive power to be improved (ΔDIC<-10 as compared with the null model $M0$), it does not serve to improve its goodness-of-fit ($\Delta R_1^2 = -1.3\%$ in comparison with the null model $M0$). Therefore, a random-slope model involving v_w does not clearly outperform the null model. The models involving v_w appear to not clearly outperform the null model, v_w thus not being an indicator of vibration annoyance.

Including MTVV in the model as an occasion-level predictor with a fixed slope enables the model's out-of-sample predictive power to be improved (ΔDIC<-10 as compared with the null model $M0$), but it does not serve to improve its goodness-of-fit ($\Delta R_1^2 = -1.6\%$ in comparison with the null model $M0$). Accordingly, a fixed-slope model involving MTVV does not clearly outperform the null model. Also, although including MTVV in the model as an occasion-level predictor with a random slope enables the model's out-of-sample predictive power to be improved (ΔDIC<-10 in comparison with the null model $M0$), it does not serve to improve its goodness-of-fit ($\Delta R_1^2 = -1.5\%$ with respect to the null model $M0$). Thus, the random-slope model involving MTVV does not clearly outperform the null model. Since the models involving MTVV do not clearly outperform the null model, MTVV appears to not be a suitable indicator of vibration annoyance.

Summary Of the non-subject-dependent indices that were tested, $f_{1,c,EC5}$ and $r_{HC,m}$ were found to be the best indicators of vibration annoyance. None of the subject-dependent indices that were tested appeared to be a good indicator of vibration annoyance.

3.2.2 Vibration acceptability data

The null model $M0$ is presented in Table 4. Figures 5 and 6 show the differences in DIC

	Coefficient (95% CI)
Fixed part	
β_{00}	-0.491 (-0.983; -0.042)
Random part	
$\sigma^2_{u_0}$	1.92 (0.801; 4.1)
DIC	355.6
$\hat{\Delta}$	0.260

Table 4: Vibration acceptability – Null model $M0$. 95% CI: 95% Bayesian credibility interval; β_{00}: intercept; $\sigma^2_{u_0}$: variance of the residual errors u_0 (for the intercept) at the individual level; DIC: Deviance Information Criterion; $\hat{\Delta}$: proportion of risk explained at the occasion level.

and in $\hat{\Delta}$, respectively, between the null model $M0$ (taken as a reference model) and the models involving occasion-level predictors.

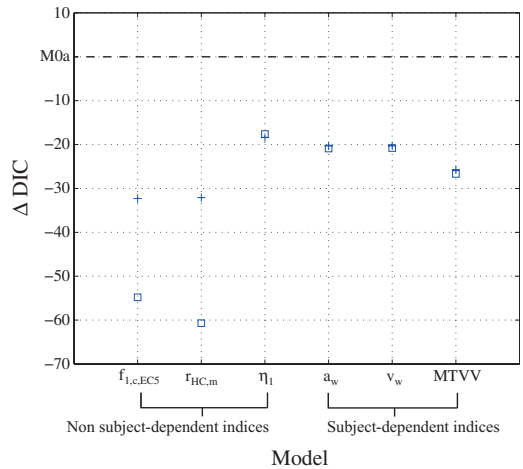

Figure 5: Vibration acceptability - Differences in DIC (ΔDIC) between null model $M0$, and the models involving occasion-level predictors. +: fixed-slope model; □: random-slope model.

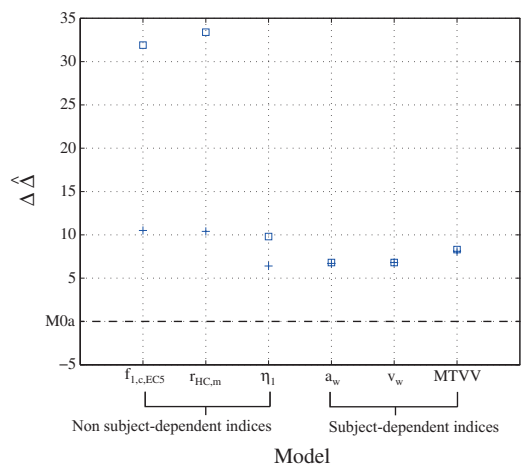

Figure 6: Vibration acceptability - Differences in $\hat{\Delta}$ ($\Delta\hat{\Delta}$) between null model $M0$, and the models involving occasion-level predictors. +: fixed-slope model; □: random-slope model.

Models involving non-subject-dependent indices Including $f_{1,c,EC5}$ in the model as an occasion-level predictor with a fixed slope enables the model's goodness-of-fit and out-of-sample predictive power to be improved ($\Delta\hat{\Delta} = 10.5\%$ and ΔDIC$\ll$-10 as compared with the null model $M0$). Thus, the fixed-slope model involving $f_{1,c,EC5}$ outperforms the null model. Making the slope random enables the model's goodness-of-fit and out-of-sample predictive power to be further improved ($\Delta\hat{\Delta} = 21.2\%$ and ΔDIC$\ll$-10 as compared with the fixed-slope model). Although in terms of these two criteria the random-slope model involving $f_{1,c,EC5}$ should be selected, there is a serious problem connected with use of this model, namely that 75% of the random slopes (the median values of these) are positive, and 25% negative. Thus, for some subjects, vibration acceptability is positively correlated with $f_{1,c,EC5}$, whereas for others vibration acceptability is negatively correlated with it. The subjects thus differ regarding the effect that $f_{1,c,EC5}$ has on vibration acceptability. This model should thus not be selected here. All in all, $f_{1,c,EC5}$ is not found to be suitable as an indicator of vibration acceptability.

Including $r_{HC,m}$ in the model as an occasion-level predictor with a fixed slope enables the model's goodness-of-fit and out-of-sample predictive power to be improved ($\Delta\hat{\Delta} = 10.4\%$ and ΔDIC $\ll$-10 as compared with the null model $M0$). A fixed-slope model involving $r_{HC,m}$ thus outperforms the null model. Making the slope random enables the model's goodness-of-fit and out-of-sample predictive power to be further improved ($\Delta\hat{\Delta} = 23\%$ and ΔDIC$\ll$-10 as compared with the fixed-slope model). Thus, in terms of both of these criteria the random-slope model involving $r_{HC,m}$ should be selected. Yet, just as with the random-slope model involving $f_{1,c,EC5}$, there is a serious problem connected with the use of this model too, 69% of the random slopes (the median values of these) being positive, and 31% negative. For the same reason as before, this model too should not be selected. All in all, $r_{HC,m}$ appears to not be a suitable indicator of vibration acceptability.

Including η_1 in the model as an occasion-level predictor with a fixed slope enables the model's goodness-of-fit and out-of-sample predictive power to be improved ($\Delta\hat{\Delta} = 6.4\%$ and ΔDIC$\ll$-10 as compared with the null model $M0$). A fixed-slope model involving η_1 thus outperforms the null model. Making the slope random enables the goodness-of-fit to be improved slightly ($\Delta\hat{\Delta} = 3.4\%$ as compared with the fixed-slope model) but does not help the out-of-sample predictive power to be improved further (ΔDIC>0 as compared with the fixed-slope model). Thus, a random-slope model involving η_1 does not clearly outperform the fixed-slope model involving η_1. All in all, in making use of the fixed-slope model, η_1 may be suitable as an indicator of vibration acceptability.

Models involving subject-dependent indices Including a_w in the model as an occasion-level predictor with a fixed slope enables the model's goodness-of-fit and out-of-sample predictive power to be improved ($\Delta\hat{\Delta} = 6.7\%$ and ΔDIC$\ll$-10 as compared with the null model $M0$). Thus, a fixed-slope model involving a_w clearly outperforms the null model. Making the slope random does not serve to further improve the model's goodness-of-fit or out-of-sample predictive power ($\Delta\hat{\Delta} = 0.1\%$ and ΔDIC>-5 as compared with the fixed-slope model). The random-slope model thus does not outperform the fixed-slope model. In making use of the fixed-slope model, a_w appears able to serve as an indicator of vibration acceptability.

		Vibration annoyance	Vibration acceptability
Non subject-dependent indices	$f_{1,c,EC5}$	+++	–
	$r_{HC,m}$	+++	–
	η_1	+	+
Subject-dependent indices	a_w	–	+
	v_w	–	+
	MTVV	–	++

Table 5: Summary of the results of the multilevel regression analyses. –, +, ++, +++: comparative degrees of relevance of the objective parameters as indicators of the subjective attributes in question.

Including v_w in the model as an occasion-level predictor with a fixed slope enables the model's goodness-of-fit and out-of-sample predictive power to be improved ($\Delta\hat{\Delta} = 6.8\%$ and ΔDIC$\ll$-10 as compared with the null model $M0$). Thus, the fixed-slope model involving v_w appears to clearly outperform the null model. Making the slope random does not serve to further improve either the model's goodness-of-fit or its out-of-sample predictive power ($\Delta\hat{\Delta} = 0\%$ and ΔDIC>-5 as compared with the fixed-slope model). The random-slope model thus does not outperform the fixed-slope model. In making use of the fixed-slope model, v_w may be suitable as an indicator of vibration acceptability.

Including MTVV in the model as an occasion-level predictor with a fixed slope enables the model's goodness-of-fit and out-of-sample predictive power to be improved ($\Delta\hat{\Delta} = 8.3\%$ and ΔDIC$\ll$-10 as compared with the null model $M0$). The fixed-slope model involving MTVV thus clearly outperforms the null model. Making the slope random does not serve to further improve the model's goodness-of-fit or out-of-sample predictive power ($\Delta\hat{\Delta} = 0.2\%$ and ΔDIC >-5 as compared with the fixed-slope model). Thus, a random-slope model does not appear able to outperform the fixed-slope model. In making use of the fixed-slope model, MTVV appears able to function well as an indicator of vibration acceptability.

Finally, one can note that (i) the goodness-of-fit of the fixed-slope model involving MTVV is slightly better than that of the fixed-slope models involving a_w or v_w ($\Delta\hat{\Delta} \geq 1.3\%$), and (ii) its out-of-sample predictive power tends to be better as well (-10< ΔDIC<-5). Thus, MTVV appears to be a better indicator of vibration acceptability than a_w or v_w are.

Summary Of the various non-subject-dependent indices that were tested, it was η_1 that turned out to be the best indicator of vibration acceptability. Of the subject-dependent indices that were tested, it was MTVV that appeared to be the best indicator of vibration acceptability. MTVV appears to also be a better indicator of vibration acceptability than η_1 is. In addition, (i) the goodness-of-fit of the fixed-slope model involving MTVV is slightly better than that of the fixed-slope model involving η_1 ($\Delta\hat{\Delta} = 1.7\%$), and (ii) its out-of-sample predictive power tends to be better as well (-10<ΔDIC<-5).

3.2.3 Summary of the outcomes

Table 5 summarizes the results of the multilevel regression analyses. The "–" symbol indicates the objective parameter in question to not be a good indicator of the subjective attribute in question. The greater the number of "+" symbols is, the more the objective parameter is regarded as being relevant as an indicator of the subjective attribute in question.

The multilevel models that pertain to the best indicators – $f_{1,c,EC5}$ and $r_{HC,m}$ for vibration annoyance and MTVV for vibration acceptability – are shown in Tables 6 and 7, respectively.

	$f_{1,c,EC5}$	$r_{HC,m}$
	Coefficient (95% CI)	Coefficient (95% CI)
Fixed part		
β_{00}	83.27 (75.19; 91.33)	78.06 (71.12; 84.90)
β_{10}	-1.35 (-1.77; -0.940)	-0.872 (-1.14; -0.603)
Random part		
σ^2_e	270.4 (220.6; 333.8)	267.8 (218.3; 330.3)
$\sigma^2_{u_0}$	517.7 (249.5; 964.0)	415.9 (219.8; 742.8)
$\sigma^2_{u_1}$	0.945 (0.333; 2.09)	0.400 (0.144; 0.870)
DIC	2562.8	2560.5
$\boldsymbol{R}^2_1$	0.563	0.566

Table 6: Vibration annoyance – Random-slope models involving $f_{1,c,EC5}$ and $r_{HC,m}$ as occasion-level explanatory variables. 95% CI: 95% Bayesian credibility interval; β_{00}: fixed intercept; β_{10}: fixed slope; σ^2_e: variance of the residual errors at the occasion level; $\sigma^2_{u_0}$: variance of the residual errors u_0 (for the intercept) at the individual level; $\sigma^2_{u_1}$: variance of the residual errors u_1 (for the slope) at the individual level; DIC: Deviance Information Criterion; R^2_1: proportion of variance explained at the occasion level. The covariance between residual errors u_0 and u_1 at the individual level is not shown.

	Coefficient (95% CI)
Fixed part	
β_{00}	0.307 (-0.296; 0.965)
β_{10}	-10.93 (-16.85; -6.11)
Random part	
$\sigma^2_{u_0}$	2.60 (1.10; 5.70)
DIC	329.9
$\hat{\Delta}$	0.341

Table 7: Vibration acceptability – Fixed-slope model involving MTVV as an occasion-level explanatory variable. 95% CI: 95% Bayesian credibility interval; β_{00}: fixed intercept; β_{10}: fixed slope for MTVV; $\sigma^2_{u_0}$: variance of the residual errors u_0 (for the intercept) at the individual level; DIC: Deviance Information Criterion; $\hat{\Delta}$: proportion of risk explained at the occasion level.

4 Discussion

Different potential indicators of vibration annoyance and of vibration acceptability were investigated. It was found that $f_{1,c,EC5}$ and $r_{HC,m}$, i.e. two non-subject-dependent objective parameters, were the best indicators for vibration annoyance, and that MTVV, i.e. a subject-dependent objective parameter, was the best indicator for vibration acceptability. Note that the damping ratio for the first eigenmode also turned out to be an important parameter in connection with both vibration acceptability and vibration annoyance. As Onysko (1970) has indicated, studies carried out in the 1960s by Wiss, Lenzen and Hurz suggested damping to also be important. Indeed, increased exposure time is thought to lead to an increase in vibration annoyance. Sufficient damping reduces the duration of exposure to the effects of each step taken by a person walking on the floor, so that walking is perceived then to a lesser degree as involving a continuous vibrational disturbance. In the present study, neither vibration acceptability nor vibration annoyance was found to be correlated with floor deflection. This result contradicts both traditions and current regulations. Notably, Onysko (1970) reported that already in 1840 Thomas Tredgold recommended making use of deflection limits. Toratti and Talja (2006) also suggested that floor deflection is related to vibrational discomfort. In the present study, certain dynamic parameters, specifically $f_{1,c,EC5}$, $r_{HC,m}$ and MTVV, were shown to be more closely correlated with vibration discomfort than floor deflection was. This result seems not illogical at all, since floor deflection is a measure of floor stiffness alone, whereas the dynamic behavior of a floor also depends upon the mass inertia of the floor.

As regards vibration acceptability, MTVV may not be practical to use in connection with design guidelines for manufacturers regarding the vibration serviceability of timber floors, since it implies that already at the design phase one needs to deal directly with walking excitation and measurement of the accelerations experienced by subjects. In fact, for random-slope models involving $f_{1,c,EC5}$ or $r_{HC,m}$, the goodness-of-fit and the out-of-sample predictive power turned out to be highest in connection with vibration acceptability. It was also observed, however, that the effect of these parameters on vibration acceptability varied considerably from subject to subject, which thus precluded their being good indicators of vibration acceptability. This corroborates the results of logistic PCA showing subjects' vibration acceptability responses to be less consistent from one subject to another than the subjects' vibration annoyance responses are. Large inter-individual differences in acceptability ratings have also been observed by Aasvang and Engdahl (2004), who studied subjective responses to aircraft noise in terms of noise annoyance and noise acceptability. Finding indicators of vibration annoyance to not represent adequate indicators of vibration acceptability, and *vice versa*, is not illogical, in view of the fact that the two subjective attributes involved are not perfectly (negatively) correlated. Indeed, a multilevel regression analysis of vibration annoyance (taken as the dependent variable) and vibration acceptability was carried out here. The proportion of variance explained at the occasion level, i.e. R_1^2, was found to be equal to 0.759, which is not particularly high.

Figures 7, 8 and 9 show, for the two vibration annoyance models (involving $f_{1,c,EC5}$ and $r_{HC,m}$, respectively) and the vibration acceptability model (involving MTVV), the

individual regression lines[1] of two subjects, together with their 95% credibility interval.

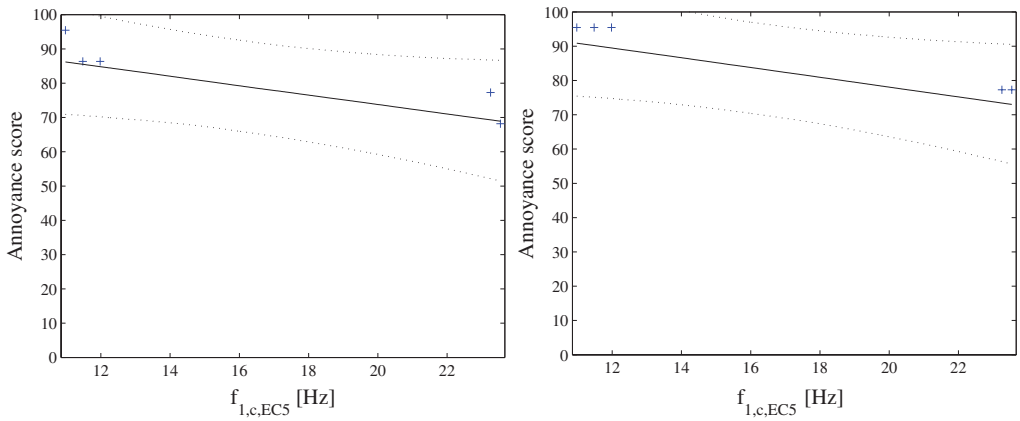

(a) Subject n°8. (b) Subject n°17.

Figure 7: Vibration annoyance model involving $f_{1,c,EC5}$ – Individual regression lines for two subjects. —: median value; – –: lower and upper limits of the 95% credibility interval;+: actual scores.

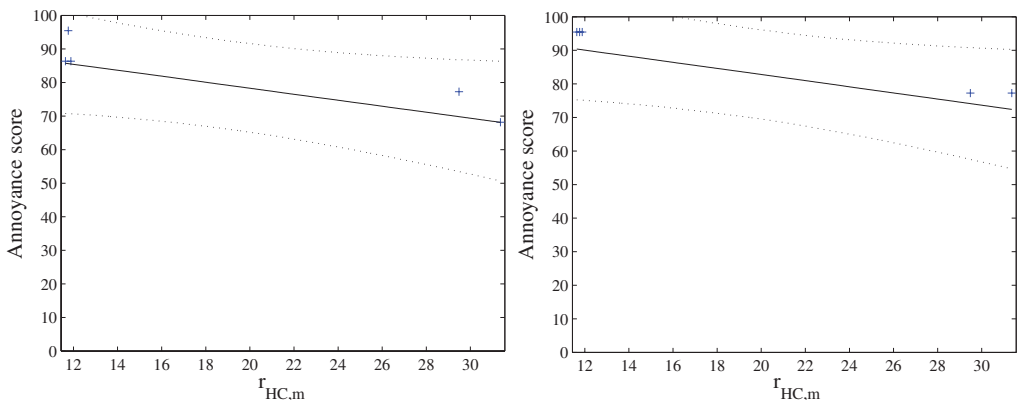

(a) Subject n°8. (b) Subject n°17.

Figure 8: Vibration annoyance model involving $r_{HC,m}$ – Individual regression lines for two subjects. —: median value; – –: lower and upper limits of the 95% credibility interval;+: actual scores.

It can be seen that, even though $f_{1,c,EC5}$ and $r_{HC,m}$ on the one hand, and $MTVV$ on the other, turned out to be the best indicators of vibration annoyance and vibration acceptability, respectively, the uncertainty regarding the individual regression lines remains

[1]For the vibration annoyance models, the individual regression lines were computed as follows: $(\beta_{00} + u_{0i}) + (\beta_{10} + u_{1i})\, f_{1,c,EC5_f}$ and $(\beta_{00} + u_{0i}) + (\beta_{10} + u_{1i})\, r_{HC,m_f}$. For the vibration acceptability model, the individual regression lines were computed as follows: $(\beta_{00} + u_{0i}) + \beta_{10}\, MTVV_{fi}$.

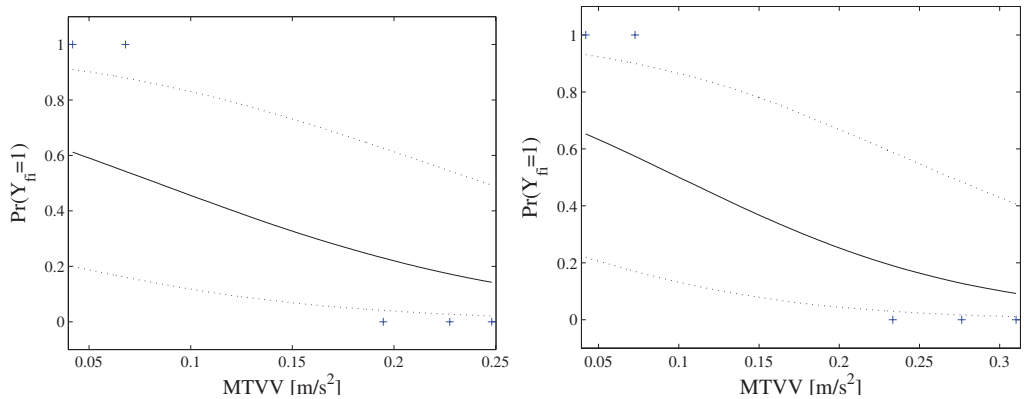

(a) Subject n°7. (b) Subject n°15.

Figure 9: Vibration acceptability model involving MTVV – Individual regression lines for two subjects. —: median value; – –: lower and upper limits of the 95% credibility interval;+: actual binary responses.

substantial. In accordance with this, the goodness-of-fit of the three models was found to be only moderate ($R_1^2 = 0.563$ and $R_1^2 = 0.566$, and $\hat{\Delta} = 0.341$, see tables 6 and 7). Nevertheless, certain trends can be noted.

For one thing, the first eigenfrequency may be an important objective parameter in connection with vibration annoyance. The lower it is, the higher the individual annoyance scores tend to be. Figure 10 shows the overall regression line[2] ($\beta_{00} + \beta_{10}\, f_{1,c,EC5}$) and its 95% credibility interval, for the vibration annoyance model involving $f_{1,c,EC5}$. It can be

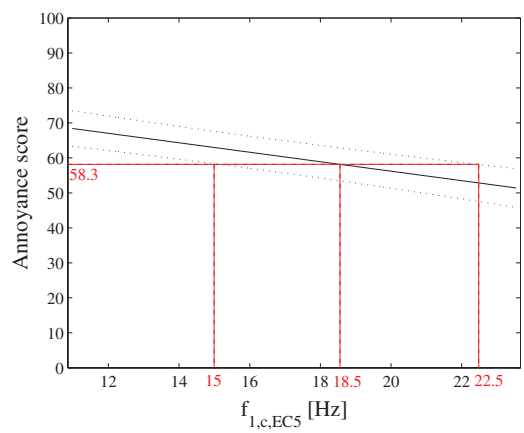

Figure 10: Vibration annoyance model involving $f_{1,c,EC5}$ – Overall regression line. —: median value; – –: lower and upper limits of the 95% credibility interval.

[2]The overall regression line provides the predicted values for an "average" subject.

noted that, on the average, the floor vibrations are not experienced as annoying (with scores < 58.3[3]) for an $f_{1,c,EC5}$ value (median value) of greater than 18.5 Hz. Taking account of the uncertainty regarding the overall regression line, this threshold value may lie somewhere between 15 and 22 Hz. This interval includes the threshold value advanced by Dolan *et al.* (1999), that of 15 Hz, for preventing wooden floor vibrations from being annoying.

Secondly, Hu and Chui's criterion may be an important objective parameter for vibration annoyance as well. The lower this criterion is, the higher the individual annoyance scores tend to be. Figure 11 shows the overall regression line ($\beta_{00} + \beta_{10}\, r_{HC,m}$), together with its 95% credibility interval, for the vibration annoyance model involving $r_{HC,m}$. One

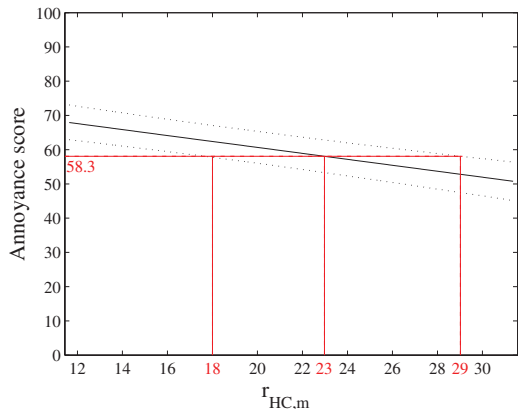

Figure 11: Vibration annoyance model involving $r_{HC,m}$ – Overall regression line. —: median value; – –: lower and upper limits of the 95% credibility interval.

can observe that, on the average, for an $r_{HC,m}$ value (median value) of greater than 23, the floor vibrations are not experienced as annoying (with scores < 58.3). Taking account of the uncertainty regarding the overall regression line, this threshold value may lie somewhere between 18 and 29. This interval includes the threshold value advanced by Hu and Chui (2004), that of 18.7, above which floors can be considered to most likely be regarded by occupants as being satisfactory.

Thirdly, MTVV turned out to be the best indicator of vibration acceptability. The lower MTVV is, the more vibrations are judged to be acceptable. Figure 12 shows the overall regression line ($\beta_{00}+\beta_{10}\, MTVV$), together with its 95% credibility interval, for the vibration acceptability model. One can observe that, on the average, the floor vibrations are judged to be acceptable ($Pr(Y_{fi}) > 0.5$) for an MTVV value (median value) of 0.03 m/s^2 or less. Taking account of the uncertainty regarding the overall regression line, this threshold value can be extended to 0.08 m/s^2. No study claiming MTVV to be an adequate indicator of vibration acceptability has been reported in the literature. Toratti and Talja (2006), notably, used the RMS velocity, v_{rms}, to draw up a vibrational classification of high-frequency floors ($f_1 > 10$ Hz).

[3]This score corresponds to the category "disturbing" of the six-point verbal scale used in SP study.

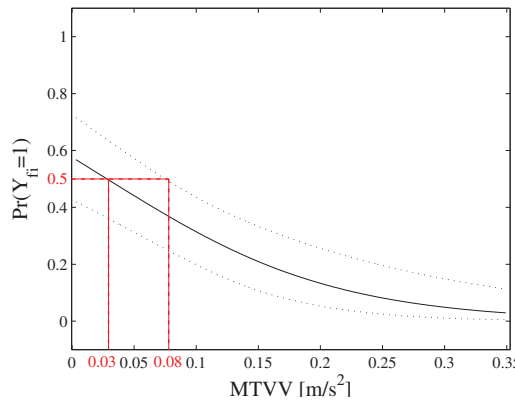

Figure 12: Vibration acceptability model involving MTVV – Overall regression line. —: median value; – –: lower and upper limits of the 95% credibility interval.

5 Conclusions

The aim of the work reported on here was to supplement current knowledge of the relationship between perceived vibrational discomfort and the objective engineering parameters involved. In two different laboratories (SP Växjö and LU), a total of 60 persons tested five different timber floors and expressed their judgments regarding the vibration performance of each of them by way of questionnaires they filled out. The data stemming from the two studies, that conducted at SP Växjö and that conducted at LU, were merged for purposes of enhancing the statistical reliability of the results. The answers the subjects provided were confronted with both measured and calculated objective parameters in efforts to determine the best design indicators of vibration acceptability and vibration annoyance, respectively. This involved use of multilevel regression. The paper can thus also be seen as exemplifying the fact that multilevel regression, not widely used as yet, can be a valuable tool for modelling repeated measures data that involves substantial inter-individual differences in rating. Two objective parameters, made use of in work reported on in the literature, were found to be the best indicators of vibration annoyance: Hu and Chui's criterion (calculated from measured quantities), $r_{HC,m}$, and the first eigenfrequency calculated according to Eurocode 5, $f_{1,c,EC5}$. The Maximum Transient Vibration Value, MTVV, determined on the basis of the accelerations experienced by the subjects, proved to be the best indicator of vibration acceptability. These findings, obtained in what can be considered a pilot study in the sense of its involving only a small sample of wooden floors (5 different ones), though there was a sufficiently large number of subjects to provide clear statistical support for the conclusions drawn concerning these floors, should be followed up by a more comprehensive study, involving a broader sample of wooden floors.

Acknowledgements

This research reported on here was funded by the Silent Spaces project, a part of the EU program Interreg IV and by the Vinnova and Formas project AkuLite.

References

H. M. E. Miedema, H. Vos: Noise annoyance from stationary sources: Relationships with exposure metric Day-Evening-Night Level (DENL) and their confidence intervals. Journal of the Acoustical Society of America **116(1)** (2004) 334–343.

W. Passchier-Vermeer, K. Zeichart: Vibrations in the living environment: Relationships between vibration annoyance and vibration metrics. Report n°98.030, TNO-PG, Leiden, The Netherlands, 1998.

J. J. Chang, J. D. Carroll: How to use MDPREF: A computer program for multidimensional analysis of preference data. Technical Report, Bell Telephone Laboratories, Murray Hill, NJ, USA, 1969.

J. J. Chang, J. D. Carroll: How to use PREFMAP and PREFMAP-2: Programs which relate preference data to multidmensional scaling solutions. Technical Report, Bell Telephone Laboratories, Murray Hill, NJ, USA, 1972.

M. R. Schroeder, D. Gottlob, K. F. Siebrasse: Comparative study of European concert halls: Correlation of subjective preference with geometric and acoustic parameters. Journal of the Acoustical Society of America **56(4)** (1974) 1195–1201.

L. J. Hu, Y. H. Chui: Development of a design method to control vibrations induced by normal walking action in wood-based floors. Proceedings of the 8th World Conference on Timber Engineering, Lahti, Finland, June 2004, pp. 217-222.

J. De Leeuw: Principal component analysis of binary data: Applications to roll-call analysis. Technical Report n°364, UCLA Department of Statistics, Los Angeles, CA, USA, 2003. Available on <`http://escholarship.org/uc/item/7n7320n0#page-1`>, viewed on 2013.02.18.

A. Gelman, J. Hill: Data analysis using regression and multilevel/hierarchical models. Cambridge University Press, New York, NY, USA, 2007.

J. J. Hox: Multilevel analysis – Techniques and applications. Second Edition. Routledge, New York, NY, USA, 2010.

W. J. Browne: MCMC Estimation in MLwiN V2.1. Centre for Multilvel Modelling, University of Bristol, Bristol, England, 2009.

The BUGS Project: DIC: Deviance Information Criterion [**online**]. Available on <`http://www.mrc-bsu.cam.ac.uk/bugs/winbugs/dicpage.shtml`>, viewed on 2012.03.28.

A. DeMaris: Explained variance in logistic regression – A Monte Carlo study of proposed measures. Sociological Methods & Research **31(1)** (2002) 27–74.

R. B. Cattell: The Scree test for the number of factors. Multivariate Behavioral Research **1** (1966) 245–276.

D. M. Onysko: Performance of wood-joist floor systems: A literature review. Information Report n°OP-X-24, Forest Products Laboratory, Canadian Forestry Service, Ottawa, Canada, 1970.

T. Toratti, A. Talja: Classification of human induced floor vibrations. Building Acoustics **13(3)** (2006) 211–221.

G. M. Aasvang, B. Engdahl: Subjective responses to aircraft noise in an outdoor recreational setting: A combined field and laboratory study. Journal of Sound and Vibration **276** (2004) 981-996.

J. D. Dolan, T. M. Murray, J. R. Johnson, D. Runte, B. C. Shue: Preventing annoying wood floor vibrations. Journal of Structural Engineering **125(1)** (1999) 19–24.

Paper C

Investigation of the vibration transmission through a lightweight junction with elastic layer using the finite element method.

J. Negreira[1], A. Sjöström[1], D. Bard[1].

[1]Lund University,
Department of Construction Sciences, Division of Engineering Acoustics,
P.O. Box 118, 221 00 Lund, Sweden.

Published in proceedings of *Internoise 2012*, New York, USA, August 2012.

Contributions: In this publication, Juan Negreira performed 95% of the work, both in terms of simulation and writing. Anders Sjöström and Delphine Bard proofread the paper and helped discussing the results.

Investigation of the vibration transmission through a lightweight junction with elastic layer using the finite element method

Juan Negreira Montero[a)]
Anders Sjöström[b)]
Delphine Bard[c)]
Department of Constuction Sciences – Division of Engineering Acoustics
Lund Tekniska Högskola, BOX 118, 22100 Lund, Sweden

When the Swedish construction code in 1994 allowed wooden multi-storey buildings, this type of lightweight structures became popular due to low cost and ease of construction[1]. A drawback in those buildings is disturbing vibrations and noise propagating in the construction, especially through the junctions - for example between floor and wall. These structures should not just meet the demands of structural integrity but also the dynamic requirements. Therefore, gaining knowledge about their dynamic behaviour is of crucial importance. To reduce noise and vibration through the junctions, rubber foam materials may be introduced between the walls and the floors and ceilings[1]. Hence, finite element simulations are useful as a prediction tool during the design phase. In this study, the properties of a junction when introducing a rubber foam material - Sylodyn® - in between were investigated by means of the finite element method using the commercial software Abaqus. The flanking transmission was specifically analysed.

1 INTRODUCTION

Lightweight structures made of timber material have a number of advantages; they may become cost effective in the future and they demand relatively short production time. However, one of the main drawbacks is related to the sound transmission, as it is becoming an increasing nuisance. The differences in weight, stiffness, density and repartition compared to traditional materials have repercussions on how the sound propagates throughout the structures. Due to this, problems with sound insulation at low frequencies through the junctions may arise. In order to avoid such problems, the weight of the construction could be increased, but this would go counter the main advantage of these constructions, i.e. being light. Another solution, which has been proved to be effective via measurements[1] but not yet accurately modelled using the finite element method (FEM), is to introduce a rubber foam material within the junction. The main

[a)] email: juan.negreira_montero@construction.lth.se
[b)] email: anders.sjostrom@construction.lth.se
[c)] email: delphine.bard@construction.lth.se

purpose is to reduce noise and vibration in the low frequency range (i.e. 20 Hz – 200 Hz). In this investigation, the influence of *Sylodyn* when placed in junctions between floor, walls and ceilings is studied. Several types of floors and ceilings as well as different placements and properties of the *Sylodyn* have been analysed.

1.1 Problem Description

In this investigation, a standard volume of a room was considered. Its inner dimensions are 3.6 m width and 6 m long, whilst the height is 3 m. In Figure 1 and 2, the drawings from *Lindbäcks Bygg's* project Brunnby Park in Upplands Väsby are shown. This lightweight structure using volume modules was chosen in order to carry out this flanking transmission investigation. The reason for this choice was its widespread use in Sweden and also because of a feasible future comparison between finite element simulations and in-situ measurements which have already been performed.

Two different placements of the *Sylodyn* were analysed as shown in Figure 3. One hereafter denoted as *case A*, where the *Sylodyn* is placed in between the top and the bottom part of the walls and the floor and ceiling on the side of the vertical partitions. The second, *case B*, where the *Sylodyn* is positioned underneath the floor and on top of the wall below. In this case, the upper wall is resting on the floor whereas the ceiling is fitted into the cavity left by the walls.

In both *case A* and *B*, the beams comprising the floor and the ceiling were considered to be placed along the shorter dimension, i.e. widthwise. Furthermore, for *case A*, the variation on the flanking transmission was also investigated when considering the beams along the lengthwise direction. A parameter study varying the material properties for the *Sylodyn* was also carried out. Finally, an analysis of the same junction without *Sylodyn* was performed.

2 FINITE ELEMENT MODEL

2.1 Introduction

Modelling a junction to represent all the phenomena involved and thus its real behaviour is a very complicated task[2]. The objective is to find a finite element model that is able to capture the phenomena that are occurring in reality. As previously mentioned, the main objective of this investigation is to study the effects of different placements of the *Sylodyn* on the flanking transmission. Hence, the relative differences between the modelled results are of greater importance than the absolute correlation between the model and the existent measurements. By doing so, one gains knowledge on the behaviour of the structure by investigating the parameters influencing the response and therefore enabling to eventually create a more refined model. With the latter model, one could try to correlate both experimental and simulation results.

As seen in Figures 1 and 2, the construction elements are composed by different materials, i.e. plasterboards, parquet, massive wood, etc. However, for this first investigation, wood was considered all over the whole model with exception of the *Sylodyn*. This simplification will not disrupt the relative differences between the different cases studied. Furthermore, only negligible vibrations are transmitted through the insulation existent in the partitions[3] and since modelling it would drastically increase the computational time, the insulation was excluded and taken into account by slightly increasing the damping of the other materials.

2.2 Materials

The structure will only be exposed to loads and displacements with low magnitude. Therefore, all non-linear behaviour was neglected and the materials may be modelled as linear elastic.

The elastomer introduced in the model to reduce the noise and vibration transmission was *Sylodyn NE*, a mixed cellular polyurethane dampening material developed by *Getzner Werkstoffe GmbH*. These viscoelastic construction elements are aligned in the path of propagation of the vibrations. Compared to existing dampening rubber, *Sylodyn* is more durable, more stable and is able to be made thinner in order to fit into small spaces[4]. *Sylodyn* can be used in many different ways, e.g., covering the whole surface, in stripes or in block shapes. In this study, it was modelled as squared blocks with dimensions 100 mm x 100 mm x 25 mm. The distance c/c (centre-to-centre) between two blocks in the junction was set to 400 mm.

In Figure 4, the load-deflection curve under compression loads for a block of *Sylodyn* is shown[4]. This curve, as all the material properties, is dependent on a parameter called shape factor; a geometric measure for the shape of an elastomeric bearing. It is defined as the ratio of the loaded area and the sum of the area of the perimeter surfaces. It has an influence in the deflection and the static load limit respectively. It can be observed that in the lower load ranges, there is a linear relationship between compression and deformation. After the linear load range, the curve moves on a degressive path, i.e. the material reacts to additional static and dynamic loads in a particularly soft manner, thus allowing for highly effective vibration isolation. For loads and deformation exceeding the degressive range, the deflection curve is progressive. The material becomes stiffer and therefore the vibration isolation is reduced. This material is not affected by overload as it recovers almost completely after load removal[4]. Furthermore, as all elastomers, *Sylodyn* reacts to dynamic loads more stiffly than to static loads.

Poisson's ratio can only be stated with adequate precision for materials that are loaded in the linear range. It was set to 0.44, whilst the loss factor considered was 0.20[4]. Due to this assumption (Hooke's law applies), the preload on the *Sylodyn* due to the walls resting on top of the blocks will not have an influence on the results. The material properties are listed in Table 1, where E [MPa] is the modulus of elasticity, ν [-] the Poisson's ratio, η [-] the loss factor, d [-] the damping ratio, ρ [kg/m^3] the mass density and G [MPa] the shear modulus.

The other material used in the model was wood. It is an anisotropic material, implying different material properties in different directions. It was modelled in *Abaqus* with the engineering constants shown in Table 1[5]. Direction 3 was considered to be along the fibre direction whilst direction 1 and 2 are perpendicular to the fibre direction. Damping prevents the structure from oscillating infinitely. It is always present in real structures and thus considered also here. It was modelled as Rayleigh damping[6] and the damping ratio was set to 3%.

2.3 Mesh

Initial calculations, i.e. convergence analyses, were carried out on single beams with different lengths and on plates with different dimensions in order to establish an appropriate mesh size that provides adequate results with low computational cost. Consequently, one ensures

that all the beams and plates assembled to create the entire model are correctly meshed and thus providing reliable results. Note the importance of this fact since we are dealing with a large model; the FE-model contains approximately 2 millions of degrees of freedom. A too fine mesh will most certainly cause an unacceptable long computation time. Only 8-nodes brick elements (C3D8R) were tried, because quadratic 20-node brick elements (C3D20R) have a tendency to create a model stiffer than reality[2]. Besides, they also cause long computation times and are therefore disregarded as element type for the complete structure.

When performing the convergence analyses, it was noticed that the biggest differences between the results of the reference mesh and the chosen FE solution are in the torsional modes; but the fact that the structure will mainly be excited by vertical loads makes the mode shapes with movement in vertical direction more important in this investigation. The vertical oscillations are also assumed to create most of the disturbing vibrations and noises that can occur in lightweight structures[2].

The most difficult challenge when creating a model of an assembled structure is to model the connections between the parts accurately. The connections determine most of the torsional rigidity and influence the behaviour of the whole structure[2]. In this study, the interactions between parts were modelled with tie constraints (full coupling). This creates stiff connections, as it happens to be the case in the real structure, where the elements are rigidly constructed using glue and screws.

The load considered was a 5 N harmonic concentrated force located at the middle of the room. A frequency sweep from 10 to 100 Hz in steps of 1 Hz was carried out. Fixed boundary conditions were applied at the free end of the walls. The different models for all studied cases can be seen in Figures 5-7. The blocks of *Sylodyn* are shown in grey colour, the floor in blue, the ceiling in red, the inner walls in yellow and the outer walls in green. Apartment separating walls (inner walls) were considered along the long edge of the room, whereas facade walls (outer walls) along the shorter sides. The height of each room was set to 1.5 m.

3 RESULTS

The following results show the performance of the junctions regarding the flanking transmission by means of plots “acceleration versus frequency”. Furthermore, the transmission from the source, located on the middle of the floor, to the ceiling underneath through the inner wall junction was investigated, i.e. the vertical transmission from the floor to the ceiling through the long side of the room. The frequency dependent acceleration was evaluated at 6 nodes along the floor, walls and ceiling, all placed 0.2 m from the junction. Likewise, the acceleration magnitudes were also evaluated on top and bottom of the *Sylodyn* blocks. An average acceleration for the 6 nodes was carried out and plotted for the different elements composing the junction. In Figure 3 the evaluation points are shown.

3.1 Case A with beams oriented widthwise

In Figure 5, one can observe that the *Sylodyn* blocks (grey) are placed between the partitions whereas the floor and the ceiling are fitted into the space created by the walls, see Figure 3. The beams are oriented widthwise.

As shown in Figure 8, the maximum acceleration magnitudes occur between 35 and 60 Hz. One can also identify that *Sylodyn* dissipates nearly all vibrations, i.e. dampens vibrations (see Figure 13), as the acceleration levels evaluated on the ceiling and the wall underneath are very low.

3.2 Case A with beams oriented lengthwise

This case is comparable with the previous case, although the beams in the floor and ceiling are now placed lengthwise, see Figure 6. The peak acceleration magnitudes existent on the floor are higher than in the previous case, probably due to the change of the orientation in the load bearing beams of the horizontal partitions. Likewise, the shape of the plots is also changed as seen in Figure 9. In this case, the acceleration peaks occur between 25 and 50 Hz as well as between 80 and 95 Hz approximately. However, the acceleration magnitudes on the ceiling and wall underneath are still very low, depicting the efficiency of the *Sylodyn* when dissipating the energy of the vibrations.

3.3 Case B with beams oriented widthwise

In Figure 7 the changed placement for the *Sylodyn* is shown. The walls on the upper floor now rest on the floor itself, being the *Sylodyn* in contact with the floor and the walls in the floor underneath. The ceiling is, as in the other cases, fitted into the cavity left by the vertical partitions. The shape of the plots resembles the ones in c*ase A* widthwise but with smaller acceleration magnitudes almost over all the frequency range as shown in Figure 10. This shows *a priori* a better performance of the junction regarding flanking transmission, although a more extensive study is needed to confirm this. As in the other cases, the *Sylodyn* performs very well when reducing the transmitted vibrations.

3.4 Parameter study

The modulus of the elasticity of the *Sylodyn* was varied in order to investigate its influence on the response of the structure. The *case A* with the beams of the floor and the ceiling along the widthwise direction was considered for this purpose. The initial value of the modulus of elasticity, i.e. 3 MPa was varied and set to 6 MPa and 9 MPa respectively. In Figure 11, the results are shown. It can be observed that the variation on the acceleration magnitude when increasing the value of the modulus of elasticity is not as large as it could be expected beforehand.

3.5 Junction without Sylodyn

The performance of the junction without *Sylodyn* was also investigated. Thus, all contacts were wood-wood connections. The performance of *case A* with beams placed widthwise was compared in both cases. The results are shown in Figure 12. It is apparent that the acceleration magnitudes evaluated at the bottom room without the *Sylodyn* are much higher, which indicates the advantages of using the *Sylodyn* as a vibration insulator in the junction.

4 CONCLUSIONS

An extensive investigation regarding the flanking transmission when introducing *Sylodyn* in a lightweight junction was carried out. It was shown that regardless of the orientation of the load bearing beams in the floor and ceiling or the placement of the *Sylodyn*, the reduction of acceleration magnitudes within the blocks of *Sylodyn* is very effective. In Figure 13 one is able to perceive how the vibrations, i.e. acceleration magnitudes, are reduced inside the block.

It was also portrayed by a parameter study that a variation in the modulus of elasticity of the *Sylodyn* does not greatly influence the vibration transmission through the junction. Likewise, it was seen that *case B* for the placement of the Sylodyn may perform better than *case A*, although a more extensive study is needed in order to confirm this fact.

In addition, the performance of a junction with *Sylodyn* was compared to the same junction without *Sylodyn*, i.e. wood-wood connections all over. It was observed that the vibrations transmitted are much higher in the latter than in the former case. Hence, the advantages of using *Sylodyn* for this type of junction were proved.

An extensive insight into the performance of the junction regarding flanking transmission has been gained. Ultimately, this will eventually allow the creation of more refined models in order to correlate both experimental and simulation results, which could be used as a prediction tool during the design phase of the structures. In these advanced models, more realistic boundary conditions as well as the real materials for the partitions may be considered.

Note that the conclusions drawn in this investigation correspond to this specific type of junction, although many junctions found in real lightweight structures have similar features.

5 ACKNOWLEDGEMENTS

This research was funded by the Silent Spaces project, a part of the EU program Interreg IV.

6 REFERENCES

1. J. Forssén et al. “Acoustics in wooden buildings. State of the art 2008. Vinnova Project 2007-01653*”. SP Technical Research Institute of Sweden Report 2008:16*. Stockholm (2008).

2. J. Negreira Montero, O. Flodén and D. Bard, “Reflection and transmission properties of a wall-floor building element: comparison between finite element model and experimental data”, *Acoustics 2012 Hong Kong* (conference proceedings), Hong Kong (May 2012).

3. L. Holterman and A. Peterson. *Vibrations in a seven-storey wood building.* Master thesis. Division of Structural Mechanics, Lund University, Sweden (2008).

4. Getzner Werkstoffe GmbH (2004). *Data sheet of the Sylodyn NE.*

5. F. Morianon, S. Fortino and T. Toratti, “A method to model wood by using Abaqus finite element software. Part 1: Constitutive model and computational details”, *VTT Technical Research Center of Finland -Report 687-*, VTT Publications, Helsinki (2008).

6. A. K. Chopra, *Dynamics of structures*, 3rd Edition, Prentice Hall, New Jersey, USA (2007)

7. L. Cremer, M. Heckl, B. A. T. Petersson. *Structure borne-sound*. 3rd Edition. Springer-Verlag. Berlin (2005).

8. K.J. Bathe, *Finite Element Proceedures*, Prentice Hall, New York, United States (1996).

9. C. Hopkins, *Sound Insulation*, Elsevier, Oxford, UK (2007).

10. L. Galbrun, “Vibration transmission through plate/beam structures typical of lightweight buildings: Applicability and limitations of fundamental theories”, *Applied Acoustics*; 71:587-596 (2010).

Table 1 – Material Properties

Wood		*Sylodyn*	
E_1 [MPa]	900	E [MPa]	3 (varied)
E_2 [MPa]	500	ν [-]	0.44
E_3 [MPa]	12500	ρ [kg/m^3]	750
G_{12} [MPa]	40	η [-]	0.1
G_{13} [MPa]	700		
G_{23} [MPa]	700		
ν_{12} [-]	0.558		
ν_{13} [-]	0.038		
ν_{23}[-]	0.015		
ρ [kg/m^3]	550		
d [-]	0.03		

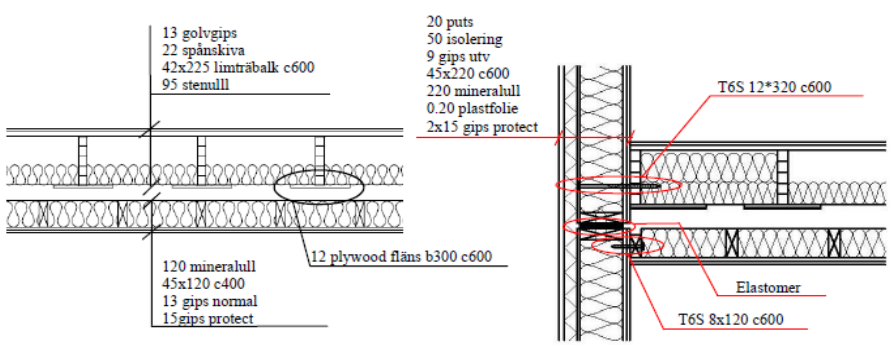

Fig. 1 - Floor/Ceiling drawings (left) and assemblage with the façade element, the so-called outer-wall (right).

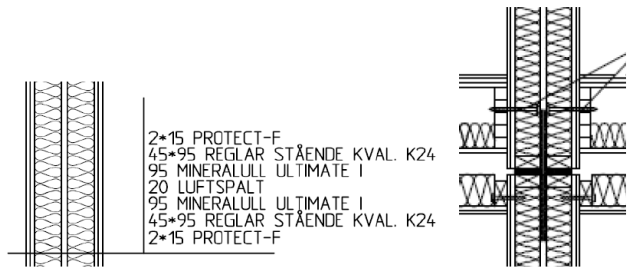

Fig. 2 - Drawings of the separating walls, i.e. inner walls (left) and the assemblage with the floor/ceiling (right).

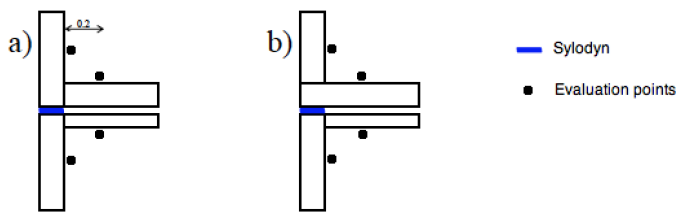

Fig. 3 - Different Sylodyn positions: (a) floor and ceiling installed between the walls and (b) floor installed upon walls. The evaluation points are dots in the figure (6 evaluation points along each line are considered).

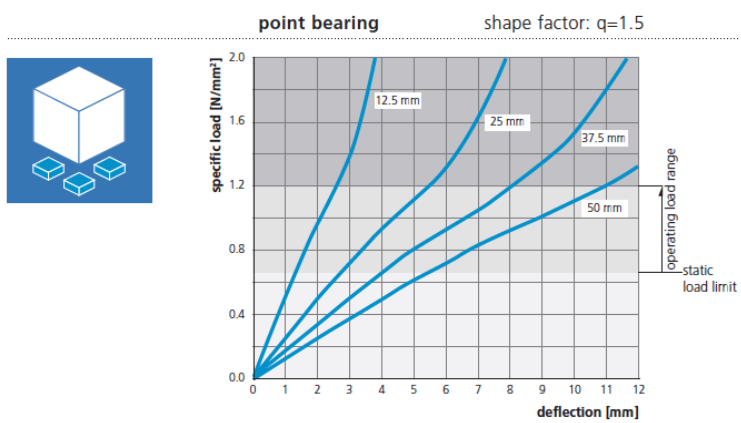

Fig. 4 - Quasy-static load-deflection curve for the Sylodyn under compression load[4].

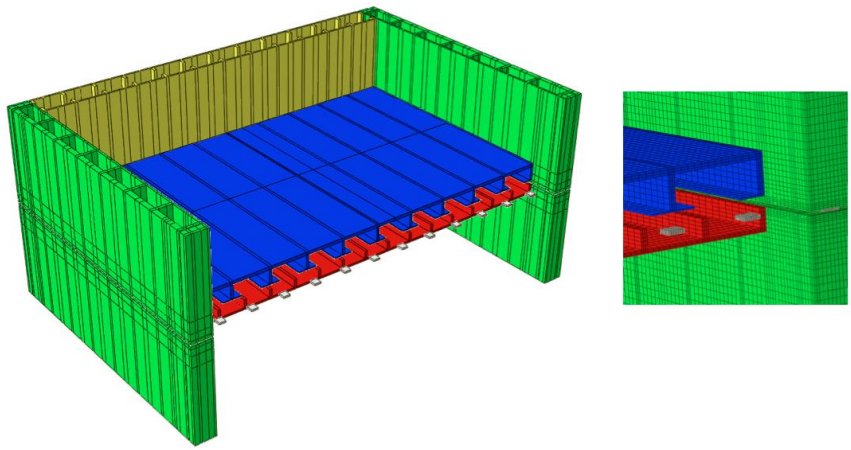

Fig. 5 - Case A with beams oriented widthwise.

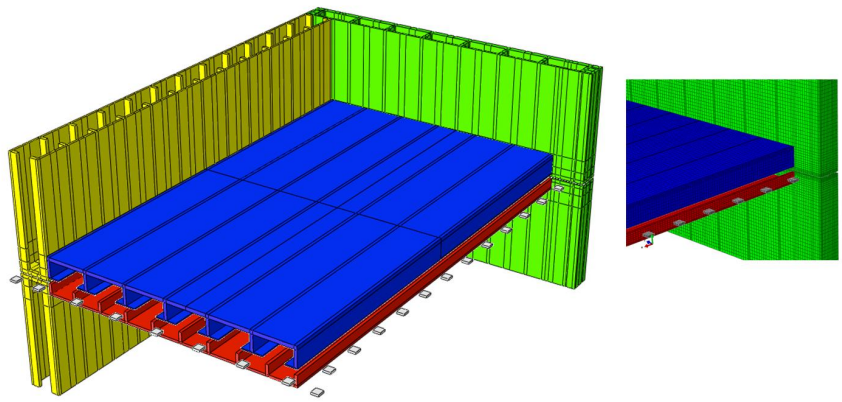

Fig. 6 - Case A with beams oriented lengthwise.

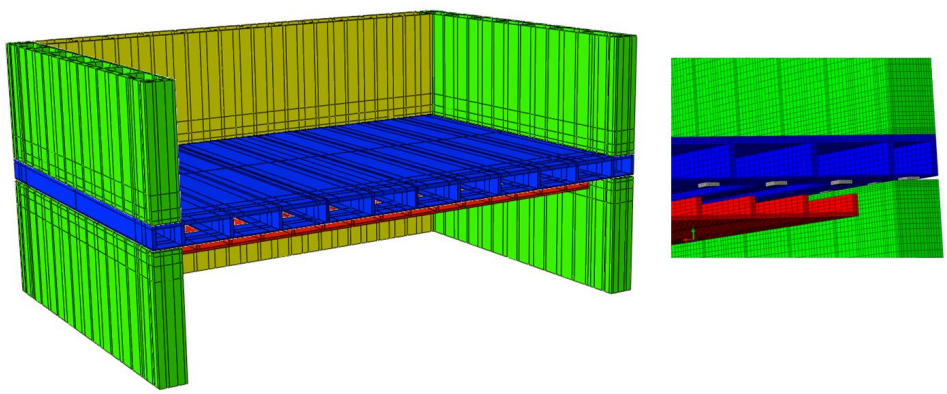

Fig. 7 - Case B with beams oriented widthwise.

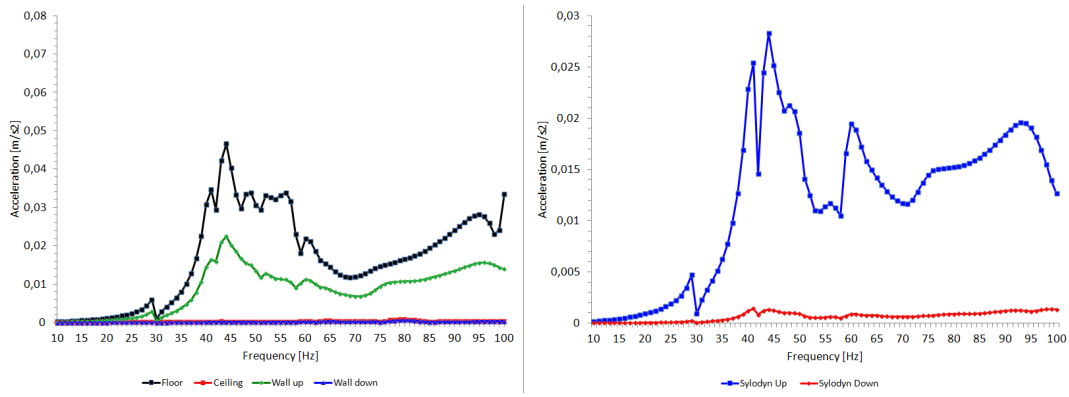

Fig. 8 - Case A widthwise. Acceleration magnitudes evaluated on the floor, ceiling, upper and bottom walls (left) and acceleration magnitudes evaluated on top and bottom of the Sylodyn (right).

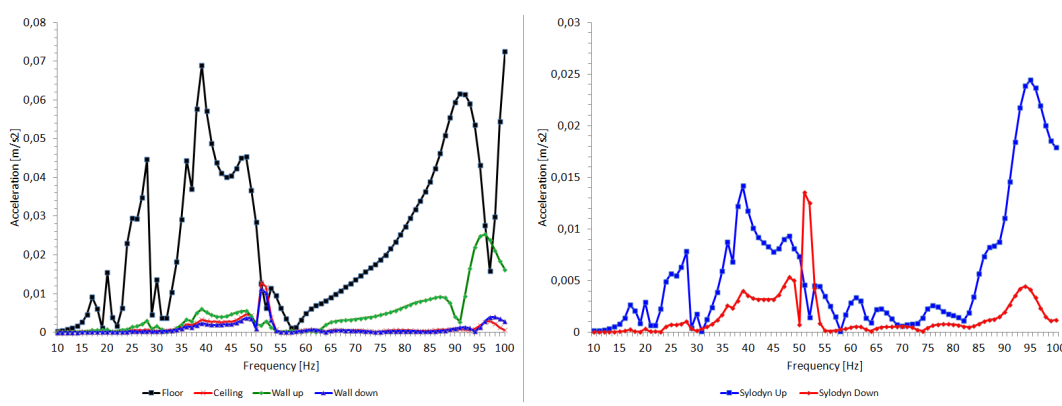

Fig. 9 - Case A lengthwise. Acceleration magnitudes evaluated on the floor, ceiling, upper and bottom walls (left) and acceleration magnitudes evaluated on top and bottom of the Sylodyn (right).

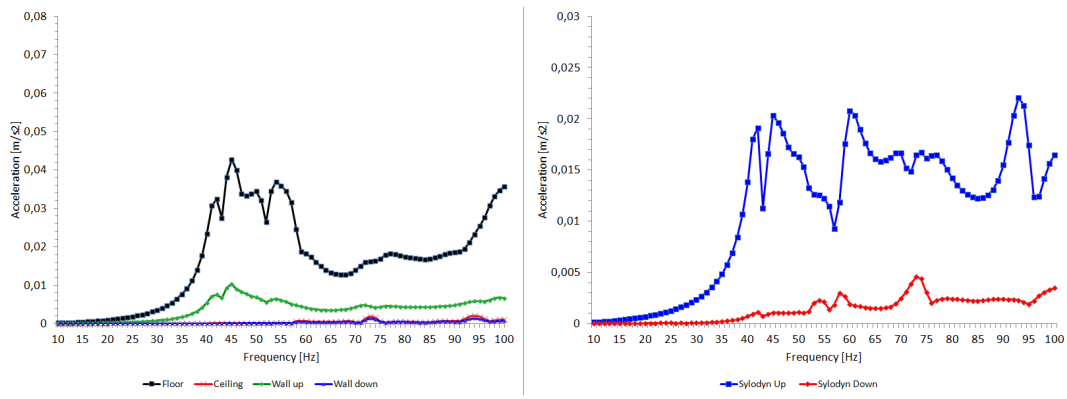

Fig. 10 - Case B widewise. Acceleration magnitudes evaluated on the floor, ceiling, upper and bottom walls (left) and acceleration magnitudes evaluated on top and bottom of the Sylodyn (right).

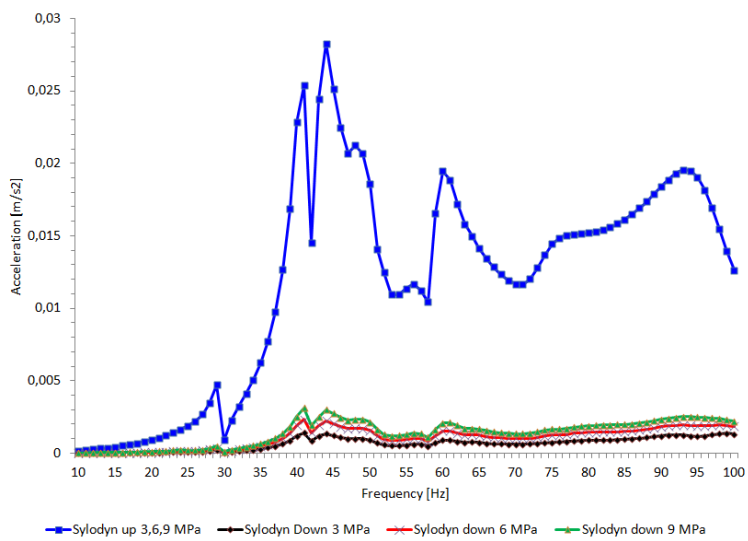

Fig. 11 - Parameter study. Comparison between the acceleration magnitudes evaluated on top and bottom of the Sylodyn blocks when varying their modulus of elasticity.

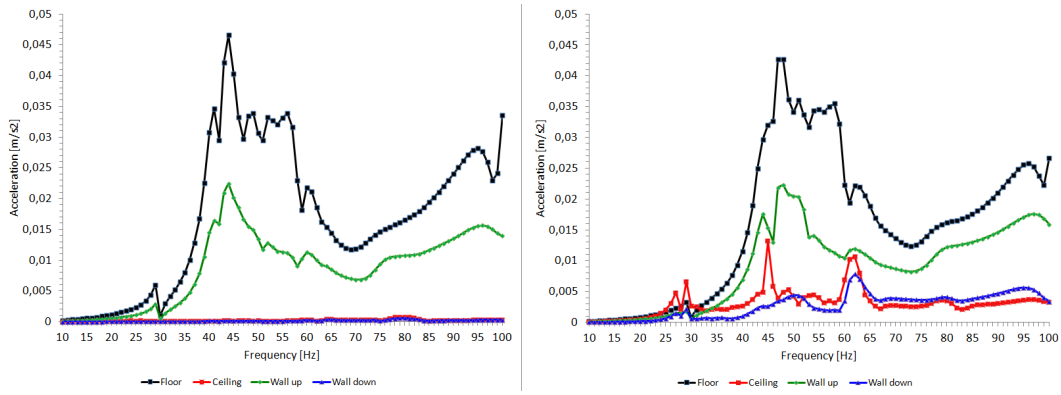

Fig. 12 - Comparison between the acceleration magnitudes for the junction using Sylodyn (left) and without Sylodyn (right). Case A widhwise was considered. The acceleration was evaluated on the floor, the ceiling and the both wall in the upper and lower floor.

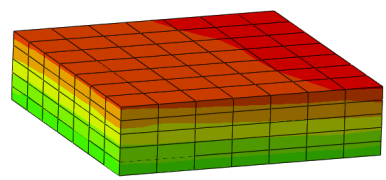

Fig. 13 -Example of reduction of the acceleration magnitudse in a block of Sylodyn for a given frequency (44 Hz) in case A widthwise. Red indicates high acceleration magnitudes whereas green shows low magnitudes.

Paper D

Characterisation of an elastomer for noise and vibration isolation in lightweight timber buildings.

J. Negreira[1], P-E. Austrell[1], O. Flodén[1], D. Bard[1].

[1]Lund University,
Department of Construction Sciences,
P.O. Box 118, 221 00 Lund, Sweden.

Submited for publication, September 2013.

Contributions: The author of the dissertation performed the measurements on the uni-axial machine, carrying out the FE simulations and analysing them, as well as writing the entire article. Per-Erik Austrell contributed with ideas about the methodology to be employed, and also discussing and analysing the results. The other authors provided with some ideas and proofread the paper.

Characterisation of an elastomer for noise and vibration isolation in lightweight timber buildings

J. Negreira[1], P.-E. Austrell[1], O. Flodén[1], D. Bard[1].

[1]Lund University, Department of Construction Sciences, P.O. Box 118, 221 00 Lund, Sweden

Abstract

Lightweight timber constructions have gained popularity in Sweden since 1994, when the national building regulations revoked a ban on constructing wooden multi-storey buildings. Since then, regulations regarding impact and airborne sound insulation have become increasingly stringent due in particular to complaints by inhabitants and the development accordingly of new building techniques. In line with this, elastomers have frequently been used at junctions between walls, floors and ceilings so as to reduce low frequency noise travelling through the structure. The development of prediction tools by using numerical methods such as the finite element (FE) method, for example, is needed in tackling flanking transmission problems during the design phase of buildings, this saving time and costs for builders. In order to create accurate models, the exact material properties involved are required as input. The properties of elastomers are often provided by manufacturers in the form of a data sheet. These properties are often closely linked to such structural effects as shape factors and boundary conditions of the samples and tests. Material properties are normally of interest for modelling arbitrary sizes and shapes of the elastomers selected, depending on the type of construction involved. Thus, accurate and handy methods for the characterisation of elastomers are needed in order to obtain precise material properties to serve as inputs for simulations. The present research concerns the characterisation of an elastomer, the properties of the elastomer material being investigated by comparing results obtained by analytical calculations, FE simulations, and mechanical testing in a uni-axial testing machine. Frequency-dependent material properties were obtained, separating geometry and material dependence. A method, one based on results of the present study, for extracting the material properties of an elastomer from the manufacturer's data sheet is thus here presented. These properties are to ultimately serve as input to commercial FE softwares for setting up models acting as prediction tools of lightweight wooden buildings.

Keywords: Lightweight, elastomer, linear viscoelasticity, finite element method, vibrations, measurements, material properties, characterisation.

1 Introduction

Although lightweight timber structures have many advantages, a high level of acoustic quality in them tends to be difficult to achieve. Even if such buildings fulfill all current regulations with respect to impact sound quality, complains amid inhabitants often arise due to structure-borne sound in the low frequency range, one of up to approximately 200 Hz. The relatively poor sound insulation at the junctions within this frequency span makes flanking transmission a problem that needs to be tackled if the comfort of the occupants in this respect is to be improved. To this end, elastomers are occasionally introduced at the junctions between floors and walls due to their sound- and vibration-insulating effects, their use being especially common in wooden buildings.

There have been, however, no reliable methods thus far for predicting the vibratory and acoustic performance of lightweight buildings, product development being carried out up to now on simply an empirical basis, i.e. through utilising observations and the experience of engineers [1]. Both time and costs could be reduced by addressing issues of flanking transmission during the design phase, for example by use of finite element (FE) simulations as predictive tools. Accurate and handy methods for the characterisation of elastomers are thus needed so as to be able to obtain the exact material properties involved to use as inputs in simulations.

In the present study, the characterisation of an elastomer was carried out. The properties of Sylodyn®, a resilient material of this sort, were investigated by comparing results stemming from analytical calculations, FE analysis through use of the commercial software *Abaqus*, and mechanical testing of the material in a uni-axial testing machine. Static and dynamic material models were established in terms of both linear elastic and viscoelastic models. In calibrating the models, data from the manufacturer and from the uni-axial tests were used in the fitting of the material models available in *Abaqus*. The load case that was investigated was a large static load to which a low degree of vibration was added. The static load comes from the dead weight of the building elements, the vibration being the noise transmitted through the junctions. Both linear and non-linear elastic models are available for taking the dead load into account, the model employed depending upon the value of the static load involved. In connection with this, one should note that the working zone for the material should always be kept within the linear range in order to maximise the insulating properties obtained. The dynamic part of the loading is dealt with by use of viscoelastic models. This approach is a rational one in its enabling the geometric and the material properties to be separated.

A general method for extracting the material properties of an elastomer from the manufacturer's data sheet for use as input to FE simulations is presented here, one based on the results of the present study.

2 Literature review

Traditionally, in single-family timber houses, the different elements converging at the junctions were connected by use of screws or nails, sometimes in combination with glue. After the construction of multi-storey wooden buildings was authorised in Sweden in

1994, more stringent sound-reduction requirements than earlier concerning impact noise were set, various new construction techniques to meet these requirements having been developed since.

An early measure taken regarding flanking transmission isolation to reduce the transmission of impact noise between floors was performed by adding additional wall plates at varying distances along the walls of the sending room or the walls of the receiving room [2]. Hanging the ceilings on resilient channels was also shown to improve the vibratory performance of timber constructions [2]. Decoupled radiation-isolated walls is another solution that was often taken [2]. The use of roller bearings to prevent shearing and avoid moment transmission was also tested more than a decade ago, this also being found to result in a decrease in the impact sound transmission [3]. Construction modifications such as adding extra mass and damping to the floor through insertion of an extra board layer, use of elastic glue between boards, and utilisation of a floating floor, have also been shown to be able to reduce vibrations created by impacts and moving about within the structure [1].

A more recent method of reducing noise and vibrations has been to place various construction elements (e.g. floor, walls, and whole rooms) on top of a resilient layer – in the form of blocks, strips or a layer covering the entire surface. Albeit this technique is used in lightweight constructions of many types, it is in volume based wooden buildings in which its use has been widespread. For a volume system, the idea is to construct prefabricated modules containing floor, walls and ceilings together with electrical, heating, water sanitation and ventilation installations [1]. Those box-like modules are then transported to the construction site and are stacked on top of each other with an elastomer being placed in between. The flexible coupling permits that the only mechanical contact between two modules in the vertical direction be by means of the elastic strips along the flanks. It is believed that, with proper design, the flanking transmission can be significantly reduced.

The solution of including elastomers in the construction obviously modifies the dynamics of the floor. One of the findings reported in [4] was that the first eigenfrequency sank when elastomers were employed and rose with increased elastomer stiffness. Measurements along those lines performed in [2] revealed that floors resting on top of elastomers will increase the modal damping and reduce the eigenfrequencies. It was also stated there, however, that the relative importance of this statement regarding the effect of vibration and impact sound pressure on site is not clearly known thus far [2].

Accordingly, in [5], comparisons between measurements and finite element simulations of a given junction were carried out. The measurements showed that insertion of elastomer pieces is beneficial if one looks simply at the vertical direction. When looking at the horizontal direction, however, i.e. a direction that can contribute strongly to the sound emission in the apartment below, use of elastomers show a positive effect in the region up to 30 Hz and above 70 Hz, but within the region 30-70 Hz, the resilient strips actually increase the velocity levels, probably due to the shear resonances that occur in particular at low frequencies. This finding was highly consistent with the results of FE simulations, which showed that the levels of acceleration in the horizontal direction increased for frequencies of between 40 and 70 Hz.

In [6], two full-scale mockups involving different junction configurations (screwed and using elastomers) were measured and compared in a laboratory environment. It was found that above approximately 70 Hz, the mean acceleration vibration level in the elastomer

configuration was significantly lower than it was in the screwed configuration. Below 70 Hz, however, the mean vibration level for the elastomer configuration was significantly higher overall than it was for the screwed junction. The authors pointed out that the elastomers, used as in that study, could heighten footstep impact noise in the low frequencies, for example, despite their improving acoustic performance at higher frequencies. The conclusions drawn there regarding the higher frequencies concur with those reported in [1], in which two volumes were stacked one on top of the other without there being an elastomer in between, i.e., wood against wood. This resulted in improved sound insulation for frequencies of 80 Hz to 500 Hz, leading to 1 dB improvement in the index respect the construction using microcellular polyurethane blocks in between to separate volumes.

In both studies [1] and [7], static loads were found to affect the insulation performance, the extent to which this occurred depending upon the storey within a building that was involved. In [1], the two-volume laboratory setup was modified by raising the uppermost one, with use of an overhead crane, to a level at which ideally, the two volumes would have mechanical contact with one another simply by means of the elastomer, at the same time as the upper volume would not transmit any static load to the lower volume. The tests conducted showed the impact sound pressure level to be reduced by 2 dB as compared with the situation in which static load was transmitted from the upper volume to the one beneath it. This confirmed what had previously been shown in [7], in which 31 nominally identical lightweight timber constructions were analysed, in each of which elastomer strips were placed between the load bearing walls and the prefabricated floors. It was found that the sound reduction was better higher up in the building. Thus, it can be concluded that when two structures are brought together, their mechanical coupling increases, compressing the elastomer and thus worsening the sound insulation.

Elastomers have a behaviour that can be described as being both elastic and viscous, dependent upon the frequency [8]. In modelling elastomers at junctions of lightweight buildings, such as by means of FE softwares, they are often dimensioned as representing a vertical single-degree-of-freedom point loaded mass-spring-dashpot system (cf. [5], [9]) so as to simplify the numerical calculations, although in practice they also act as shearing isolators in the horizontal plane and as their not being strictly point-loaded [2]. In addition, according to [9], there is a need of modelling the rotational stiffness and damping of an elastomer in a manner that matches the results of experiments and FE simulations.

If a general conclusion can be drawn from the literature, it is that in using resilient strips between different parts of lightweight buildings, it is of crucial importance to select the most adequate properties for the material and to prepare it accordingly if the degree of isolation aimed at is to be achieved. For instance, a load higher than the recommended one compresses the elastomer to a level at which its isolating properties are greatly reduced, which is believed to sometimes be the case for some buildings nowadays.

All in all, it can be concluded that there is still a lack of sufficient knowledge regarding the vibrational performance of elastomers in lightweight buildings. In order to gain a better understanding of their performance, use of accurate FE prediction tools having reliable material properties as input are needed. Determining how such properties can be achieved is thus a major aim in the investigation reported on here.

3 Governing theory: linear viscoelasticity

Viscous materials resist straining linearly over time when a load is applied. Elastic materials, in turn, when stretched, return to their original state once the stress ceases. Viscoelastic materials possess both viscous and elastic properties to varying degrees when they undergo deformations. Their material properties depend on time or, in the frequency domain, on frequency. Specifically, if the material is subjected to deformations or stresses small enough that its rheological properties do not depend upon the value of the deformation stress, the material is said to behave in a linear viscoelastic way, this being the simplest response of a viscoelastic material. It is the case for the elastomers under study here, as vibrations in dwellings due to its occupants or to machinery there are normally of small amplitude.

Buildings are subjected both to transient loads (people walking, objects striking the floor, and the like) and harmonic ones (rotatory machinery, for example). However, for reasons of computational costs, FE models of such constructions are often subjected to steady-state dynamic loading. The response of linear viscoelastic materials to a stationary sinusoidal strain history is thus of interest in the application under study here, for which such materials present a certain lag in strain. Also, the effective stiffness of such materials depends upon the rate of application of the load. Thus, by performing some mathematical manipulations such as shown in [10], for example, the stress corresponding to a harmonic strain can be expressed through a simple multiplication by a complex function, the so-called complex modulus ($E^*(\omega)$), as

$$\sigma^* = E^*(\omega)\epsilon^*, \tag{1}$$

Equation (1) can be also expressed as

$$\sigma^* = \sigma_0 e^{i\omega t+\delta} = |E^*|e^{i\arg(E^*)}\epsilon_0 e^{i\omega t} = |E^*|\epsilon_0 e^{i(\omega t+\arg(E^*))}, \tag{2}$$

ϵ_0 being the amplitude of the strain, i the complex number, t the time, ω the angular frequency and $\arg(E^*)$ the phase lag. Comparing Equations (1) and (2), leads to an interpretation of the complex modulus in terms of measurable quantities as

$$|E^*| = E^{dyn} = \frac{\sigma_0}{\epsilon_0} \qquad \text{and} \qquad \arg(E^*) = \delta, \tag{3}$$

meaning that the absolute value $|E^*(\omega)|$ is the amplitude ratio of the stress to the strain (this being termed the *dynamic modulus*, E^{dyn}), and the phase angle $\arg(E^*)$ being the phase shift between the stress and the strain; see Figure 1. The complex modulus can thus be expressed in polar form as

$$E^* = \frac{\sigma^*}{\epsilon^*} = \frac{\sigma_0 e^{i(\omega t+\delta)}}{\epsilon_0 e^{i\omega t}} = \frac{\sigma_0}{\epsilon_0}e^{i\delta}, \tag{4}$$

and in rectangular form as

$$E^* = E^{dyn}\cos\delta + iE^{dyn}\sin\delta = E_s + iE_l, \tag{5}$$

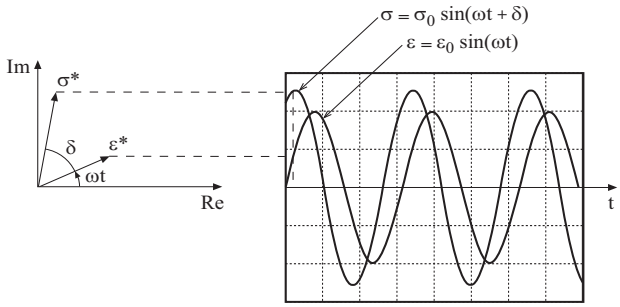

Figure 1: The real and the imaginary parts of the complex strain and stress that represent the harmonic motion.

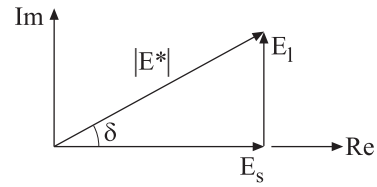

Figure 2: Complex representation of dynamic elastic modulus E^*.

where the real part of it, E_s, is called *storage modulus* (its representing the in-phase response, i.e. the elastic response) whereas the imaginary part E_l is termed *loss modulus* (its representing the out-of-phase response, i.e. the energy dissipation that occurs); see Figure 2.
An alternative form to this rectangular formulation is

$$E^* = E_s(1 + \tan\delta), \tag{6}$$

the term $\tan\delta$ being termed the loss factor. The relation between the polar and the rectangular form of the complex modulus can be simplified for small values of δ, as in the particular case under study here. These approximations are

$$\sin\delta \approx \tan\delta \approx \delta \qquad \text{and} \qquad \cos\delta \approx 1, \tag{7}$$

In addition, dynamic measurements of linear viscoelastic materials under harmonic loading show curves of dynamic modulus and damping which basically look like those shown in Figure 3, in which E_0 is the instantaneous Young's modulus for very fast loading and E^∞ is the long-term modulus for a very slow loading rate or none at all. Both the instantaneous and the long-term modulus are connected to other constants, namely the shear G and the bulk K modulus, by relationships of linear elasticity; see Equations (11) and (12).

The shear modulus G^*, which describes the material's response to shear strain, is defined as the ratio of the shear stress to the shear strain. It is given, in complex rectangular form, as

$$G^* = G_s + iG_l, \tag{8}$$

where G_s and G_l are the storage and the loss shear modulus respectively. Similarly, the bulk modulus K^* describes the material's response to uniform pressure, and is defined as the ratio of the infinitesimal pressure increase to the resulting relative decrease in the volume, according to (in rectangular form)

$$K^* = K_s + iK_l, \tag{9}$$

where K_s and K_l are the storage and the loss bulk modulus respectively.

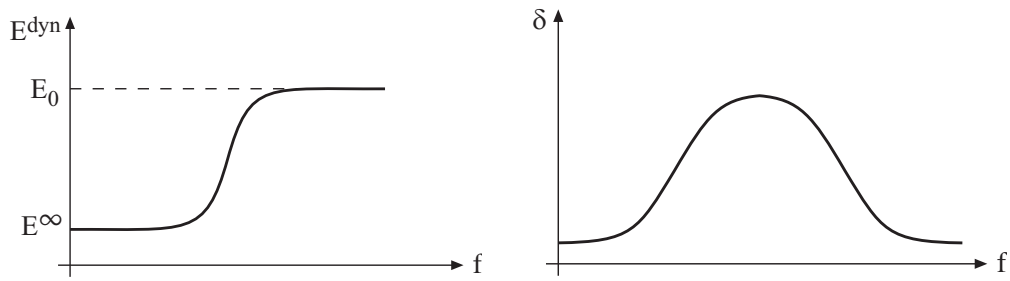

(a) Dynamic modulus. (b) Damping.

Figure 3: Dynamic measurements of linear viscoelastic materials.

4 Extraction of material properties

In the present study, Sylodyn was investigated, its being a closed-cell polyurethane material manufactured by Getzner Werkstoffe. Its material parameters were determined from the manufacturer's data sheet, together with static measurements and FE simulations. Since buildings of the sort for which the predictive tools are sought are often subjected to serviceability vibrations of small amplitude, a linear viscoelastic model was chosen, due to the small size of the deformations. An advantage of this choice is that it yields a linear dynamic system for a structure containing elastomers at the junctions. Also, through use of material parameters, elements of any size and shape can be included in the structural model employed in the dynamic analysis carried out (different construction types use different elastomer configurations).

4.1 Static parameters

Isotropic linear elasticity serves as the basis for the linear viscoelastic model and thus two parameters define the static behaviour. Looking at different commercial FE softwares (*Abaqus* [11] was the one specifically employed here), material behaviour can be defined in terms of a shear and a bulk modulus. This is a natural choice for a rubber-like material, since the behaviour that occurs in shear is usually fairly linear, even in the case of rather large strains. Also, the bulk behaviour can be characterised rather accurately in terms of a constant.

4.1.1 Measurements

Preliminary static compression tests on Sylodyn samples situated between lubricated plates, so as to obtain homogeneous state of stress and thus eliminate structural effects, were performed in an uni-axial testing machine. The results of the testing, which yielded a static Young's modulus $E^{\infty} = \Delta\sigma/\Delta\epsilon = 3.2$ MPa, are shown in Figure 4. This, together with the data contained in the data sheet of the manufacturer, will be the only measurement data used for extracting all material parameters used as input to the finite element software.

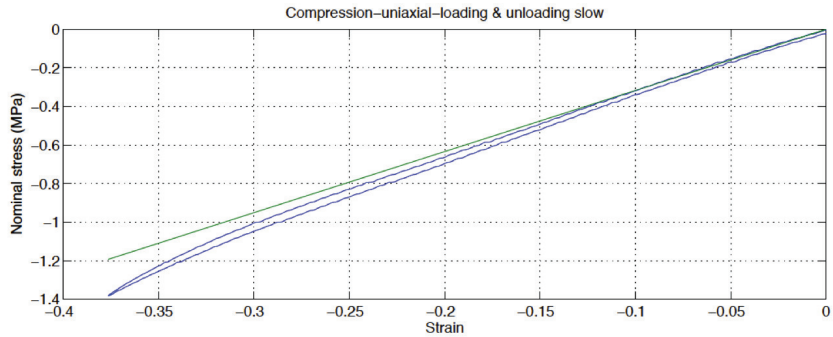

Figure 4: Compression-tests results. Loading and unloading curves (slow).

4.1.2 FE calibration

In the data sheet of the Sylodyn NE [12], a compression modulus is defined and is determined experimentally for different configurations (blocks, strip and surface) and shape factors of the elastomer (cf. Figure 6). What a shape factor represents is defined in Equation (10) and in Figure 5. Although this compression modulus is related to the Young's modulus of the material, it is not a material parameter. It depends upon the shape factor and the boundary conditions of the test piece employed. Such is often the case when manufacturers provide data concerning materials they produce, this hindering use of the properties in connection with an arbitrary size or shape.

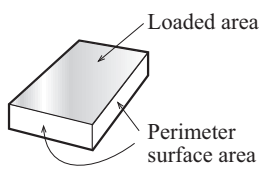

$$q = \frac{\text{loaded area}}{\text{perimeter surface area}} \tag{10}$$

Figure 5: Shape factor parameters.

FE simulations made in endeavoring to calibrate the model by mimicking the tests performed in [12], as shown in the plots displayed in Figure 6, were carried out for separate material and structural dependent properties. In so doing, the following steps were performed:

1. A block of Sylodyn having the shape factor $q = 1.5$, calculated according to Equation (10), and the thickness t=12.5 mm, was modelled, employing the same boundary conditions as those used for the tests shown in Figure 6. The blocks were meshed with hybrid elements (C3D8RH in *Abaqus*), which are generally used for nearly incompressible materials so as to avoid numerical issues. Use of a linear elastic material model (which is the basis for the linear viscoelastic model which will be eventually used) was considered. A Poisson's ratio of $\nu^{\infty} = 0.44$ was assumed initially, this being a reasonable value for a slightly compressible material, which the elastomer dealt with in here is. Also, a density measured simply as $\rho = m/V$

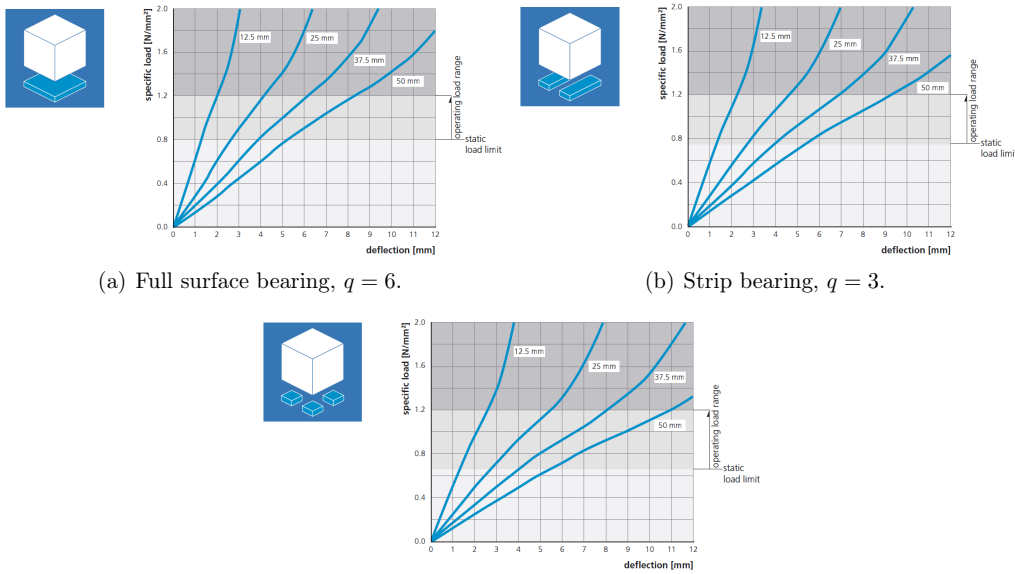

(a) Full surface bearing, $q = 6$.

(b) Strip bearing, $q = 3$.

(c) Point bearing, $q = 1.5$.

Figure 6: Quasi-static load deflection curve measured at a velocity of deformation of 1% of the thickness per second; testing between flat steel-plates; recording of the 3$^{\text{rd}}$ loading; testing at room temperature [12].

in [kg/m^3] was assigned to the block. The Young's modulus E^∞ was then varied by following an iterative process until the simulated curve and the correspondent plot given in the data sheet matched; see Figure 7. The result obtained for $q = 1.5$ and the thickness 12.5 mm., $E^\infty = 3.25$ MPa, was then also tried for the other thicknesses considered in [12], i.e. 25, 37.5 and 50 mm., yielding rather close matches throughout.

2. A block with a shape factor of $q = 6$ and for which $t = 12.5$ mm was created, its being assigned the density of the material and the Young's modulus obtained in the previous step, i.e. $E^\infty = 3.25$ MPa. This time, the Poisson's ratio was varied in an iterative manner, a rather close match being obtained for a value of $\nu^\infty = 0.42$; see Figure 8. Again, using this value, each of the thicknesses were tried for $q = 6$, again a rather close match being achieved.

3. Once this calibration was carried out, the three properties obtained, namely $\rho = 750$ kg/m^3, $E^\infty = 3.25$ MPa and $\nu^\infty = 0.42$, were ascribed to the material. The rest of the curves of the data sheet with $q = 3$ (for thicknesses of 12.5, 25, 37.5 and 50 mm), were reproduced, portraying the static parameters obtained to provide a close match for this one case as well. This thus indicates the properties obtained and to be used thereafter to be reliable. Plots relating the calibrated FE models to measurements shown in [12] are shown in Figure 9.

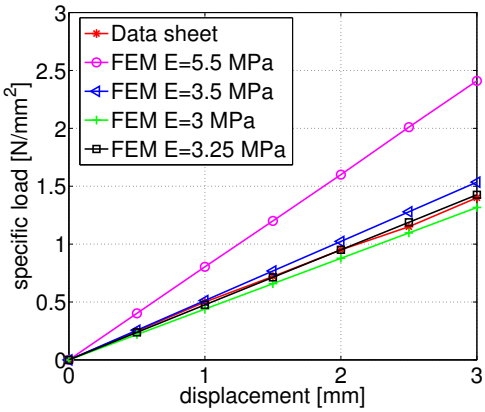

Figure 7: Iterative calibration for varying E, $q = 1.5$, $t = 12.5$ mm, $\nu = 0.44$, $\rho = 750$ kg/m^3.

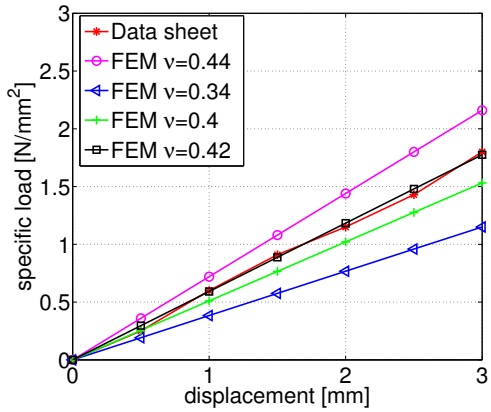

Figure 8: Iterative calibration for varying ν, $q = 6$, $t = 12.5$ mm, $E = 3.25$ MPa, $\rho = 750$ kg/m^3.

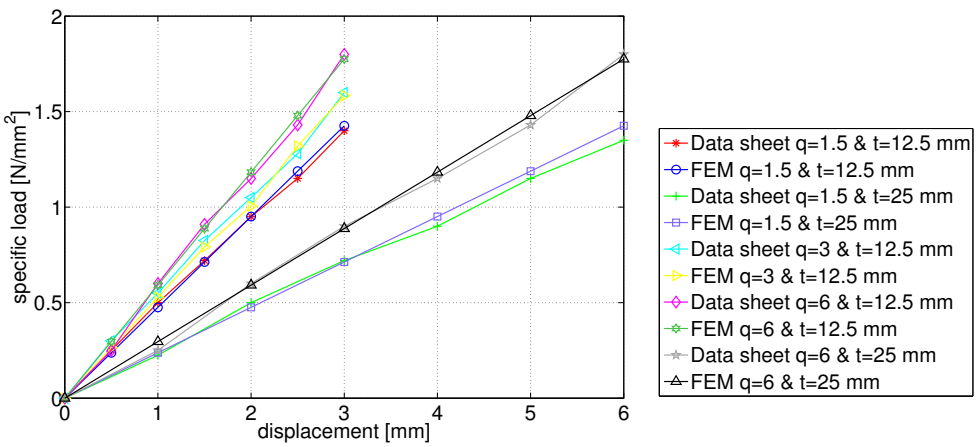

Figure 9: Comparison between the FE results and the data sheet tests for different shape factors and thicknesses of the test samples. For simplicity's sake and for clarity of the plot, not all cases under study are shown.

The Young's modulus and the Poisson's ratio need then to be converted to shear and bulk modulus by use of Equations (11) and (12) respectively.

$$G^{\infty} = \frac{E^{\infty}}{2(1+\nu^{\infty})} \tag{11}$$

$$K^{\infty} = \frac{E^{\infty}}{3(1-2\nu^{\infty})} \tag{12}$$

The FE simulations and the static measurements were shown to be consistent. The value of the Poisson's ratio also appears reasonable in view of the material being nearly incompressible. Inserting the values through the calibration into Equations (11) and (12) results in $G^{\infty} = 1.14$ MPa and $K^{\infty} = 6.8$ MPa, these being the basis for the viscoelastic parameters considered next.

4.2 Dynamic parameters

It is desirable to analyse lightweight structures containing elastomers in steady-state dynamic analyses. In terms of linear dynamic analyses, this means solving for displacement amplitudes and phase lag in linear systems of equations containing complex numbers. Accordingly, the material parameters are given in the form of complex numbers depending on the frequency. The extraction of the values for the dynamic shear and bulk modulus is taken up hereafter.

4.2.1 Methodology – justification of the scaling method

Hypothesis: The entire scaling process relies on the hypotheses, or underlying assumption, that a frequency dependent proportionality factor $\alpha(f)$ can be defined as follows for the conversion to material parameters suitable for use as input in the FE simulations:

$$\alpha(f) = \underbrace{\frac{E^{dyn}(f)}{E^{\infty}} = \frac{G^{dyn}(f)}{G^{\infty}} = \frac{K^{dyn}(f)}{K^{\infty}}}_{Homogeneous\ (I)} = \underbrace{\frac{E_c^{dyn}(f)}{E_c^{\infty}}}_{Inhomogeneous\ (II)}, \tag{13}$$

E being the Young's modulus of the material, G the shear modulus, and K the bulk modulus. Note that the subscript c denotes structural dependent properties, the superscript ∞ indicates static dynamic properties and the term dyn is used to denote the modulus of the complex dynamic magnitude in question (E^*, G^* or K^*). The phase lag of these dynamic magnitudes will be dealt with later. The relationship is derived in the following manner.

Proof of term (I) in Equation (13): Particularising, for the present case under study, the complex dynamic quantities E^*, G^* and K^*, it yields (if the frequency dependence of ν is neglected)

$$G^* = \frac{E^*}{2(1+\nu)} = \frac{1}{2(1+0.42)} \cdot E^* = 0.70 \cdot E^*, \tag{14}$$

$$K^* = \frac{E^*}{3(1-2\nu)} = \frac{1}{3(1-2\cdot 0.42)} \cdot E^* = 2.08 \cdot E^*. \tag{15}$$

There is thus, a proportionality (a constant scaling) for transformation of the dynamic elastic modulus into both dynamic shear and bulk modulus, all the latter parameters being non-structural dependent. These constant factors have the values, for this one case under study, of 0.70 and 2.08 respectively.

The dynamic proportionality factor $\alpha(f)$ to transform static to dynamic non-structural dependent properties can be defined and discussed in accordance with

$$E^{dyn} = \alpha(f)E^{\infty} \begin{cases} \alpha(f) = 1 \text{ for } f = 0 \text{ Hz} \\ \alpha(f) = E_0/E^{\infty} \text{ for } f = \infty \text{ Hz} \end{cases} \tag{16}$$

where the latter definition given in Equation (16) can be proved by comparing it with Figure 3(a). This assumption (approach) is also employed in [10] (Section 9.5.1). In the same manner, due to the proportionality shown earlier in Equations (14)-(15), it can be assumed that

$$G^{dyn} = \alpha(f)G^{\infty} \quad \text{and} \quad K^{dyn} = \alpha(f)K^{\infty}, \tag{17}$$

meaning that the dynamic stiffness in the various loading cases varies in the same manner with frequency. Hence, in accordance with Equations (14)-(17), it can be stated that

$$\alpha(f) = \frac{E^{dyn}(f)}{E^{\infty}} = \frac{G^{dyn}(f)}{G^{\infty}} = \frac{K^{dyn}(f)}{K^{\infty}}, \tag{18}$$

which defines $\alpha(f)$ as being ratios of different dynamic to static constants, without any structural dependence being involved.

Proof of term (II) in Equation (13): To be obtained next is $\alpha(f)$ defined as the ratio of the structural dependent dynamic to static properties. By inhomogeneous loading is meant that the boundary conditions result in a change in stiffness as compared to the homogeneous case. In compression, for example, the situation is that described in Figure 10. The behaviour of the tests shown there is governed by the following equations:

$$\begin{aligned} \frac{P}{A} &= E_c^{\infty}\frac{u_c}{H} \quad \text{for Figures 10(a) and 10(c),} \\ \frac{P}{A} &= E^{\infty}\frac{u}{H} \quad \text{for Figures 10(b) and 10(d).} \end{aligned} \tag{19}$$

where u is the vertical displacement of the sample test when it is compressed, H is the original height of it, A is the cross section of it, P the compressive force and E_c^{∞} and E^{∞} are the Young's modulus (the structural and the non-structural dependent one, respectively).

It can thus be stated, in comparing the two equations given in (19), that a proportionality factor k_c exists in accordance with

$$E_c^{\infty} = k_c E^{\infty}, \tag{20}$$

the boundary conditions affecting the instantaneous modulus in the same way, i.e.

$$E_c^{0} = k_c E^{\infty}, \tag{21}$$

and thus

$$E_c^{dyn}(f) = \underbrace{k_c E^{\infty}}_{E_c^{\infty}}\alpha(f), \tag{22}$$

and finally

$$\alpha(f) = \frac{E_c^{dyn}}{E_c^{\infty}}. \tag{23}$$

Equation (23) justifies together with Equation (18) the assumption given in Equation (13).

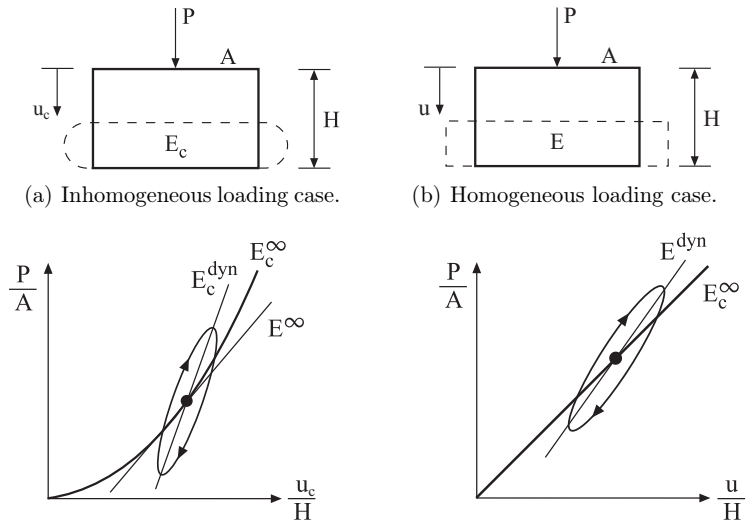

(a) Inhomogeneous loading case.

(b) Homogeneous loading case.

(c) Inhomogeneous loading case response plot.

(d) Homogeneous loading case response plot.

Figure 10: Compression test between non lubricated plates (a), allowing the material to bulge and thus creating structural effects together with its response (c); and compression test between lubricated plates (b), showing ideal behaviour eliminating any structural effect, together with its stress-strain response (d).

4.2.2 Application – obtaining the material properties

Through use of the underlying assumption discussed in the previous section, the material properties were extracted from the data contained in the data sheet. The Sylodyn NE data sheet [12], yields a dynamic compression modulus (E_c^{dyn}) and a loss angle ($\tan\delta$) for a case mixing in a structural dependence as discussed; see Figure 11. The parameters $E_c^{dyn}(f)$ and $\delta(f)$, with f being given in Hertz and the subindex c denoting the structural dependent properties, can be looked upon as the absolute value and the phase angle of a complex quantity being dependent upon the frequency E_c^*, where

$$E_c^{dyn} = |E_c^*| \qquad \text{and} \qquad \delta = \arg E_c^*. \tag{24}$$

Looking at Figure 11(a), one finds that E_c^{dyn} is weakly dependent upon the frequency, its having a value of around 6 MPa. The dynamic modulus is always larger than the static one [10], and in this case it is even higher, due to structural effects (cf. Figure 10(c)). Thus, in order to find G^* and K^*, these being the dynamic complex shear and the bulk modulus, respectively, the values need to be properly scaled, so as to eliminate structural effects, as explained in Section 4.2.1.

In [13], it was shown that the losses represented by δ are no more than weakly dependent upon the boundary conditions, and that they can thus be taken as corresponding to

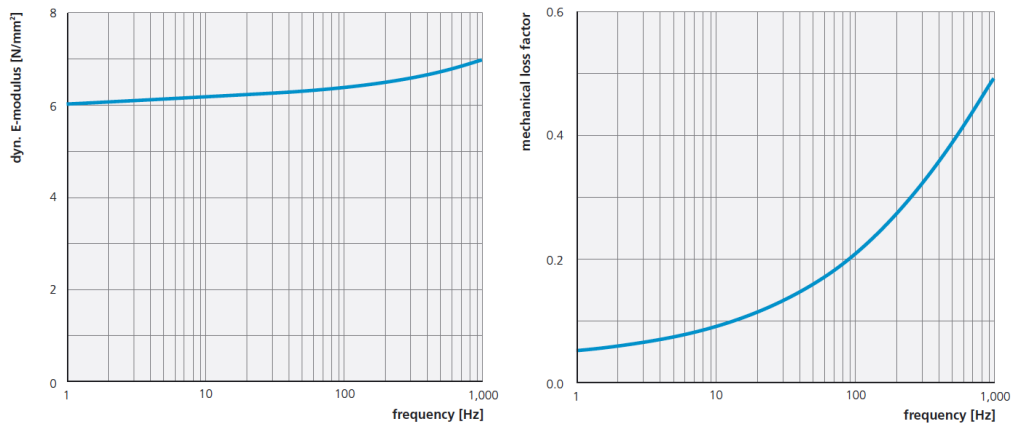

(a) Dynamic Young's modulus.

(b) Loss factor.

Figure 11: DMA-tests; mastercurve with a reference temperature of 21°C; tests within the linear area of the load deflection curve, at low specific loads [12].

the phase angle of the complex material parameters, i.e. they can be directly taken from the data sheet.

Finding material parameters for the input to the FE simulations is thus a matter of carrying out a proper scaling of the dynamic stiffness given in the data sheet.

The scaling of the shear modulus, G, is done by combining Equations (17) and (23) in the following manner:

$$G^{dyn}(f) = \alpha(f) \cdot G^{\infty} = \frac{E_c^{dyn}(f)}{E_c^{\infty}} \cdot G^{\infty}, \tag{25}$$

where $E_c^{dyn}(f)$ can be taken directly from Figure 11(a) for each frequency of interest, and E_c^{∞} can be taken from Figure 12. In the latter Figure, it can also be seen that E_c^{∞} has a value for the lowest shape factor ($q = 1.5$) which is fairly constant (one of approximately 6 MPa) if the preload is less than about 0.6 MPa, which should be the operating range for the material (therefore the value of E_c^{∞} should be taken from the curve termed as *static* and below the value of 0.6 MPa in the horizontal axis). The static shear modulus G^{∞} present in Equation (25) was determined earlier by use of Equation (11). Note that both Figures 11(a) and 12 have redundant data, i.e. they are equivalent in some respects. Thus, if the material is operating in the recommended range, the curves termed as *10 Hz* and *30 Hz* in Figure 12 are equivalent to the values given in Figure 11(a) if one looks in the horizontal axis at the values for the frequencies of 10 Hz and 30 Hz, since these yield the same value for $E_c^{dyn}(f)$. Since no value for 0 Hz is given in Figure 11(a), the value for E_c^{∞} has to be obtained from the curve *static* in Figure 12, as was explained earlier.

Accordingly, the material parameters can be obtained directly from the static parameters by scaling them in terms of a frequency-structural dependent parameter $\alpha(f)$, as determined for each frequency directly from the data sheet [12].

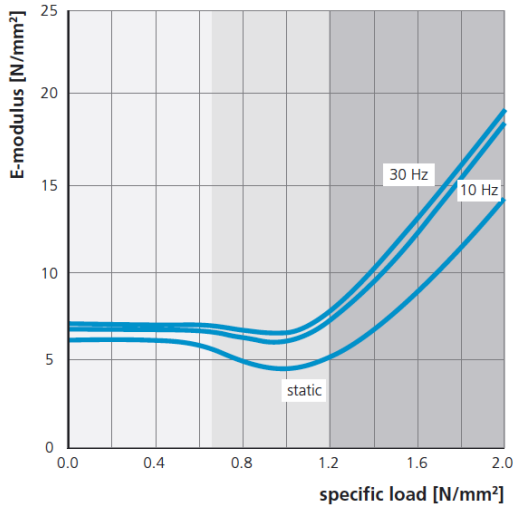

Figure 12: Static modulus of elasticity as a tangent modulus taken from the load deflection curve; dynamic modulus of elasticity due to sinusoidal excitation with a velocity level of 100 dBv re. $5{\cdot}10^{-8}$ m/s; test according to DIN 53513, $q = 1.5$ [12].

The loss angle δ, as already mentioned, is not affected by the boundary conditions or by structural effects [13]. This has not just been shown experimentally, it in fact is inherent in the assumption of proportionality. This means that the phase angle for $G^*(f)$ can be taken directly also from the data sheet (cf. Figure 11(b)), with use of the simplification given in Equation (7), i.e. that

$$\arg G^*(f) = \delta(f). \tag{26}$$

The parameters determined thus far ($G^{dyn}(f)$ and $\delta(f)$) give the complex shear modulus in polar form. *Abaqus* requires G^* and K^* in a rectangular form, i.e. $G^* = G_s + iG_l$, with G_s and G_l being the storage and loss modulus, respectively. The conversion can be done by applying the simple trigonometric principles of

$$\begin{aligned} G_s &= G^{dyn} \cos\delta, \\ G_l &= G^{dyn} \sin\delta. \end{aligned} \tag{27}$$

For the complex bulk modulus, the same procedure applies, where

$$K^{dyn}(f) = \alpha(f) \cdot K^{\infty} = \frac{E_c^{dyn}(f)}{E_c^{\infty}} \cdot K^{\infty}, \tag{28}$$

$\alpha(f)$ having the same values and thus being obtained in the same way as for the case of the dynamic shear modulus, and K^{∞} being calculated on the basis of Equation (12). Again, the phase angle for $K^*(f)$ is taken directly from the data sheet (cf. Figure 11(b)) making use of the simplifications given in Equation (7)

$$\arg K^*(f) = \delta(f). \tag{29}$$

The bulk modulus is hence given, in rectangular form, as

$$\begin{aligned} K_s &= K^{dyn} \cos\delta, \\ K_l &= K^{dyn} \sin\delta. \end{aligned} \tag{30}$$

Results obtained in employing this scaling procedure for use in *Abaqus* are presented in Section 5.1.

5 Verification

In this section, the method developed here is tested for purposes of verification.

5.1 Material properties

The material properties of the elastomer in question that were obtained in employing this method are presented in Tables 1 and 2.

Table 1: Linear viscoelastic properties (of the dynamic shear modulus). For simplicity's sake, only certain frequencies amongst all that were determined are presented. The values for other frequencies can be obtained either through the linear interpolation between the values presented in the table or through obtaining $\alpha(f)$ from Figures 11(a) and 12.

	Data Sheet			Scale factor	MTS&FEM	Scaling Eq.(25)	*Abaqus* Input	
f [Hz]	E_c^{dyn} [MPa]	E_c^{∞} [MPa]	$\delta \approx \tan\delta$	$\alpha(f)$	G^{∞} [MPa]	G^{dyn} [MPa]	G_s [MPa]	G_l [MPa]
1	6.0000	6	0.0500	1.0000	1.14	1.1400	1.1385753	0.05697625
5	6.1000	6	0.0700	1.0167	1.14	1.1590	1.15616161	0.08106376
10	6.2000	6	0.0900	1.0333	1.14	1.1780	1.17323232	0.10587693
15	6.2125	6	0.0100	1.0354	1.14	1.1804	1.18031598	0.01180355
20	6.2250	6	0.1200	1.0375	1.14	1.1828	1.17424441	0.14158961
25	6.2300	6	0.1100	1.0383	1.14	1.1837	1.17654583	0.12994457
30	6.2500	6	0.1300	1.0417	1.14	1.1875	1.17747975	0.15394054

Table 2: Linear viscoelastic properties (of the dynamic bulk modulus). For simplicity's sake, only certain frequencies amongst all that were determined are presented. The values for other frequencies can be obtained either through the linear interpolation between the values presented in the table or through obtaining $\alpha(f)$ from Figures 11(a) and 12.

	Data Sheet			Scale factor	MTS&FEM	Scaling Eq.(28)	*Abaqus* Input	
f [Hz]	E_c^{dyn} [MPa]	E_c^{∞} [MPa]	$\delta \approx \tan\delta$	$\alpha(f)$	K^{∞} [MPa]	K^{dyn} [MPa]	K_s [MPa]	K_l [MPa]
1	6.0000	6	0.0500	1.0000	6.8	6.8000	6.79150177	0.33985835
5	6.1000	6	0.0700	1.0167	6.8	6.9133	6.89640258	0.48353822
10	6.2000	6	0.0900	1.0333	6.8	7.0267	6.99822787	0.63154661
15	6.2125	6	0.0100	1.0354	6.8	7.0408	7.04048129	0.07040716
20	6.2250	6	0.1200	1.0375	6.8	7.0550	7.00426493	0.84456962
25	6.2300	6	0.1100	1.0383	6.8	7.0607	7.01799269	0.77510799
30	6.2500	6	0.1300	1.0417	6.8	7.0833	7.02356341	0.91824184

5.1.1 Dynamic finite element calibration

The material properties presented in the tables stemming from the method developed set the scene for viscoelastic linear dynamic calculations that were performed in *Abaqus*. A block of Sylodyn (q=1.5 and t=12.5 mm) was modelled, the properties shown in Section 5.1 being ascribed to it, as well as the same boundary conditions as those involved in the tests performed in [12]. A frequency sweep was carried out and the dynamic modulus was obtained simply as $|E^*| = \sigma_{nom}/\epsilon = (R/A)/(u/H)$; R being the reaction force on the surface of the block, and A, u and H being defined in Figure 10. As one can see, there is a fairly close agreement between the data as taken from Figure 11(a) and a block of Sylodyn modelled with use of the same shape factor and the same material data as obtained through use of the scaling process that was developed; see Figure 13.

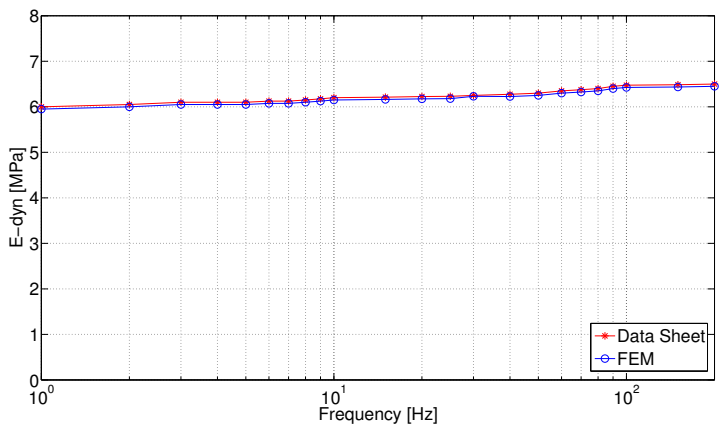

Figure 13: Verification of the dynamic properties obtained.

6 Conclusions

Low frequency prediction tools for assessing vibratory performance of lightweight buildings are needed due to frequency with which complaints in this respect arise on the part of the inhabitants. Since the current standards leave low frequencies out of the scope, acoustic comfort may not met, even when buildings fulfil all of the regulations currently in force. Assessing the dynamic behaviour of a building accurately requires of FE models representing the geometry involved in great detail, as any geometric variations may have an effect. Likewise, reliable input of the material properties in question are needed, since even small changes can have a marked effect on the results obtained.

In wooden buildings, elastomers are often introduced at the junctions in order to reduce noise and vibration transmission. In setting up the FE prediction tools referred to here, it is of particular interest to have knowledge of the material properties involved, so as to be able to model elastomers of any size and shape. The properties of rubber-like materials and elastomers are often given on data sheets by the manufacturers in data

sheets, these often being bonded to structural effects such as shape factors or boundary conditions, possibly limiting and hindering their use for a general arbitrary case. In the present study, a method for determining the material properties of elastomers based on laboratory testing, material modelling, and FE simulations was developed. Ultimately, the method can be expected to permit the material properties to be obtained simply on the basis of the manufacturer's data sheet and knowledge of the static modulus of elasticity of the material. This can facilitate the introduction of accurate material properties into FE commercial softwares in a handy way.

Several models of the junctions in modelling these in FE softwares are possible. A simplified approach is to treat an elastomer as a discrete 1-degree-of-freedom spring-and-dashpot system to be able to speed up the calculations. The authors are currently involved in the development of a 6-degree-of-freedom spring-dashpot system that can mimic the behaviour of the elastomer blocks placed at the junctions. The need for this approach is specifically pointed out in [9]. This is expected to eventually permit the effective use of substructuring reduction techniques, for assembling parts into a FE model of an entire building, where this can be seen a far more suitable and efficient approach for time-consuming FE simulations.

Acknowledgements

This research was funded by the Silent Spaces project a part of the EU program Interreg IV. The authors very appreciate of the financial support provided.

References

[1] F. Ljunggren, A. Ågren: Potential solutions to improved sound performance of volume based lightweight multistory timber buildings. Applied Acoustics **72** (2011) 231–240.

[2] A. Ågren, F. Ljunggren, Å. Bolmsvik: Flanking transmission in light weight timber houses with elastic flanking isolators. Proceedings of Internoise, New York, USA, 2012.

[3] S. Ljunggren: Measurement of the performance of noise controlling devices in buildings of massive wood. Working Report 2001:42001. Department of Civil and Architectural Engineering, Division of Building Technology, KTH, Stockholm, Sweden, 2001.

[4] K. Jarnerö, Å. Bolmsvik, A. Brandt, A. Olsson: Effects of flexible supports on vibration performance of floors. Proceedings of Euronoise 2012, Prague, Czech Republic, 2012.

[5] Å. Bolmsvik, A. Linderholt, K. Jarnerö: FE modeling of a lightweight structure with different junctions. Proceedings of Euronoise, Prague, Czech Republic, 2012.

[6] Å. Bolmsvik, A. Brandt: Damping assessment of light wooden assembly with and without damping material. Engineering Structures **49** (2013) 434–447.

[7] R. Ökvist, F. Ljunggren, A. Ågren: Variations in sound insulation in nominal identical prefabricated lightweight timber constructions. Journal of building acoustics, **17**(2) 2009, 91–103.

[8] Å. Bolmsvik: Structural-acoustic vibrations in wooden assemblies – Experimental modal analysis and finite element modelling. PhD thesis. Linnaeus University, Sweden, 2012.

[9] Å. Bolmsvik, A. Linderholt, A. Brandt, T. Ekevid: FE Modelling of Light Wooden Assemblies. Submitted to Engineering Structures. January 2013.

[10] P-E. Austrell: Modeling of elasticity and damping for filled elastomers. PhD thesis, Division of Structural Mechanics, Lund University, Sweden, 1997.

[11] Dassault Systèmes: Abaqus theory manual, Version 6.11, 2012.

[12] Getzner Werkstoffe GmbH (2004). Data sheet of the Sylodyn NE.

[13] A. K. Olsson, P-E. Austrell: Finite element analysis of a rubber bushing considering rate and amplitude dependence effects. Proceedings of 3rd European Conference on Constitutive Models for Rubber (ECCMR), London, UK, 2003.

[14] J. Forssén, W. Kropp, J. Brunskog, S. Ljunggren, D. Bard, G. Sandberg, F. Ljunggren, A. Ågren, O. Hallström, H. Dybro, K. Larsson, K. Tillberg, L-G. Sjökvist, B. Östman, K. Hagberg, Å. Bolmsvik, A. Olsson, C-G. Ekstrand, M. Johansson: Acoustics in wooden buildings. State of the art 2008. Vinnova project 2007-01653, Report 2008:16, Stockholm: SP Trätek (Technical Research Institute of Sweden), 2008.

[15] F. Ljunggren: Using elastic layers to improve sound insulation in volume based multistory lightweight buildings. Proceedings of Internoise, Ottawa, Canada, 2009.

[16] A. Ågren: Acoustic highlights in Nordic light weight building tradition – focus on ongoing development in Sweden. Proceedings of BNAM, Bergen, Norway, 2010.

[17] M. Meyers, K. Chawla: Mechanical Behavior of Materials. Cambridge University Press, New York, USA, 2009.

[18] L. Cremer, M. Heckl, B. A. T. Petersson: Structure-borne sound. Springer. Berlin, Germany, 2004.

[19] O. A. B. Hassan: Building acoustics and vibrations – Theory and practice. World Scientific, Singapore, 2009.

[20] R. Ökvist, F. Ljunggren, A. Ågren: Variation in sound insulation in multistory lightweight timber constructions. Proceedings of Internoise, Ottawa, Canada, 2009.

[21] Å. Bolmsvik, T. Ekevid: Flanking transmission in a timber-framed building – A comparison of structural vibrations in measurements and FE analyses, Submitted to The International Journal of Acoustics and Vibration , January 2013.

[22] Å. Bolmsvik, T. Ekevid: FE modeling of wooden building assemblies. Proceedings of Internoise 2010, Lisbon, Portugal, 2010.

[23] F. Ljunggren: Long-term effects of elastic glue in lightweight timber constructions. Proceedings of Forum Acusticum. Aalborg, Denmark, 2011.

[24] A. K. Chopra: Dynamics of structures, Prentice Hall, New Jersey, USA, 2007.

[25] N. Ottosen, H. Petersson: Introduction to the finite element method. Prentice Hall, England, 1992.

[26] K.J. Bathe: Finite Element Procedures, Prentice Hall, New York, United States, 1996.

[27] C. Hopkins: Sound Insulation, Elsevier, Oxford, UK, 2007